# Functional biodiversity and seasonal transitions of pelagic protists in Disko Bay, Greenland

Dissertation

vorgelegt zur Erlangung des Grades *Doctor rerum naturalium* (Dr. rer. nat.)

2021

von

**Claudia Sabine Bruhn**

M. Sc. Water Science

B. Sc. Biologie

Fachbereich 2 (Biologie/Chemie) der

Universität Bremen

ALFRED-WEGENER-INSTITUT
HELMHOLTZ-ZENTRUM FÜR POLAR- UND MEERESFORSCHUNG

Sektion für Ökologische Chemie

In Kooperation mit der Arctic Station,
Universität Kopenhagen,
Qeqertarsuaq, Grönland

Author: Claudia S. Bruhn

Cover Design: Stella Wenzel

Universität Bremen

**Versicherung an Eides Statt**

Ich,
Claudia Sabine Bruhn,
Matr.-Nr.: 3115137,

versichere an Eides Statt durch meine Unterschrift, dass ich die vorstehende Arbeit selbständig und ohne fremde Hilfe angefertigt und alle Stellen, die ich wörtlich dem Sinne nach aus Veröffentlichungen entnommen habe, als solche kenntlich gemacht habe, mich auch keiner anderen als der angegebenen Literatur oder sonstiger Hilfsmittel bedient habe.
Ich versichere an Eides Statt, dass ich die vorgenannten Angaben nach bestem Wissen und Gewissen gemacht habe und dass die Angaben der Wahrheit entsprechen und ich nichts verschwiegen habe.
Die Strafbarkeit einer falschen eidesstattlichen Versicherung ist mir bekannt, namentlich die Strafandrohung gemäß § 156 StGB bis zu drei Jahren Freiheitsstrafe oder Geldstrafe bei vorsätzlicher Begehung der Tat bzw. gemäß § 161 Abs. 1 StGB bis zu einem Jahr Freiheitsstrafe oder Geldstrafe bei fahrlässiger Begehung.

_____

Ort, Datum

_____

Unterschrift

Datum des Kolloqiums: 24.01.2022

1. Gutachterin: Prof. Dr. Bente Edvardsen

2. Gutachterin: Dr. Sylke Wohlrab

*"In the end, our society will be defined not only by what we create, but what we refuse to destroy."*

John C. Sawhill

## Table of Contents

## List of abbreviations

| | |
|---|---|
| ANOVA | analysis of variance |
| ASV | amplicon sequence variant |
| Chl *a* | chlorophyll *a* |
| CTD probe | conductivity-temperature-depth probe |
| DA | domoic acid |
| HAB | harmful algal bloom |
| N:P ratio | ratio of nitrogen to phosphorus |
| OTU | operational taxonomic unit |
| PAR | photosynthetically active radiation (wavelength of 400 to 700 nm) |
| PCR | polymerase chain reaction |
| POC | particulate organic carbon |
| PON | particulate organic nitrogen |
| RUE | resource use efficiency |
| SPATT | solid phase adsorption toxin tracking |
| SSU rRNA | small subunit of the ribosomal RNA |

## Abstract

Environments are changing more and more due to the ongoing climate change. This will and is altering ecosystems all over the World. The Arctic is warming up at approximately double the rate than other regions. To understand how the marine ecosystem will be affected by this, it is necessary to understand how it is behaving in the first place. For marine pelagic ecosystems, protists are recognized as one of the most important organism groups. They form the basis of the marine food web, encompassing most of the primary producers of biomass, which are further consumed by higher trophic levels. The community usually follows seasonal patterns in abundance and dominance of different taxonomic groups throughout the year. Due to the relative inaccessibility, protist seasonal patterns have not been studied extensively in the Arctic environment before.

Especially during the phototrophic spring bloom, a high amount of biomass is created, which is providing nourishment for other microorganisms, small mesozooplankton, bigger animals and eventually the local population and marine megafauna. Therefore, this study focused on the months leading into and out of the annual spring bloom event in an Arctic environment, and how the local protist community reacted to the changing circumstances. As a highly seasonal study area, this provided the opportunity to investigate several typical Arctic phenomena during two field studies in 2017 (from spring to summer) and 2018 (from winter to spring), including seasonal sea ice and very dark periods in winter, and the continuously shining midnight sun in summer. Embedded in contextual data, an approach with state of the art metabarconding was utilized to shed light on the pelagic protist diversity. To get additional insight, the samples were size fractionated into picoplankton (0.2 to 3 µm), nanoplankton (3 to 20 µm) and microplankton (20 to 200 µm). For Illumina sequencing, the V4 region of eukaryotic SSU rRNA gene was targeted with haptophyte-optimized primers. Afterwards, annotation via PR$^2$, and – in some cases – phylogenetic placement for species confirmation, were performed. For all 36 samplings from 22 sampling dates, a total of 5,522 different ASVs assignable to protist taxa were found. The winter community in 2018 consisted of many mixotrophic, heterotrophic and parasitic organisms, which were displaced by phototrophs towards the spring bloom, especially in the microplankton size fraction. When looking at the transition from spring to summer in 2017, pico- and nanoplankton had only a small percentage of phototrophs, but more heterotrophs and mixotrophs. Microplankton progressed from predominantly phototrophs during the spring bloom to mostly mixotrophs in summer.

Both years had a phototrophic, diatom dominated spring bloom with relatively low diversity and high biomass, while the times before and after the bloom event were much more diverse. These periods were characterized by a higher percentage of ciliates and dinoflagellates

in winter, and additionally more haptophytes and cryptophytes in summer. Parasitism seemed very prevalent in winter, while in summer, most protists were mixotrophs and heterotrophs.

The influence of environmental factors on these transition patterns were part of this study. The initiation of the spring bloom event was found to happen in accordance with sea ice break-up and shallowing of the ocean's mixed layer depth. However, the spring bloom did not initiate at the bottom of the sea ice, but at a depth of approximately 55 m, coinciding with the halocline. Additionally, day length increase and the light's spectral composition changes were measured above water. Therefore, the shallowing of the mixed layer depth, the increase in day length and change in spectral composition were probable factors in the bloom initiation, and not only the light intensity. The bloom had a low diversity, but high resource use efficiency (RUE) with high biomass. This shows that the spring community was, compared to the other observed seasons, the most productive one. The decline of RUE towards summer indicated ecological niches opening up as the spring community became less efficient in using the given resources. This was confirmed with a subsequent community shift in the microplankton size fraction from phototrophs to mixotrophs. The potential for harmful algal blooms (HABs) was detected during the spring bloom, as particulate domoic acid (DA) concentration increased. This was in accordance with the detected peak of relative abundance of the potentially DA-producing genera *Pseudo-nitzschia* and *Nitzschia*. Particulate dinoflagellate-related toxins peaked while potentially toxic dinoflagellate taxa were in their highest relative abundance in summer. However, dissolved dinoflagellate-related HAB toxins were present throughout the rest of the year, indicating long retention times of the toxins in the water column.

This work overall contributes to a better understanding of the interplay of protist organisms with each other and with their environment in an Arctic context. In the future, this may help to understand the changes that are currently provoked and how they will affect these small but significant organisms, and therefore the whole marine ecosystem.

## Zusammenfassung

Durch den Klimawandel verändert sich unsere Umwelt mehr und mehr. Diese Veränderungen beeinflussen bereits Ökosysteme auf der gesamten Welt und werden auch weiterhin zu mehr Veränderungen führen. Alleine die Arktis erwärmt sich ungefähr doppelt so schnell wie andere Regionen. Um allerdings evaluieren zu können, was diese Erwärmung mit dem marinen Ökosystem der Arktis macht, muss zuerst das Ökosystem an sich verstanden werden. Für marine pelagische Ökosysteme sind Protisten einer der wichtigsten Primärproduzenten. Sie produzieren einen Großteil der Biomasse, die von Organismen höherer Trophiestufen konsumiert werden. Protistengemeinschaften verfolgen normalerweise ein saisonales Muster von Menge und Anteil der verschiedenen Taxa. Durch die relativ schlechte Erreichbarkeit und die herausfordernde Logistik von Studien in der Arktis sind saisonale Muster der Protisten noch nicht ausreichend untersucht.

Vor allem während der phototrophen Frühlingsblüte des mikrobiellen Planktons wird eine große Menge Biomasse produziert. Diese Biomasse ist die Ernährungsgrundlage für andere Mikroorganismen, kleine Herbivoren, größere Tiere und letzten Endes für die lokale Bevölkerung und marine Megafauna. Aus diesem Grund wurde diese Studie angesetzt um insbesondere die Monate, die in die und aus der Frühlingsblüte führen, zu untersuchen: Es wurde untersucht, wie die Arktis sich zu dieser Zeit verändert, wie die Protistengemeinschaft auf diese Veränderungen reagiert und diskutiert, was das für Konsequenzen für die Zukunft haben könnte. Der Studienort in der Diskobucht, West Grönland, hat es dabei ermöglicht, verschiedene typisch arktische Phänomene der Saisonalität der Arktis als Kontext der beiden Feldstudien in 2017 (vom Frühling in den Sommer) und 2018 (vom Winter in den Frühling) zu erforschen. Saisonales Meereis, sehr dunkle Perioden im Winter sowie die kontinuierlich scheinende Mitternachtssonne im Sommer gehören zu einigen dieser extremen Phänomenen. Eine Herangehensweise mittels modernem Metabarcoding wurde genutzt, um die anwesenden pelagischen Protisten zu identifizieren und ihre Diversität zu eruieren. Für eine detailliertere Einsicht in die Größenverteilung wurden die Proben in Picoplankton (0,2 bis 3 µm), Nanoplankton (3 bis 20 µm) und Microplankton (20 bis 200 µm) eingeteilt. Mit Illumina-Sequenzierung, die mit Hilfe von für Haptophyten optimierten Primern vorgenommen wurde, wurde die eukaryotische V4-region des SSU rRNA Gens als Ziel für PCR-Reaktionen genutzt. Anschließend wurden Annotationen mittels $PR^2$ und ggf. phylogenetischen Platzierungen zur taxonomischen Bestätigung besonders abundanter Sequenzen durchgeführt. Für alle 36 Probennahmen von 22 verschiedenen Tagen konnten insgesamt 5.522 verschiedene ASVs Protisten zugeordnet werden. Die Wintergemeinschaft in 2018 bestand insbesondere aus mixotrophen, heterotrophen und parasitären Organismen, welche zum Frühling hin durch phototrophe ausgetauscht wurden, insbesondere im Microplankton. In dem Übergang von

Frühling zu Sommer 2017 waren kaum phototrophe im Pico- und Nanoplankton vertreten, dafür aber mehr heterotrophe und mixotrophe Organismen. Im Microplankton hingegen war ein Übergang von vorwiegend phototrophen während der Frühlingsblüte zu mixotrophen Organismen im Sommer sichtbar.

Beide Jahre hatten eine phototrophe Frühlingsblüte, die von Diatomeen dominiert wurde und eine relativ geringe Diversität, aber dafür eine hohe Biomasse aufzuweisen hatte. Die Zeiten vor und nach der Blüte waren im Vergleich dazu besonders divers. Es gab insgesamt einen höheren Anteil an Ciliaten und Dinoflagellaten im Winter und zusätzlich dazu mehr Haptophyten und Cryptophyten im Sommer. Insbesondere im Winter schien Parasitismus eine weit verbreitete Strategie gewesen zu sein, während im Sommer hauptsächlich mixotrophe und heterotrophe Protisten detektiert wurden.

Der Einfluss von Umweltfaktoren auf diese Abfolgen der Protisten war ebenfalls Teil dieser Studie. Der Anfang der Frühlingsblüte geschah im Zusammenhang mit dem Aufbrechen und Schmelzen des Meereises und der Abflachung der durchmischten Schicht des Meeres. Die Blühte begann allerdings nicht direkt unter dem Meereis, sondern auf einer Tiefe von ca. 55 m, was der Halokline entsprach. Zusätzlich wurden die stetig länger werdenden Tage und die spektrale Komposition des Sonnenlichtes über Wasser gemessen. Deshalb waren vermutlich die flacher werdende durchmischte Meeresschicht, die verlängerte Beleuchtung und die spektrale Lichtzusammensetzung Faktoren für die Initiiation der Frühlingsblüte und nicht nur die Lichtintensität. Die Blüte hatte eine geringe Diversität aber eine hohe Ressourcen-Nutzungs-Effizienz (RUE) mit hoher Biomasse. Das zeigte, dass die Frühlingsblüte, im Vergleich zu den anderen beobachteten Jahreszeiten, die produktivste war. Der Rückgang der RUE im Sommer deutete an, dass ökologische Nischen frei wurden, da die Frühjahrsgemeinschaft weniger effizient darin wurde, die gegebenen Ressourcen zu nutzen. Dies bestätigte sich mit einem darauffolgenden Wechsel des Microplanktons von phototrophen zu mixotrophen Protisten. Das Potenzial für toxische Algenblüten (HABs) wurde auch bereits während der Frühlingsblüte erkannt, als die Konzentration partikulärer Domoinsäure (DA) gestiegen ist. Dies war in Übereinstimmung mit einem höheren Aufkommen der Genera *Pseudo-nitzschia* und *Nitzschia*, die bekannte Produzenten von DA sind. Partikuläre toxine, die sich auf Dinoflagellaten zurückführen ließen, hatten ihr Maximum als potenziell toxische Dinoflagellaten-Taxa stärker in der Protistengemeinschaft vertreten waren. Gelöste, von Dinoflagellaten stammende Toxine waren jedoch den Rest des Jahres im Wasser detektierbar, was auf eine lange Verweildauer der Toxine im Wasser hindeutete.

Insgesamt leistet diese Arbeit einen Beitrag dazu, die Wechselwirkungen zwischen Protisten miteinander und mit ihrer Umwelt im arktischen Kontext besser zu verstehen. In Zukunft kann dies dabei helfen, die Veränderungen, die sich im Moment ereignen, und ihren

Einfluss auf diese kleinen aber wichtigen Organismen und damit auf das gesamte Ökosystem, besser zu erkennen.

# Introduction

## The marine ecosystem

The marine ecosystem consists of a multitude of different niches and organisms, which interact with each other. Apart from that, the marine ecosystem has also been recognized as a key factor of the global carbon and nitrogen cycle, influencing the whole world (Fawcett & Ward, 2011). As primary producers, pelagic phytoplankton forms the basis of the marine food web, producing a substantial amount of biomass through photosynthesis, relieving the atmosphere from $CO_2$ and providing $O_2$ (Falkowski, 1994; Field *et al.*, 1998). The produced biomass subsequently sinks into deeper ocean layers or is exported, either to other heterotrophic or mixotrophic microorganisms or to higher trophic levels (Fig. 1). The next non-microbial trophic level usually consists of crustaceans, such as copepods, or other mesozooplankton. The mesozooplankton in turn gets eaten by larger animals. Like such, the productivity of marine protists defines the available food sources for animals and eventually the amount of fish and marine mammals that can be harvested by the local population.

**Terminology**

**Protists** – polyphyletic group of eukaryotic microorganisms (Whittaker & Margulis, 1978), in this case excluding fungi

**Phytoplankton** – drifting unicellular organisms that carry out photosynthesis, comprising both eukaryotes and prokaryotes (Marañón, 2009)

**Phototroph** – an organism obtaining energy from visible light as a primary energy source, utilizing photosynthesis (Peretó, 2011)

**Heterotroph** – an organism that needs organic compounds as carbon sources for the synthesis of its own cellular compounds (Gomez, 2011)

**Phagotrophy** – the act of ingesting other cells (Jékely *et al.*, 2007)

**Mixotroph** – an organism that employs both photosynthesis and phagotrophy to obtain energy (Ward, 2019)

**Zooplankton** – heterotrophic planktonic organism (Ward, 2019). In this case, referring to planktonic animals.

Seasonal regions usually have a pronounced phototrophic phytoplankton spring bloom (Sommer & Lengfellner, 2008), which quickly depletes the available nutrients in the mixed layer of the ocean (e.g. Sakshaug & Skjodal, 1989; Larsen *et al.*, 2004). A summer community of mixotrophic protists, such as dinoflagellates, typically follows this (Raymont, 1980; Smayda & Trainer, 2010; Flynn *et al.*, 2019). However, in some regions, other effects such as upwelling can deliver more nutrients from lower ocean layers to the surface water, enabling further blooms (Calil *et al.*, 2011; Fawcett & Ward, 2011). In some temperate and tropical areas, no clear seasonality can be observed at all (Winder & Cloern, 2010). In the Arctic, seasonal influences are widely believed to be more important to bloom formation, although upwelling at the edges of marine-terminating glaciers, driven by meltwater, have already been observed in Greenland, delivering nutrients and triggering local protist blooms that were independent from annual seasonality (Meire *et al.*, 2017). These upwelling events directly contributed to higher halibut yields in the direct proximity (Meire *et al.*, 2017), emphasizing the direct link between these ecosystem levels. In the Arctic, the food web tends to be shorter than in temperate regions, at

times only consisting of five levels (Hobson & Welch, 1992), which ultimately illustrates the importance of the healthy linkage between the different trophic levels even further (Fig. 1).

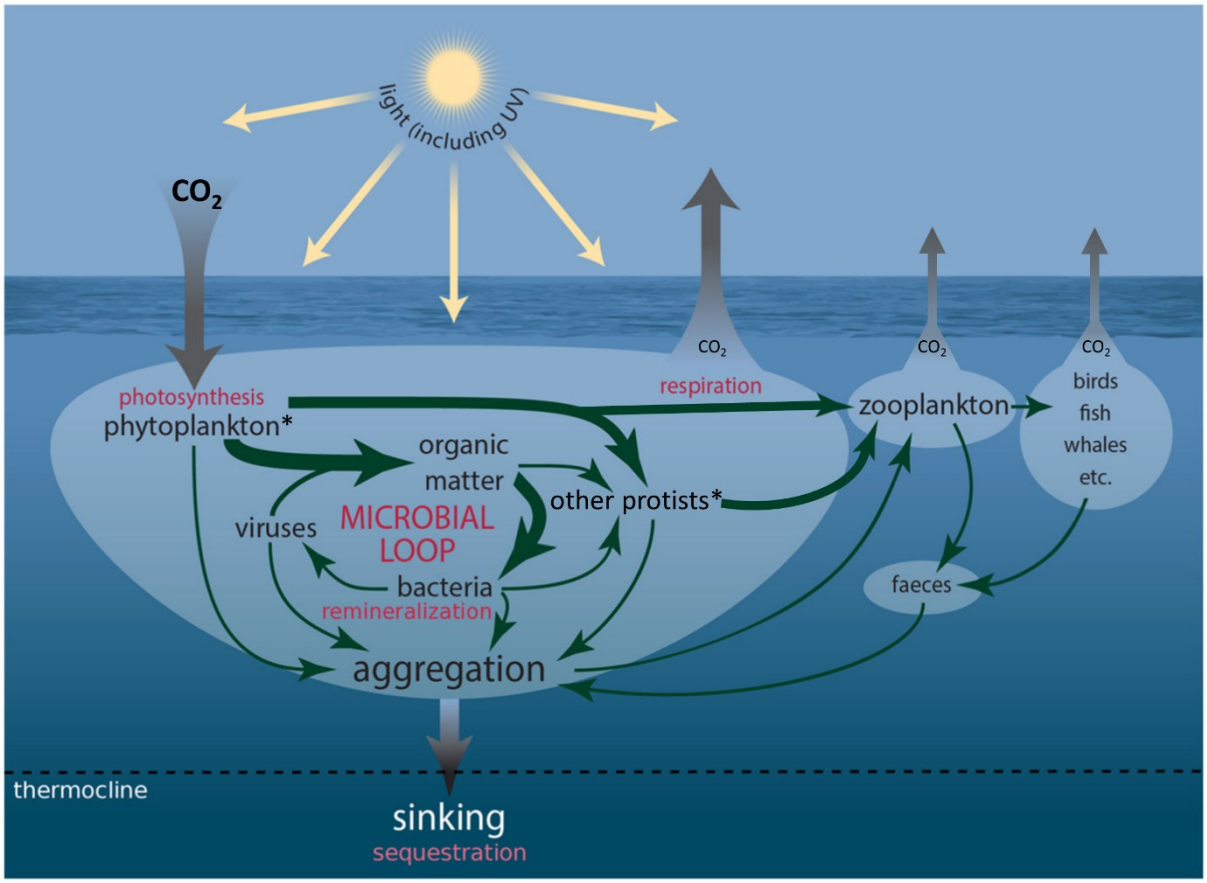


***Figure 1: Connections and schematics of marine protists, the marine food web, and their role in the biological carbon pump.*** *Note that pelagic protists are divided between phytoplankton (i.e. photosynthetic microorganisms, here also including prokaryotic phytoplankton) and other protists (both marked with *). Modified from Deppeler & Davidson, 2017.*

Marine microorganisms also include prokaryotes, which can utilize dissolved organic carbon from other microbes, thereby regenerating nutrients, which are ultimately made available to protists through sequestration by the prokaryotes or phagotrophy by the protists. This so-called microbial loop ads an additional level of complexity to the microbial ecology of the ocean (Pomeroy *et al.*, 2007). Marine protists by themselves already operate in different trophic modes, showing that even single celled organisms occupy different ecological niches. Traditionally, it was believed that protists only have the two trophic modes of phototrophy and heterotrophy, ignoring additional niches in the marine ecosystem (Flynn *et al.*, 2013). The habitual usage of the term mixoplankton is rather new, describing protists that combine aspects of phototrophy and phagotrophy (Flynn *et al.*, 2019). While the recognition of the concept of

mixotrophy itself dates back almost 100 years for plants (Christy, 1923), the usage for marine protists is just slowly gaining attention (Faure *et al.*, 2019; Leles *et al.*, 2019). The acknowledgement of mixotrophy as an additional trophic mode takes direct influence on the understanding of the biochemical cycling of nutrients and trophic dynamics within the ecosystem (Flynn *et al.*, 2019).

## Nutrients and resources

An important study topic for ecologists is the relationship between the community diversity and the community functioning, especially the resulting stability of the ecosystem with higher or lower diversity (McCann, 2000; Ptacnik *et al.*, 2008). One approach to estimate these factors is the calculation of the so-called resource use efficiency (RUE), which was derived from the concept of transfer efficiency by Odum (1957). Resource use efficiency is defined as the unit of biomass per unit of limiting nutrient in an ecosystem (de Wit, 1992; Hodapp *et al.*, 2019), being based on Liebig's law of the minimum (Liebig, 1840). It displays how well a given ecosystem can transfer nutrients into biomass, showing its general efficiency. One possibility to describe the nutrient ratios of a marine ecosystem is the Redfield-Ratio (Redfield, 1934), which in a modified version describes the ratio of carbon to nitrogen to phosphorus as 106:16:1 (C:N:P, Redfield *et al.*, 1963). In 1933, Redfield measured several samples from various positions of the Atlantic, Indian and Pacific Ocean, and the Barents Sea for nutrients, and discovered that the seawater in all areas approximated the same N:P ratio. This was in turn in accordance with the nutrient ratios of the marine plankton (Redfield, 1934). Since then, the ratio, although regularly modified and fine-tuned, has been widely accepted as a fundamental principle of marine research. In this ratio, an ecosystem is usually considered to be "in balance" (Nature Geoscience, 2014). In addition, it was generally hypothesized that phosphorus, as the macronutrient with the lowest value in this ratio, is the limiting nutrient of the ecosystem (Paytan & McLaughlin, 2007). However, in further studies, it has been shown that nitrogen fixation is not as efficient in a marine environment as believed before (Ryther & Dunstan, 1971). Therefore, the marine ecosystem is now considered to be generally limited by nitrogen and not by phosphorus concentration (Smith, 1984). Putting the RUE (based on nitrogen) in context with the diversity could potentially explain shifts in the protist community and therefore parts of the seasonal succession patterns of the different protist taxa. Still, nitrogen might not be the only limiting nutrient in an ecosystem (as illustrated by e. g. Hodapp *et al.*, 2019).

## The Arctic as an extreme environment

The tilt of the Earth's axis results in seasonality, which is more extreme towards the North and South Poles. While there is little variation in day length and season along the equator, days get longer and shorter – depending on the season – the farther the distance from the equator (Fig. 2). The latitude of approximately 66.3 °N marks the so-called Arctic Circle (Laskar, 1986; Tanner, 2021), which is the latitude where it is continuously night/day for a full 24 h at least once per year. Higher north, the amount of days with full sun/full night increases. Therefore, this latitude marks the border of the Arctic for most definitions. However, the climate-oriented definition of the Arctic varies from this. This is mostly due to the fact that water currents may result in a considerably milder climate in some regions north of the Arctic Circle. The Gulf Stream warms e.g. northern Scandinavia, resulting in it to belong to the climatic sub-Arctic. On the other hand, the entirety of Greenland belongs to the climatic Arctic (with part of it in the low Arctic and part of it in the high Arctic), although the southernmost part is located south of the Arctic Circle (Meltofte *et al.*, 2017, Fig. 3). Ultimately, the North Pole area is characterized by the Arctic Ocean, which to date is continuously covered with thick multiyear sea ice. The extent of the sea ice fluctuates annually, with the usual maximum sea ice extend in March and the usual minimum in September (Parkinson & Cavalieri, 2002). The Arctic is an extreme environment that also seems to be much more vulnerable to climate change (Overpeck *et al.*, 1997; McBean *et al.*, 2005; IPCC, 2007). The Arctic is one of the quickest changing ecosystems on Earth, warming at a significantly higher rate than other regions (Moritz *et al.*, 2002; Mauritsen, 2016).

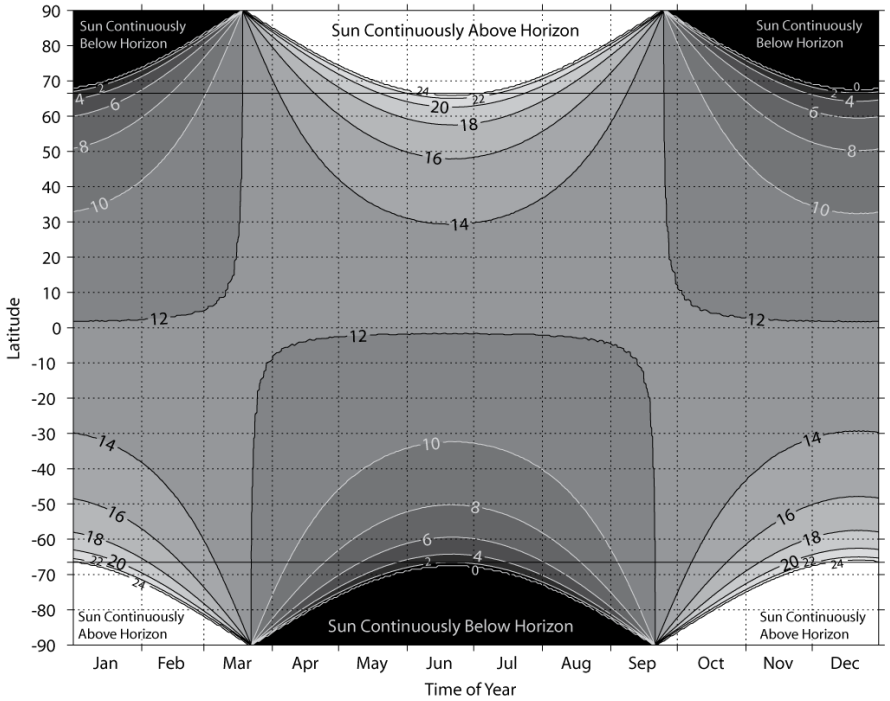


***Figure 2: Amount of day length in dependence of the latitude and time of the year on Earth.*** *Different shades of grey reflect the amount of night hours and day hours per day in their respective hues. From Hudson, 2007.*

## Disko Bay as a study area

Just after Antarctica, Greenland holds the second biggest reservoir of fresh water in its ice sheet, holding enough water to raise the sea level by 7.4 m if completely melted (Morlighem *et al.*, 2017). Greenland's western coast is much more densely populated than its eastern coast, mostly due to heavy pack ice that inhibits travel and transport by sea in the East (Fuchs & Whittard, 1930). Disko Bay is an area located at the western side of Greenland, belonging to the climatic low Arctic. Apart from the mainland, this bay contains the largest Greenlandic island, which is called Disko Island or Qeqertarsuaq (Greenlandic for "big island", Fig. 4). Disko Bay is a comparably well-established site for fisheries and tourism, the former providing also the most important export goods for Greenland in general (Brett, 2003; Vahl & Kleemann, 2019). The area is one of the most densely populated regions in Greenland, with many inhabitants heavily relying on marine resources through hunting and fishing of marine animals (Vahl & Kleemann, 2019).

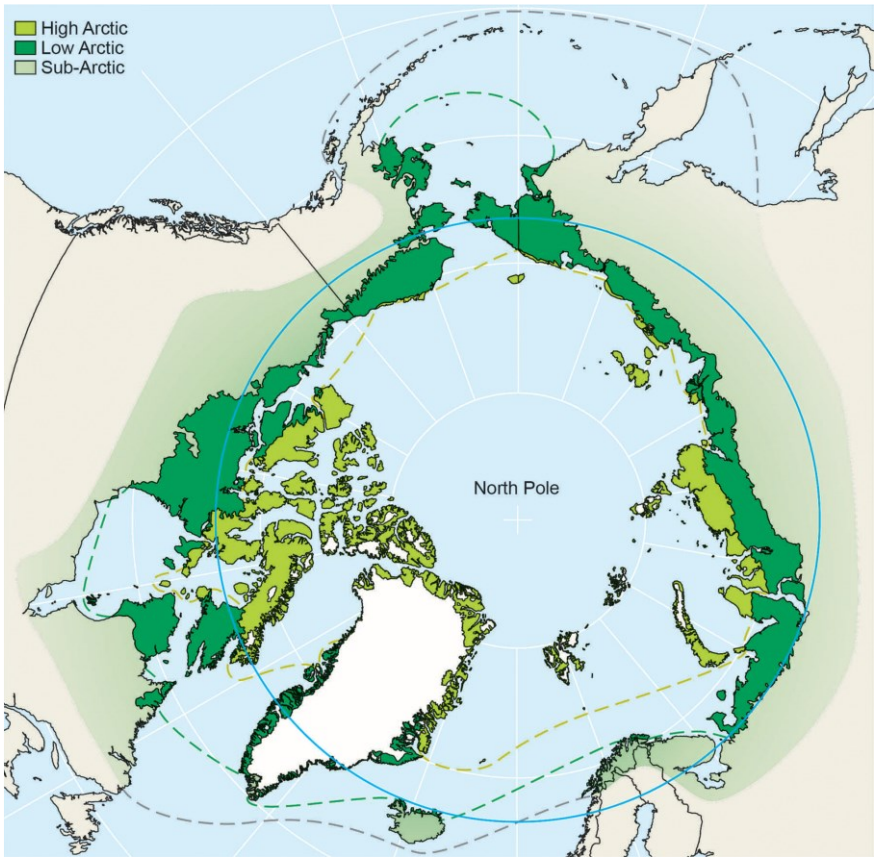


***Figure 3: Map of the northern hemisphere with marked zones for the high Arctic, low Arctic and sub-Arctic.*** *The continuous blue line represents the Arctic Circle. From Meltofte, 2017.*

Jakobyhavn Isbræ is the most productive glacier of the northern hemisphere, which is located in the eastern part of the Disko Bay, calving and melting into it (Motyka *et al.*, 2011, Fig. 4). Both ice melt – also from icebergs – and sub-glacial freshwater flow get delivered into the bay area, which at times can decrease the ocean salinity (Buch, 1990). Additionally, the bay is seasonally covered with sea ice, which obstructs light to possible primary producers in the ocean and hinders logistics. Disko Island is home to the oldest Arctic research station, simply

called Arctic Station, which was founded in 1906 by the botanist Morten Petersen Porsild (Porsild, 1906). A village, inhabited by approximately 840 people, is also situated on the island. The depth of the bay goes down to approximately 400 m below sea level and has warm Atlantic waters streaming into it, originating from the Irminger current (Fig. 4).

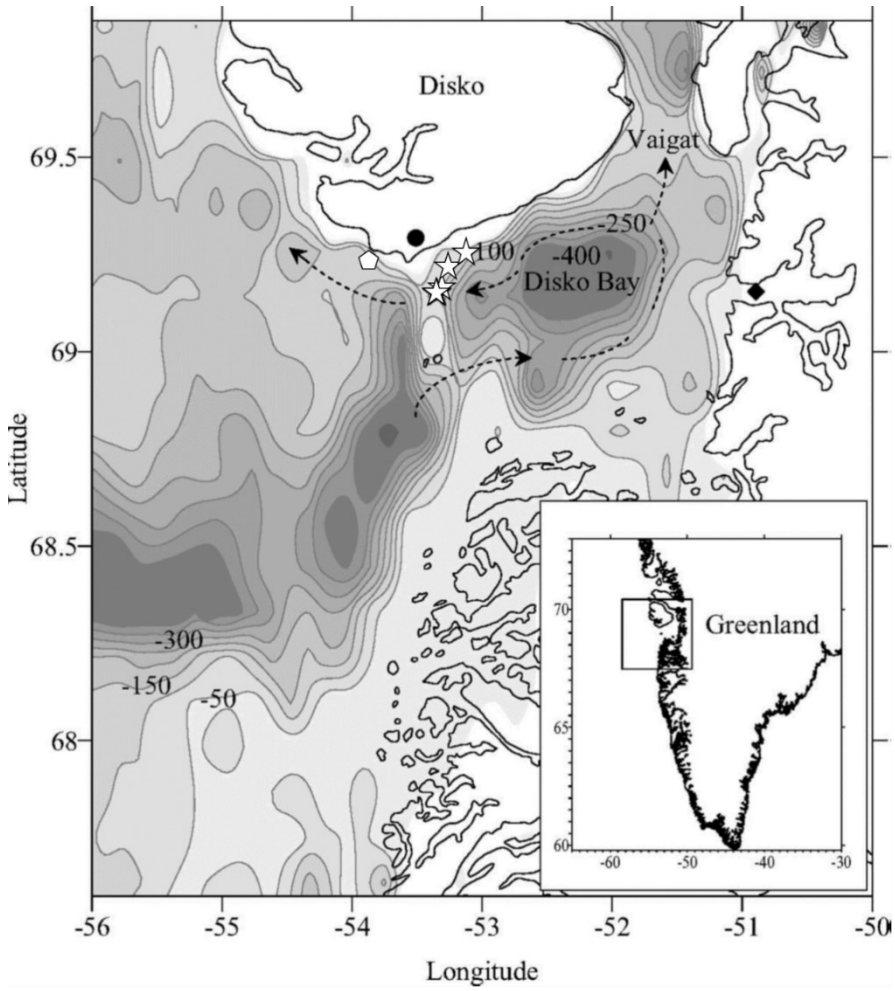


***Figure 4: Map, showing southwest Greenland and, in detail, Disko Bay.*** *The arrows indicate the flow of currents south of the island. The black dot represents the Arctic station, and the black diamond the calving glacier Jakobyhavn Isbræ. Regularly used sampling stations utilized in the presented studies are shown with white stars. The location marked with the white pentagon is representing the location, where SPATT toxin monitoring was conducted. Modified from Hansen* et al.*, 2012*.

## The spring bloom in the Arctic

At approximately 69.2 °N, Disko Bay is a very seasonal area, which also influences the local phytoplankton spring bloom and its patterns. At the latitude of Qeqertarsuaq, the polar night and the midnight sun both persist for almost three months each. At the end of the winter, seasonal sea ice usually obstructs light from penetrating deep into the ocean. As a characteristical Arctic phenomenon, sea ice can be discussed as influencing the Arctic spring bloom event. Protists that are incorporated into the sea ice typically consist of large cells, which are mainly diatoms (Gradinger & Ikävalko, 1998; Riedel *et al.*, 2007; Różańska *et al.*, 2008). Pennate diatoms, such as *Nitzschia frigida*, are the most common taxon present in the sea ice

(Niemi *et al.*, 2011), while the pelagic community is net heterotrophic with little interaction with the sea ice community (Leu *et al.*, 2015). At the end of winter, a quickly melting snow cover, together with increasing day length and solar angle lead to a stronger light penetration through the sea ice (Nicolaus *et al.*, 2012). Subsequently, a first ice algal bloom develops at the lowermost centimeters of the sea ice, already providing food for other trophic levels (Leu *et al.*, 2015). Initially, as the sea ice breaks up, the pelagic community is seeded in part by the sea ice algae community, which later on evolves into a typical pelagic spring community (Michel *et al.*, 1993). The breakup of the seasonal sea ice and stronger stratification are widely believed to be the reasons for a rich pelagic phytoplankton spring bloom, which is net phototrophic (Hansen *et al.*, 2012). The spring bloom is often dominated by diatoms (Hansen *et al.*, 2012), which was also already observed in Disko Bay (Tammilehto *et al.*, 2017). However, the Arctic spring bloom can also be dominated by phototrophic haptophytes, like *Phaeocystis* spp., which prevailed in the spring bloom close to Spitsbergen in 2011 (Marquardt *et al.*, 2016). The spring bloom is usually followed by a secondary bloom in summer (Hansen *et al.*, 2012), containing more mixotrophic organisms such as dinoflagellates (Raymont, 1980; Smayda & Trainer, 2010; Flynn *et al.*, 2019). The protist blooms are in turn grazed upon by calanoid copepods. In the past, a change from predominant *Calanus hyperboreus* and *C. glacialis* to the smaller and less fat *C. finnmarchicus* was observable in the study area of Disko Bay (Møller & Nielsen, 2020).

## Non-beneficial impacts of protists on the marine ecosystem

As important as the protist community is for a healthy marine ecosystem, as problematic are some of its members. The haptophyte genus *Phaeocystis* is an example, which is often found in Arctic surface waters during early spring (Marquardt *et al.*, 2016), sometimes when sea ice is still covering the ocean (Pavlov *et al.*, 2017). *Phaeocystis* spp. are considered to be climate altering species, because they can produce the climate active compound dimethylsulfide (Stefels & van Boeckel, 1993; Verity *et al.*, 2007). Additionally, they seem to be a less preferred food source for mesozooplankton compared to other phytoplankton taxa (Weisse *et al.*, 1994; Nejstgaard *et al.*, 2007). As *Phaeocystis* spp. were already observed in parts of the Arctic, more frequently occurring community shifts from mainly diatoms to mainly *Phaeocystis* spp. could have great impact on the marine ecosystem.

Additionally to this, many coastal regions are affected by so-called harmful algal blooms (HABs; Anderson *et al.*, 2012). These blooms can be the overabundance either or both of biomass and/or share of specific toxigenic protist species. Toxigenic species are sometimes diatoms such as *Pseudo-Nitzschia* spp. or *Nitzschia* spp. (Lundholm *et al.*, 2018), or – more often – toxigenic dinoflagellates (Smayda, 1997). Nevertheless, other taxa such as the haptophyte

*Chrysochromulina leadbeateri* may also cause HABs (Karlson *et al.*, 2021). A global increase in HABs has been observed (Van Dolah *et al.*, 2000; Hallegraeff, 2003; Anderson *et al.*, 2012), suggesting a link to climate change (Gobler, 2020). More prevalent HABs in Arctic waters, namely in Disko Bay, would have devastating effects on the local residents, which are heavily relying on marine resources (Vahl & Kleemamm, 2019). Although HABs have, until recently, not been viewed as a substantial threat in the Arctic, there have been several observations suggesting otherwise. The Alaskan Arctic already started to have recurring toxic blooms of the dinoflagellate *Alexandrium catenella* (Anderson *et al.*, 2021). *Alexandrium catenella* is one of the species able to produce saxitoxins, the causative agent for paralytic shellfish poisoning. Moreover, *A. catenella* is able to form cysts, which lay dormant in the benthic part of the ocean, with the potential to germinate and bloom into a HAB once the conditions are favorable (Fisher *et al.*, 2018). These cysts have been found to be available as massive deposits in the Alaskan Arctic, suggesting that they could also be available and ready to germinate at other Arctic locations, where this species was not yet an issue (Anderson *et al.*, 2021). In the Attu region, not far south from Disko Bay, saxitoxin-producing *A. catenella* has already been detected, which even led to an exceed of the limit of 800 µg saxitoxin per kg shellfish in 2003 (Baggesen *et al.*, 2012). Other dinoflagellate-derived toxins have also been recorded at high latitudes, such as pectenotoxin-1 in the Chuckchi Sea, or azaspiracid-producing *Amphidoma languida* in the sub-Arctic Irminger Sea (Tillmann *et al.*, 2015). Domoic acid (DA), the toxin produced by some *Pseudo-Nitzschia* and *Nitzschia* spp., which is the causative agent for amnesic shellfish poisoning, was as well detected in West Greenland north of the Arctic circle (Elferink *et al.*, 2017). Marine mammals in the Alaskan Arctic and sub-Arctic have already shown signs of severe poisoning through HAB toxins, illustrating the harm that could be done to higher trophic levels of the ecosystem, especially via bioaccumulation (Lefebvre *et al.*, 2016; Hendrix *et al.*, 2021). The threat of regular HABs in the Arctic, having a big impact on the local population and ecosystems, is therefore most imminent.

# Outline

**The overarching aim of this study was to investigate the species and functional transitions in the protist community and therefore the seasonality of the basis of the marine ecosystem in the Arctic environment of Disko Bay in West Greenland. The transition periods to and from the important spring bloom event should be understood better, illuminating their underlying factors.**

To achieve this, a metabarcoding approach targeting the eukaryotic V4 region of the SSU rRNA gene was utilized. Amplicon sequence variants (ASVs) belonging to protist taxa were subsequently manually assigned to functional groups based on their trophic modes. These analyses were the basis for diversity measures and further taxonomic analyses to understand the community better. These data were put into context with more factors: the mixed layer depth and other oceanographic data gave insights into possible physical interactions with the immediate environment (temperature, salinity, local fluorescence, photosynthetic active radiation: PAR in the water, and others). Additional monitoring of sea ice presence helped to discuss the influence of this typical Arctic phenomenon on the protist community. Light measurements from a weather station could complement the physical data in the winter time. For investigating the general amount of biomass and the ratio of carbon to nitrogen in particles, particulate organic nitrogen (PON) and particulate organic carbon (POC) were measured. These measures had the advantage of including all organisms and not only photosynthetic organisms that bear chlorophyll. Still, chlorophyll *a* (Chl *a*) measurements were utilized to quantify the presence of phototrophs in the water. Nutrients in the water showed possible limitations of the organisms and the changing living conditions of the protist community. Eventually, HAB toxin contents were monitored directly in the cell samples and via SPATT (solid phase adsorption toxin tracking) samplers to help detect possible HAB-related organisms in the protist community.

Two intense field campaigns of each three months (spring to summer in 2017, and winter to spring in 2018) to study the protist community transitions in Disko Bay were the basis of the following three chapters. First, the protist community of the local ecosystem itself will be discussed in its natural succession patterns (chapters 1 and 2), and afterwards the act of producing toxins will be examined, embedded in the transition patterns of the first two chapters (chapter 3). The combination of these chapters will provide a different view on the protist community transitions and their interaction with their environment. Therefore, the dissertation is an in-depth study of the protist community throughout the seasons in Disko Bay.

## Chapters of this Dissertation

As stated before, the dissertation is consisting of three distinct chapters. They are presented in the forms of a submitted manuscript (chapter 1), a manuscript ready to be submitted (chapter 2), and a reprint of an independently published paper (chapter 3). For better readability, the styles are adapted to this dissertation. The content of the published paper remains unchanged from the published version. The supplemental material of the respective chapters can be found at the end of each of them. The following summaries are putting the chapters into context with the dissertation topic and aims. The chapters in this dissertation can be divided into the following core topics, dealing with segments of the overarching aim.

## Chapter 1 – Winter to Spring

### Transition from a mixotrophic/heterotrophic protist community during the dark winter to a photoautotrophic spring community in Arctic surface waters

Claudia Sabine Bruhn, Nina Lundholm, Per Juel Hansen, Sylke Wohlrab, Uwe John

Currently under peer review in: *Scientific Reports*

Preprint available under https://doi.org/10.21203/rs.3.rs-951783/v1

Chapter 1 is an in-depth study of the spring bloom initiation from early February to end of April 2018. It was possible to track the initiation of the spring bloom that commenced under the seasonal sea ice, while the spectral composition and the day length changed significantly from day to day. The interactions with sea ice, mixed layer depth, and the initiation of the bloom were the main topics of this chapter. To investigate the progression towards the spring bloom in terms of diversity, metabarcoding was utilized, targeting the eukaryotic V4-region. For further analysis of the available protists, the ASVs were divided into their major trophic modes. Biomass and photosynthetic activity were measured through POC and Chl *a*. With a CTD probe, it was possible to measure light penetration through the sea ice. Furthermore, the local fluorescence, showing the position of the phytoplankton in the water column, was measured. A weather station close to the bay area was providing information about the spectral composition and daily insolation above water, rounding off the fractional sampling data with continuous data. The presented study brings metabarcoding with functional analyses, oceanographic data, and

continuous light measurements into context with each other and aims to explain the initiation of the phytoplankton spring bloom in Disko Bay, tackling the following main questions:

- How does the spring bloom develop initially?
- Does the spring bloom develop just below the sea ice, where light intensity is highest?
- How do the breakage of the seasonal sea ice & more light influence its development?
- Is a distinct winter protist community existing or is the winter community just a dormant spring community?

**Author contributions**

C.S.B., N.L., and U.J. planned the study. C.S.B. coordinated and performed the sampling and processing of the samples, the analysis of the samples as well as most of the analyses of the data. U.J. produced the phylogenetic placement of the most abundant ASVs. C.S.B. curated the placement. P.J.H. and C.S.B. assigned trophic modes to the different ASVs. S.W. and C.S.B. wrote the scripts for analyzing the data. S.W. performed statistical analyses. All authors interpreted the resulting data. C.S.B. wrote the manuscript and prepared the graphs. The supplementary material was also prepared by C.S.B. The manuscript was revised by S.W., P.J.H., N.L., and U.J. All authors reviewed the final manuscript before submission and confirmed its originality.

## Chapter 2 – Spring to Summer

### Community composition and resource use efficiency shifts from spring to summer in Arctic pelagic protists

Claudia Sabine Bruhn, Sylke Wohlrab, Nina Lundholm, Per Juel Hansen, Uwe John

Manuscript to be submitted to: *Frontiers in Microbiology*

The second chapter focuses on the progression from the spring bloom into a summer community in 2017. Here, a connection between RUE with nitrogen as a limiting nutrient and the protist community diversity was made. Analyses of dissolved nutrients as well as PON were the basis for the nitrogen content of the ecosystem, while metabarcoding was used to assess the diversity of the community. It was possible to demonstrate that changes from the RUE correlate with the community transition from a spring community to a summer community. Different

productivity levels (assessed as RUE) of the different community compositions were also visible, with the phototrophic spring bloom being the most productive season. However, the diatoms that dominated this part of the season were not able to sustain for long, being replaced by less productive mixotrophs. Main questions of this chapter were:

- What is the fate of the spring bloom towards summer?
- Is the spring bloom really the most productive season?
- Is a high diversity the key to higher productivity in the marine protist community?
- How does the trophic mode, i.e. the niche of the organism, influence their productivity?

**Author contributions**

C.S.B., N.L., U.J., and S.W. planned the study. C.S.B. conducted the samplings, the processing of the samples, and most of the analyses. All authors interpreted the results of the analyses. S.W. and C.S.B. wrote the R-scripts for data analyses. C.S.B. executed the analyses. P.J.H. and C.S.B. assigned the trophic modes to the respective ASVs. C.S.B. performed the phylogenetic placement of the most abundant ASVs and the subsequent curation of the species names. The graphs and the manuscript were prepared by C.S.B and Fig. 3 was modified by S.W. The work was revised by S.W., P.J.H., N.L., and U.J. Eventually, all authors reviewed the final manuscript and confirmed its originality.

## Chapter 3 – HAB generating Species in Disko Bay

### Seasonal plankton succession is in accordance with phycotoxin occurrence in Disko Bay, West Greenland

Claudia Sabine Bruhn, Sylke Wohlrab, Bernd Krock, Nina Lundholm, Uwe John

Published in: *Harmful Algae*

https://doi.org/10.1016/j.hal.2021.101978

Chapter 3 concentrates on the HAB potential of the local protist community in Disko Bay. For this, a comprehensive study of the local protist community with regard to the potentially toxigenic species was conducted. Additionally to the metabarcoding approach, known HAB toxins were extracted from the sampling sites, and an almost year-round observation of

dissolved toxins via SPATT samplers was performed close to the sampling sites. Nine potentially toxigenic taxa were detected within the six months of investigation. The two diatom taxa and seven dinoflagellate taxa were integrated in the natural transition patterns of the bloom. Additionally, nine different dissolved toxins were detected over the course of one full year with the exception of one month. This chapter demonstrates that several toxigenic species were available in the Disko Bay area and that they were indeed producing toxins with the potential of causing harm to the ecosystem in the future. The main questions that this chapter should answer were:

- Are there toxin producing species in Disko Bay? If yes, how does the presence of these species change over the seasons?
- Is there a link between successional species and community patterns and toxin sequestration?
- How may HAB species influence and challenge the Arctic ecosystem and its beneficiaries in the future, especially with the ongoing climate change?

**Author contributions**

C.S.B., N.L., and U.J. planned the study. C.S.B. performed the field sampling and processing of the samples. B.K. supervised the toxin analyses after sample preparation and extraction by C.S.B. The manuscript was conzeptualized by all authors. S.W. and C.S.B. wrote the scripts for data analyses. C.S.B. prepared the graphs and the manuscript. All authors reviewed the manuscript and confirmed its originality before submission.

# Chapter 1

**Transition from a mixotrophic/heterotrophic protist community during the dark winter to a photoautotrophic spring community in Arctic surface waters**

Submitted manuscript

# Transition from a mixotrophic/heterotrophic protist community during the dark winter to a photoautotrophic spring community in Arctic surface waters

Claudia Sabine Bruhn[1,*], Nina Lundholm[2], Per Juel Hansen[3], Sylke Wohlrab[1,4], Uwe John[1,4,*]

[1]: Alfred Wegener Institute, Helmholtz Centre for Polar and Marine Research, Am Handelshafen 12, 27570 Bremerhaven, Germany

[2]: Natural History Museum of Denmark, University of Copenhagen, Øster Farimagsgade 5, 1353 Copenhagen, Denmark

[3]: University of Copenhagen, Strandpromenaden 5, 3000 Helsingør, Denmark

[4]: Helmholtz Institute for Functional Marine Biodiversity at the University of Oldenburg, Ammerländer Heersstraße 231, 26129 Oldenburg, Germany

[*]Corresponding authors: Claudia S. Bruhn, claudia.bruhn@awi.de, and Uwe John, uwe.john@awi.de

**Abstract**

Unicellular plankton communities (protists) are the basis of the marine food web. The spring bloom is especially important, because of its high biomass. However, it is poorly described how the protist community structure in Arctic surface waters develops from winter to spring. We show that mixotrophy and parasitism are the prominent trophic modes in the dark winter period. The transition period was characterized by a high relative abundance of mixotrophic dinoflagellates, while centric diatoms and the haptophyte *Phaeocystis pouchetii* dominated the successive phototrophic spring bloom event. Our observations indicate the presence of a characteristic winter community and a community shift from winter to spring, and not just a dormant spring community waiting for better circumstances. The spring bloom initiation commenced while sea ice was still obstructing the light penetration into the water column. The initiation coincided with a change in day length and spectral composition of the light, rather than with an increased light intensity. The initial increase in fluorescence, and therefore photosynthetic activity, was detected relatively deep in the water column, at ~55 m depth. This suggests that water column stratification and a complex interplay of abiotic factors eventually promote the spring bloom initiation.

**Keywords:** sea ice, succession patterns, metabarcoding, spring bloom formation, parasites, functional diversity, time series

## 1. Introduction

The Arctic is one of the fastest changing environments due to climate change [1-3]. This has already affected the Arctic biosphere, and will lead to further changes in the future [4]. The base of the complex marine pelagic food web consists of unicellular organisms, such as bacteria and eukaryotic unicellular plankton (protists) occupying different ecological niches, and providing the food source for higher trophic levels.

Because of their crucial role in the ecosystem, marine protists are frequent study subjects. Community studies of Arctic pelagic waters often focus on transect or snapshot studies [5-8], which do not properly display the temporal dynamics. The pelagic winter protist community in the Arctic has been characterized as most likely heterotrophic [9, 10] with phototrophic diatoms being present mostly in a stage of dormancy, e.g. as resting spores [11, 12].

The periods with ice cover have been declining during the past decades due climate change and this is expected to impact the timing and dynamics of the spring bloom, and the trophic modes of the protist community [13, 14]. Phytoplankton blooms have occasionally been found to develop before the sea ice melts [15-17], and recent studies have recognized the abundance of parasitic and mixotroph protists in sea ice presence [18, 19]. The seeding of the pelagic phototrophic spring bloom event by sea ice algae has also been discussed, especially in relation to multiyear sea ice [20, 21]. While the pattern of phototroph dominance during the spring bloom event is comparably well-described [22, 33, 36], the community structure of the winter community and its transition towards the vernal bloom is less investigated [10], especially in relation to seasonal sea ice. To understand the link between the biosphere and climate change in an ecosystem such as the Arctic, it is important to understand the general biotic patterns and their interactions with their environment. Therefore, a study of how the marine protist community evolves from the winter composition to a spring bloom composition is necessary. With the presented work, we aim to discuss the impact of the occurrence of seasonal sea ice and other abiotic parameters in their interplay with the protist community structure transition, with special focus on the functional groups of the observed organisms.

## 2. Results

### 2.1 Environmental observations

#### 2.1.1 Oceanographical context

The CTD measurements resulted in several depth profiles, of which photosynthetically active radiation (PAR), water density, chlorophyll fluorescence, and salinity are presented (Fig. 1). PAR measurements showed some penetration of light into the water at the beginning of the study up until March 7 and again from April 23 and onwards (Fig. 1a). Between these dates, there was

almost no light penetrating into the water column. The measured density of the water column showed a slight shallowing of a few meters of the layers (Fig. 1d). Fluorescence values started to increase around March 30 at a depth of approximately 55 m (Fig. 1c). Additionally, it formed two layers at 40 m and 7 m depth between April 5 and April 9, respectively. Afterwards, on April 13, fluorescence was detected as deep as 100 m. Salinity values showed different layers in the water column, which shallowed over time (Fig. 1b).

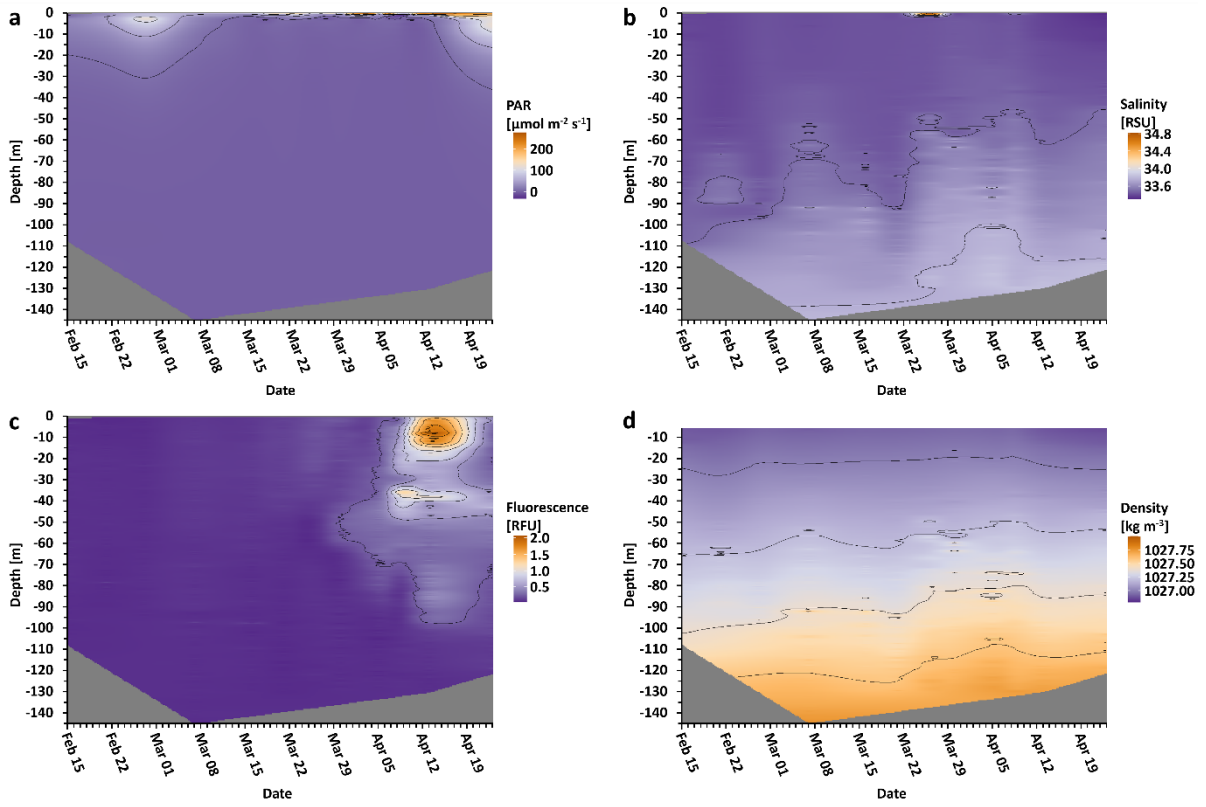


***Figure 1: Oceanographic data in depth profile over time.*** *Depicted are photosynthetic active radiation (**a**, PAR), salinity (**b**), fluorescence (**c**), and the density of the water (**d**). Isolines are displayed for orientation regarding the different values. Grey areas indicate unmeasured depths.*

### 2.1.2 Sea ice presence

In the following, we distinguish between the overall sea ice presence in the entire bay area and sea ice directly at the sampling station. Sea ice was present, but did not cover the full bay throughout the whole period. In the Disko Bay area, the sea ice cover reached a maximum coverage of 99 % on February 12, and covered at least 75 % until April 25, when the ice slowly started to break up (Fig. 2a, black line). At the sampling station, sea ice was building up between March 7 and March 16 (Fig. 2a, white area), when it reached a thickness of more than 40 cm with an additional snow cover. After April 5, the ice at the sampling station began to melt again, rendering the sampling on April 13 to be from the sea ice edge and the sampling on April 23 from the water surface.

### 2.1.3 Light

The day length increased during the sampling period, which therefore led to an increased total daily light intensity (Fig. 2b). The spectral composition of the light above the water also changed during the study (Fig. 2b). While incoming longwave radiation (4500 to 42000 nm wavelength) only experienced a slight increase in the daily average, incoming shortwave radiation (300 to 2800 nm wavelength) increased two to three times as much during the observed time period. The daily average of PAR increased even more rapidly, compared to longwave and shortwave radiation.

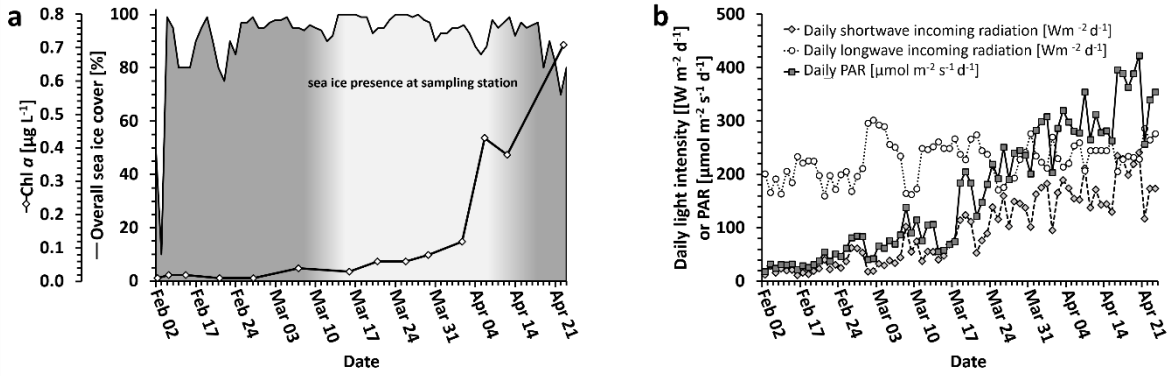


***Figure 2: Light and ice conditions. a: Local photosynthetic biomass (solid line with diamonds) in relation to sea ice coverage (solid line).*** *The sea ice coverage of the entire bay area is shown as a black line. The sea ice at the sampling station is indicated as the white coloring below the line.* ***b: Light quality change over time above water****. Incoming longwave radiation and incoming shortwave radiation as well as PAR are displayed as daily averages.*

### 2.2 Community structure changes

Biomass data were represented as particulate organic carbon (POC), particulate organic nitrogen (PON) and chlorophyll *a* (Chl *a*). POC and PON were measured to 63.7 µg $mL^{-1}$ POC and 4.9 µg $L^{-1}$ PON on the first day of measurement (February 10), and decreased until 14.0 µg $L^{-1}$ POC on March 21 and 0.8 µg $L^{-1}$ PON on February 21 (Table 1). Afterwards, both POC and PON increased until the end of the sampling campaign to their highest values of 70.8 µg $L^{-1}$ POC (on April 23) and 12.7 µg $L^{-1}$ PON (on April 13). In contrast, Chl *a* gradually increased from almost unmeasurable with 0.01 µg $L^{-1}$ on February 21 to 1.26 µg $L^{-1}$ on April 19 (Figure 2a).

| | FEB 10 | FEB 15 | FEB 21 | FEB 27 | MAR 07 | MAR 16 | MAR 21 | MAR 26 | APR 05 | APR 13 | APR 19 | APR 23 |
|---|---|---|---|---|---|---|---|---|---|---|---|---|
| **POC [µG $L^{-1}$]** | 68.40 | 63.72 | 43.29 | 16.36 | 33.46 | 31.41 | 14.01 | 16.18 | 23.79 | 66.13 | 49.82 | 70.79 |
| **PON [µG $L^{-1}$]** | 3.73 | 4.94 | 0.8 | 6.44 | 6.41 | 5.83 | 3.77 | 3.51 | 4.64 | 12.67 | 8.24 | 12.19 |

***Table 1: POC and PON as biomass proxies.*** *Data were retrieved from Bruhn et al. [37].*

In total, 4,009 different ASVs were assigned to protists in the metabarcoding analyses. The 300 most abundant protist ASVs accounted for 81 to 98 % of all reads, depending on the sampling date, of which 97 % were present in all three monthly phases. On the other hand, ASVs that were unique to a certain month were the overall least abundant ASVs, ranging from 14.3 % (February exclusive ASVs) over 5.4 % (April exclusive ASVs) to 4.7 % (March exclusive ASVs) of all reads.

A range from 44.9 % in picoplankton, over 36.9 % in nanoplankton to 21.8 % in microplankton of all protist ASVs were shared among all three time phases (Fig. 3). The highest number of unique ASVs per month is detected in February and the smallest number in April.

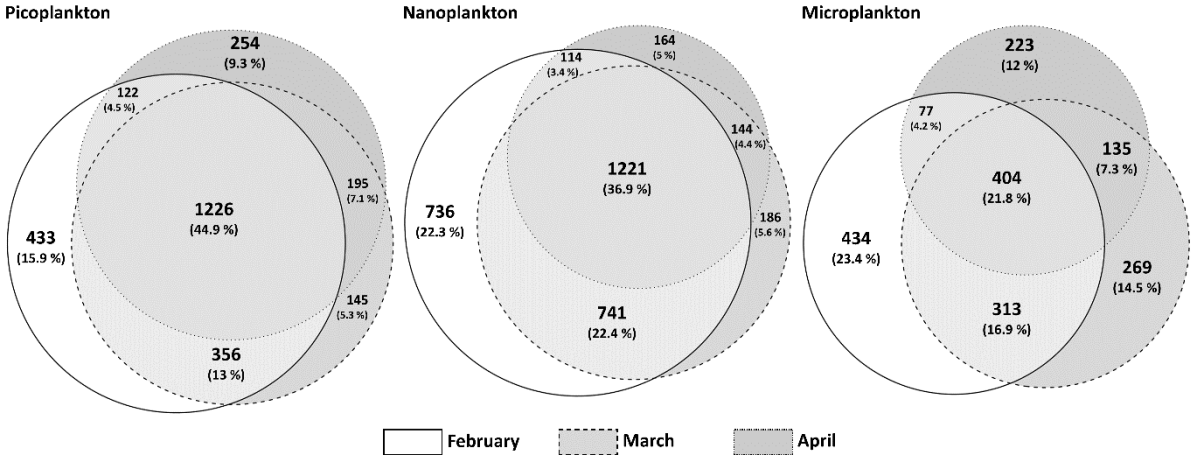


***Figure 3: Venn-Diagram adaptation of ASVs per monthly phase and size fraction.*** *A presence/absence-matrix was the basis for this visualization, where shared ASVs per calendar month are depicted in the overlaps. The circles are proportional to the number of unique ASVs.*

In February, the protist communities in all size fractions were mostly heterotroph, parasitic and mixotroph. The percentage of ASVs linked to heterotrophic taxa declined strongly during the sampling period, whereas ASVs linked to phototrophic species increased with time leading to a phototroph dominated community in April (Fig. 4a). ASVs linked to phototrophic taxa were mainly diatoms, especially in the nanoplankton and microplankton size fractions. In

picoplankton and nanoplankton, a considerable amount of reads initially accounted for parasitic protists, but were displaced by mixotrophic protists in March and April. Over time, Shannon diversity declined in all size fractions (Fig. 4b). Picoplankton and nanoplankton have significantly different Shannon diversity indices between the three monthly phases (with ANOVA, $F_{(2,12)} = 33.1$, $p < 0.05$ for picoplankton and $F_{(2,12)} = 16.6$, $p < 0.05$ for nanoplankton), with significantly lower Shannon diversity indices in April compared to February and March, but no difference between February and March (Tukey adjusted p-values < 0.05). In microplankton, the three monthly phases also differed significantly (ANOVA, $F_{(2.12)} = 16.4$, $p < 0.05$), with significantly lower Shannon diversity indices in April and March compared to February, but no difference between April and March (Tukey adjusted p-values < 0.05).

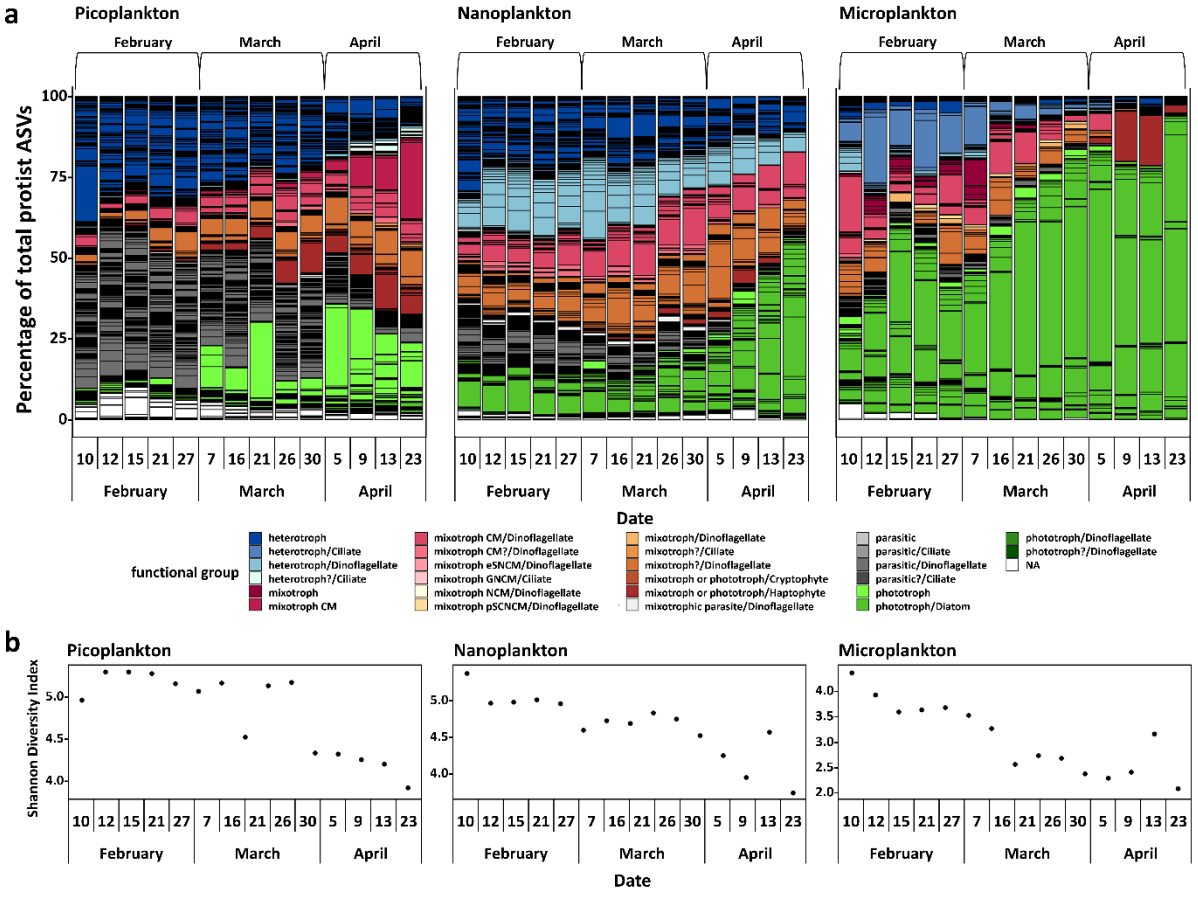


***Figure 4: Protist community analyses.*** *Normalized protist ASVs, divided by functional group and size fraction and additionally divided into three phases by calendar month (**a**). CM=constitutive mixotroph, eSNCM=endo-symbiotic specialist non-constitutive mixotrophs, GNCM=generalist non-constitutive mixotrophs, NCM=non-constitutive mixotroph, pSNCM=plastidic specialist non-constitutive mixotrophs. It was not possible to assign the definite trophic mode to each ASV, hence a putative trophic mode (indicated with a question mark or NA) is displayed. The Shannon Diversity Index based on taxonomic diversity (**b**) is also displayed.*

When evaluating the 50 most abundant ASVs of ciliates, cryptophytes, diatoms, dinoflagellates (excluding Syndiniales), and haptophytes individually, the successional patterns of some putative species stand out (Fig. 5). In the following, the putative species belonging to the ASVs will be called by the respective species name assigned after phylogenetic placement analyses and are meant as presumed species names. Ciliates were diverse and difficult to identify to species level. Most noteworthy, one ASV of an unidentified heterotrophic tintinnid declined in abundance in the microplankton size fraction, accounting for > 20 % of all microplankton reads on February 12 to < 2 % on April 23 (Fig. 5a). Cryptophytes, which are either mixotrophs or phototrophs, were mainly found in the picoplankton size fraction. Here, *Teleaulax gracilis*, *Falcomonas daucoides* and the *Plagioselmis* stage of *Teleaulax amphioxeia* all increased in abundance with time (Fig. 5b).

The most abundant diatom in the microplankton size fraction was *Porosira glacialis*, followed by *Thalassiosira antarctica* var. *borealis*. In nanoplankton, the most abundant diatoms were *Chaetoceros gelidus*, *Navicula flagillifera* and other *Navicula* species. *Chaetoceros gelidus* had the highest relative abundance in February and March, declining with time. On the other hand, *Navicula flagellifera* and other *Navicula* spp. were the most relatively abundant diatoms towards the bloom initiation in April. *Skeletonema* sp. was the most important diatom of the picoplankton size fraction, and it increased in relative abundance during bloom initiation in April (Fig. 5c).

Overall, dinoflagellates made up the most abundant group based on absolute sequence read numbers. However, species groups have different amounts of rRNA copies per cell in their genomes and dinoflagellates are known to have particular high amounts of copy numbers, making a direct comparison across groups challenging, but this is less impacted when comparing within a group. All of the 50 most abundant dinoflagellate taxa are most likely constitutive mixotrophs and heterotrophs. In the picoplankton size fraction *Gymnodinium* spp. and *Karenia* sp. increased in relative abundance over time, whereas *Karlodinium* sp. stayed more or less at the same level throughout the study period. In the nanoplankton, *Gymnodinium* spp. neither increased nor decreased, while *Tripos* sp. and *Prorocentrum* sp. increased in the spring period, whereas *Karenia* sp. and *Gyrodinium* sp. decreased. In the microplankton size fraction, *Torodinium robustum* and *Tripos* sp. decreased in relative abundance. *Alexandrium ostenfeldii* was also a fairly abundant species in the microplankton size fraction, and was present throughout the whole sampling period, but had a very low relative abundance from April 9 on (Fig. 5d).

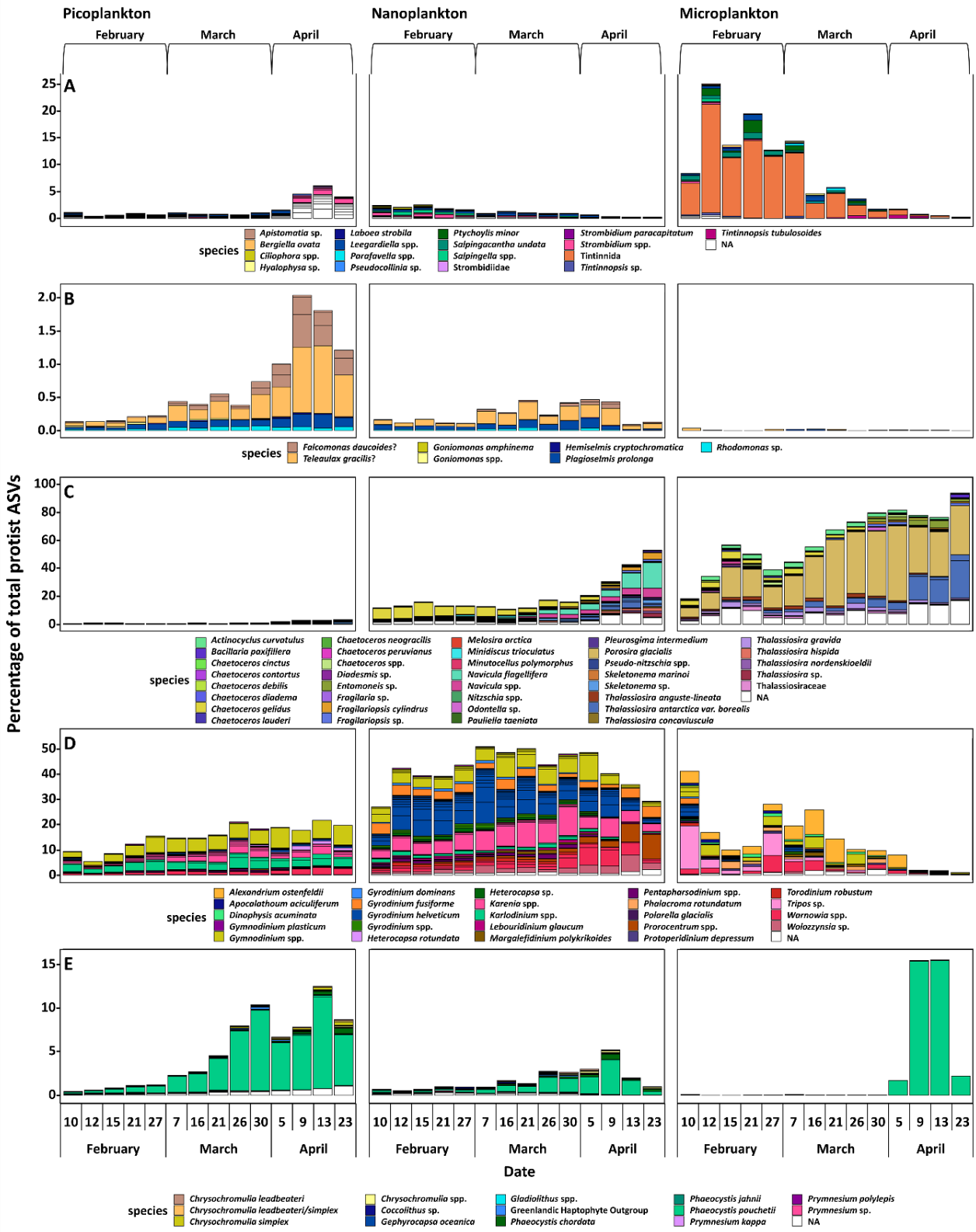


***Figure 5: most important ASVs of the taxonomic groups*** *of ciliates (a), cryptophytes (b), diatoms (c), dinoflagellates, excluding Syndiniales (d), and haptophytes (e). Displayed are a maximum of the 50 most abundant ASVs, if applicable. Each species name is to be understood as putative, as the species themselves were not confirmed via microscopic investigation but only through phylogenetic placement.*

When analyzing haptophytes, a clade of six unidentifiable ASVs was found, which were distantly related to *Chrysochromulina* spp. The mixotroph or phototroph *Phaeocystis pouchetii* was the most prominent haptophyte. It increased in relative abundance over time in all three size fractions (existing both as single cells and in large colonies). In microplankton, *P. pouchettii* was almost non-existent until April 9, whereas in the nanoplankton fraction, it gradually increased in abundance and peaked on April 9 (Fig. 5e).

**3. Discussion**

The winter communities were dominated by parasites, heterotrophs and mixotrophs during February (Fig. 4a). In more temperate coastal regions, where more light is available, small heterotrophic protists are also dominating the winter population [23], showing that this may be a general strategy for winter communities. However, especially the picoplankton and nanoplankton size fractions revealed a high relative abundance of parasitic organisms during winter, and not only general heterotrophs. At times, the picoplankton fraction consisted almost entirely of parasites and heterotrophs, which underlines the importance of these two trophic modes for the winter community. Most marine parasitic protists are relatively small and target considerably larger cells as host organisms [24, 25], indicating that most of the parasitic protists detected in the study were most likely in their free-living stage, showing up in the picoplankton fraction. Very few parasites were detected in the microplankton fraction, further supporting the conjecture that few of the parasites were inside microplankton host cells, unless these cells were broken up by the filtration process. In Antarctic waters, parasitic protists have been detected as being surprisingly prevalent in winter [26], probably associated with the sea ice lead, i.e. long openings in the sea ice cover [18]. Parasitic protists usually do not stay alive for prolonged periods of time without their host organisms and they complete their free-living stages within a few hours to days [24, 27, 28]. Most of the parasitic organisms were dinoflagellates, specifically Syndiniales. Resting spores as an overwintering strategy for parasites have not been described yet, although such a strategy is a possibility [29]. Syndiniales often infect ciliates, dinoflagellates, cercozoons and crabs [29], i.e. groups of mixotrophic and heterotrophic organisms, but apparently not or only rarely diatoms [30]. In Disko Bay, heterotrophic and especially mixotrophic dinoflagellates were detected in all size fractions. The overall biomass (assessed as POC) was, however, extremely low (Table 1). Little is known about the autecology of parasitic dinoflagellates in the ocean, in particular because of their difficult maintenance under laboratory conditions. The existing laboratory experiments suggest that they are not fit to live without their host organisms for an extended period of time [24, 28]. It is possible that the parasitic organisms observed were simply very successful in finding their host organisms and completing their life cycles with an output of many new individual cells (dinospores), but we cannot exclude alternative survival strategies. The presence of mixotrophic organisms, mainly constitutive

mixotrophs, may be related to them having had an advantage over organisms which are less flexible in their trophic mode, because they gain energy from both harvesting the little light available and additional food uptake.

Also later, during the early stages of the spring bloom, mixotrophs, especially dinoflagellates (CMs), contributed substantially to the total photosynthetic protist community in the pico- and nanoplankton size fractions (March, phase 2). This may have been a response to the slightly increased day length (Fig. 2b), although the light reaching into the water was still negligible (Fig. 1a). Similar observations in the community structure have recently been made in the Young Sound fjord in Northeast Greenland. Here, a bloom of mixotrophic haptophytes developed in ice covered surface waters during early spring [19]. The two locations differ considerably with regard to salinity and nutrient concentrations. Nevertheless, mixotrophs seemed to have had an advantage at both locations, because they compensate for low levels of photosynthesis with their ability to ingest other organisms. The mixotrophic ability seems to give them the flexibility to quickly adapt to increasing light availability, thereby giving them an advantage over pure photoautotrophs at this seasonal time point. It is even possible that mixotrophy dominates the pelagic food web during much of the year in the Arctic, due to this increased persistence [74].

April (phase 3) marked the initiation of the spring bloom. The spring bloom community was mainly characterized by photosynthetic diatoms, especially in the nanoplankton and microplankton size fractions. In the dark winter period in the Arctic, the primary source of energy for phototrophs is naturally lacking, while other nutrients are sufficient. One possible overwintering strategy for diatoms are resting spores, which can germinate when the conditions are more favorable [31-33]. Another strategy for fast adaptation to better conditions of phototrophs, mainly diatoms, is the quick photosynthetic reactivation of resting cells after a period of darkness, as resting cells only display a much-reduced metabolic rate [34]. The presence of diatoms throughout all phases, albeit in small proportions, also reflected by low Chl *a* measurements (Fig. 2a), suggests the utilization of the latter or both strategies. As stated before, diatoms are usually not the primary target of the parasitic Syndiniales. Thus, diatoms seem to combine the advantages of the ability to photosynthesize, being r-strategists, surviving as resting cells and with not being targeted by parasitic organisms, possibly giving them the critical advantage for overgrowing the other organisms both proportionally and in absolute abundance, leading to the spring bloom event.

Diatoms are typical spring bloom organisms and are often the dominant taxa in Arctic spring blooms [22, 35-37]. The genera, *Thalassiosira* spp. and *Navicula* spp. have previously been detected as important spring bloom species in the Baffin Bay area, not far from the sampled position, albeit much later in the year and two years prior in 2016 [36]. *Porosira*

*glacialis* is also a cold-water diatom, commonly found in the northern hemisphere [38, 39], and was also one of the dominating phototrophs in the microplankton size fraction (Fig. 5c).

*Phaeocystis* spp. are often abundant in Arctic surface waters during the early spring where the surface waters are still covered by sea ice [9, 40]. *Phaeocystis* spp. are often regarded as a climate altering species, because they are able to produce dimethylsulfide [41, 42]. They are considered a less desirable food source for zooplankton compared to other phytoplankton taxa [43, 44]. Interestingly, in our study, *P. pouchetii*, seemed to start as solitary cells in phase 1 and 2 (in the picoplankton fraction) making them potential prey for microplankton (Fig. 5e). Later in phase 3, towards the bloom, this species started to form larger colonies. The colony formation observed here may have been a defense mechanism against smaller copepod species [44]. However, larger copepods, such as *Calanus* spp., are typically occurring in larger quantities just around the spring bloom event [73], and can subsequently graze on these colonies. *Phaeocystis* spp. have an advantage over diatoms, because they are not dependent on silicate concentrations, which diminish quickly during the spring bloom [37]. Compared to some other Arctic phytoplankton species, *Phaeocystis* spp. have a wider tolerance towards temperature, as they are also commonly found in the Atlantic [45]. This increased fitness makes them a possible candidate for gaining importance in the spring bloom event in the future. We can confirm presence of *P. pouchetii* in the Arctic winter community, as also shown close to Svalbard [46], underlining a considerable resilience in harsh conditions.

The diversity analyses showed that the community in winter was generally more diverse than towards and during the spring bloom event (Fig. 4b). Interestingly, the smaller the organisms, the more similar the phases were in terms of presence or absence of ASVs (Fig. 3). The largest differences were thus seen in the microplankton size fraction, in which only 21.8 % of ASVs were shared among all size fractions. These findings are similar to a comparative study of ASVs from Iceland and Greenland [8], in which the microplankton size fraction was most dissimilar compared to smaller size fractions. Locally adapted populations of larger celled species are shown to have lower flexibility and to be more plastic than smaller cells, which might differentiate more rapidly into distinct ecotpyes, giving them some adaptational flexibility [8, 75]. Therefore, these cells may be viewed as more specialized in the different phases, resulting in a more drastic community shift. In a global context, it has been shown that the highest phytoplankton diversity often is detected at intermediate biomasses, while especially high and low biomass correlate with lower diversity [47]. In our case, we found that the low biomass winter community was surprisingly diverse (Fig. 4b) and that the diversity, by means of ASVs and Shannon diversity index, decreased with the onset of the spring bloom. This suggests a highly diverse winter community followed by a spring bloom, in which only few diatom ASVs started to dominate the community in both relative and absolute abundance, as the conditions

became favorable for them. Additionally, the overall less diverse microplankton size fraction reacted quicker by means of community shifts to a changing environment than the smaller size fractions, again supporting the hypothesis that larger celled species react quicker to environmental changes due to higher niche specificity.

Studies in the Arctic have been investigating the phytoplankton spring bloom both in areas with sea ice [17, 48] and without sea ice [10]. The ice cover has often been discussed as a factor involved in the initiation of the spring bloom because snow and ice cover will lower the penetration of light into the water column, depriving phototrophs of their energy source [48, 20]. However, the transition from a sea ice covered surface water environment to surface waters without sea ice cover has rarely been studied. Here, we present data on the bloom dynamics starting in the dark winter period to the breakage of the sea ice and formation of a spring bloom. The slow increase in Chl *a* unmistakably shows the initiation of the spring bloom event at a time when the sea ice was still largely covering the Bay (Fig. 2a). Biomass is, at this time, not yet strongly increasing, but when taking POC into consideration, the amount of phototrophs (measured as Chl *a*) is increasing in relation to the total amount of biomass, showing the imminence of the spring bloom (Fig. 2a, Table 1).

A number of publications have shown that phytoplankton growth is possible under very low light conditions, as often observed in surface waters under the sea ice [15-17]. It has also been shown that once the light penetrates the ice, photosynthetic capabilities are quickly reactivated, usually within a few hours to a day [34]. In the present study, the light penetrating the ice was extremely limited at the time of increasing photosynthetic activity (Fig. 1a, c), while the spectral light quality and the average insolation per day above water changed considerably (Fig. 2b). It is well known that the wavelength is also influenced by possible and variable cloud cover [49], but the overall tendency of the wavelength shifts were clearly seen in the daily averages of the light intensity in the present study (Fig. 2b). Shortwave radiation that penetrates water deeper than longwave radiation, increased more strongly during this period. This suggests that light quality and average light irradiation per day in combination may be more important for bloom initiation than the light intensity itself. Low light intensity can possibly be compensated for by longer light duration and different wavelength composition. Still, it is standing out that the fluorescence measurement shows that the bloom started at a depth of approximately 55 m, which coincided with the approximate halocline at that time (Fig. 1b, c). The early start of ice algal blooms initiating directly under the sea ice has been discussed previously [20], but our study suggests that the pelagic spring bloom was not seeded from the sea ice or from the bottom of the sea ice as pennate diatoms typically dominate sea ice communities. Instead, we observed typical centric pelagic bloom species, similar to the findings of Arrigo *et al.* [50, 51]. In combination with the depth of the developing bloom, this does not

suggest a seeding of the bloom by sea ice algae. Apart from that, it is possible that the breakage of the sea ice could have led to increased turbulences in the upper ocean layers. This could help non-motile cells such as diatoms to stay in the illuminated layers of the ocean, increasing the amount of possibly absorbed photons due to residence in lighter areas of the ocean, eventually enabling their growth. During the initiation of the spring bloom, the local area was still completely covered with sea ice. However, open patches further away from the sampling area may have been suficient to increase the mixing in the suggested way and to lead to advective effects.

**Conclusion**

During winter, the protistan community mostly consisted of parasites, heterotrophs, and mixotrophs, which is probably a natural adaptation to a life at low light availability [18, 19]. The transitional period was characterized by a high relative abundance of mixotrophs, which most likely have a trophic advantage due to their flexibility. The community shift towards a spring bloom community already started before the sea ice retreated. Past studies have forecasted and shown an increase in primary productivity when the sea ice retreats, based on satellite data [51, 52]. However, *in situ* studies, such as ours, confirm that blooms of microbial plankton not only occur [15, 16, 17, 19, 40], but also start growing while ice is still covering the surface waters. We also show that the period prior to the phytoplankton spring bloom is most likely not a period of dormancy, but only a period of low biomass, because changes in the community are still occurring. This suggests that sea ice retreat is not the major factor of initiating the phytoplankton spring bloom in the Arctic. Rather, an interplay of the factors of light intensity, spectral composition and day-length, as well as oceanographic factors such as nutrient availability and mixed layer depth are involved, making the spring bloom initiation and the shift from the winter community a multifactorial event.

## 4. Materials and Methods

### 4.1 Study site description and sampling procedure

Sampling was performed off the southern coast of Disko Island, West Greenland, close to the Arctic Station in Qeqertarsuaq. The area is characterized by coastal proximity, annual seasonal sea ice, and influence of the calving glacier Jakobshavn Isbræ. Samples were taken between February 10 and April 23, 2018 around noon. The sampling started at 69°12.95’ N, 53°31.25’ W, which had a water depth of approx. 140 m. As this location became inaccessible due to sea ice formation and growth, the sampling station was moved to 69°14.2’ N, 53°29.9’ W, depth: ca. 140 m, from March 16, 2018, approximately 2.5 km away from the first position. The alternative position was chosen as the best compromise between comparability to the first location and probable accessibility throughout the sampling period. The samples were taken approximately

every four days with a 25 L Niskin water sampler (KC Denmark, Denmark) either from the water surface or through a manually drilled hole in the ice. The samples, taken at the depths 5 m, 10 m, 20 m, 30 m, and 40 m were transferred to polyethylene containers (pre-treated with 3 % hydrochloric acid and flushed twice with the respective sample), stored cold and dark, and processed on the same day.

### 4.2 Sea ice and contextual data

The water sampling was accompanied by an SBE 911plus CTD (Sea-Bird Scientific, Washington, USA) to collect temperature, photosynthetic active radiation (PAR), fluorescence and salinity data. For continuous environmental data above sea level, light from a station located at 69°15'12.558'' N, 53°30'50.863'' W, 25 m above sea level was provided by Greenland Environmental Monitoring (GEM) program, subprogram "GeoBasisDisko". Sea ice was observed both locally at the sampling location on the sampling day, and daily of the whole bay area by visual sea ice monitoring of the Arctic Station provided by the University of Copenhagen, Denmark.

### 4.3 Sample preparation and analysis

As biomass during the Arctic winter is rather low and sampling of larger volumes of water are logistically limited, we applied a pooling approach of the upper 40 m of the water column. Equal volumes (10 L) of water from five depths (5, 10, 20, 30 and 40 m) were pooled in order to obtain these depth-integrated samples. Data for chlorophyll *a* (Chl *a*), and particulate organic carbon and nitrogen (POC and PON) as biomass and nutrition status proxies were retrieved from supplementary material of Bruhn *et al.* [37]. The following method of size fractionation might have impacted the integrity of more fragile cells, which could have fragmentized under the pressure of the vacuum filtration. The reads of a few larger taxa such as *Strombidium* spp. (Fig. 5a) in the picoplankton size fraction may have been the result of this method. On the other hand, these findings could also hint at the presence of considerably smaller gametes. Overall, this method holds more scientific value than it has drawbacks, allowing e.g. insights in seasonal colony formation of the haptophyte *Phaeocystis pouchetii*, and was successfully applied in other field studies several times [53, 8, 37]. Therefore, the remaining 47.5 L pooled sample was size fractionated through a series of filters. Prefiltering through a 200 µm nylon mesh removed most multicellular zooplankton, also resulting in a loss of some larger protist species and colonies. Afterwards, the complete sample was filtered through a 20 µm nylon mesh to obtain the microplankton size fraction. Further filtration steps were carried out with polycarbonate filters and a vacuum pump at minimum -500 mbar, resulting in the filtration of 3 L through a 3 µm pore size (for obtaining the nanoplankton size fraction) and 1 L through a 0.2 µm pore size (for obtaining the picoplankton size fraction). The cells were carefully flushed off the surface of the

filters. Afterwards, they were frozen in extraction buffer and transported for extraction in the home institution. The DNA from these three size fractions (0.2 – 3 µm or picoplankton, 3 – 20 µm or nanoplankton, 20 – 200 µm or microplankton) was extracted using a NucleoSpin Soil kit (Macherey-Nagel, Germany). The 16S rRNA Metagenomic Sequencing Library Preparation protocol (Illumina, California, USA) was used. However, the protocol was adapted with primers targeting the eukaryotic V4-region [54] modified to include haptophytes, which are otherwise mostly underrepresented when using the original primers [55]. Nevertheless, this method still tends to overestimate the abundance of dinoflagellates, because their genome usually displays a high copy number of ribosomal operons [56]. After sequencing 300 bp paired-end with a MiSeq System (Illumina, California, USA), amplicon sequence variants (ASVs) were generated with the R-packages DADA2 [57], ShortRead [76], Biostrings [77] and stringr [78], and annotated with the PR$^2$-database; version 4.11.1; [58]. The species were marked with their respective trophic mode, if known, by manual curation (see table in supplementary data for applied criteria). Afterwards, the 50 most abundant ASVs from the taxonomic groups of dinoflagellates, haptophytes, cryptophytes, diatoms and ciliates were determined after excluding low abundance ASVs and non-protist ASVs. These ASVs were analyzed and their identity confirmed through phylogenetic placement.

For this, alignments with longer reference sequences of the different target groups (dinoflagellates, haptophytes, cryptophytes, diatoms, or ciliates) have been generated with MAFFT, using the L-INSI settings and the "—add fragments --reorder" option. Afterwards, a phylogenetic tree was calculated with RAxML for 1000 bootstrap analyses, separately for dinoflagellates, haptophytes, cryptophytes, diatoms, and ciliates, respectively resulting in one maximum likelihood tree per taxonomic group. These trees served as a reference for the phylogenetic assignment or confirmation of the 50 most abundant ASV sequences of the aforementioned taxonomic groups. Alignments and resulting trees have been manual curated and analyzed.

Further analyses were performed with R, version 4.0.3 [59], with RStudio version 1.3.1093 [60], and the packages effects [61], eulerr [62], ggplot2 [63], lubridate [64], MBA [65], mgcv [66], phyloseq [67], plyr [68], RColorBrewer [69], reshape2 [70], tidyverse [71], and vegan [72]. Low abundance ASVs and non-protist ASVs were excluded. Read numbers were then normalized to average sequencing depth and afterwards set to 100 % reads, to be able to assess the relative abundance in context with biomass. To facilitate some analyses, the samplings were summarized into three phases divided by the calendar month they were taken in. This resulted in phase 1 from February 10 to 27 (containing five samplings), phase 2 from March 7 to 30 (containing five samplings), and phase 3 from April 5 to 23 (containing four samplings).

**References**


1. Overpeck, J. *et al.* Arctic Environmental Change of the Last Four Centuries. *Science.* **278**, 1251–1257 (1997).
2. McBean, G. *et al.* Arctic Climate: Past and Present. *Arct. Clim. Impact Assess.* 21–60 (2005).
3. Pachauri, R. K., Reisinger A. (Eds., Core Writing Team). IPCC: Climate Change 2007: Synthesis Report. Contribution of Working Groups I, II and III to the Fourth Assessment Report of the Intergovernmental Panel on Climate Change. IPCC, Geneva, Switzerland, 104 pp. (2007).
4. Hoegh-Guldberg, O. & Bruno, J. F. The Impact of Climate Change on the World's Marine Ecosystems. *Science.* **328**, 1523–1529 (2010).
5. Baggesen, C. *et al.* Molecular phylogeny and toxin profiles of *Alexandrium tamarense* (Lebour) Balech (Dinophyceae) from the west coast of Greenland. *Harmful Algae* **19**, 108–116 (2012).
6. Tillmann, U., Kremp, A., Tahvanainen, P. & Krock, B. Characterization of spirolide producing *Alexandrium ostenfeldii* (Dinophyceae) from the western Arctic. *Harmful Algae* **39**, 259–270 (2014).
7. Elferink, S. *et al.* Molecular diversity patterns among various phytoplankton size-fractions in West Greenland in late summer. *Deep. Res. Part I* **121**, 54–69 (2017).
8. Elferink, S. *et al.* Comparative Metabarcoding and Metatranscriptomic Analysis of Microeukaryotes Within Coastal Surface Waters of West Greenland and Northwest Iceland. *Front. Mar. Sci.* **7**, 1–20 (2020).
9. Marquardt, M., Vader, A., Stübner, E. I., Reigstad, M. & Gabrielsen, T. M. Strong Seasonality of Marine Microbial Eukaryotes in a High-Arctic Fjord (Isfjorden, in West Spitsbergen, Norway). *Appl. Environ. Microbiol.* **82**, 1868–1880 (2016).
10. Kubiszyn, A. M. *et al.* The annual planktonic protist community structure in an ice-free high Arctic fjord (Adventfjorden, West Spitsbergen). *J. Mar. Syst.* **169**, 61–72 (2017).
11. Zhang, Q., Gradinger, R. & Spindler, M. Dark Survival of Marine Microalgae in the High Arctic (Greenland Sea). *Polarforschung* **65**, 111–116 (1998).
12. Hegseth, E. N. & Tverberg, V. Effect of Atlantic water in flow on timing of the phytoplankton spring bloom in a high Arctic fjord (Kongsfjorden, Svalbard). *J. Mar. Syst.* **113–114**, 94–105 (2013).
13. Alexander, V. & Niebauer, H. J. Oceanography of the eastern Bering Sea ice-edge zone in spring. *Limnol. Oceanogr.* **26**, 1111–1125 (1981).
14. Hunt Jr., G. L. *et al.* Climate change and control of the southeastern Bering Sea pelagic ecosystem. *Deep. Res. Part II* **49**, 5821–5853 (2002).
15. Arrigo, K. R. *et al.* Under Arctic Sea Ice. *Science.* **336**, 1408 (2012).

16. Spall, M. A. *et al.* Deep-Sea Research II Role of shelfbreak upwelling in the formation of a massive under-ice bloom in the Chukchi Sea. *Deep. Res. Part II* **105**, 17–29 (2014).
17. Massicotte, P. *et al.* Green Edge ice camp campaigns: understanding the processes controlling the under-ice Arctic phytoplankton spring bloom. *Earth Sysem Sci. Data* **12**, 151–176 (2020).
18. Clarke, L. J., Bestley, S., Bissett, A. & Deagle, B. E. A globally distributed Syndiniales parasite dominates the Southern Ocean micro-eukaryote community near the sea-ice edge. *ISME J.* **13**, 734–737 (2019).
19. Søgaard, D. H. *et al.* An under - ice bloom of mixotrophic haptophytes in low nutrient and freshwater - influenced Arctic waters. *Sci. Rep.* **11**, 1–9 (2021).
20. Leu, E. *et al.* Arctic spring awakening – Steering principles behind the phenology of vernal ice algal blooms. *Prog. Oceanogr.* **139**, 151–170 (2015).
21. Olsen, L. M. *et al.* The seeding of ice algal blooms in Arctic pack ice: The multiyear ice seed repository hypothesis. *J. Geophys. Res. Biosci.* **122**, 1529–1548 (2017).
22. Tammilehto, A., Watts, P. C. & Lundholm, N. Isolation by Time During an Arctic Phytoplankton Spring Bloom. *Eukaryot. Microbiol.* **64**, 248–256 (2017).
23. Morán, X. A. G., Calvo-díaz, A., Arandia-Gorostidi, N. & Huete-Stauffer, T. M. Temperature sensitivities of microbial plankton net growth rates are seasonally coherent and linked to nutrient availability. *Environ. Microbiol.* **20**, 3798–3810 (2018).
24. Alacid, E., Reñé, A. & Garcés, E. New Insights into the Parasitoid *Parvilucifera sinerae* Life Cycle: The Development and Kinetics of Infection of a Bloom-forming Dinoflagellate Host. *Protist* **166**, 677–699 (2015).
25. Gómez, F., Moreira, D. & López-García, P. Life cycle and molecular phylogeny of the dinoflagellates *Chytriodinium* and *Dissodinium*, ectoparasites of copepod eggs. *Eur. J. Protistol.* **45**, 260–270 (2009).
26. Cleary, A. C. & Durbin, E. G. Unexpected prevalence of parasite 18S rDNA sequences in winter among Antarctic marine protists. **38**, 401–417 (2016).
27. Reñé, A., Alacid, E., Figueroa, R. I., Rodríguez, F. & Garcés, E. Life-cycle, ultrastructure, and phylogeny of *Parvilucifera corolla* sp. nov. (Alveolata, Perkinsozoa), a parasitoid of dinoflagellates. *Eur. J. Protistol.* **58**, 9–25 (2017).
28. John, U. *et al.* An aerobic eukaryotic parasite with functional mitochondria that likely lacks a mitochondrial genome. *Sci. Adv.* **5**, 1–11 (2019).
29. Guillou, L. *et al.* Widespread occurrence and genetic diversity of marine parasitoids belonging to Syndiniales (Alveolata). *Environ. Microbiol.* **10**, 3349–3365 (2008).
30. Tillmann, U., Hesse, K.-J. & Tillmann, A. Large-scale parasitic infection of diatoms in the Northfrisian Wadden Sea. *J. Sea Res.* **42**, 255–261 (1999).

31. McQuoid, M. R. & Hobson, L. A. Importance of resting stages in diatom seasonal succession. **50**, 44–50 (1995).
32. Tsukazaki, C., Ishii, K., Matsuno, K., Yamaguchi, A. & Imai, I. Distribution of viable resting stage cells of diatoms in sediments and water columns of the Chukchi Sea, Arctic Ocean. *Phycologia* **57**, 440–452 (2019).
33. Luostarinen, T. *et al.* An annual cycle of diatom succession in two contrasting Greenlandic fjords: from simple sea-ice indicators to varied seasonal strategists. *Mar. Micropaleontol.* **158**, 1–15 (2020).
34. Kvernvik, A. C. *et al.* Fast Reactivation of Photosynthesis in Arctic Phytoplankton during the Polar Night. *Phycol. Soc. Am.* **54**, 461–470 (2018).
35. Krause, J. W. *et al.* Biogenic silica production and diatom dynamics in the Svalbard region during spring. *Biogeosciences* **15**, 6503–6517 (2018).
36. Lafond, A. *et al.* Late spring bloom development of pelagic diatoms in Baffin Bay. *Elem. Sci. Anthr.* **7**, 1–24 (2019).
37. Bruhn, C. S., Wohlrab, S., Krock, B., Lundholm, N. & John, U. Seasonal plankton succession is in accordance with phycotoxin occurrence in Disko Bay, West Greenland. *Harmful Algae* **103**, 101978 (2021).
38. McMinn, A., Pankowski, A. & Delfatti, T. Effect of Hyperoxia on the Growth and Photosynthesis of Polar Sea Ice Microalgae. *J. Phycol.* **41**, 732–741 (2005).
39. Svenning, J. B., Dalheim, L., Eilertsen, H. C. & Vasskog, T. Temperature dependent growth rate, lipid content and fatty acid composition of the marine cold-water diatom *Porosira glacialis*. *Algal Res.* **37**, 11–16 (2019).
40. Pavlov, A. K. *et al.* Altered inherent optical properties and estimates of the underwater light field during an Arctic under-ice bloom of *Phaeocystis pouchetii*. *J. Geophys. Res. Ocean.* **122**, 4939–4961 (2017).
41. Stefels, J. & van Boeckel, W. H. M. Production of DMS from dissolved DMSP axenic cultures of the marine phytoplankton species *Phaeocystis* sp. *Mar. Ecol. Prog. Ser.* **97**, 11–18 (1993).
42. Verity, P. G. *et al.* Current understanding of *Phaeocystis* ecology and biogeochemistry, and perspectives for future research. *Biogeochemistry* **83**, 311–330 (2007).
43. Weisse, T., Tande, K., Verity, P., Hansen, F. & Gieskes, W. The trophic significance of *Phaeocystis* blooms. *J. Mar. Syst.* **5**, 67–79 (1994).
44. Nejstgaard, J. C. *et al.* Zooplankton grazing on *Phaeocystis*: a quantitative review and future challenges. *Biogeochemistry* **83**, 147–172 (2007).
45. Hoppe, C. J. M., Wolf, K. K. E., Schuback, N., Tortell, P. D. & Rost, B. Compensation of ocean acidification effects in Arctic phytoplankton assemblages. *Nat. Clim. Chang.* **8**, 529–533 (2018).

46. Vader, A., Marquardt, M., Meshram, A. R. & Gabrielsen, T. M. Key Arctic phototrophs are widespread in the polar night. *Polar Biol.* **38**, 13–21 (2015).
47. Irigoien, X., Huisman, J. & Harris, R. P. Global biodiversity patterns of marine phytoplankton and zooplankton. *Lett. to Nat.* **429**, 863–867 (2004).
48. Terrado, R., Lovejoy, C., Massana, R. & Vincent, W. F. Microbial food web responses to light and nutrients beneath the coastal Arctic Ocean sea ice during the winter – spring transition. *J. Mar. Syst.* **74**, 964–977 (2008).
49. Kapsch, M.-L., Graversen, R. G., Tjernström, M. & Bintanja, R. The Effect of Downwelling Longwave and Shortwave Radiation on Arctic. *Am. Meteorol. Soc.* 1143–1159 (2016). doi:10.1175/JCLI-D-15-0238.1
50. Arrigo, K. R. *et al.* Journal of Geophysical Research : Oceans. *J. Geophys. Res. Ocean.* **122**, 9350–9369 (2017).
51. Arrigo, K. R., van Dijken, G. & Pabi, S. Impact of a shrinking Arctic ice cover on marine primary production. *Geophys. Res. Lett.* **35**, 1–6 (2008).
52. Renaut, S., Devred, E. & Babin, M. Northward Expansion and Intensification of Phytoplankton Growth During the Early Ice-Free Season in Arctic. *Geophys. Res. Lett.* **45**, 10,590-10,598 (2018).
53. Krock, B., Tillmann, U., John, U. & Cembella, A. D. Characterization of azaspiracids in plankton size-fractions and isolation of an azaspiracid-producing dinoflagellate from the North Sea. *Harmful Algae* **8**, 254–263 (2009).
54. Stoeck, T., Bass, D., Nebel, M., Christen, R. & Meredith, D. Multiple marker parallel tag environmental DNA sequencing reveals a highly complex eukaryotic community in marine anoxic water. *Mol. Ecol.* **19**, 21–31 (2010).
55. Piredda, R. *et al.* Diversity and temporal patterns of planktonic protist assemblages at a Mediterranean LTER site. *FEMS Microbiol. Ecol.* **93**, 1–14 (2017).
56. Guo, L., Sui, Z. & Liu, Y. Quantitative analysis of dinoflagellates and diatoms community via Miseq sequencing of actin gene and v9 region of 18S rDNA. *Sci. Rep.* 1–9 (2016). doi:10.1038/srep34709
57. Callahan, B. J. *et al.* DADA2: High-resolutiuon sample inference from Illumina amplicon data. *Nat. Methods* **13**, 581–583 (2016).
58. Guillou, L. *et al.* The Protist Ribosomal Reference database ($PR^2$): a catalog of unicellular eukaryote Small Sub-Unit rRNA sequences with curated taxonomy. *Nucleic Acids Res.* **41**, 597–604 (2012).
59. R Core Team. R: A language and environment for statistical computing. *Stat. Comput. Vienna, Austria* (2020).
60. R Team. RStudio: Integrated Development Environment for R. *PBC, Boston, MA*

61. Fox, J. & Weisberg, S. An R Companion to Applied Regression, 3rd Edition. *Thousand Oaks, CA* (2019).
62. Larsson, J. eulerr: Area-proportional Euler and Venn Diagrams with Ellipses. R package version 6.1.0.
63. Wickham, H. ggplot2: Elegant Graphics for Data Analysis. *Springer-Verlag, NY* (2016).
64. Grolemund, G. & Wickham, H. Dates and Times Made Easy with lubridate. *J. Stat. Softw.* **40**, 1–25 (2011).
65. Finley, A., Banerjee, S. & Hjelle, Ø. MBA: Multilevel B-Spline Approximation. R package version 0.0-9. (2017).
66. Wood, S. N., Pya, N. & Saefken, B. Smoothing parameter and model selection for general smooth models (with discussion). *J. Am. Stat. Assoc.* **111**, 1548–1575 (2016).
67. McMurdie, P. J. & Holmes, S. phyloseq: An R package for reproducible interactive analysis and graphics of microbiome census data. *PLoS One* **8**, e61217 (2013).
68. Wickham, H. The Split-Apply-Combine Strategy for Data Analysis. *J. Stat. Softw.* **40**, 1–29 (2011).
69. Neuwirth, E. RColorBrewer: ColorBrewer Palettes. R package version 1.1-2. (2014).
70. Wickham, H. Reshaping Data with the reshape Package. *J. Stat. Softw.* **21**, 1–20 (2007).
71. Wickham, H. Welcome to the tidyverse. *J. Open Source Softw.* **4**, 1686 (2019).
72. Oksanen, J. *et al.* vegan: Community Ecology Package. R package version 2.5-6. (2019).
73. Møller, E. F. & Nielsen, T. G. Borealization of Arctic zooplankton — smaller and less fat zooplankton species in Disko Bay, Western Greenland. 1175–1188 (2020).
74. Stoecker, D. K. & Lavrentyev, P. J. Mixotrophic Plankton in the Polar Seas: A Pan-Arctic Review. *Front. Mar. Sci.* **5**, 1–12 (2018).
75. Wohlrab, S. *et al.* Metatranscriptome Profiling Indicates Size-Dependent Differentiation in Plastic and Conserved Community Traits and Functional Diversification in Dinoflagellate Communities. *Front. Mar. Sci.* **5**, 1–13 (2018).
76. Morgan, M. *et al.* ShortRead: a Bioconductor package for input, quality assessment and exploration of high-throughput sequence data. *Bioinformatics*, **25**, 2607–2608 (2009).
77. Paès, H., Aboyoun, P., Gentleman, R. & DebRoy, S. Biostrings: Efficient manipulation of biological strings. R package version 2.62.0 (2021).
78. Wickham, H. stringr: Simple, Consistent Wrappers for Common String Operations. R package version 1.4.0. (2019)

**Acknowledgements**

Our thanks go to Nancy Kühne for providing technical assistance in the laboratory. We also thank Regin Rønn, Kjeld Akaraaq Mølgaard, Abel Brandt, and Johannes Mølgaard for their help on location during the field campaign in Greenland. The expedition was conducted within the

framework of the Disko Marine Basis Program. The POC and PON analyses were done with Florian Koch, who we thank for his support. Claudia Sabine Bruhn and Uwe John were financially and logistically supported through the PACES II research program of the Alfred Wegener Institute, Helmholtz Centre for Polar and Marine Research. The Ministry for Science and Culture of Lower Saxony and the Volkswagen Foundation through the "Niedersächsisches Vorab" grant program (grant number ZN3285) provided funding for Sylke Wohlrab. The Danish Research Council for Nature and Universe (9040-00248B) provided funding to Nina Lundholm. The Danish Ministry of the Environment provided funding for Per Juel Hansen and Nina Lundholm through the Marine Basis Disko Program as part of the Greenland Environmental Monitoring Program (GEM).

**Competing Interests**

No competing interests have been declared by the authors.

# Chapter 1

**Supplementary**

**Material**

**Supplementary Table 1:** Criteria for assigned trophic mode of organisms.

| *Assigned trophic mode* | *Assigned to* |
|---|---|
| *heterotroph* | Anything not within the other heterotroph groups that lacks photosynthetic plastids |
| *heterotroph/Ciliate* | A phagotrophic (heterotrophic) ciliate, that does not follow a parasitic lifestyle |
| *heterotroph/Dinoflagellate* | A heterotrophic dinoflagellate – a phagotrophic dinoflagellate without chloroplasts that does not display a parasitic lifestyle |
| *heterotroph?/Ciliate* | A ciliate that is suspected to be a phagotrophic heterotroph, and does not display a parasitic lifestyle |
| *mixotroph* | Mixoplankton – a planktonic protist that combine *phototrophy* and *phagotrophy* |
| *mixotroph CM* | A constitutive mixoplankonic protist that has an innate, constitutive, ability to conduct photosynthesis and that is also able to phagocytise. (Cf. *NCM*.) |
| *mixotroph CM/Dinoflagellate* | A dinoflagellate with its own chloroplast(s) that combines phototrophy and phagotrophy |
| *mixotroph CM?/Dinoflagellate* | A dinoflagellate that is suspected being a constitutive mixotroph |
| *mixotroph eSNCM/Dinoflagellate* | A specialist non-constitutive mixoplanktonic dinoflagellate that harbours endo/ecto symbionts |
| *mixotroph GNCM/Ciliate* | A generalist non-constitutive mixoplanktonic ciliate that lacks an innate, constitutive, ability to perform photosynthesis and acquires its phototrophic potential from various other organisms. (Cf. CM, GNCM, SNCM.) |
| *mixotroph NCM/Dinoflagellate* | A non-constitutive mixoplanktonic dinoflagellate that lacks an innate, constitutive, ability to conduct photosynthesis and thus acquires its phototrophic potential from (an)other organism(s). (Cf. CM, GNCM, SNCM.) |
| *mixotroph pSNCM/Dinoflagellate* | A plastidic specialist non-constitutive mixoplankton; these acquire and exploit only the plastids originating from another organism. (Cf. CM, GNCM, SNCM.) |
| *mixotroph/Dinoflagellate* | Mixoplanktonic dinoflagellate |
| *mixotroph?/Ciliate* | A ciliate suspected of a mixotrophic lifestyle |
| *mixotroph?/Dinoflagellate* | A dinoflagellate suspected of a mixotrophic lifestyle |
| *mixotroph or* | A photosynthetic cryptophyte in which it is unknown to |

| | |
|---|---|
| *phototroph/Cryptophyte* | which extent is capable of phagotropy |
| *mixotroph or phototroph/Haptophyte* | A photosynthetic haptophyte in which it is unknown to which extent is capable of phagotropy |
| *mixotrophic parasite/Dinoflagellate* | A parasitic dinoflagellate which has its own chloroplasts |
| *parasitic* | The organisms are classified as parasitic, but do not fit into the other categories |
| *parasitic/Ciliate* | A parasitic ciliate |
| *parasitic/Dinoflagellate* | A parasitic dinoflagellate, in essence belonging to Syndiniales |
| *parasitic?/Ciliate* | A ciliate that is suspected of being a parasite |
| *phototroph* | A photosynthetic organism |
| *phototroph/Diatom* | Diatoms are exclusively phototrophic – they do not have the ability of phagocytosis; therefore all diatoms were summarized in this category |
| *phototroph/Dinoflagellate* | A phototrophic dinoflagellate |
| *phototroph?/Dinoflagellate* | A dinoflagellate that is suspected of being a phototroph |
| *NA* | It was not possible to assign a trophic mode, either due to poor identification or to lack of information on the assigned taxon |

## Ciliates: Phylogenetic Placement

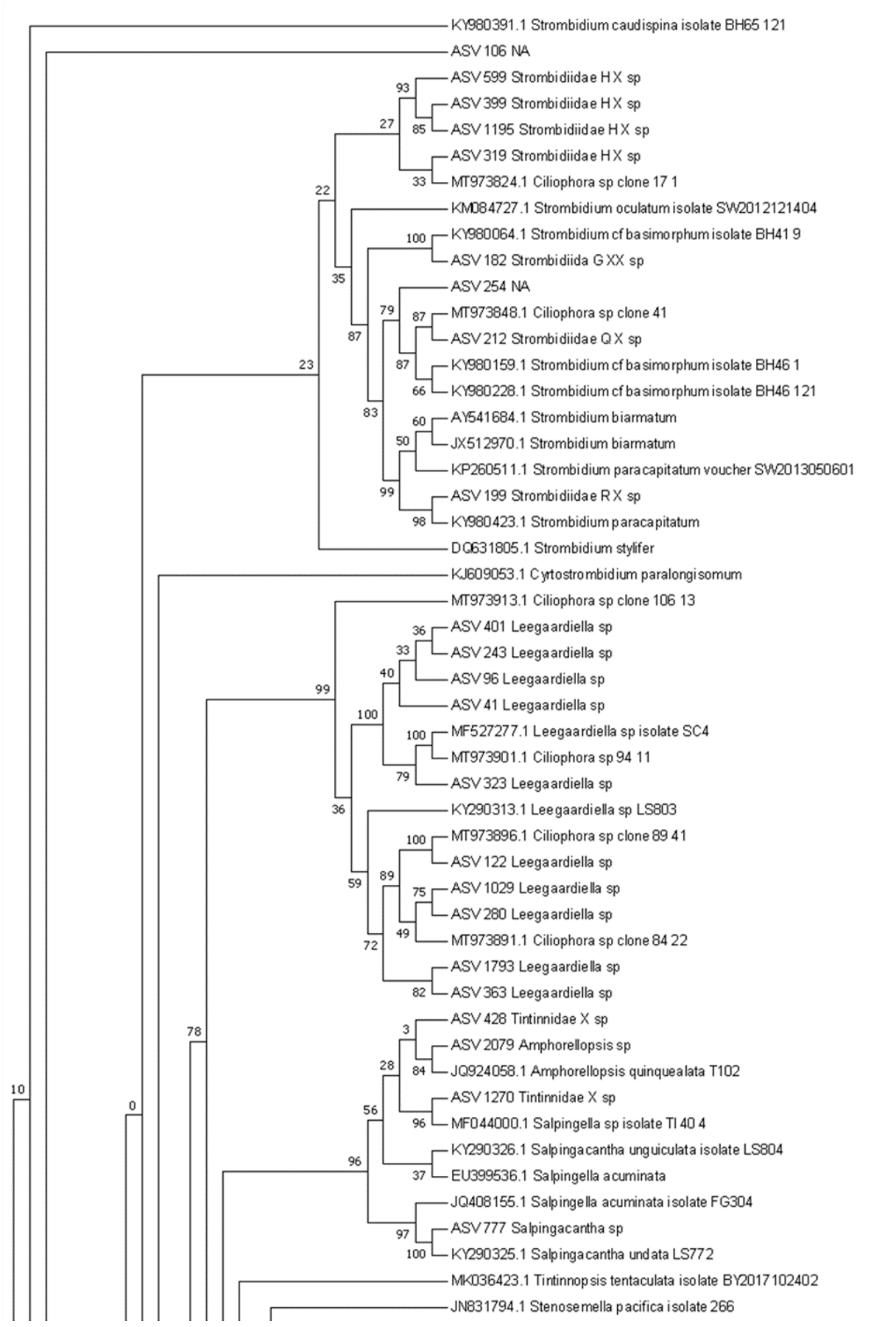

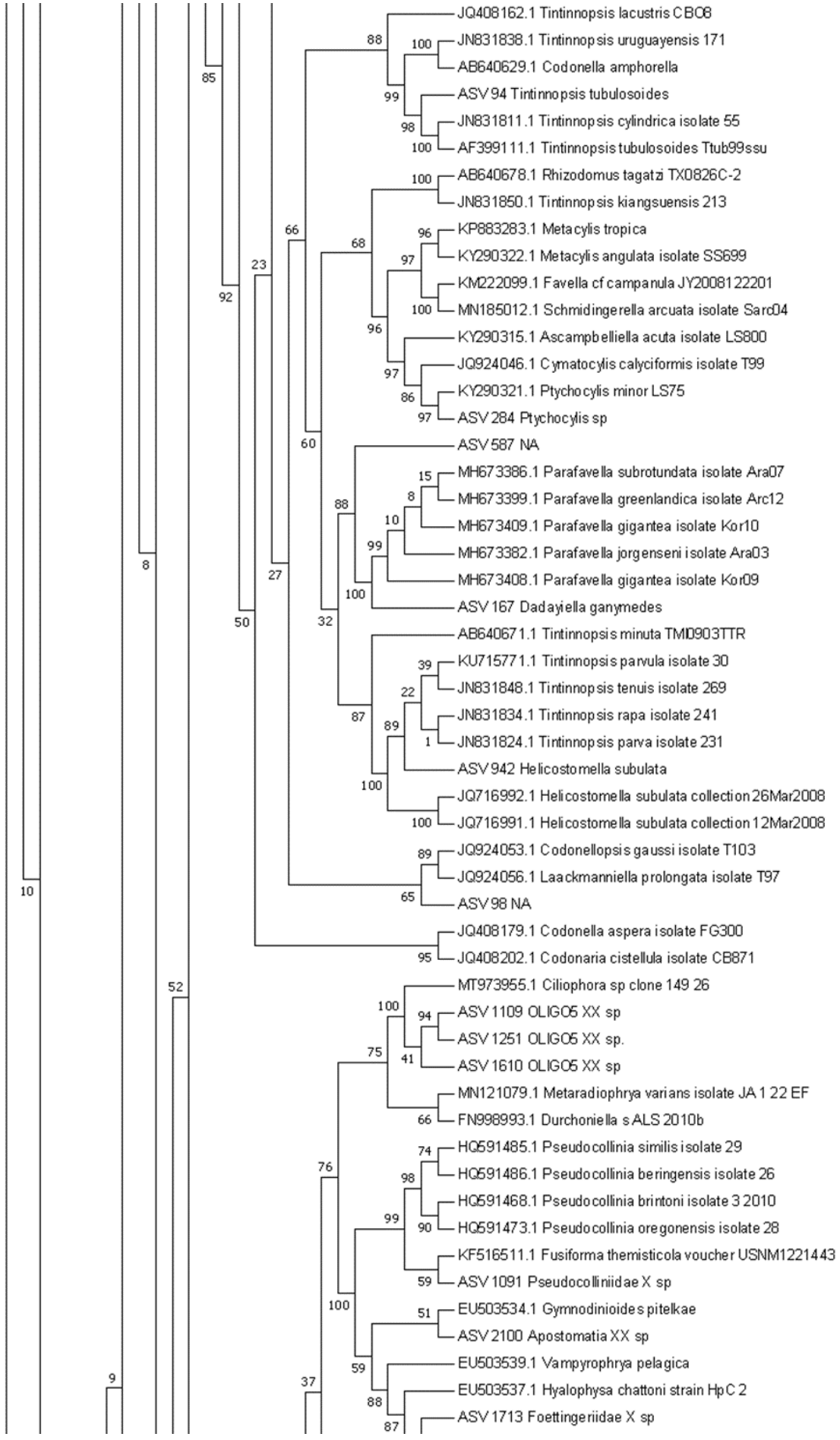
JQ408162.1 Tintinnopsis lacustris CBC8
JN831838.1 Tintinnopsis uruguayensis 171
AB640629.1 Codonella amphorella
ASV 94 Tintinnopsis tubulosoides
JN831811.1 Tintinnopsis cylindrica isolate 55
AF399111.1 Tintinnopsis tubulosoides Ttub99ssu
AB640678.1 Rhizodomus tagatzi TX0826C-2
JN831850.1 Tintinnopsis kiangsuensis 213
KP883283.1 Metacylis tropica
KY290322.1 Metacylis angulata isolate SS699
KM222099.1 Favella cf campanula JY2008122201
MN185012.1 Schmidingerella arcuata isolate Sarc04
KY290315.1 Ascampbelliella acuta isolate LS800
JQ924046.1 Cymatocylis calyciformis isolate T99
KY290321.1 Ptychocylis minor LS75
ASV 284 Ptychocylis sp
ASV 587 NA
MH673386.1 Parafavella subrotundata isolate Ara07
MH673399.1 Parafavella greenlandica isolate Arc12
MH673409.1 Parafavella gigantea isolate Kor10
MH673382.1 Parafavella jorgenseni isolate Ara03
MH673408.1 Parafavella gigantea isolate Kor09
ASV 167 Dadayiella ganymedes
AB640671.1 Tintinnopsis minuta TMD903TTR
KU715771.1 Tintinnopsis parvula isolate 30
JN831848.1 Tintinnopsis tenuis isolate 269
JN831834.1 Tintinnopsis rapa isolate 241
JN831824.1 Tintinnopsis parva isolate 231
ASV 942 Helicostomella subulata
JQ716992.1 Helicostomella subulata collection 26Mar2008
JQ716991.1 Helicostomella subulata collection 12Mar2008
JQ924053.1 Codonellopsis gaussi isolate T103
JQ924056.1 Laackmanniella prolongata isolate T97
ASV 98 NA
JQ408179.1 Codonella aspera isolate FG300
JQ408202.1 Codonaria cistellula isolate CB871
MT973955.1 Ciliophora sp clone 149 26
ASV 1109 OLIGO5 XX sp
ASV 1251 OLIGO5 XX sp.
ASV 1610 OLIGO5 XX sp
MN121079.1 Metaradiophrya varians isolate JA 1 22 EF
FN998993.1 Durchoniella s ALS 2010b
HQ591485.1 Pseudocollinia similis isolate 29
HQ591486.1 Pseudocollinia beringensis isolate 26
HQ591468.1 Pseudocollinia brintoni isolate 3 2010
HQ591473.1 Pseudocollinia oregonensis isolate 28
KF516511.1 Fusiforma themisticola voucher USNM1221443
ASV 1091 Pseudocolliniidae X sp
EU503534.1 Gymnodinioides pitelkae
ASV 2100 Apostomatia XX sp
EU503539.1 Vampyrophrya pelagica
EU503537.1 Hyalophysa chattoni strain HpC 2
ASV 1713 Foettingeriidae X sp

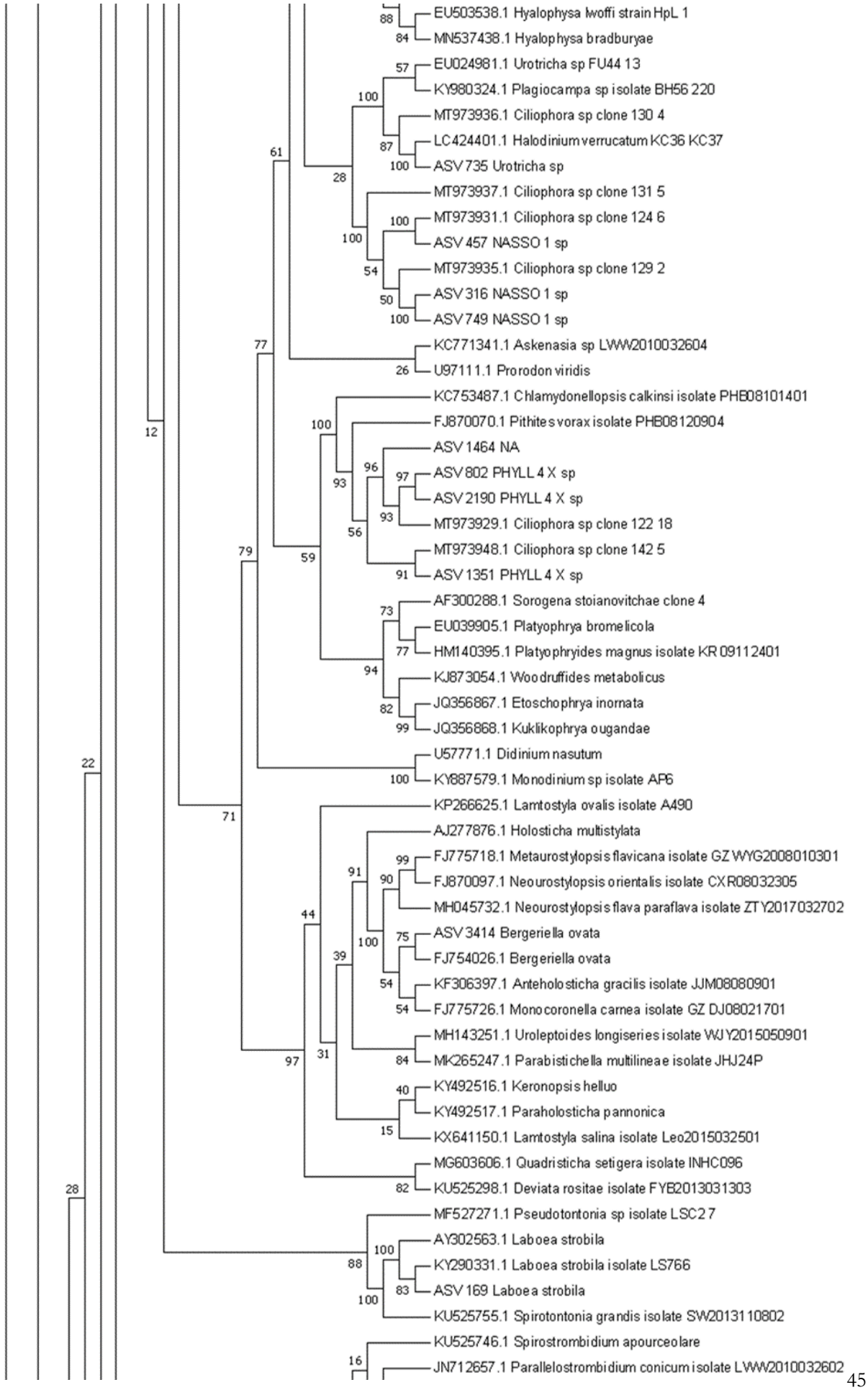
EU503538.1 Hyalophysa lwoffi strain HpL 1
MN537438.1 Hyalophysa bradburyae
EU024981.1 Urotricha sp FU44 13
KY980324.1 Plagiocampa sp isolate BH56 220
MT973936.1 Ciliophora sp clone 130 4
LC424401.1 Halodinium verrucatum KC36 KC37
ASV 735 Urotricha sp
MT973937.1 Ciliophora sp clone 131 5
MT973931.1 Ciliophora sp clone 124 6
ASV 457 NASSO 1 sp
MT973935.1 Ciliophora sp clone 129 2
ASV 316 NASSO 1 sp
ASV 749 NASSO 1 sp
KC771341.1 Askenasia sp LWW2010032604
U97111.1 Prorodon viridis
KC753487.1 Chlamydonellopsis calkinsi isolate PHB08101401
FJ870070.1 Pithites vorax isolate PHB08120904
ASV 1464 NA
ASV 802 PHYLL 4 X sp
ASV 2190 PHYLL 4 X sp
MT973929.1 Ciliophora sp clone 122 18
MT973948.1 Ciliophora sp clone 142 5
ASV 1351 PHYLL 4 X sp
AF300288.1 Sorogena stoianovitchae clone 4
EU039905.1 Platyophrya bromelicola
HM140395.1 Platyophryides magnus isolate KR 09112401
KJ873054.1 Woodruffides metabolicus
JQ356867.1 Etoschophrya inornata
JQ356868.1 Kuklikophrya ougandae
U57771.1 Didinium nasutum
KY887579.1 Monodinium sp isolate AP6
KP266625.1 Lamtostyla ovalis isolate A490
AJ277876.1 Holosticha multistylata
FJ775718.1 Metaurostylopsis flavicana isolate GZ WYG2008010301
FJ870097.1 Neourostylopsis orientalis isolate CXR08032305
MH045732.1 Neourostylopsis flava paraflava isolate ZTY2017032702
ASV 3414 Bergeriella ovata
FJ754026.1 Bergeriella ovata
KF306397.1 Anteholosticha gracilis isolate JJM08080901
FJ775726.1 Monocoronella carnea isolate GZ DJ08021701
MH143251.1 Uroleptoides longiseries isolate WJY2015050901
MK265247.1 Parabistichella multilineae isolate JHJ24P
KY492516.1 Keronopsis helluo
KY492517.1 Paraholosticha pannonica
KX641150.1 Lamtostyla salina isolate Leo2015032501
MG603606.1 Quadristicha setigera isolate INHC096
KU525298.1 Deviata rositae isolate FYB2013031303
MF527271.1 Pseudotontonia sp isolate LSC2 7
AY302563.1 Laboea strobila
KY290331.1 Laboea strobila isolate LS766
ASV 169 Laboea strobila
KU525755.1 Spirotontonia grandis isolate SW2013110802
KU525746.1 Spirostrombidium apourceolare
JN712657.1 Parallelostrombidium conicum isolate LWW2010032602

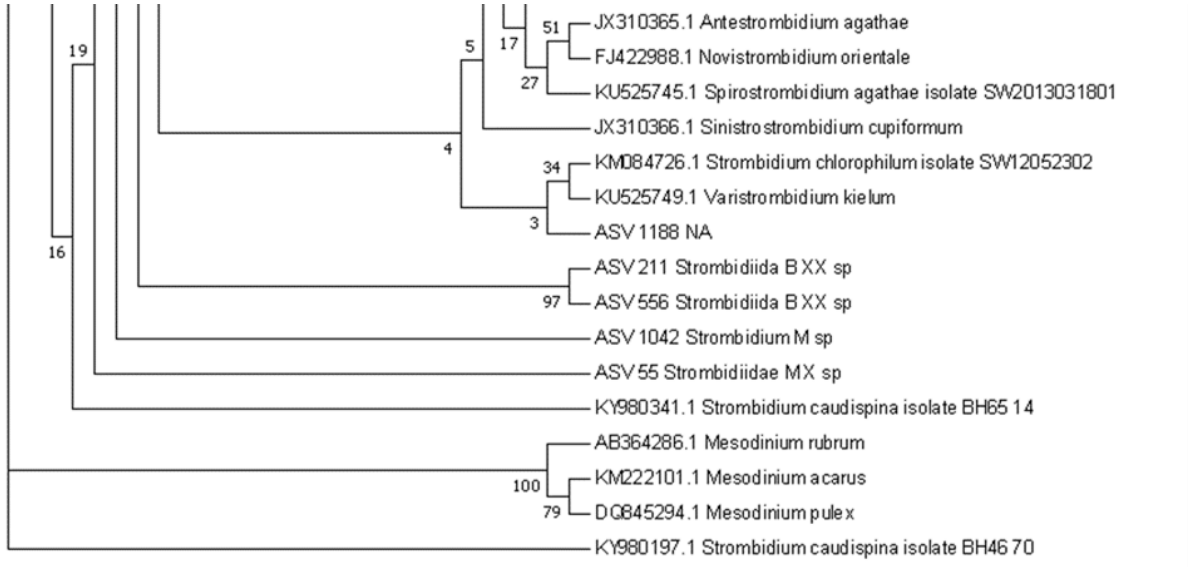


The initial identification of the presented ASVs was based on PR$^2$ and has subsequently been curated according to the shown phylogenetic placement.

## Cryptophytes: Phylogenetic Placement

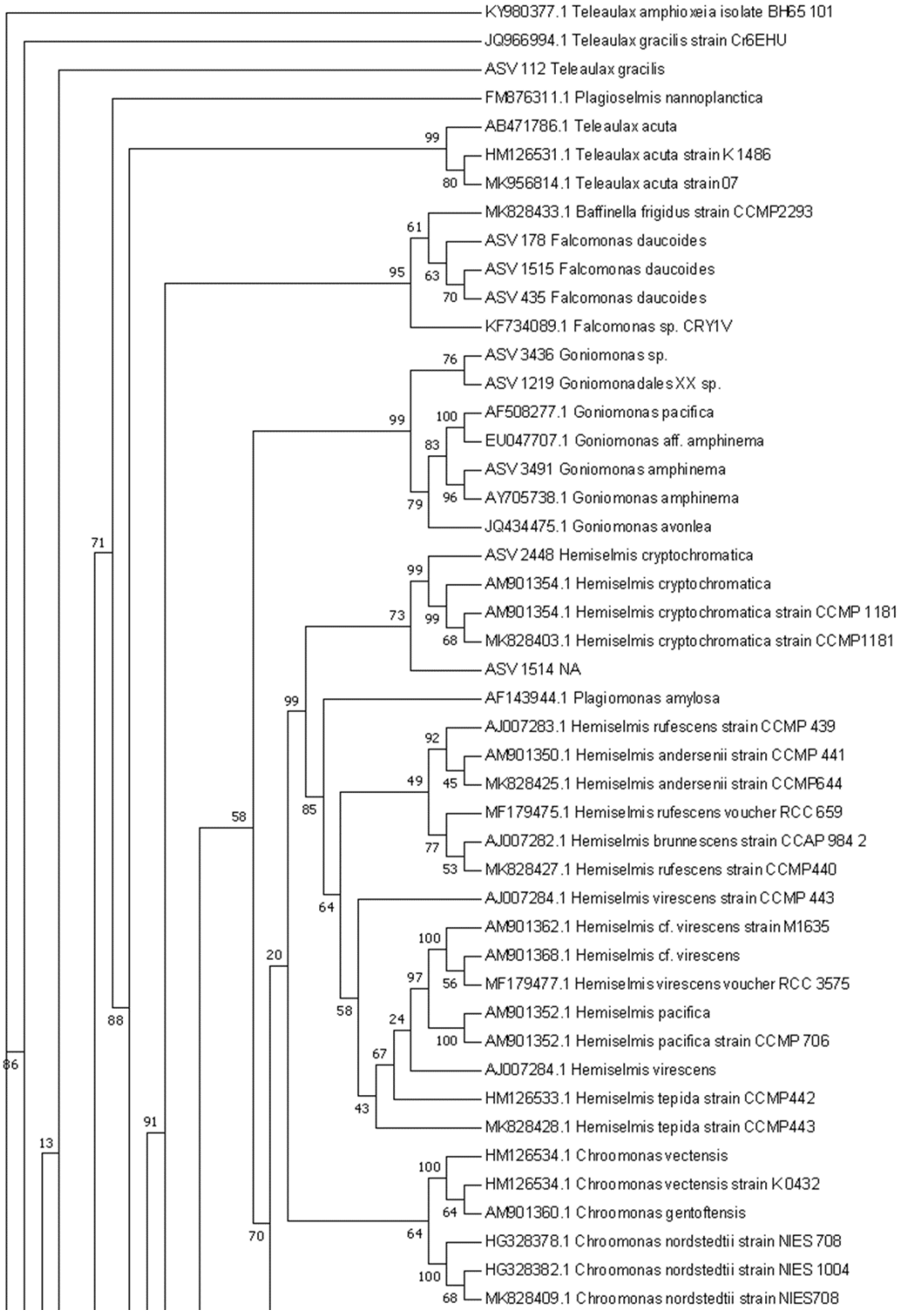

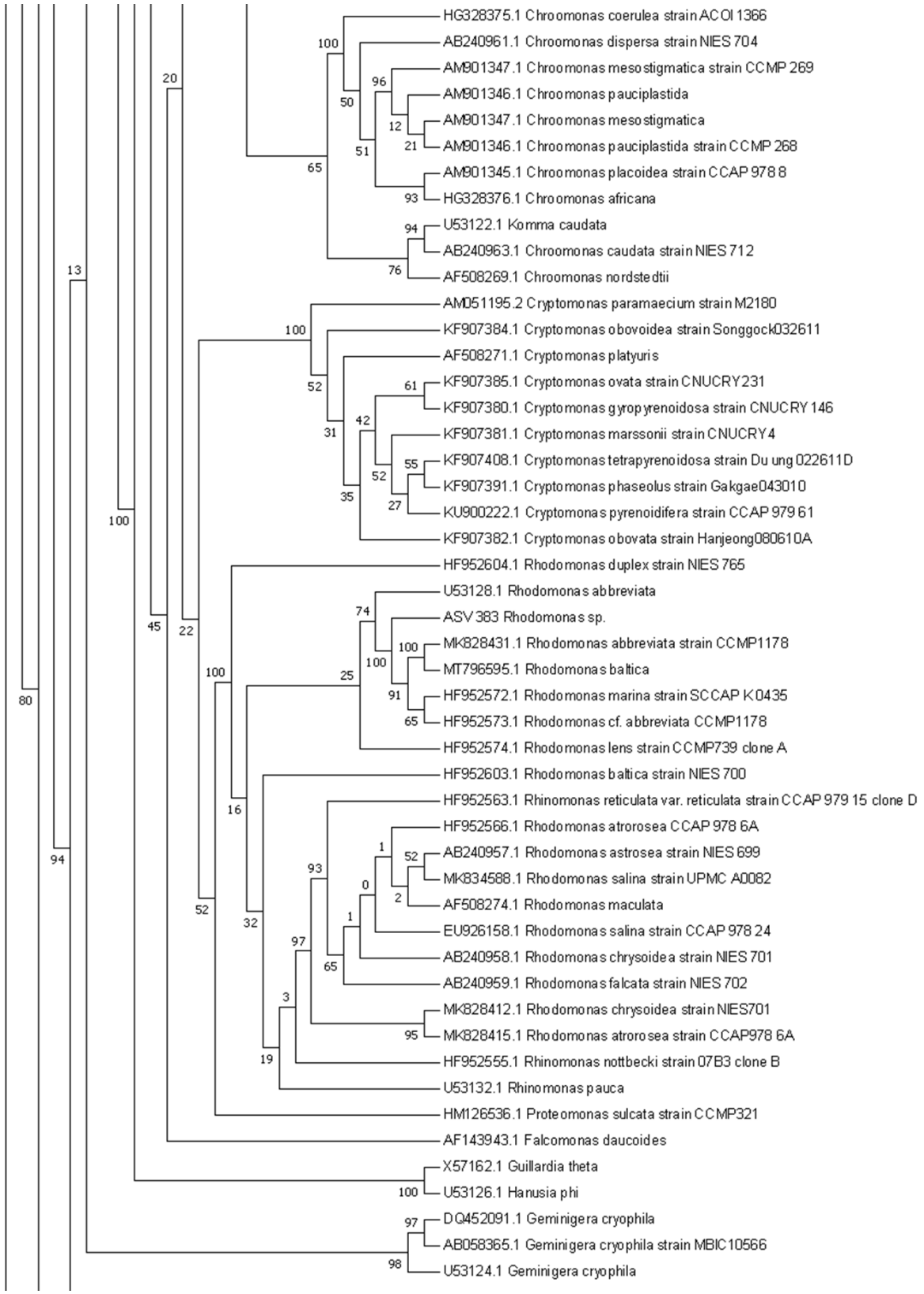
HG328375.1 Chroomonas coerulea strain ACOI 1366
AB240961.1 Chroomonas dispersa strain NIES 704
AM901347.1 Chroomonas mesostigmatica strain CCMP 269
AM901346.1 Chroomonas pauciplastida
AM901347.1 Chroomonas mesostigmatica
AM901346.1 Chroomonas pauciplastida strain CCMP 268
AM901345.1 Chroomonas placoidea strain CCAP 978 8
HG328376.1 Chroomonas africana
U53122.1 Komma caudata
AB240963.1 Chroomonas caudata strain NIES 712
AF508269.1 Chroomonas nordstedtii
AM051195.2 Cryptomonas paramaecium strain M2180
KF907384.1 Cryptomonas obovoidea strain Songgock032611
AF508271.1 Cryptomonas platyuris
KF907385.1 Cryptomonas ovata strain CNUCRY231
KF907380.1 Cryptomonas gyropyrenoidosa strain CNUCRY 146
KF907381.1 Cryptomonas marssonii strain CNUCRY4
KF907408.1 Cryptomonas tetrapyrenoidosa strain Du ung 022611D
KF907391.1 Cryptomonas phaseolus strain Gakgae043010
KU900222.1 Cryptomonas pyrenoidifera strain CCAP 979 61
KF907382.1 Cryptomonas obovata strain Hanjeong080610A
HF952604.1 Rhodomonas duplex strain NIES 765
U53128.1 Rhodomonas abbreviata
ASV 383 Rhodomonas sp.
MK828431.1 Rhodomonas abbreviata strain CCMP1178
MT796595.1 Rhodomonas baltica
HF952572.1 Rhodomonas marina strain SCCAP K0435
HF952573.1 Rhodomonas cf. abbreviata CCMP1178
HF952574.1 Rhodomonas lens strain CCMP739 clone A
HF952603.1 Rhodomonas baltica strain NIES 700
HF952563.1 Rhinomonas reticulata var. reticulata strain CCAP 979 15 clone D
HF952566.1 Rhodomonas atrorosea CCAP 978 6A
AB240957.1 Rhodomonas astrosea strain NIES 699
MK834588.1 Rhodomonas salina strain UPMC A0082
AF508274.1 Rhodomonas maculata
EU926158.1 Rhodomonas salina strain CCAP 978 24
AB240958.1 Rhodomonas chrysoidea strain NIES 701
AB240959.1 Rhodomonas falcata strain NIES 702
MK828412.1 Rhodomonas chrysoidea strain NIES701
MK828415.1 Rhodomonas atrorosea strain CCAP978 6A
HF952555.1 Rhinomonas nottbecki strain 07B3 clone B
U53132.1 Rhinomonas pauca
HM126536.1 Proteomonas sulcata strain CCMP321
AF143943.1 Falcomonas daucoides
X57162.1 Guillardia theta
U53126.1 Hanusia phi
DQ452091.1 Geminigera cryophila
AB058365.1 Geminigera cryophila strain MBIC10566
U53124.1 Geminigera cryophila

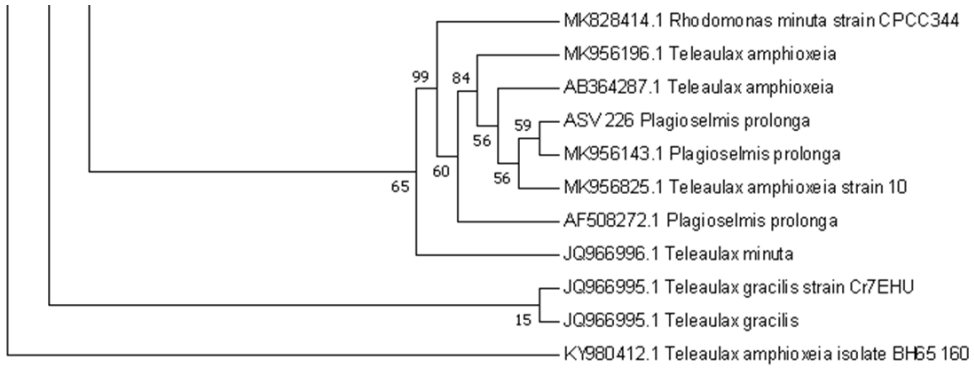


The initial identification of the presented ASVs was based on PR$^2$ and has subsequently been curated according to the shown phylogenetic placement.

## Diatoms: Phylogenetic Placement

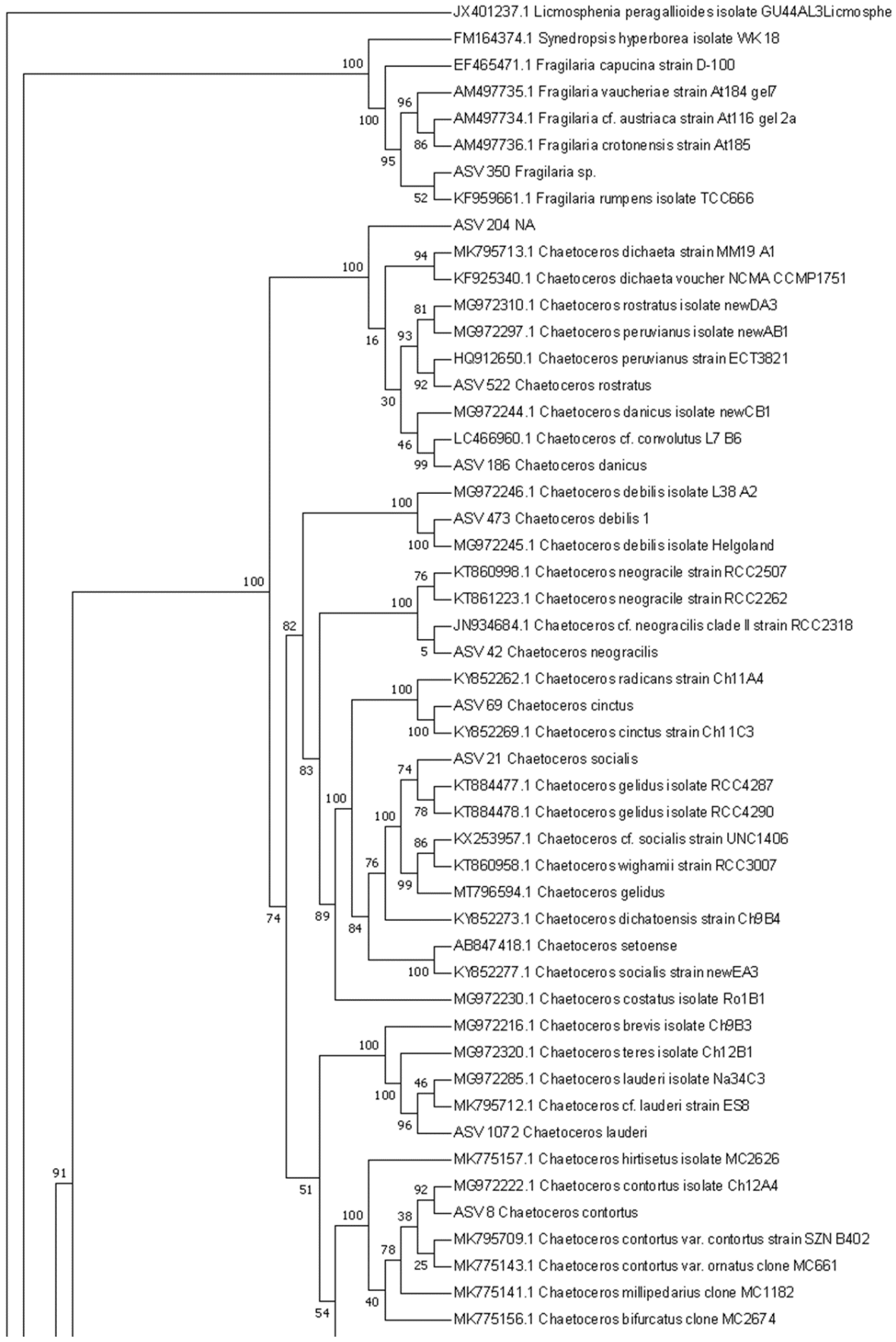

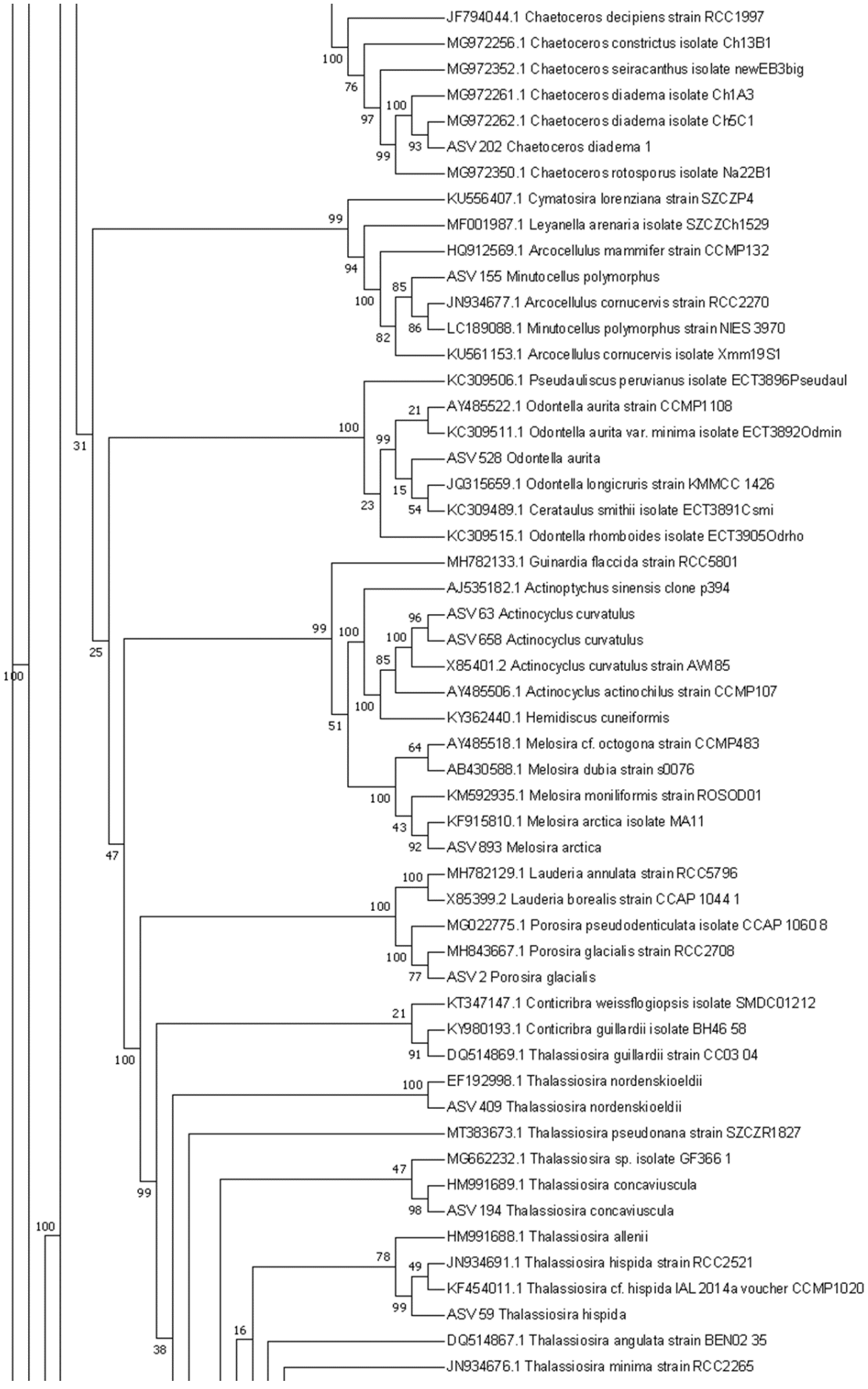
JF794044.1 Chaetoceros decipiens strain RCC1997
MG972256.1 Chaetoceros constrictus isolate Ch13B1
MG972352.1 Chaetoceros seiracanthus isolate newEB3big
MG972261.1 Chaetoceros diadema isolate Ch1A3
MG972262.1 Chaetoceros diadema isolate Ch5C1
ASV 202 Chaetoceros diadema 1
MG972350.1 Chaetoceros rotosporus isolate Na22B1
KU556407.1 Cymatosira lorenziana strain SZCZP4
MF001987.1 Leyanella arenaria isolate SZCZCh1529
HQ912569.1 Arcocellulus mammifer strain CCMP132
ASV 155 Minutocellus polymorphus
JN934677.1 Arcocellulus cornucervis strain RCC2270
LC189088.1 Minutocellus polymorphus strain NIES 3970
KU561153.1 Arcocellulus cornucervis isolate Xmm19S1
KC309506.1 Pseudauliscus peruvianus isolate ECT3896Pseudaul
AY485522.1 Odontella aurita strain CCMP1108
KC309511.1 Odontella aurita var. minima isolate ECT3892Odmin
ASV 528 Odontella aurita
JQ315659.1 Odontella longicruris strain KMMCC 1426
KC309489.1 Cerataulus smithii isolate ECT3891Csmi
KC309515.1 Odontella rhomboides isolate ECT3905Odrho
MH782133.1 Guinardia flaccida strain RCC5801
AJ535182.1 Actinoptychus sinensis clone p394
ASV 63 Actinocyclus curvatulus
ASV 658 Actinocyclus curvatulus
X85401.2 Actinocyclus curvatulus strain AWI85
AY485506.1 Actinocyclus actinochilus strain CCMP107
KY362440.1 Hemidiscus cuneiformis
AY485518.1 Melosira cf. octogona strain CCMP483
AB430588.1 Melosira dubia strain s0076
KM592935.1 Melosira moniliformis strain ROSOD01
KF915810.1 Melosira arctica isolate MA11
ASV 893 Melosira arctica
MH782129.1 Lauderia annulata strain RCC5796
X85399.2 Lauderia borealis strain CCAP 1044 1
MG022775.1 Porosira pseudodenticulata isolate CCAP 10608
MH843667.1 Porosira glacialis strain RCC2708
ASV 2 Porosira glacialis
KT347147.1 Conticribra weissflogiopsis isolate SMDC01212
KY980193.1 Conticribra guillardii isolate BH46 58
DQ514869.1 Thalassiosira guillardii strain CC03 04
EF192998.1 Thalassiosira nordenskioeldii
ASV 409 Thalassiosira nordenskioeldii
MT383673.1 Thalassiosira pseudonana strain SZCZR1827
MG662232.1 Thalassiosira sp. isolate GF366 1
HM991689.1 Thalassiosira concaviuscula
ASV 194 Thalassiosira concaviuscula
HM991688.1 Thalassiosira allenii
JN934691.1 Thalassiosira hispida strain RCC2521
KF454011.1 Thalassiosira cf. hispida IAL 2014a voucher CCMP1020
ASV 59 Thalassiosira hispida
DQ514867.1 Thalassiosira angulata strain BEN02 35
JN934676.1 Thalassiosira minima strain RCC2265

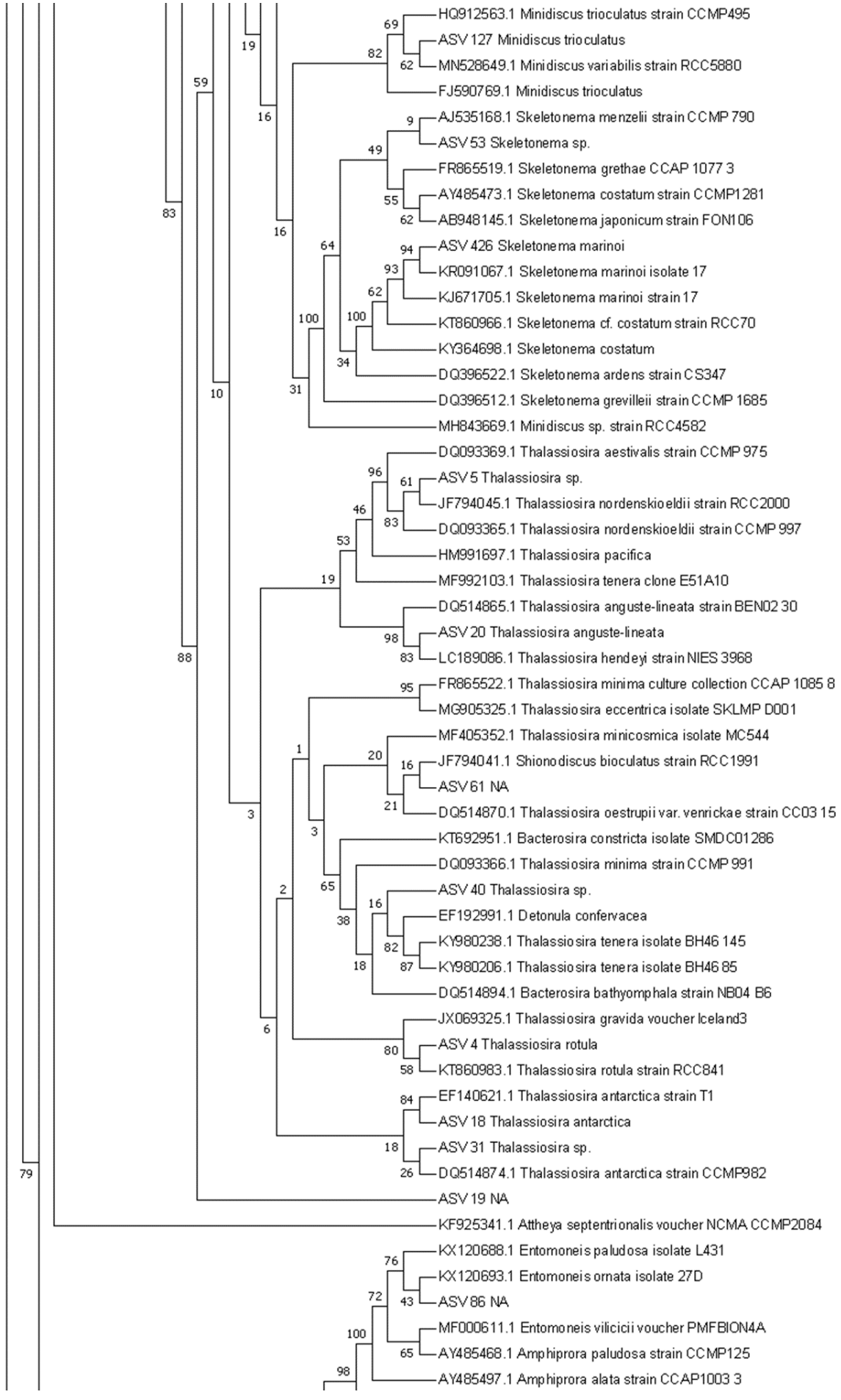
HQ912563.1 Minidiscus trioculatus strain CCMP495
ASV 127 Minidiscus trioculatus
MN528649.1 Minidiscus variabilis strain RCC5880
FJ590769.1 Minidiscus trioculatus
AJ535168.1 Skeletonema menzelii strain CCMP 790
ASV 53 Skeletonema sp.
FR865519.1 Skeletonema grethae CCAP 1077 3
AY485473.1 Skeletonema costatum strain CCMP1281
AB948145.1 Skeletonema japonicum strain FON106
ASV 426 Skeletonema marinoi
KR091067.1 Skeletonema marinoi isolate 17
KJ671705.1 Skeletonema marinoi strain 17
KT860966.1 Skeletonema cf. costatum strain RCC70
KY364698.1 Skeletonema costatum
DQ396522.1 Skeletonema ardens strain CS347
DQ396512.1 Skeletonema grevilleii strain CCMP 1685
MH843669.1 Minidiscus sp. strain RCC4582
DQ093369.1 Thalassiosira aestivalis strain CCMP 975
ASV 5 Thalassiosira sp.
JF794045.1 Thalassiosira nordenskioeldii strain RCC2000
DQ093365.1 Thalassiosira nordenskioeldii strain CCMP 997
HM991697.1 Thalassiosira pacifica
MF992103.1 Thalassiosira tenera clone E51A10
DQ514865.1 Thalassiosira anguste-lineata strain BEN02 30
ASV 20 Thalassiosira anguste-lineata
LC189086.1 Thalassiosira hendeyi strain NIES 3968
FR865522.1 Thalassiosira minima culture collection CCAP 1085 8
MG905325.1 Thalassiosira eccentrica isolate SKLMP D001
MF405352.1 Thalassiosira minicosmica isolate MC544
JF794041.1 Shionodiscus bioculatus strain RCC1991
ASV 61 NA
DQ514870.1 Thalassiosira oestrupii var. venrickae strain CC03 15
KT692951.1 Bacterosira constricta isolate SMDC01286
DQ093366.1 Thalassiosira minima strain CCMP 991
ASV 40 Thalassiosira sp.
EF192991.1 Detonula confervacea
KY980238.1 Thalassiosira tenera isolate BH46 145
KY980206.1 Thalassiosira tenera isolate BH46 85
DQ514894.1 Bacterosira bathyomphala strain NB04 B6
JX069325.1 Thalassiosira gravida voucher Iceland3
ASV 4 Thalassiosira rotula
KT860983.1 Thalassiosira rotula strain RCC841
EF140621.1 Thalassiosira antarctica strain T1
ASV 18 Thalassiosira antarctica
ASV 31 Thalassiosira sp.
DQ514874.1 Thalassiosira antarctica strain CCMP982
ASV 19 NA
KF925341.1 Attheya septentrionalis voucher NCMA CCMP2084
KX120688.1 Entomoneis paludosa isolate L431
KX120693.1 Entomoneis ornata isolate 27D
ASV 86 NA
MF000611.1 Entomoneis vilicicii voucher PMFBION4A
AY485468.1 Amphiprora paludosa strain CCMP125
AY485497.1 Amphiprora alata strain CCAP1003 3

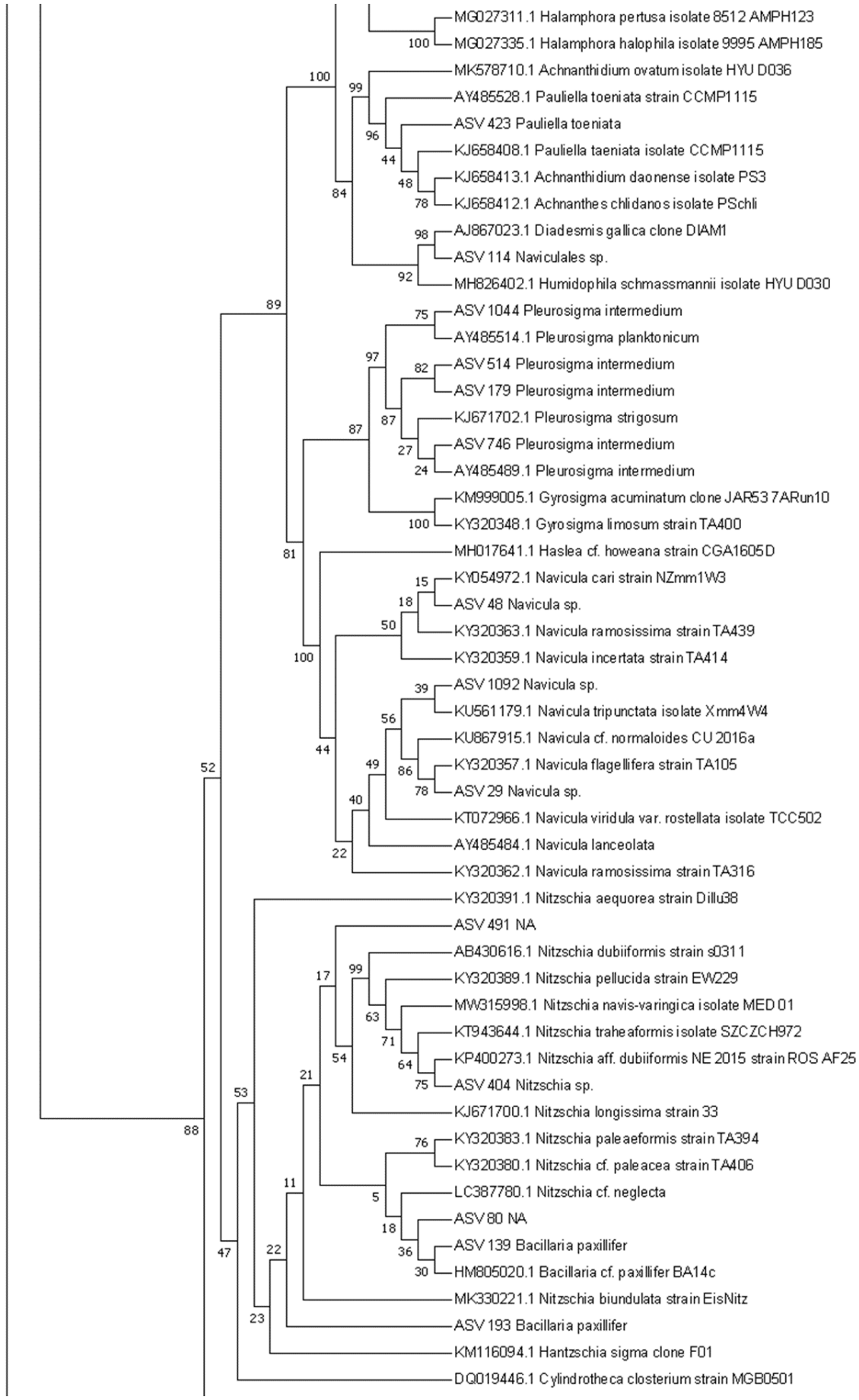
MG027311.1 Halamphora pertusa isolate 8512 AMPH123
MG027335.1 Halamphora halophila isolate 9995 AMPH185
MK578710.1 Achnanthidium ovatum isolate HYU D036
AY485528.1 Pauliella toeniata strain CCMP1115
ASV 423 Pauliella toeniata
KJ658408.1 Pauliella taeniata isolate CCMP1115
KJ658413.1 Achnanthidium daonense isolate PS3
KJ658412.1 Achnanthes chlidanos isolate PSchli
AJ867023.1 Diadesmis gallica clone DIAM1
ASV 114 Naviculales sp.
MH826402.1 Humidophila schmassmannii isolate HYU D030
ASV 1044 Pleurosigma intermedium
AY485514.1 Pleurosigma planktonicum
ASV 514 Pleurosigma intermedium
ASV 179 Pleurosigma intermedium
KJ671702.1 Pleurosigma strigosum
ASV 746 Pleurosigma intermedium
AY485489.1 Pleurosigma intermedium
KM999005.1 Gyrosigma acuminatum clone JAR53 7ARun10
KY320348.1 Gyrosigma limosum strain TA400
MH017641.1 Haslea cf. howeana strain CGA1605D
KY054972.1 Navicula cari strain NZmm1W3
ASV 48 Navicula sp.
KY320363.1 Navicula ramosissima strain TA439
KY320359.1 Navicula incertata strain TA414
ASV 1092 Navicula sp.
KU561179.1 Navicula tripunctata isolate Xmm4W4
KU867915.1 Navicula cf. normaloides CU 2016a
KY320357.1 Navicula flagellifera strain TA105
ASV 29 Navicula sp.
KT072966.1 Navicula viridula var. rostellata isolate TCC502
AY485484.1 Navicula lanceolata
KY320362.1 Navicula ramosissima strain TA316
KY320391.1 Nitzschia aequorea strain Dillu38
ASV 491 NA
AB430616.1 Nitzschia dubiiformis strain s0311
KY320389.1 Nitzschia pellucida strain EW229
MW315998.1 Nitzschia navis-varingica isolate MED 01
KT943644.1 Nitzschia traheaformis isolate SZCZCH972
KP400273.1 Nitzschia aff. dubiiformis NE 2015 strain ROS AF25
ASV 404 Nitzschia sp.
KJ671700.1 Nitzschia longissima strain 33
KY320383.1 Nitzschia paleaeformis strain TA394
KY320380.1 Nitzschia cf. paleacea strain TA406
LC387780.1 Nitzschia cf. neglecta
ASV 80 NA
ASV 139 Bacillaria paxillifer
HM805020.1 Bacillaria cf. paxillifer BA14c
MK330221.1 Nitzschia biundulata strain EisNitz
ASV 193 Bacillaria paxillifer
KM116094.1 Hantzschia sigma clone F01
DQ019446.1 Cylindrotheca closterium strain MGB0501

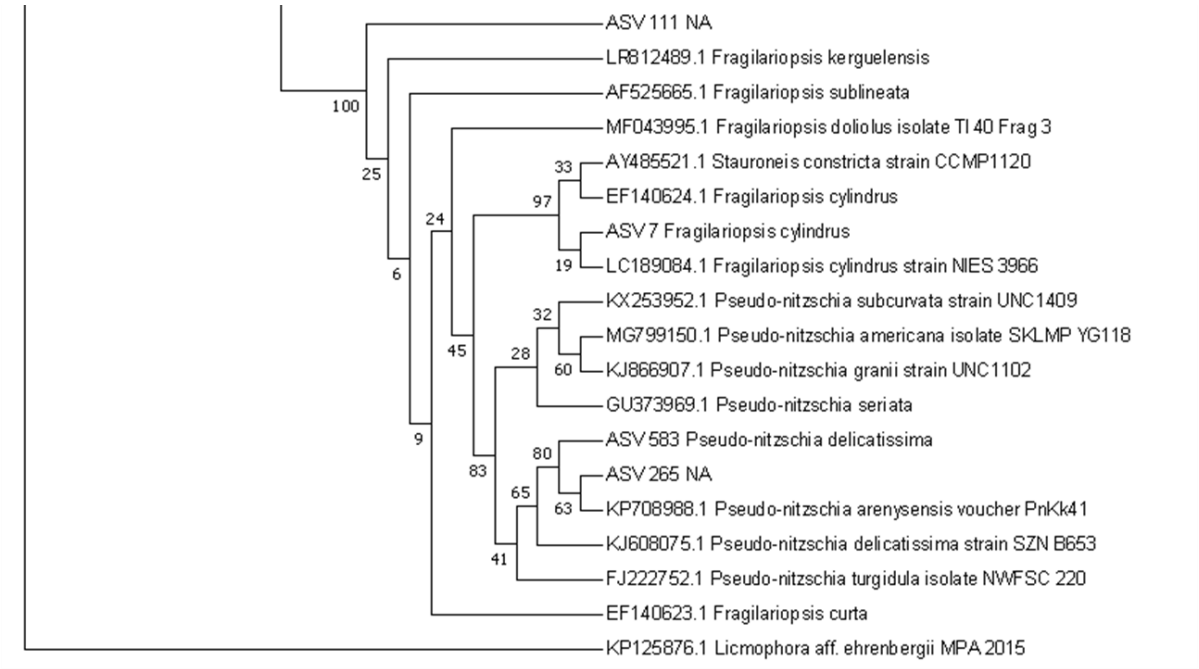


The initial identification of the presented ASVs was based on PR$^2$ and has subsequently been curated according to the shown phylogenetic placement.

## Dinoflagellates: Phylogenetic Placement

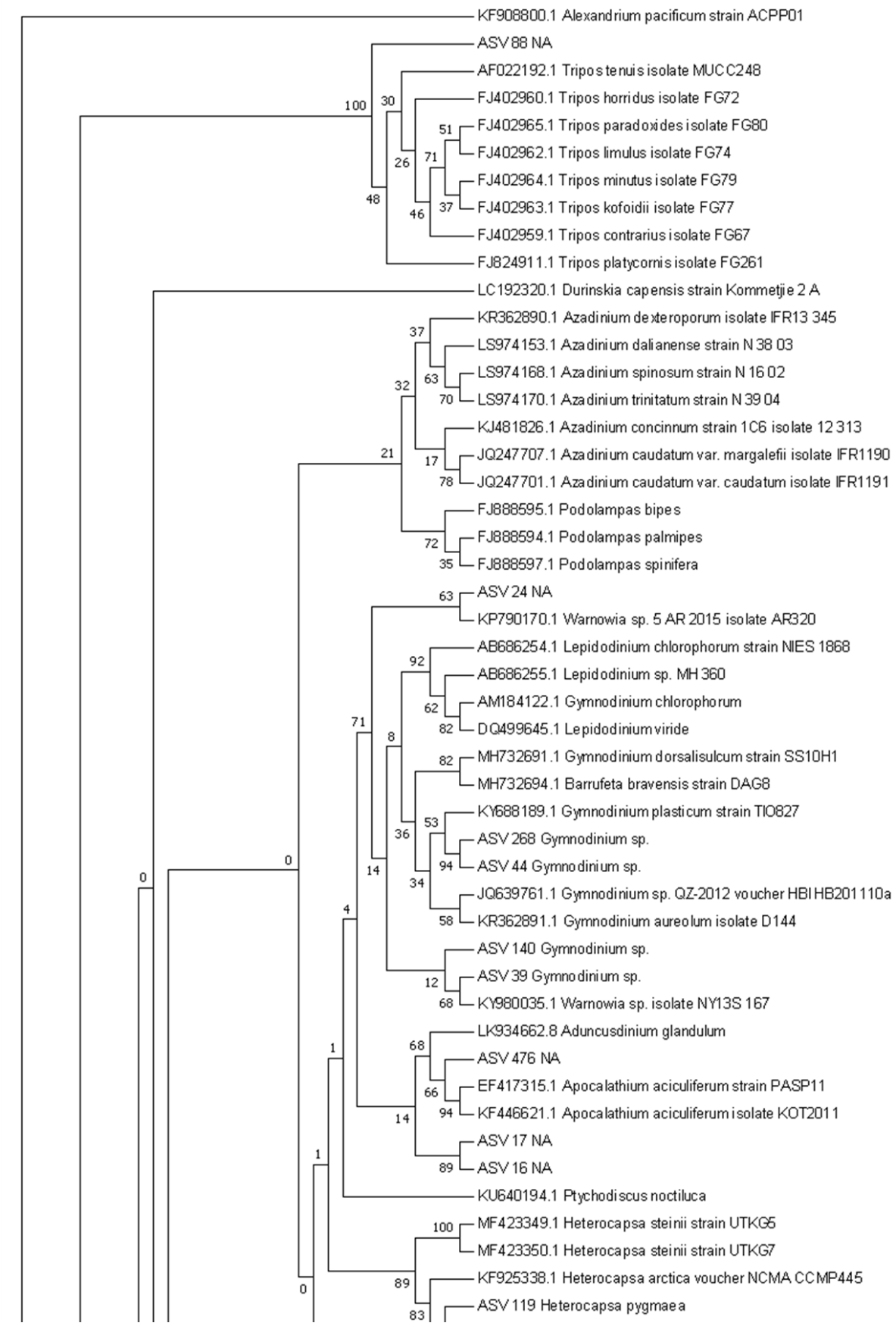

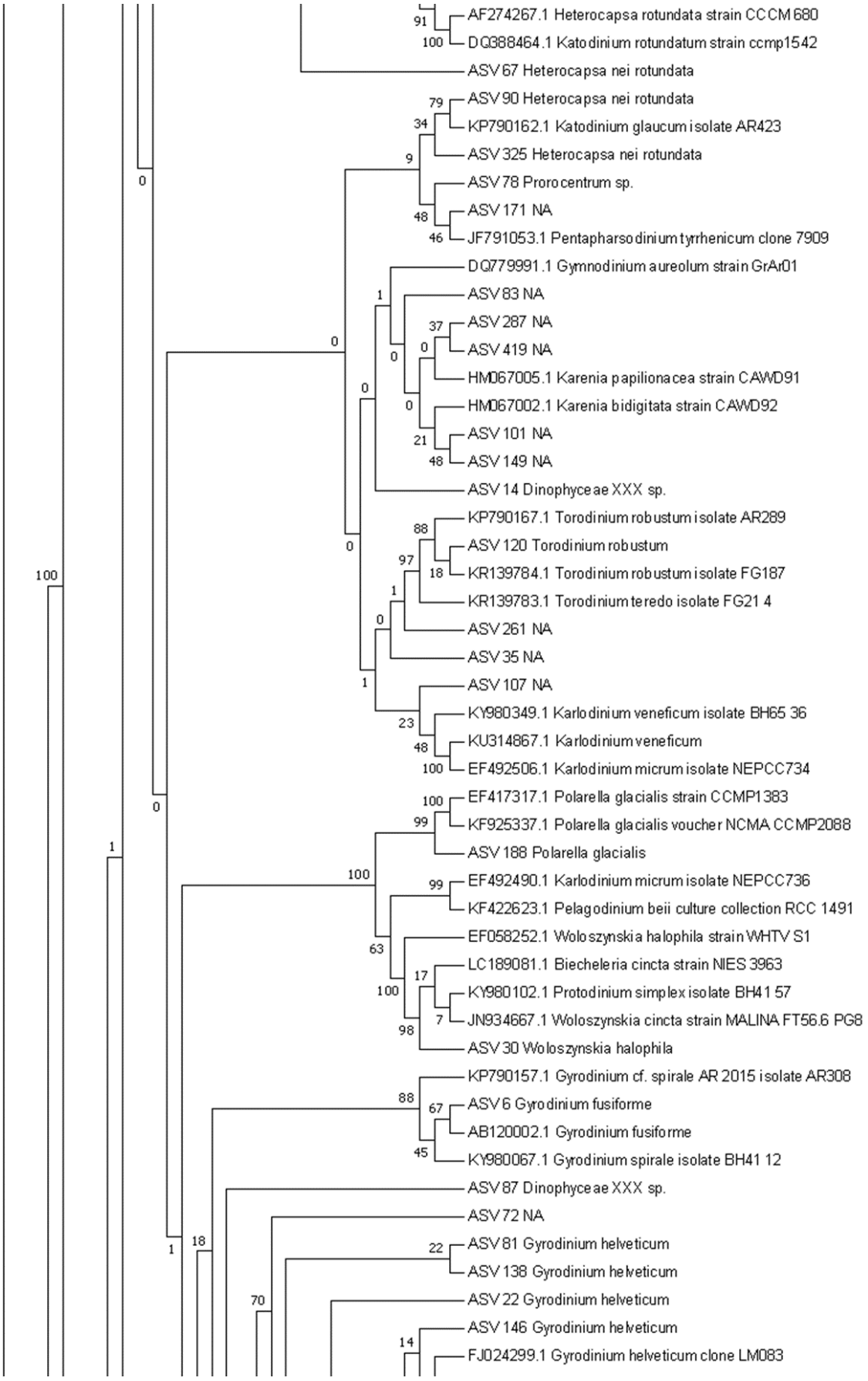
AF274267.1 Heterocapsa rotundata strain CCCM680
DQ388464.1 Katodinium rotundatum strain ccmp1542
ASV 67 Heterocapsa nei rotundata
ASV 90 Heterocapsa nei rotundata
KP790162.1 Katodinium glaucum isolate AR423
ASV 325 Heterocapsa nei rotundata
ASV 78 Prorocentrum sp.
ASV 171 NA
JF791053.1 Pentapharsodinium tyrrhenicum clone 7909
DQ779991.1 Gymnodinium aureolum strain GrAr01
ASV 83 NA
ASV 287 NA
ASV 419 NA
HM067005.1 Karenia papilionacea strain CAWD91
HM067002.1 Karenia bidigitata strain CAWD92
ASV 101 NA
ASV 149 NA
ASV 14 Dinophyceae XXX sp.
KP790167.1 Torodinium robustum isolate AR289
ASV 120 Torodinium robustum
KR139784.1 Torodinium robustum isolate FG187
KR139783.1 Torodinium teredo isolate FG21 4
ASV 261 NA
ASV 35 NA
ASV 107 NA
KY980349.1 Karlodinium veneficum isolate BH65 36
KU314867.1 Karlodinium veneficum
EF492506.1 Karlodinium micrum isolate NEPCC734
EF417317.1 Polarella glacialis strain CCMP1383
KF925337.1 Polarella glacialis voucher NCMA CCMP2088
ASV 188 Polarella glacialis
EF492490.1 Karlodinium micrum isolate NEPCC736
KF422623.1 Pelagodinium beii culture collection RCC 1491
EF058252.1 Woloszynskia halophila strain WHTV S1
LC189081.1 Biecheleria cincta strain NIES 3963
KY980102.1 Protodinium simplex isolate BH41 57
JN934667.1 Woloszynskia cincta strain MALINA FT56.6 PG8
ASV 30 Woloszynskia halophila
KP790157.1 Gyrodinium cf. spirale AR 2015 isolate AR308
ASV 6 Gyrodinium fusiforme
AB120002.1 Gyrodinium fusiforme
KY980067.1 Gyrodinium spirale isolate BH41 12
ASV 87 Dinophyceae XXX sp.
ASV 72 NA
ASV 81 Gyrodinium helveticum
ASV 138 Gyrodinium helveticum
ASV 22 Gyrodinium helveticum
ASV 146 Gyrodinium helveticum
FJ024299.1 Gyrodinium helveticum clone LM083

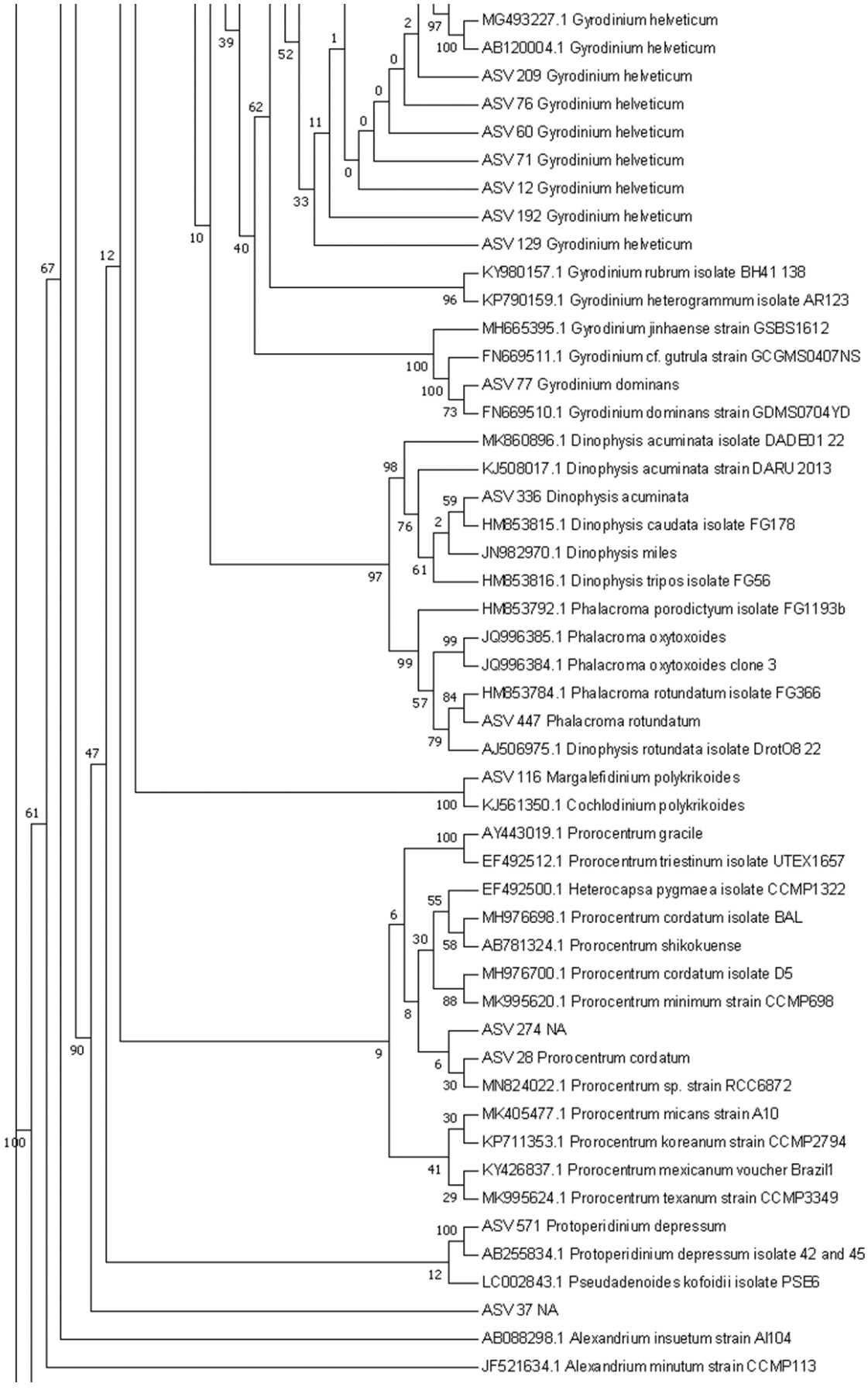
MG493227.1 Gyrodinium helveticum
AB120004.1 Gyrodinium helveticum
ASV 209 Gyrodinium helveticum
ASV 76 Gyrodinium helveticum
ASV 60 Gyrodinium helveticum
ASV 71 Gyrodinium helveticum
ASV 12 Gyrodinium helveticum
ASV 192 Gyrodinium helveticum
ASV 129 Gyrodinium helveticum
KY980157.1 Gyrodinium rubrum isolate BH41 138
KP790159.1 Gyrodinium heterogrammum isolate AR123
MH665395.1 Gyrodinium jinhaense strain GSBS1612
FN669511.1 Gyrodinium cf. gutrula strain GCGMS0407NS
ASV 77 Gyrodinium dominans
FN669510.1 Gyrodinium dominans strain GDMS0704YD
MK860896.1 Dinophysis acuminata isolate DADE01 22
KJ508017.1 Dinophysis acuminata strain DARU 2013
ASV 336 Dinophysis acuminata
HM853815.1 Dinophysis caudata isolate FG178
JN982970.1 Dinophysis miles
HM853816.1 Dinophysis tripos isolate FG56
HM853792.1 Phalacroma porodictyum isolate FG1193b
JQ996385.1 Phalacroma oxytoxoides
JQ996384.1 Phalacroma oxytoxoides clone 3
HM853784.1 Phalacroma rotundatum isolate FG366
ASV 447 Phalacroma rotundatum
AJ506975.1 Dinophysis rotundata isolate DrotO8 22
ASV 116 Margalefidinium polykrikoides
KJ561350.1 Cochlodinium polykrikoides
AY443019.1 Prorocentrum gracile
EF492512.1 Prorocentrum triestinum isolate UTEX1657
EF492500.1 Heterocapsa pygmaea isolate CCMP1322
MH976698.1 Prorocentrum cordatum isolate BAL
AB781324.1 Prorocentrum shikokuense
MH976700.1 Prorocentrum cordatum isolate D5
MK995620.1 Prorocentrum minimum strain CCMP698
ASV 274 NA
ASV 28 Prorocentrum cordatum
MN824022.1 Prorocentrum sp. strain RCC6872
MK405477.1 Prorocentrum micans strain A10
KP711353.1 Prorocentrum koreanum strain CCMP2794
KY426837.1 Prorocentrum mexicanum voucher Brazil1
MK995624.1 Prorocentrum texanum strain CCMP3349
ASV 571 Protoperidinium depressum
AB255834.1 Protoperidinium depressum isolate 42 and 45
LC002843.1 Pseudadenoides kofoidii isolate PSE6
ASV 37 NA
AB088298.1 Alexandrium insuetum strain AI104
JF521634.1 Alexandrium minutum strain CCMP113


The initial identification of the presented ASVs was based on PR$^2$ and has subsequently been curated according to the shown phylogenetic placement.

## Haptophytes: Phylogenetic Placement

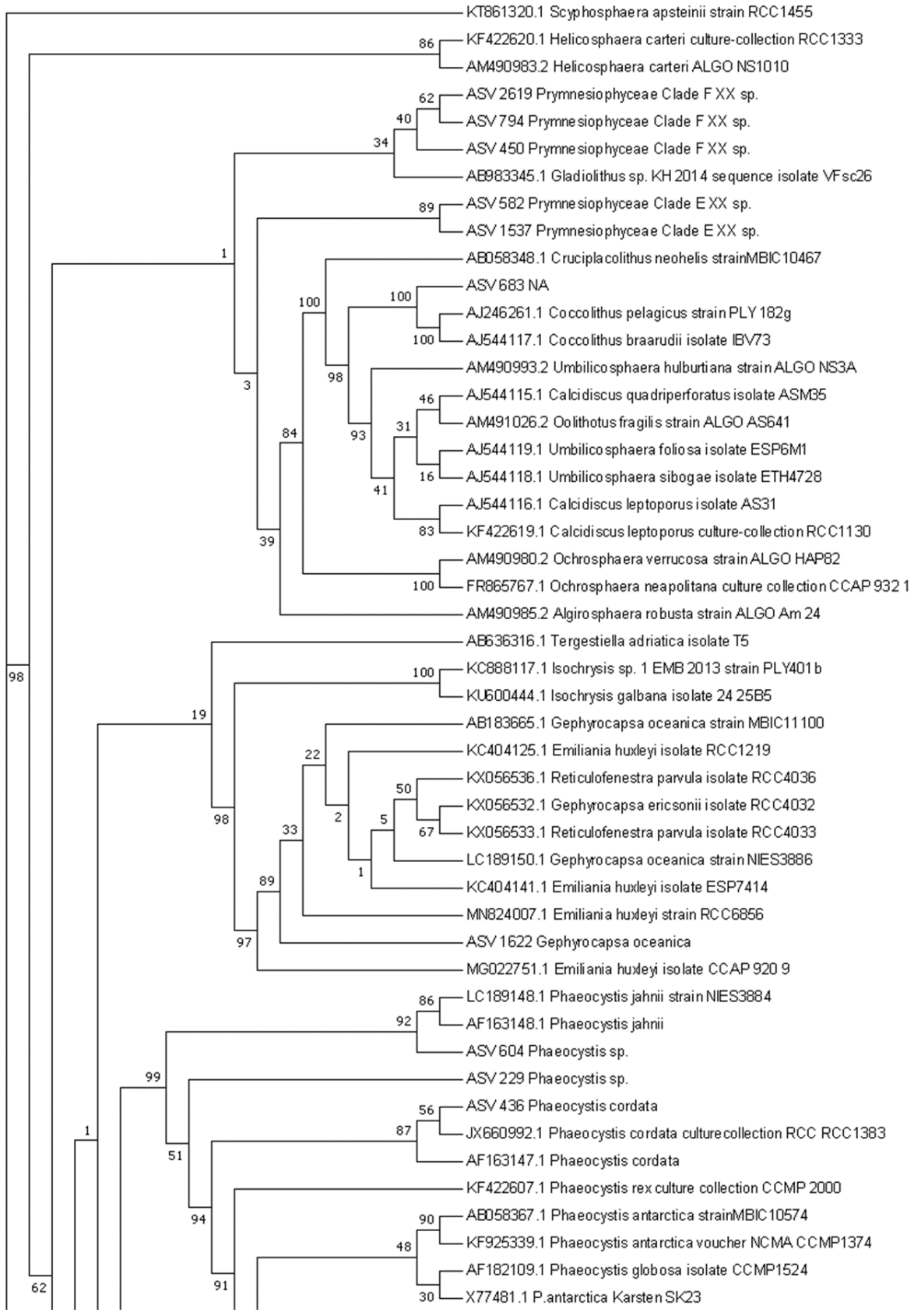

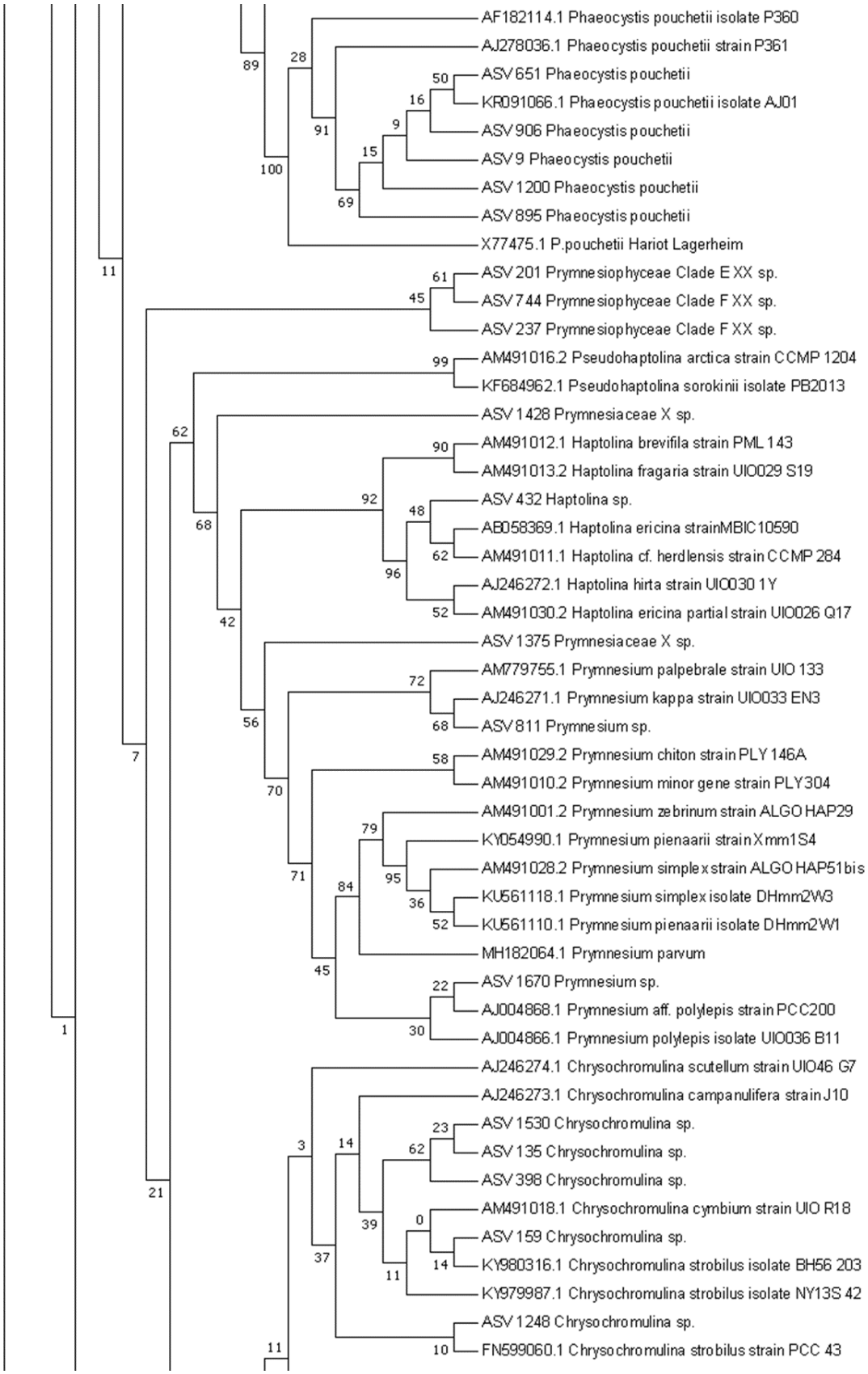
AF182114.1 Phaeocystis pouchetii isolate P360
AJ278036.1 Phaeocystis pouchetii strain P361
ASV 651 Phaeocystis pouchetii
KR091066.1 Phaeocystis pouchetii isolate AJ01
ASV 906 Phaeocystis pouchetii
ASV 9 Phaeocystis pouchetii
ASV 1200 Phaeocystis pouchetii
ASV 895 Phaeocystis pouchetii
X77475.1 P.pouchetii Hariot Lagerheim
ASV 201 Prymnesiophyceae Clade E XX sp.
ASV 744 Prymnesiophyceae Clade F XX sp.
ASV 237 Prymnesiophyceae Clade F XX sp.
AM491016.2 Pseudohaptolina arctica strain CCMP 1204
KF684962.1 Pseudohaptolina sorokinii isolate PB2013
ASV 1428 Prymnesiaceae X sp.
AM491012.1 Haptolina brevifila strain PML 143
AM491013.2 Haptolina fragaria strain UIO029 S19
ASV 432 Haptolina sp.
AB058369.1 Haptolina ericina strainMBIC10590
AM491011.1 Haptolina cf. herdlensis strain CCMP 284
AJ246272.1 Haptolina hirta strain UIO030 1Y
AM491030.2 Haptolina ericina partial strain UIO026 Q17
ASV 1375 Prymnesiaceae X sp.
AM779755.1 Prymnesium palpebrale strain UIO 133
AJ246271.1 Prymnesium kappa strain UIO033 EN3
ASV 811 Prymnesium sp.
AM491029.2 Prymnesium chiton strain PLY 146A
AM491010.2 Prymnesium minor gene strain PLY304
AM491001.2 Prymnesium zebrinum strain ALGO HAP29
KY054990.1 Prymnesium pienaarii strain Xmm1S4
AM491028.2 Prymnesium simplex strain ALGO HAP51bis
KU561118.1 Prymnesium simplex isolate DHmm2W3
KU561110.1 Prymnesium pienaarii isolate DHmm2W1
MH182064.1 Prymnesium parvum
ASV 1670 Prymnesium sp.
AJ004868.1 Prymnesium aff. polylepis strain PCC200
AJ004866.1 Prymnesium polylepis isolate UIO036 B11
AJ246274.1 Chrysochromulina scutellum strain UIO46 G7
AJ246273.1 Chrysochromulina campanulifera strain J10
ASV 1530 Chrysochromulina sp.
ASV 135 Chrysochromulina sp.
ASV 398 Chrysochromulina sp.
AM491018.1 Chrysochromulina cymbium strain UIO R18
ASV 159 Chrysochromulina sp.
KY980316.1 Chrysochromulina strobilus isolate BH56 203
KY979987.1 Chrysochromulina strobilus isolate NY13S 42
ASV 1248 Chrysochromulina sp.
FN599060.1 Chrysochromulina strobilus strain PCC 43

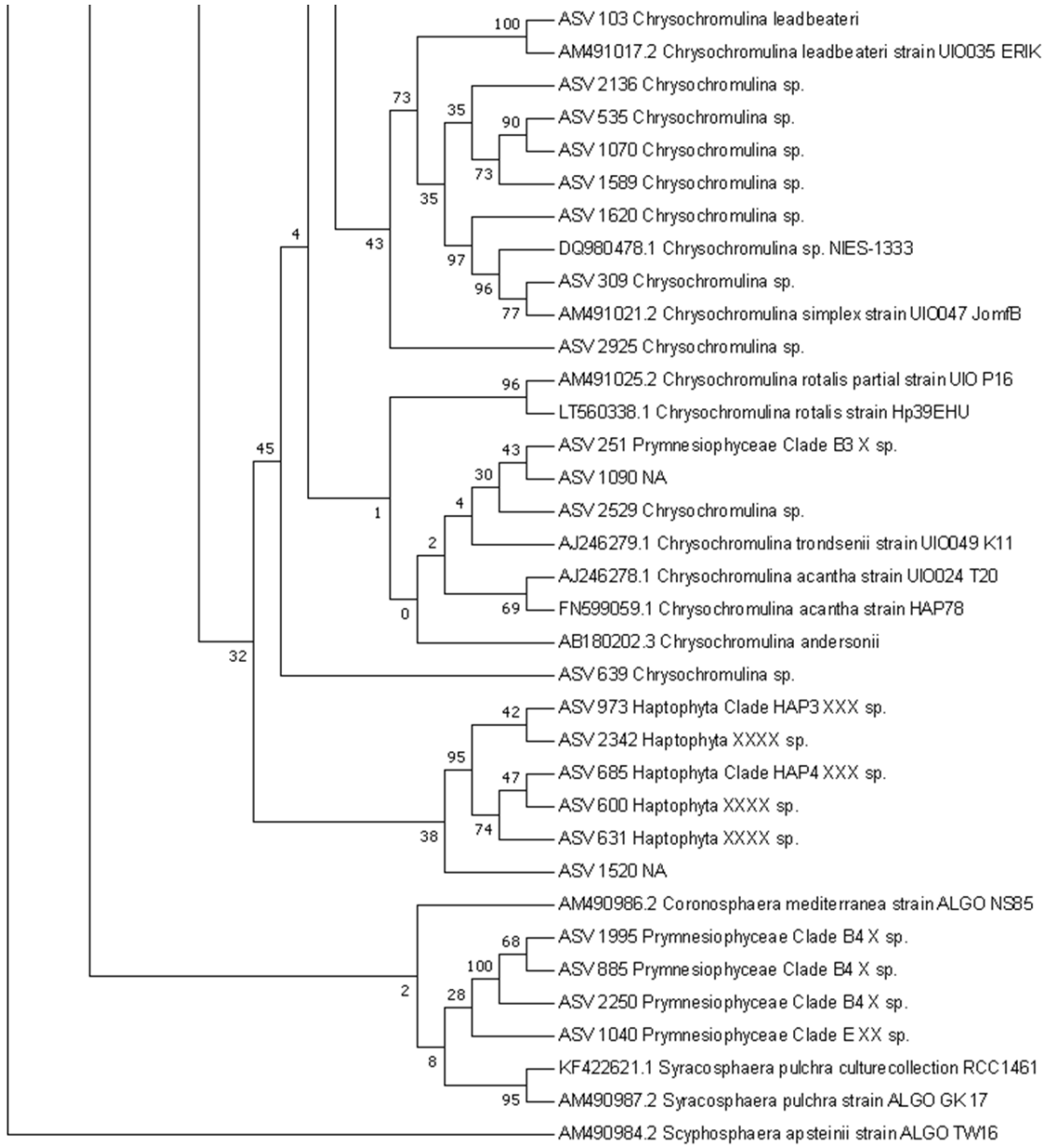


The initial identification of the presented ASVs was based on PR$^2$ and has subsequently been curated according to the shown phylogenetic placement.

# Chapter 2

**Community composition and resource use efficiency shift from spring to summer in Arctic pelagic protists**

Manuscript

# Community composition and resource use efficiency shift from spring to summer in Arctic pelagic protists

Claudia Sabine Bruhn[1,*], Sylke Wohlrab[1,2], Nina Lundholm[3], Per Juel Hansen[4] , Uwe John[1,2]

[1]: Alfred Wegener Institute, Helmholtz Centre for Polar and Marine Research, Am Handelshafen 12, 27570 Bremerhaven, Germany

[2]: Helmholtz Institute for Functional Marine Biodiversity at the University of Oldenburg, Ammerländer Heersstraße 231, 26129 Oldenburg, Germany

[3]: Natural History Museum of Denmark, University of Copenhagen, Øster Farimagsgade 5, 1353 Copenhagen, Denmark

[4]: University of Copenhagen, Strandpromenaden 5, 3000 Helsingør, Denmark

[*]corresponding authors: claudia.bruhn@awi.de, and uwe.john@awi.de

## Abstract

Marine pelagic protist communities are often driven by seasonal progressions between a phototrophic dominated spring bloom and a more diverse mixotrophic and heterotrophic summer community. The typical Artic spring community is usually dominated by phototrophic diatoms and/or mixotrophic haptophytes, while the summer community mainly consists of mixotrophic as well as heterotrophic ciliates and dinoflagellates. Snapshot- and transect studies are most common in the Arctic. Therefore, the transition of communities is still poorly understood and underlying factors are not well investigated. In this study, we present a metabarcoding survey that covers a course of approximately three months, including the shift from a protist spring community towards a summer community. Additionally, we investigated the relationship between biodiversity and ecosystem functioning in the respective progressing community. While the resource use efficiency (RUE) for nitrogen seemed to be rather high during the spring bloom event, it plateaued quickly and decreased towards the summer. Shortly after the decline in RUE, a shift from a mainly phototrophic community towards a heterotrophic/mixotrophic community was observed, while the community diversified. This suggests that the relatively low ability of a protist community to use some of the resources (here nitrogen) is an indicator of ecological niches opening up, enabling the community to diversify and to fill these niches. The diatom-dominated phytoplankton spring bloom remains one of the

most efficient biomass producing periods in the Arctic. Additionally, RUE was indicating the community shift, and may be used as an indicator in future studies.

Keywords: metabarcoding, functional diversity, trophic mode, biodiversity-ecosystem function

## 1. Introduction

The Arctic is characterized by a strong seasonality and therefore, a clearly defined seasonal pattern of pelagic marine protists can be observed. This pattern consists of a very pronounced phototrophic spring bloom with high biomass, while winter and summer hold much less biomass (Tammilehto *et al.*, 2017). The intense spring bloom marks the start of the productive season of high latitude areas (Sakshaug, 2004; Hodal *et al.*, 2012), and results in the generation of a high share of the ocean's annual primary production (Sakshaug, 2004). Nutrients are quickly depleted during the spring bloom (Bruhn *et al.*, 2021a), while the summer community, with much less available nutrients, is typically more diverse (Gran-Stadniczeñko *et al.*, 2018; Bruhn *et al.*, 2021a). The summer community is often characterized by less phototrophic and more mixotrophic protists, which combine traits from heterotrophs and phototrophs, utilizing both phagotrophy and photosynthesis as means to obtain energy (Stoecker & Lavrentyev, 2018; Flynn *et al.*, 2019).

The spring bloom in the Arctic and its high productivity are often topics of research. The drivers of the productivity are estimated to be irradiance and sea ice break up or other external factors (Ardyna *et al.*, 2014; Bruhn *et al.*, 2021b). For evaluation of the internal factors of productivity, the measure of resource use efficiency (RUE) can be utilized. RUE is the measure of biomass generated out of available nutrients and can be taken as an index of how efficiently available species are utilizing the given nutrients (Hodapp *et al.*, 2019). The concept law of the minimum (Liebig, 1840) is used to determine the limiting nutrient in a biological system. In a marine system, the limiting macronutrient is often nitrogen (Smith, 1984), or, when looking at bloom-forming diatoms, silicate (Conley & Malone, 1992). Resource use efficiency reflects how well a given community transfers nutrients into biomass, and has often been linked to the community's diversity (Tilman *et al.*, 1982; Ptacnik *et al.*, 2008). A meta-study of Ptacnik *et al.* (2008) resulted in the discovery that a general positive relationship between biodiversity and RUE in natural phytoplankton communities is observable. In line, a high biodiversity in the protist plankton community has been proposed to be beneficial for the whole ecosystem, resulting in a higher productivity and thus a higher ability to fix carbon, delivering more resources to higher trophic levels by grazing (Ptacnik *et al.*, 2008).

The pronounced seasonality of the Arctic makes this area interesting for researching RUE and its link to biodiversity of planktonic protists, because community shifts can be expected. So far, investigations of Arctic seasonal protist communities are available, but scarce (Marquardt *et al.*, 2016; Massicotte *et al.*, 2020), while transect and snapshot studies are more common (Baggesen *et al.*, 2012; Tillmann *et al.*, 2014; Elferink *et al.*, 2017). To use the approach of RUE for gaining further insight into the protist community shifts, longer studies are necessary. Here, we apply RUE for gaining a better understanding about the transition processes and mechanisms, which drive the transition from a spring bloom into the diverse summer protist community over the course of approximately three months.

To our knowledge, no study so far explores community transition and biodiversity in the context of RUE in an Arctic environment. To realize such a study holds valuable information about the productivity of the different groups within the protist community and their impact on the marine ecosystem as a whole. For instance, this can hold more information about how different taxa contribute to the fixing of carbon and therefore, the global carbon pump (Falkowski, 1994; Field *et al.*, 1998).

## 2. Material and Methods

### 2.1 Sampling locations and procedure

The sampling was performed at three distinct locations in the Disko Bay area, close to Qeqertarsuaq, West Greenland. The precise locations of the stations were 53.5444444 °E, 69.2111111 °N (hereafter referred to as station 1), 53.5208333 °E, 69.2158333 °N (hereafter referred to as station 2), and 53.4266667 °E, 69.2538889 °N (hereafter referred to as station 3). The station depths were 60, 140 and 325 m, respectively.

The sampling was performed between May 4 and July 27 2017, twice per month with 10 to 19 days between each sampling. An exception to this is an additional sampling on May 1, which was only performed on station 3 and only three days prior to the next sampling. It was meant as a test sampling, but delivered data that was valuable for this study, and thus was implemented in the study. Sampling at the three stations was always performed within a few hours on the same day as close to noon as possible.

From each station, water samples were taken with a 25 L Niskin water sampler (KC Denmark, Denmark) from the depths of 5 m, 10 m, 20 m, 30 m, and 40 m. The samples were collected in one 10 L polyethylene container per depth and station. The containers had been pre-treated with 3 % hydrochloric acid and flushed twice with the respective sample before

collection. The filled containers were stored cold and dark until sample processing on the same day.

### 2.2 Sample processing

Divided by the stations, 10 L per depth were pooled to obtain a manually integrated sample of the upper 40 m of the water column. Samples for analyses such as particulate organic nitrogen (PON), particulate organic carbon (POC), nutrients and chlorophyll *a* (Chl *a*) were taken from this integrated sample. The remaining 47.5 L were the basis for the size fractionation of the protist community, achieved through a series of filters. The initial filtration through a nylon mesh with 200 µm openings removed most of the multicellular zooplankton, which were not part of this study. As a consequence, some of the larger protist species or their colonies might have been discarded. The resulting filtrate was poured through a 20 µm nylon mesh, resulting in the microplankton size fraction with cell sizes ranging from 20 to 200 µm. Following filtration steps were carried out with polycarbonate filters and a vacuum pump not going below -500 mbar of pressure. For the nanoplankton size fraction, 3 L of the flow-through from the aforementioned microplankton size fraction were filtrated through a 3 µm polycarbonate filter, resulting in the size range of 3 to 20 µm. Of this filtrate, 1 L was again filtrated, this time through a 0.2 µm pore sized polycarbonate filter, resulting in the picoplankton size fraction ranging from 0.2 to 3 µm. The resulting samples were transferred into extraction buffer and frozen at -20 °C until DNA extraction using the NucleoSpin Soil kit from Macherey-Nagel (Germany).

### 2.3 Metabarcoding and phylogenetic analyses

For metabarcoding, the 16S Metagenomic Sequencing Library preparation protocol by Illumina (California, USA), modified with primers targeting the eukaryotic V4-region, was used (Piredda *et al.*, 2017). The resulting libraries of approximately 300 bp paired-end metabarcodes were sequenced with a MiSeq System (Illumina, California, USA). The resulting amplicon sequence variants (ASVs) were generated with the R-packages DADA2 (Callahan *et al.*, 2016), ShortRead (Morgan *et al.*, 2009), Biostrings (Paès *et al.*, 2021), and stringr (Wickham, 2019), and afterwards annotated via $PR^2$ database (version 4.11.1; Guillou *et al.*, 2012). For community analyses, sequences assigned to fungi and animals as well as low abundance ASVs (ASVs that were present not more than three times in 10 % of the samples) were excluded. Functional groups were assigned to the ASVs on the base of Bruhn *et al.* (2021b) and ASVs not assignable to any functional group were excluded from further analyses to keep all graphs comparable. The functional groups of heterotrophs (meaning not using photosynthesis), parasites (as a special form of heterotrophy), phototrophs (deriving energy exclusively from photosynthesis) and several different types of mixotrophs (employing both photosynthesis and phagotrophy) were

differentiated. The detailed criteria for functional group assignment can be taken from Bruhn *et al.* (2021b). Because of the close proximity – both regarding data outcome and distance, the three stations were averaged for community analyses to obtain a better overview of the general trends.

Additionally, the 50 most abundant ASVs (if applicable) from the taxa ciliates, cryptophytes, diatoms, dinoflagellates and haptophytes were phylogenetically analyzed. The ASV sequences were aligned with reference sequences via MAFFT (Katoh *et al.*, 2002), and phylogenetically analyzed using the maximum likelihood approach via MEGA7 (Felsenstein, 1985; Nei & Kumar, 2000; Kumar *et al.*, 2016). One hundred replicates of the bootstrap test were performed and combined in a consensus phylogenetic tree. Afterwards, the assignment of ASVs to species names was manually curated. The ASV abundance analyses were done in R, version 4.0.3 (R Core Team, 2021), with RStudio version 1.3.1093 (RStudio Team, 2020). Further used packages for analyses and visualization were ggplot2 (Wickham, 2016), phyloseq (McMurdie & Holmes, 2013), plyr (Wickham, 2011), and vegan (Oksanen *et al.*, 2019).

### 2.4 Resource use efficiency (RUE) analyses for protist community evaluation

In the marine context, nitrogen is usually considered the limiting nutrient as opposed to phosphorus in fresh water environments (Smith, 1984). Hence, total nitrogen was used as a factor for calculating RUE. Total nitrogen content of the water samples was calculated by converting nitrate, nitrite and ammonia values to grams of elemental nitrogen per liter and summating those values with particulate organic nitrogen values. The original values were published by Bruhn *et al.* (2021a). Chlorophyll *a* values are usually used as a biomass proxy (Ptacnik *et al.*, 2008). However, we decided to use particulate organic carbon (POC) to estimate biomass, because this value does not exclude non-phototrophic organisms, which can reach rather high abundances and are also accounted for in the community analysis. The resulting RUE was calculated as the ratio of units of POC per unit of nitrogen. The ASVs of the different size fractions were summated for RUE and richness analyses with the R-package vegan (Oksanen *et al.*, 2019) and visualized with ggplot2 (Wickham, 2016).

### 2.5 Diversity index calculation (Fisher alpha diversity)

For the size fractionated diversity analyses, we used Fisher alpha diversity (Fisher *et al.*, 1943). This index is based on the log scale, and therefore puts more emphasis on rare ASVs than Shannon-Weaver and Simpson diversity indices (Barjau-González *et al.*, 2012). Due to the PCR amplification step of the used metabarcoding approach, differences between rare and frequent

ASVs are artificially enlarged. In a time series like in the present study, rarer ASVs in one sampling may become more abundant in another one. This is why we decided to use Fisher alpha diversity, which helps to compensate the PCR-derived overrepresentation and provides a more accurate representation of the investigated community. Additionally, an additive model (GAM as described in Wood, 2011; Wood, 2017) was used to estimate trends and differences in trends for the Fisher alpha diversity calculated for each plankton size fraction. Comparisons in the additive model are based on the microplankton size fraction as reference base line. Analyses were performed in R with the 'mgcv' package (Wood, 2017).

## 3. Results

### 3.1 Functional group succession

After removal of non-protist and low abundance ASVs, a total of 1,683 different ASVs were detected. These ASVs could largely be assigned to one of 27 different functional groups or putative functional groups (Suppl. Table 1). Only one ASV was unassignable to any, which was an unidentified alveolate.

The functional groups of the observed communities in the three spatial stations all show similar succession patterns (Suppl. Fig.1). In the picoplankton size fraction, phototrophs were at a low percentage throughout the whole sampling period, while the highest percentages in ASV reads were different mixotrophs and heterotrophs (Fig. 1). On May 14, an increase of constitutive mixotrophs (i.e. photosynthetic organisms that also utilize phagotrophy; Mitra *et al.*, 2016) could be observed, accounting for more than half of the picoplankton reads. The nanoplankton size fraction had a relative majority of heterotrophic organisms, of which heterotrophic dinoflagellates had the highest share. The microplankton size fraction was dominated by phototrophic diatoms in early May, and the percentage afterwards gradually decreased over time. The share of diatoms decreased to under 50 % on the sampling on July 12, at which time constitutive mixotrophs – both dinoflagellates and non-dinoflagellates – became the most relatively abundant functional group. Heterotrophic organisms also gradually increased their share of ASV reads in the microplankton size fraction up until July 12. On July 27, the relative abundance of heterotrophic organisms again was approximately as low as in the beginning of the sampling period.

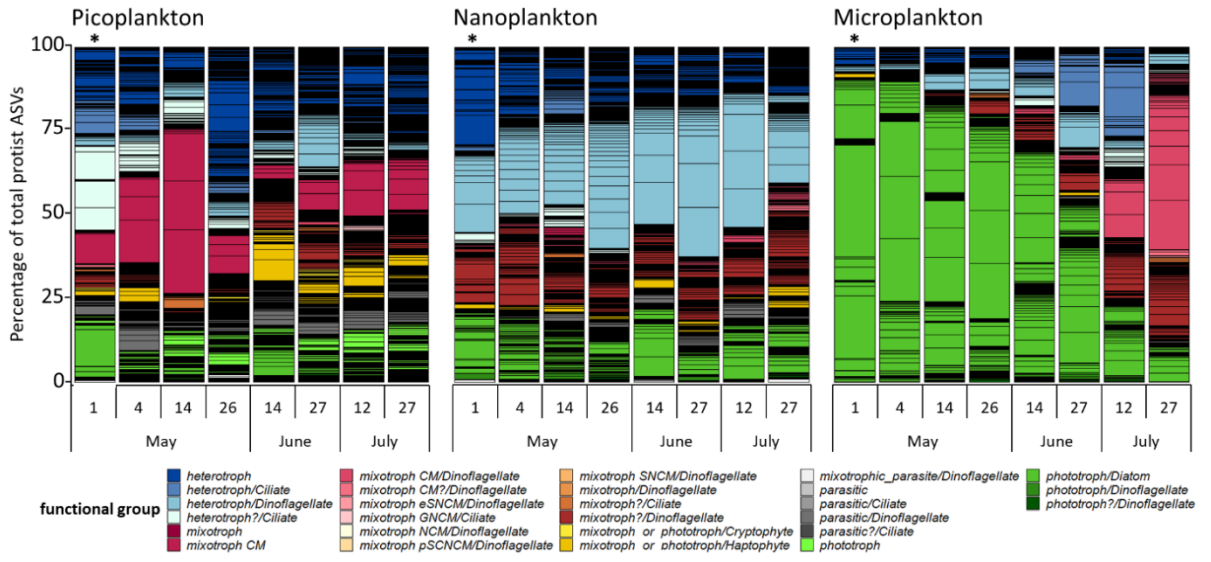


***Figure 1: Functional groups and their relative share of all protist ASVs and their succession over time.*** *The three stations were averaged, except for May 1 (*), which only consists of data from station 3. CM=constitutive mixotroph, eSNCM=endo-symbiotic specialist non-constitutive mixotrophs, GNCM=generalist non-constitutive mixotrophs, NCM=non-constitutive mixotroph, pSNCM=plastidic specialist non-constitutive mixotrophs. Question marks indicate ASVs from protists with ambiguous trophic modes.*

Further details of the functional groups are given through the analyses of the 50 most abundant ASVs (regarding their relative abundance) of the taxonomic groups of ciliates, cryptophytes, diatoms, dinoflagellates, and haptophytes (Fig. 2). In the following, the term "50 most abundant" will be used when meaning the 50 most abundant ASVs in relation to their relative abundance to all ASVs. Within the ciliates (Fig. 2A), the most abundant ASVs were detected in the picoplankton size fraction, but 14 of the 50 most abundant ciliate ASVs could not be assigned to the species level. The most abundant assignable ASVs belonged to the heterotroph ciliate *Leegardiella* spp. Cryptophytes (Fig. 2B) only had ten distinct ASVs in our analyses. *Falcomonas daucoides* and *Teleaulax gracilis* were the most abundantly detected species. According to their ASV assignment, especially in the picoplankton size fraction, where they had their highest relative abundance on June 27. It was not possible to assign these species to the respective ASVs with confidence, which resulted in the assignment of the putative species names and the marking of the species name with an interrogation mark. *Goniomonas* sp. did not have an obvious succession pattern with rather low relative abundances except for May 14, where it reached a relative abundance of 0.22 % of all protist ASVs of the picoplankton size fraction. The microplankton size fraction was devoid of cryptophytes.

The majority of the 50 most abundant diatoms were detected in the microplankton size fraction (Fig. 2C), where they accounted for more than 66 % of all protist ASVs on May 1, with

over 25 % of those assigned to *Porosira glacialis*. After the decline of *P. glacialis*, *Thalassiosira antarctica* var. *borealis* increased in abundance. From June 14 on, the relative abundance of these 50 diatom ASVs decreased below 20 % and stayed approximately at this level until the end of the sampling period.

Because *Gyrodinium helveticum* is a known freshwater dinoflagellate, we suspect a misidentification of this species. Existing reference sequences from marine isolates and our findings are resulting in the need of a systematic evaluation of its reference data and the corresponding isolates. We decided to label the respective ASVs "*Gyrodinium* cf. *helveticum*", to not add to this misidentification. The most abundant dinoflagellates exhibited a shift from *Gyrodinium* cf. *helveticum* to *Gyrodinium fusiforme* in the nanoplankton size fraction (Fig. 2D). In the microplankton size fraction, several *Alexandrium ostenfeldii* ASVs were increasing strongly in relative abundance with time.

Among the haptophytes, *Phaeocystis pouchettii* had the highest relative ASV abundance (Fig. 2E). It was mainly present in the picoplankton size fraction (as single cells), with a slight increase in relative abundance towards the summer, similar to *Chrysochromulina leadbeateri*, which also increased in relative abundance towards the summer. Seven ASVs from the most abundant haptophytes could not be assigned to a species. From this, six unidentified haptophyte ASVs phylogenetically clustered together forming a clade within the haptophytes, which was mostly present in the picoplankton size fraction.

### 3.2 Resource use efficiency and diversity changes

During the observed time, RUE as ratio of unit of POC per unit of nitrogen ranged between 0.45 and 6.03, fluctuating in a distinct pattern. Station 1 had its maximum RUE on June 14, station 2 on May 14 and station 3 on May 26, respectively (Fig. 3A). This resulted in the average RUE of the three stations to increase until May 26, after which a downward trend was seen. The ASV-based richness analysis showed an overall increase over time, ranging from 879 to 1,521 different ASVs being present at the same time in all three size fractions combined (Fig. 3B). Between the sampling from May 26 and June 14, a decrease in the slope of the incline was visible, after which the slope increased again until the end of the sampling period. The functional richness was also calculated for all three size fractions combined and individually, but no apparent increase or decrease trend was visible (Suppl. Table 2).


***Figure 2: Most abundant ASVs of the taxonomic groups of ciliates (A), cryptophytes (B), diatoms (C), dinoflagellates excluding Syndiniales (D), and haptophytes.*** *The three stations were averaged, except for May 1 (*), which only consists of data from station 3. The 50 most abundant ASVs, if applicable, are displayed. The respective species names after confirmation through phylogenetic placement were used. Because identification is only based on this, all species names are to be understood as putative.*

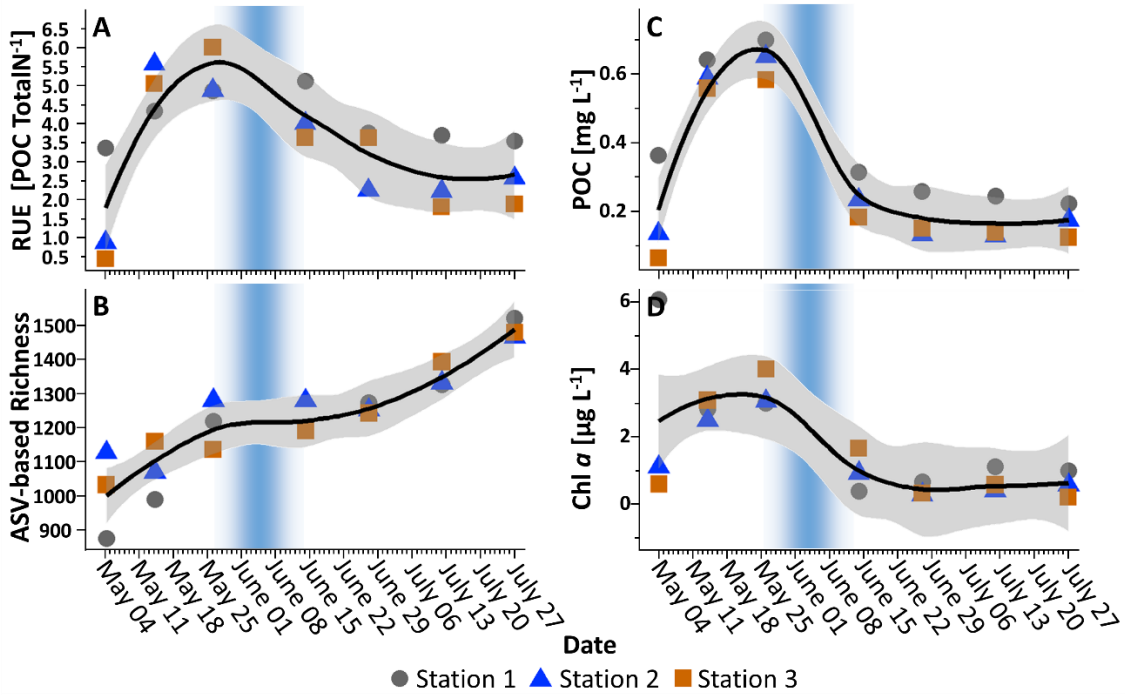


***Figure 3: RUE (A), ASV richness (B), and biomass as POC (C) and Chl a (D) of all size fractions over time.*** *RUE is shown as the unit of biomass as POC per unit of measured nitrogen, both dssolved (nitrite, nitrate and ammonia) and particulate (PON). ASV richness values are based on ASV numbers. The black line represents the mean of the three stations, whereas the grey area displays the 95 % confidence interval. The blue area marks the time of a pattern change from spring to summer community.*

Fisher alpha diversity and time (sampling day) were positively correlated in all of the three size fractions (Fig. 4). When using an additive model, pico- and nanoplankton were significantly different when compared to microplankton, with p=0.000652 for picoplankton and p=3.00e$^{-06}$ for nanoplankton. The estimated difference between the microplankton and picoplankton size fractions is linear, i.e. the increase in diversity in the picoplankton is more pronounced than in the microplankton size fraction, although the overall pattern is similar. The Fisher diversity index of the nanoplankton size fraction behaved differently than the other size fractions. Instead of a steady increase, the values resembled a sigmoid curve, first increasing strongly and then decreasing to a local minimum average on June 26, to increase again afterwards, rising above all values from previous days.

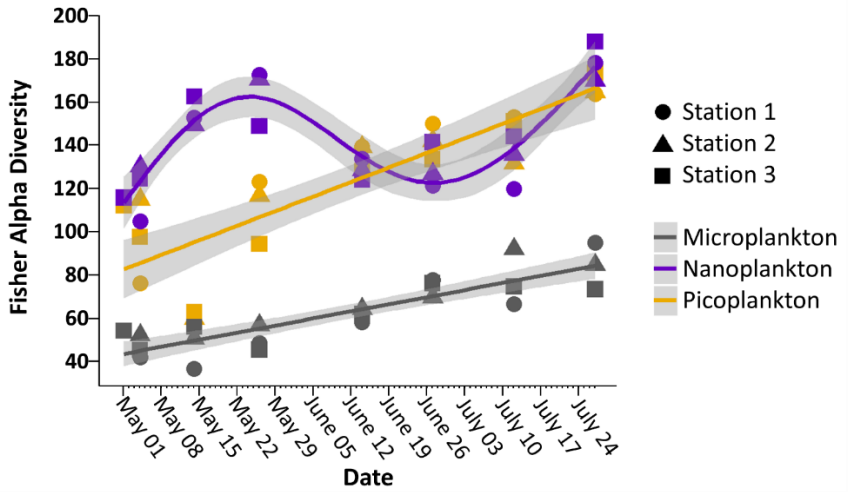


***Figure 4: Fisher alpha diversity of the different size fractions over time.*** *The patterns for picoplankton, nanoplankton, and microplankton are shown. The solid lines represent fits based on a generalized additive model, with the grey area showing the 95 % confidence intervals.*

## 4. Discussion

### 4.1 Control of primary producers by nutrient shortage

The observed succession patterns in the plankton in the Disko Bay were similar to previous observations in Arctic waters. Phototrophic diatoms dominated the protist community in spring similar to what has been observed in the same area in 2011 (Tammilehto *et al.*, 2017). Mixotrophs, especially constitutive mixotrophs, followed after, developing into a summer community characterized by e.g. mixotrophic dinoflagellates, comparable to earlier observations in Disko Bay (Levinsen *et al.*, 2000), and comparable to temperate regions (Raymont, 1980; Smayda & Trainer, 2010; Flynn *et al.*, 2019). In this study, only the microplankton size fraction showed a majority in relative abundance of diatoms in spring, while the pico- and nanoplankton size fractions also had a high share of heterotrophs and mixotrophs (Fig. 1). The Chl *a* peak in spring coincided with a high percentage of phototroph amplicon sequence reads in the microplankton size fraction (Fig. 3D). Thus, the majority of the photosynthetic activity was performed by larger species in the microplankton size fraction, mainly diatoms. From spring to summer, diatoms in the microplankton size fraction got – when taking relative abundance into account – replaced by mixotrophs, mainly dinoflagellates (Fig. 1), and Chl *a* declined (Fig. 3D). Therefore, fewer photosynthetic organisms were present in summer, and the photosynthesis of the community was mostly carried out by dinoflagellates and other mixotrophic organisms. Apart from an effect of depleted silicate on the change in community, mixotrophs may also have an advantage over the specialist diatoms in their trophic flexibility, being able to adapt to

generally lower nutrient availability. In the Arctic, mixotrophs have been suggested to have a particularly important role for primary production (Stoecker & Levrentyev, 2018). Arctic conditions favor the more generalist approach of mixotrophs over pure photo- or heterotrophs, as the strong seasonality puts more stress on resource use for growth and their related conditions. Mixotrophs are much more flexible in acquiring scarce resources and therefore have an advantage in the community (reviewed in Stoecker & Lavrentyev, 2018; Mitra *et al.*, 2016).

In a temperate region and a freshwater lake, a positive correlation between functional diversity and RUE have been observed (Ye *et al.*, 2019). We found no apparent correlation between functional diversity and RUE, as the amount of functional groups present was somewhat the same throughout the sampling period. Resource use efficiency even had a clear downward trend after the spring bloom, while the present functional groups remained largely the same. This could highlight that diatoms are much better at transferring nutrients to higher trophic levels than other phototrophic or mixotrophic organisms, emphasizing the importance of a diatom dominated spring bloom, in particular in the marine Arctic food web.

The community change was reflected in the RUE and in the taxonomic diversity. When Chl *a* levels dropped and the microplankton community shifted from diatoms to mixotrophs, the RUE dropped and the overall richness plateaued for a short while (Fig. 3A, B, indicated with a blue area). All three size fractions showed an overall increase in their Fisher alpha diversity. In contrast to this, studies with plants generally came to the conclusion that a higher diversity results in a higher RUE (Hector *et al.*, 1999; Loureau *et al.*, 2012). Planktonic protists, especially generalist non-constitutive mixotrophs, show a lower correlation of traits to nutrient uptake and RUE, thus behaving very differently from terrestrial plants. The traits of competing for the same resources may be the cause for lowered RUE when new species are introduced into the system (Hodapp *et al.*, 2019). Resources are redistributed between the species and if the "newly introduced" species have a lower RUE, the RUE of the whole community will be reduced (Nijs & Impens, 2000). This suggests the decline of the RUE to be a result of the community shift. On the other hand, it could also be that the RUE decline indicates ecological niches opening up, as the original species can no longer use the provided resources in an ideal way. This could be explained with multiple resource limitations (as discussed e.g. by Hodapp *et al.*, 2019). In this study, diatoms are possibly limited by silicate content and not by nitrogen, while the following constitutive mixotrophs do not need silicate to grow and are able to fill the opening ecological niches. At the beginning of the spring bloom event, nutrients were replete but were quickly depleted, as described in other studies (Leu *et al.*, 2006; Bruhn *et al.*, 2021a). The shift from diatoms to constitutive mixotrophic dinoflagellates driven by silicate limitation has also been seen e.g. in the Yellow Sea (Liang *et al.*, 2019) and the northern Arabian Sea (Xiang *et al.*, 2019). With mixotrophs, new resources, meaning feeding on other organisms, are added to the

calculation of the limiting resources, enabling a further diversification (as seen in the richness and in the general trends of the Fisher alpha diversity of the different size fractions) of the present species. In a modeling approach backed by experiments, higher temperature was found to be a factor resulting in a lower RUE (Thomas *et al.*, 2017). The diatom *Thalassiosira pseudonana* was less able to cope with low nutrients when the temperature was higher. If the observed protist community behaves similarly to this, the increasing temperature in the Arctic due to climate change (IPCC 2007) hint at the possibility that the available nutrients will probably not support the same amount of biomass in the future as they do now. This would lead to the conclusion that in the future, with increasing warmth due to climate change, less biomass would be produced and less food would be available for the upper trophic levels in the marine ecosystem.

### 4.2 Control of primary producers by higher trophic levels

Low RUE values may also be caused by grazing activity. Calanoid copepods are the most important mesozooplankton in Arctic waters (Arashkevich *et al.*, 2002; Ashjian *et al.*, 2003). As the next trophic level, copepods and other smaller metazoans are directly linked to the protist community. It has already been demonstrated that copepods react quickly to increased phytoplankton biomass, adapting to the available food source e.g. in the form of a pelagic diatom spring bloom (Forest *et al.*, 2011). The copepods are known to have a high abundance in Disko Bay just after the phytoplankton spring bloom peak (Møller & Nielsen, 2020). This suggests a top-down regulation (grazing) of the observed community productivity. Since 1992, the copepod species have been observed to change from a majority of *Calanus hyperboreus* and *C. glacialis* to an increasing part being the smaller and less fat *C. finmarchicus* (Møller & Nielsen, 2020). The change in copepod composition may result in different grazing patterns and therefore may lead to different protist communities in the future as well. It has already been observed that larger species are more able to feed on *Phaeocystis* colonies than smaller copepods (Nejstgaard *et al.*, 2007), supporting the hypothesis that selective grazing can alter the protist community. In addition to grazing from animals, the approach of utilizing POC as a biomass indicator includes also heterotrophic micrograzers, which may graze on other protists, possibly decreasing the RUE values but not the process of creating biomass from the available nutrients.

### 4.3 Size fractionation is giving more insights into the detailed community changes

Ciliates showing up in the pico- and nanoplankton size fractions illustrate that the filtration method does result in the physical destruction of some cells, making the remnants show up in a

smaller size fraction than their complete cells belong to (Fig. 1A). However, the method can reveal additional information, e.g. if *Phaeocystis* sp. is organized in colonies or solitary cells, making the reads appear in different size fractions (as shown in Bruhn *et al.*, 2021b). In our case, the size fractionation elaborated about patterns in biodiversity and species succession patterns that would have otherwise not been observed. All size fractions increased in biodiversity over the monitored time period, with picoplankton having the largest increase and microplankton the smallest. The Fisher alpha diversity of the nanoplankton size fraction, however, followed the pattern of a sigmoid curve, while the other size fractions had a linear relationship (Fig. 4). In comparison, the functional diversity of the nanoplankton size fraction did not notably change over time (Fig. 1). This hints at community changes not in the functional diversity, but in species succession with similar or identical functional diversity. The reason behind these differences might be the cell size itself, which is the reason for many differences in advantages and disadvantages in an ecosystem: In contrast to larger cells, smaller ones have lower sinking losses, higher nutrient uptake rates due to a higher surface-to-volume ratio (Reynolds, 2006), and probably higher cell division rates. On the other hand, Arctic copepods seem to prefer grazing on phototrophs (Forest *et al.*, 2011), which, in the presented case, were mainly larger cells, being present in the microplankton size fraction. The sigmoid curve pattern of the nanoplankton diversity indicates fluctuating impacts of these factors over the course of the observed time.

Some species changes that are indicated in the diversity analyses can be evaluated further when taking the 50 most abundant ASVs of the larger groups into account (Fig. 2). Many non-phototrophic microorganisms are still unclassified, showing the need for more species reference data in the databases to elucidate strains that are not cultivatable (del Campo *et al.*, 2013). This is reflected by the vast amount of unidentified but relatively abundant ciliates in the present study (Fig. 1A). Within the cryptophytes, both putative *Teleaulax daucoides* and *Plagioselmis prolonga* were identified, with a slight increase in relative abundance of *P. prolonga* towards the summer. This indicates that both putative species are possibly the diploid/haploid stages of the same organism and follow the succession patterns as described in Altenburger *et al.* (2020). The unusually abundant appearance of *Goniomonas* sp. on May 14 may be explained by a patchy spatial distribution. However, little is known about the specific distributional patterns of *Goniomonas* spp., meaning that this remains speculative.

For the strictly phototrophic diatoms, the most abundant family is Thalassiosiraceae, which is mostly present in the microplankton size fraction. The shift from microplanktonic *Porosira glacialis* to *Thalassiosira antarctica* var. *borealis* can be observed in May. In coastal waters of Antarctica, it was already found that *T. antarctica*, a close relative to *T. antarctica* var. *borealis*, which was found in this study, favors slightly warmer waters than *P. glacialis* (Pike *et*

*al.*, 2009). This may have parallels with our findings in the northern hemisphere. Summer warms up the water temperature, possibly favoring the prevalence of *T. antarctica* var. *borealis* over *P. glacialis.*

In the nanoplankton size fraction of the most abundant dinoflagellates, a reciprocal shift from *Gyrodinium cf. helveticum* towards *G. fusiforme* is visible (Fig. 2D). Some *Gyrodinium* species are prevalent grazers, known to graze on *Phaeocystis* spp. (Grattepanche *et al.*, 2011). The sudden relative increase of *Phaeocystis pouchettii* (Fig. 2E) coincides with the shift from *G. fusiforme* to *G.* cf. *helveticum*. This could mean that *G. fusiforme* is targeting *P. pouchettii* more as a food source than *G*. cf. *helveticum*, making it possible for *P. pouchetti* to grow in relative abundance. *Gyrodinium helveticum* is a typical freshwater dinoflagellate, which was detected e.g. in Lake Baikal (Annenkova *et al.*, 2009) or a Japanese lake (Takano & Horiguchi, 2004). However, based on molecular data, several very close relatives have been found in marine waters, suggesting the prevalence of a marine sister clade of *G. helveticum* (Gómez *et al.*, 2020), which is most likely also what was identified as *G.* cf. *helveticum* in the present study. *Margalefidinium polykrikoides* is a known warm water dinoflagellate, which also can cause harmful algal blooms (Azanza *et al.*, 2008; Gobler *et al.*, 2008; Richlen *et al.*, 2010). It was also detected in the presented study in the Arctic, which is rather unusual, but could be also hinting at an unidentified close relative with a very similar barcode sequence within the V4 region of the SSU rRNA.

**Conclusion**

A community shift from a pelagic spring bloom to a summer community was observed. While the bloom itself was dominated by microplanktonic phototrophic Thalassiosiraceae, the niche of phototrophy was later taken up by mixotrophic dinoflagellates. The RUE was highest when the diversity was below its median, highlighting the efficient productivity of diatoms during the spring bloom event. The spring bloom event therefore is one of the most productive, if not the most productive, time in the Arctic marine ecosystem. After the biomass maximum, i.e. the spring bloom, RUE decreased and richness increased. This hints at biological niches opening up which are filled by newly upcoming taxa. The reasons for this shift may lie in either regulation by nutrient availability and/or regulation by grazers of the seasonally changing ecosystem.

While the trophic diversity changed much more in the microplankton size fraction than in the smaller size fractions, all size fractions increased in diversity. However, the nanoplankton size fraction displayed a more dynamic pattern than the other two size fractions, hinting at more understudied reciprocal changes from organisms occupying a similar niche, such as the shift from *G. fusiforme* to *G.* cf. *helveticum*.

**Acknowledgements**

We thank Nancy Kühne for her technical assistance in the laboratory. Regin Rønn, Kjeld Akaraaq Mølgaard, Abel Brandt, and Johannes Mølgaard deserve our thanks for their help during the sampling campaign in Greenland. Our thanks for the support of POC and PON analyses go to Florian Koch. Thanks also go to Kai-Uwe Ludichowski who supported nutrient analyses.

The work of Claudia Sabine Bruhn, Sylke Wohlrab, and Uwe John was financially supported under the POF IV topic 6 and subtopic 2 research program of the Alfred Wegener Institute, Helmholtz Centre for Polar and Marine Research. Part of the funding for Sylke Wohlrab was provided by HIFMB, a collaboration between the Alfred-Wegener-Institute, Helmholtz-Center for Polar and Marine Research, and the Carl-von-Ossietzky University Oldenburg, initially funded by the Ministry for Science and Culture of Lower Saxony (MWK) and the Volkswagen Foundation through the "Niedersächsisches Vorab" grant program (grant number ZN3285). Nina Lundholm was funded through the Danish Research Council for Nature and Universe (9040-00248B). The Marine Basis Disko Program as part of the Greenland Environmental Monitoring Program (GEM) by the Danish Ministry of the Environment funded Per Juel Hansen and Nina Lundholm.

**Competing interests**

The authors declare no competing interests.

**References**

Altenburger, A., Blossom, H.E., Garcia-Cuetos, L., Jakobsen, H.H., Carstensen, J., Lundholm, N., *et al.* (2020) Dimorphism in cryptophytes — The case of *Teleaulax amphioxeia*/*Plagioselmis prolonga* and its ecological implications. *Sci Adv* **6**: eabb1611.

Annenkova, N. V., Belykh, O.I., Denikina, N.N., and Belikov, S.I. (2009) Identification of Dinoflagellates from the Lake Baikal on the Basis of Molecular Genetic Data. *Dokl Biol Siences* **426**: 1–4.

Arashkevich, E., Wassmann, P., Pasternak, A., and Wexels Riser, C. (2002) Seasonal and spatial changes in biomass, structure, and development progress of the zooplankton community in the Barents Sea. *J Mar Syst* **38**: 125–145.

Ashjian, C.J., Campbell, R.G., Welch, H.E., Butler, M., and van Keuren, D. (2003) Annual cycle in abundance, distribution, and size in relation to hydrography of important copepod species in the western Arctic Ocean. *Deep Res Part I* **50**: 1235–1261.

Azanza, R. V, David, L.T., Borja, R.T., Baula, I.U., and Fukuyo, Y. (2008) An extensive *Cochlodinium* bloom along the western coast of Palawan, Philippines. *Harmful Algae* **7**: 324–330.

Baggesen, C., Moestrup, Ø., Daugbjerg, N., Krock, B., Cembella, A.D., and Madsen, S. (2012) Molecular phylogeny and toxin profiles of *Alexandrium tamarense* (Lebour) Balech (Dinophyceae) from the west coast of Greenland. *Harmful Algae* **19**: 108–116.

Barjau-González, E., Rodríguez-Romero, J., Galván-Magaña, F., and López-Martínez, J. (2012) Changes in the taxonomic diversity of the reef fish community of San José Island, Gulf of California, Mexico. *Biodivers Conserv* **21**: 3543–3554.

Bruhn, C.S., Wohlrab, S., Krock, B., Lundholm, N., and John, U. (2021a) Seasonal plankton succession is in accordance with phycotoxin occurrence in Disko Bay, West Greenland. *Harmful Algae* **103**.

Bruhn, C.S., Lundholm, N., Hansen, P.J., Wohlrab, S., and John, U. (2021b) Transition from a mixotrophic/heterotrophic protist community during the dark winter to a photoautotrophic community in spring in Arctic surface waters. Manuscript.

Callahan, B. J., McMurdie, P. J., Rosen, M. J., Han, A. W., Johnson, A. J. A, and Holmes, S. P. (2016) DADA2: High-resolution sample inference from Illumina amplicon data. *Nat. Methods* **13**: 581–583.

Conley, D.J. and Malone, T.C. (1992) Annual cycle of dissolved silicate in Chesapeake Bay: implications for the production and fate of phytoplankton biomass. *Mar Ecol Prog Ser* **81**: 121–128.

del Campo, J., Balagué, V., Forn, I., Lekunberri, I., and Massana, R. (2013) Culturing Bias in Marine Heterotrophic Flagellates Analyzed Through Seawater Enrichment Incubations. *Microb Ecol* **66**: 489–499.

Elferink, S., Neuhaus, S., Wohlrab, S., Toebe, K., Voß, D., Gottschling, M., *et al.* (2017) Molecular diversity patterns among various phytoplankton size-fractions in West Greenland in late summer. *Deep Res Part I* **121**: 54–69.

Falkowski, P.G. (1994) The role of phytoplankton photosynthesis in global biogeochemical cycles. *Photosynth Res* **39**: 235–258.

Felsenstein, J. (1985) Confidence limits on phylogenies: an approach using the bootstrap. **39**: 783–791.

Field, C.B., Behrenfeld, M.J., and Randerson, J.T. (1998) Primary Production of the Biosphere: Integrating Terrestrial and Oceanic Components. *Science* **281**: 237–241.

Fisher, R.A., Corbet, A.S., and Williams, C.B. (1943) The Relation Between the Number of Species and the Number of Individuals in a Random Sample of an Animal Population. *J Anim Ecol* **12**: 42–58.

Flynn, K.J., Stoecker, D.K., Mitra, A., Raven, J.A., Glibert, P.M., Hansen, P.J., *et al.* (2013) Misuse of the phytoplankton – zooplankton dichotomy: the need to assign organisms as mixotrophs within plankton functional types. *J Plankt Res* **35**: 3–11.

Flynn, K.J., Mitra, A., Anestis, K., Anschütz, A.A., Calbet, A., Duarte Ferreira, G., *et al.* (2019) Mixotrophic protists and a new paradigm for marine ecology: where does plankton research go now? *J Plankton Res* **41**: 375–391.

Forest, A., Galindo, V., Darnis, G., Pineault, S., Lalande, C., Tremblay, J.-É., and Fortier, L. (2011) Carbon biomass, elemental ratios (C:N) and stable isotopic composition ($\delta^{13}C$, $\delta^{15}N$) of dominant calanoid copepods during the winter-to-summer transition in the Amundsen Gulf (Arctic Ocean). *J Plankton Res* **33**: 161–178.

Gobler, C.J., Berry, D.L., Anderson, O.R., Burson, A., Koch, F., Rodgers, B.S., *et al.* (2008) Characterization, dynamics, and ecological impacts of harmful *Cochlodinium polykrikoides* blooms on eastern Long Island, NY, USA. *Harmful Algae* **7**: 293–307.

Gómez, F., Artigas, L.F., and Gast, R.J. (2020) Phylogeny and synonymy of *Gyrodinium heterostriatum* comb. nov. (Dinophyceae), a Common unarmored Dinoflagellate in the World Oceans. *ACTA Protozool* **59**: 77–87.

Gran-Stadniczeñko, S., Egge, E., Hostyeva, V., Logares, R., Eikrem, W., and Edvardsen, B. (2019) Protist Diversity and Seasonal Dynamics in Skagerrak Plankton Communities as Revealed by Metabarcoding and Microscopy. *J Eukaryot Microbiol* **66**: 494–513.

Grattepanche, J.-D., Breton, E., Brylinski, J.-M., Lecuyer, E., and Christaki, U. (2011) Succession of primary producers and micrograzers in a coastal ecosystem dominated by *Phaeocystis globosa* blooms. *J Plankton Res* **33**: 37–50.

Griffith, A.W. and Gobler, C.J. (2016) Temperature controls the toxicity of the ichthyotoxic dinoflagellate *Cochlodinium polykrikoides*. *Mar Ecol Prog Ser* **545**: 63–76.

Guillou, L., Bachar, D., Audic, S., Bass, D., Berney, C., Bittner, L., *et al.* (2013) The Protist Ribosomal Reference database (PR²): a catalog of unicellular eukaryote Small Sub-Unit rRNA sequences with curated taxonomy. *Nucleic Acids Res* **41**: D597–D604.

Hector, A., Schmid, B., Beierkuhnlein, C., Caldeira, M.C., Diemer, M., Dimitrakopoulos, P.G., *et al.* (1999) Plant Diversity and Productivity Experiments in European Grasslands. *Science* **286**: 1123–1127.

Hodal, H., Falk-Petersen, S., Hop, H., Kristiansen, S., and Reigstad, M. (2012) Spring bloom dynamics in Kongsfjorden, Svalbard: nutrients, phytoplankton, protozoans and primary production. *Polar Biol* **35**: 191–203.

Hodapp, D., Hillebrand, H., and Striebel, M. (2019) "Unifying" the Concept of Resource Use Efficiency in Ecology. *Front Ecol Evol* **6**: 1–14.

Katoh, K., Misawa, K., Kuma, K., and Miyata, T. (2002) MAFFT: a novel method for rapid multiple sequence alignment based on fast Fourier transform. *Nucleic Acids Res* **30**: 3059–3066.

Kumar, S., Stecher, G., and Tamura, K. (2016) MEGA7: Molecular Evolutionary Genetics Analysis Version 7.0 for Bigger Datasets. *Mol* **33**: 1870–1874.

Leu, E., Falk-Petersen, S., Kwaśniewski, S., Wulff, A., Edvardsen, K., and Hessen, D.O. (2006) Fatty acid dynamics during the spring bloom in a High Arctic fjord: importance of abiotic factors versus community changes. *Can J Fish Aquat Sci* **63**: 2760–2779.

Levinsen, H., Nielsen, T.G., and Hansen, B.W. (2000) Annual succession of marine pelagic protozoans in Disko Bay, West Greenland, with emphasis on winter dynamics. *Mar Ecol Prog Ser* **206**: 119–134.

Liang, Y., Zhang, G., Wan, A., Zhao, Z., Wang, S., and Liu, Q. (2019) Nutrient-limitation induced diatom-dinoflagellate shift of spring phytoplankton community in an off shore shell fish farming area. *Mar Pollut Bull* **141**: 1–8.

Liebig, J. von (1840) Die organische Chemie in ihrer Anwendung auf Agricultur und Physiologie, Vieweg (Braunschweig).

Loreau, M., Sapijanskas, J., Isbell, F., and Hector, A. (2012) Niche and fitness differences relate the maintenance of diversity to ecosystem function: Comment. *Ecology* **93**: 1482–1487.

Marquardt, M., Vader, A., Stübner, E.I., Reigstad, M., and Gabrielsen, T.M. (2016) Strong Seasonality of Marine Microbial Eukaryotes in a High-Arctic Fjord (Isfjorden, in West Spitsbergen, Norway). *Appl Environ Microbiol* **82**: 1868–1880.

Massicotte, P., Amiraux, R., Amyot, M.-P., Archambault, P., Ardyna, M., Arnaud, L., *et al.* (2020) Green Edge ice camp campaigns: understanding the processes controlling the under-ice Arctic phytoplankton spring bloom. *Earth Sysem Sci Data* **12**: 151–176.

McMurdie, P.J. and Holmes, S. (2013) phyloseq: An R package for reproducible interactive analysis and graphics of microbiome census data. *PLoS One* **8**: e61217.

Mitra, A., Flynn, K.J., Tillmann, U., Raven, J.A., Caron, D., Stoecker, D.K., *et al.* (2016) Defining Planktonic Protist Functional Groups on Mechanisms for Energy and Nutrient Acquisition: Incorporation of Diverse Mixotrophic Strategies. *Protist* **167**: 106–120.

Møller, E.F. and Nielsen, T.G. (2020) Borealization of Arctic zooplankton — smaller and less fat zooplankton species in Disko Bay, Western Greenland. *Limnol Oceanogr* **65**: 1175–1188.

Morgan, M., Anders, S., Lawrence, M., Aboyoun, P., Pagès, H., and Gentleman, R. (2009) ShortRead: a bioconductor package for input, quality assessment and exploration of high-throughput sequence data. *Bioinformatics* **25**(19): 2607–2608.

Nei, M. and Kumar, S. (2000) Molecular evolution and phylogenetics, *Oxford University Press, Oxford*.

Nejstgaard, J.C., Tang, K.W., Steinke, M., Dutz, J., Koski, M., Antajan, E., and Long, J.D. (2007) Zooplankton grazing on *Phaeocystis*: a quantitative review and future challenges. *Biogeochemistry* **83**: 147–172.

Nijs, I. and Impens, I. (2016) Underlying Effects of Resource Use Efficiency in Diversity-Productivity. *Oikos* **91**: 204–208.

Oksanen, J., Blanchet, F.G., Friendly, M., Kindt, R., Legendre, P., McGlinn, D., *et al.* (2019) vegan: Community Ecology Package. R package version 2.5-6.

Pachauri, R. K., Reisinger A. (Eds., Core Writing Team). IPCC, 2007: Climate Change 2007: Synthesis Report. Contribution of Working Groups I, II and III to the Fourth Assessment Report of the Intergovernmental Panel on Climate Change. *IPCC, Geneva, Switzerland,* 104 pp.

Paès, H., Aboyoun, P., Gentleman, R. and DebRoy, S. (2021) Biostrings: Efficient manipulation of biological strings. R package version 2.62.0.

Pike, J., Crosta, X., Maddison, E.J., Stickley, C.E., Denis, D., Barbara, L., and Renssen, H. (2009) Observations on the relationship between the Antarctic coastal diatoms *Thalassiosira antarctica* Comber and *Porosira glacialis* (Grunow) Jørgensen and sea ice concentrations during the late Quaternary. *Mar Micropaleontol* **73**: 14–25.

Piredda, R., Tomasino, M.P., Erchia, A.M.D., Manzari, C., Pesole, G., Montresor, M., *et al.* (2017) Diversity and temporal patterns of planktonic protist assemblages at a Mediterranean LTER site. *FEMS Microbiol Ecol* **93**: 1–14.

Ptacnik, R., Solimini, A.G., Andersen, T., Tamminen, T., Brettum, P., Lepisto, L., *et al.* (2008) Diversity predicts stability and resource use efficiency in natural phytoplankton communities. *PNAS* **105**: 5134–5138.

R Core Team (2021) R: A language and environment for statistical computing. R Found Stat Comput Vienna, Austria.

Raymont, J.E.G. (1980) Plankton and Productivity in the Oceans, 2nd ed. *Pergamon Press, Ltd*.

Reynolds, C.S. (2006) The Ecology of Phytoplankton, *Cambridge University Press, Cambridge*.

Richlen, M.L., Morton, S.L., Jamali, E.A., Rajan, A., and Anderson, D.M. (2010) The catastrophic 2008–2009 red tide in the Arabian gulf region, with observations on the identification and phylogeny of the fish-killing dinoflagellate *Cochlodinium polykrikoides*. *Harmful Algae* **9**: 163–172.

RStudio Team (2020) RStudio: Integrated Development for R. RStudio, PBC, Boston, MA.

Sakshaug, E. (2004) Primary and Secondary Production in the Arctic Seas. In The Organic Carbon Cycle in the Arctic Ocean. Stein, R. and Macdonald, R.W. (eds). *Berlin: Springer*, pp. 57–81.

Smayda, T.J. and Trainer, V.L. (2010) Progress in Oceanography Dinoflagellate blooms in upwelling systems: Seeding, variability, and contrasts with diatom bloom behaviour. *Prog Oceanogr* **85**: 92–107.

Smith, S. V. (1984) Phosphorus versus nitrogen limitation. *Limnol Oceanogr* **29**: 1149–1160.

Sprong, P.A.A., Fofonova, V., Wiltshire, K.H., Neuhaus, S., Ludwichowski, K.U., Käse, L., *et al.* (2020) Spatial dynamics of eukaryotic microbial communities in the German Bight. *J Sea Res* **163**: 101914.

Stoecker, D.K. and Lavrentyev, P.J. (2018) Mixotrophic Plankton in the Polar Seas: A Pan-Arctic Review. *Front Mar Sci* **5**: 1–12.

Takano, Y. and Horiguchi, T. (2004) Surface ultrastructure and molecular phylogenetics of four unarmored heterotrophic dinoflagellates, including the type species of the genus *Gyrodinium* (Dinophyceae). *Phycol Res* **52**: 107–116.

Tammilehto, A., Watts, P.C., and Lundholm, N. (2017) Isolation by Time During an Arctic Phytoplankton Spring Bloom. *J Eukaryot Microbiol* **64**: 248–256.

Thomas, M.K., Aranguren-Gassis, M., Kremer, C.T., Gould, M.R., Anderson, K., Klausmeier, C.A., and Litchman, E. (2017) Temperature-nutrient interactions exacerbate sensitivity to warming in phytoplankton. *Glob Chang Biol* **23**: 3269–3280.

Tillmann, U., Kremp, A., Tahvanainen, P., and Krock, B. (2014) Characterization of spirolide producing *Alexandrium ostenfeldii* (Dinophyceae) from the western Arctic. *Harmful Algae* **39**: 259–270.

Tilman, D., Kilham, S.S., and Kilham, P. (1982) Phytoplankton Community Ecology: The Role of Limiting Nutrients. *Ann Rev Ecol Syst* **13**: 349–372.

Wickham, H. (2019) stringr: Simple, Consistent Wrappers for Common String Operations. R package version 1.4.0.

Wickham, H. (2016) ggplot2: Elegant Graphics for Data Analysis. *Springer-Verlag, NY*.

Wickham, H. (2011) The Split-Apply-Combine Strategy for Data Analysis. *J Stat Softw* **40**: 1–29.

Wood, S.N. (2017) Generalized Additive Models: An Introduction with R, 2nd ed. Chapman and Hall/*CRC Press*.

Wood, S.N. (2011) Fast stable restricted maximum likelihood and marginal likelihood estimation of semiparametric generalized linear models. *J R Stat Soc* **73**: 3–36.

Xiang, C., Tan, Y., Zhang, H., Liu, J., Ke, Z., and Li, G. (2019) The key to dinoflagellate (*Noctiluca scintillans*) blooming and outcompeting diatoms in winter off Pakistan, northern Arabian Sea. *Sci Total Environ* **694**: 133396.

Ye, L., Chang, C.-W., Matsuzaki, S.S., Takamura, N., Widdicombe, C.E., and Hsieh, C. (2019) Functional diversity promotes phytoplankton resource use efficiency. *J Ecol* **107**: 2353–2363.

# Chapter 2

**Supplementary**

**Material**

**Supplementary Table 1:** Criteria for assigned trophic mode of organisms.

| *Assigned trophic mode* | *Assigned to* |
|---|---|
| *heterotroph* | Anything not within the other heterotroph groups that lacks photosynthetic plastids |
| *heterotroph/Ciliate* | A phagotrophic (heterotrophic) ciliate, that does not follow a parasitic lifestyle |
| *heterotroph/Dinoflagellate* | A heterotrophic dinoflagellate – a phagotrophic dinoflagellate without chloroplasts that does not display a parasitic lifestyle |
| *heterotroph?/Ciliate* | A ciliate that is suspected to be a phagotrophic heterotroph, and does not display a parasitic lifestyle |
| *mixotroph* | Mixoplankton – a planktonic protist that combine *phototrophy* and *phagotrophy* |
| *mixotroph CM* | A constitutive mixoplankonic protist that has an innate, constitutive, ability to conduct photosynthesis and that is also able to phagocytise. (Cf. *NCM*.) |
| *mixotroph CM/Dinoflagellate* | A dinoflagellate with its own chloroplast(s) that combines phototrophy and phagotrophy |
| *mixotroph CM?/Dinoflagellate* | A dinoflagellate that is suspected being a constitutive mixotroph |
| *mixotroph eSNCM/Dinoflagellate* | A specialist non-constitutive mixoplanktonic dinoflagellate that harbours endo/ecto symbionts |
| *mixotroph GNCM/Ciliate* | A generalist non-constitutive mixoplanktonic ciliate that lacks an innate, constitutive, ability to perform photosynthesis and acquires its phototrophic potential from various other organisms. (Cf. CM, GNCM, SNCM.) |
| *mixotroph NCM/Dinoflagellate* | A non-constitutive mixoplanktonic dinoflagellate that lacks an innate, constitutive, ability to conduct photosynthesis and thus acquires its phototrophic potential from (an)other organism(s). (Cf. CM, GNCM, SNCM.) |
| *mixotroph pSNCM/Dinoflagellate* | A plastidic specialist non-constitutive mixoplankton; these acquire and exploit only the plastids originating from another organism. (Cf. CM, GNCM, SNCM.) |
| *mixotroph/Dinoflagellate* | Mixoplanktonic dinoflagellate |
| *mixotroph?/Ciliate* | A ciliate suspected of a mixotrophic lifestyle |
| *mixotroph?/Dinoflagellate* | A dinoflagellate suspected of a mixotrophic lifestyle |

| | |
|---|---|
| *mixotroph or phototroph/Cryptophyte* | A photosynthetic cryptophyte in which it is unknown to which extent is capable of phagotropy |
| *mixotroph or phototroph/Haptophyte* | A photosynthetic haptophyte in which it is unknown to which extent is capable of phagotropy |
| *mixotrophic parasite/Dinoflagellate* | A parasitic dinoflagellate which has its own chloroplasts |
| *parasitic* | The organisms are classified as parasitic, but do not fit into the other categories |
| *parasitic/Ciliate* | A parasitic ciliate |
| *parasitic/Dinoflagellate* | A parasitic dinoflagellate, in essence belonging to Syndiniales |
| *parasitic?/Ciliate* | A ciliate that is suspected of being a parasite |
| *phototroph* | A photosynthetic organism |
| *phototroph/Diatom* | Diatoms are exclusively phototrophic – they do not have the ability of phagocytosis; therefore all diatoms were summarized in this category |
| *phototroph/Dinoflagellate* | A phototrophic dinoflagellate |
| *phototroph?/Dinoflagellate* | A dinoflagellate that is suspected of being a phototroph |
| *NA* | It was not possible to assign a trophic mode, either due to poor identification or to lack of information on the assigned taxon |

**Supplementary Figure 1: Relative abundance of protist ASVs over time at the different stations, divided by functional group.** (A) Station 1, (B) station 2, (C) station 3.

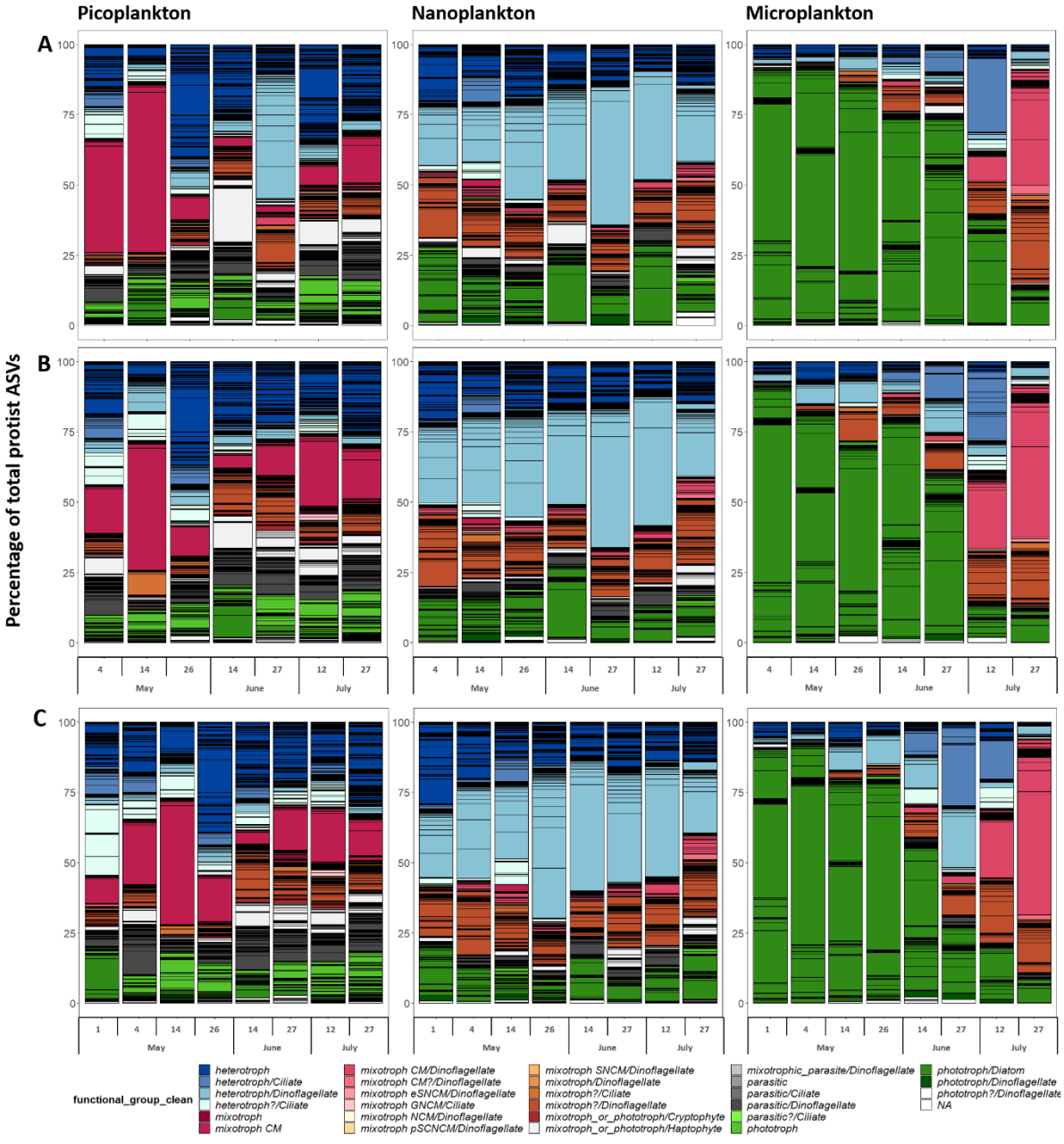

**Supplementary Table 2: functional richness, ASV-based richness and RUE over time and sampling location.**

| date | Station | functRichness | ASVRichness | RUE |
|---|---|---|---|---|
| 04.05.2017 | 1 | 24 | 879 | 3.37305757 |
| 14.05.2017 | 1 | 25 | 992 | 4.34136551 |
| 26.05.2017 | 1 | 24 | 1220 | 4.87175144 |
| 14.06.2017 | 1 | 24 | 1195 | 5.13545662 |
| 27.06.2017 | 1 | 23 | 1275 | 3.7720714 |
| 12.07.2017 | 1 | 23 | 1327 | 3.71018737 |
| 27.07.2017 | 1 | 23 | 1521 | 3.55573565 |
| 04.05.2017 | 2 | 22 | 1129 | 0.87585959 |
| 14.05.2017 | 2 | 22 | 1072 | 5.58259447 |
| 26.05.2017 | 2 | 25 | 1281 | 4.89088571 |
| 14.06.2017 | 2 | 24 | 1280 | 4.01713565 |
| 27.06.2017 | 2 | 25 | 1253 | 2.25285291 |
| 12.07.2017 | 2 | 25 | 1332 | 2.23169791 |
| 27.07.2017 | 2 | 26 | 1466 | 2.57575669 |
| 04.05.2017 | 3 | 26 | 1035 | 0.44536643 |
| 14.05.2017 | 3 | 26 | 1162 | 5.07165522 |
| 26.05.2017 | 3 | 25 | 1138 | 6.02770468 |
| 14.06.2017 | 3 | 27 | 1192 | 3.6445968 |
| 27.06.2017 | 3 | 27 | 1244 | 3.64249048 |
| 12.07.2017 | 3 | 27 | 1394 | 1.81373531 |
| 27.07.2017 | 3 | 27 | 1480 | 1.89079954 |

## RUE

| sample | date | N to P liquid | C to N particulate | Chl a g/L | POC g/L | aqN µmol/L | aqN g/L | PON g/L | TotalN g/L | aqP g/L | RUE-POC:TotalN |
|---|---|---|---|---|---|---|---|---|---|---|---|
| I_1_NB_02_DNA | 04.05.2017 | 10.6538462 | 5.267650687 | 6.05273E-06 | 0.000363691 | 2.77 | 0.00003878 | 6.90424E-05 | 0.000107822 | 8.05318E-06 | 3.373057569 |
| I_3_NB_02_DNA | 14.05.2017 | 13.5111111 | 10.2742761 | 2.8169E-06 | 0.000639943 | 6.08 | 0.00008512 | 6.2286E-05 | 0.000147406 | 1.39382E-05 | 4.341365505 |
| I_4_NB_02_DNA | 26.05.2017 | 17.4444444 | 9.033712916 | 2.98303E-06 | 0.000697272 | 4.71 | 0.00006594 | 7.71856E-05 | 0.000143126 | 8.36292E-06 | 4.871751439 |
| I_5_NB_02_DNA | 14.06.2017 | 8.8 | 6.425519333 | 3.75587E-07 | 0.000315128 | 0.88 | 0.00001232 | 4.90432E-05 | 6.13632E-05 | 3.09738E-06 | 5.135456621 |
| I_7_NB_02_DNA | 27.06.2017 | 9.63157895 | 6.014042036 | 6.50054E-07 | 0.000259236 | 1.83 | 0.00002562 | 4.31051E-05 | 6.87251E-05 | 5.88501E-06 | 3.772071401 |
| I_8_NB_02_DNA | 12.07.2017 | 18.4166667 | 6.950206229 | 1.10509E-06 | 0.000246244 | 2.21 | 0.00003094 | 3.54298E-05 | 6.63698E-05 | 3.71685E-06 | 3.710187374 |
| I_9_NB_02_DNA | 27.07.2017 | 13.1333333 | 6.334085023 | 9.75081E-07 | 0.000223574 | 1.97 | 0.00002758 | 3.52969E-05 | 6.28769E-05 | 4.64606E-06 | 3.555735653 |
| | | | | | | | | | | | |
| | | | | | | | | | | | |
| II_1_NB_02_DNA | 04.05.2017 | 17.6666667 | 8.899489707 | 1.08342E-06 | 0.000136958 | 10.07 | 0.00014098 | 1.53894E-05 | 0.000156369 | 1.7655E-05 | 0.875859589 |
| II_3_NB_02_DNA | 14.05.2017 | 14.1818182 | 9.549435664 | 2.46298E-06 | 0.000587018 | 3.12 | 0.00004368 | 6.14715E-05 | 0.000105152 | 6.81423E-06 | 5.582594466 |
| II_4_NB_02_DNA | 26.05.2017 | 15.3103448 | 9.208223872 | 3.04081E-06 | 0.000648423 | 4.44 | 0.00006216 | 7.04178E-05 | 0.000132578 | 8.98239E-06 | 4.890885706 |
| II_5_NB_02_DNA | 14.06.2017 | 5.64285714 | 6.476979711 | 9.02853E-07 | 0.000233973 | 1.58 | 0.00002212 | 3.61239E-05 | 5.82439E-05 | 8.67265E-06 | 4.017135646 |
| II_7_NB_02_DNA | 27.06.2017 | 12.95 | 5.847639284 | 2.67244E-07 | 0.000132883 | 2.59 | 0.00003626 | 2.27241E-05 | 5.89841E-05 | 6.19475E-06 | 2.252852915 |
| II_8_NB_02_DNA | 12.07.2017 | 7.52777778 | 6.351149096 | 3.75587E-07 | 0.000130541 | 2.71 | 0.00003794 | 2.05539E-05 | 5.84939E-05 | 1.11506E-05 | 2.231697912 |
| II_9_NB_02_DNA | 27.07.2017 | 10.5862069 | 6.970397571 | 5.48935E-07 | 0.000175592 | 3.07 | 0.00004298 | 2.51911E-05 | 6.81711E-05 | 8.98239E-06 | 2.575756689 |
| | | | | | | | | | | | |
| | | | | | | | | | | | |
| III_1_NB_02_DNA | 04.05.2017 | 16.3934426 | 8.242631707 | 5.77826E-07 | 6.59127E-05 | 10 | 0.00014 | 7.99656E-06 | 0.000147997 | 1.8894E-05 | 0.445366426 |
| III_3_NB_02_DNA | 14.05.2017 | 8.05 | 8.59843424 | 3.0697E-06 | 0.00055741 | 3.22 | 0.00004508 | 6.48269E-05 | 0.000109907 | 1.23895E-05 | 5.071655225 |
| III_4_NB_02_DNA | 26.05.2017 | 17.2307692 | 8.930147141 | 3.99422E-06 | 0.000581598 | 2.24 | 0.00003136 | 6.51275E-05 | 9.64875E-05 | 4.02659E-06 | 6.027704677 |
| III_5_NB_02_DNA | 14.06.2017 | 12.8461538 | 6.787209134 | 1.6468E-06 | 0.000184032 | 1.67 | 0.00002338 | 2.71146E-05 | 5.04946E-05 | 4.02659E-06 | 3.644596801 |
| III_7_NB_02_DNA | 27.06.2017 | 14.625 | 5.998074599 | 3.10581E-07 | 0.000151924 | 1.17 | 0.00001638 | 2.53287E-05 | 4.17087E-05 | 2.4779E-06 | 3.642490483 |
| III_8_NB_02_DNA | 12.07.2017 | 15.9583333 | 5.935489605 | 5.6338E-07 | 0.000140047 | 3.83 | 0.00005362 | 2.35949E-05 | 7.72149E-05 | 7.4337E-06 | 1.813735313 |
| III_9_NB_02_DNA | 27.07.2017 | 23.7857143 | 6.310988288 | 1.95016E-07 | 0.000125856 | 3.33 | 0.00004662 | 1.99424E-05 | 6.65624E-05 | 4.33633E-06 | 1.890799544 |

# Chapter 3

**Seasonal plankton succession is in accordance with phycotoxin occurrence in Disko Bay, West Greenland**

Publication

# Seasonal plankton succession is in accordance with phycotoxin occurrence in Disko Bay, West Greenland.

Claudia Sabine Bruhn[1,*], Sylke Wohlrab[1,2], Bernd Krock[1], Nina Lundholm[3], Uwe John[1,2,*]

[1]: Alfred Wegener Institute, Helmholtz Centre for Polar and Marine Research, Am Handelshafen 12, 27570 Bremerhaven, Germany

[2]: Helmholtz Institute for Functional Marine Biodiversity, Ammerländer Heersstraße 231, 26129 Oldenburg, Germany

[3]: Natural History Museum of Denmark, University of Copenhagen, Øster Farimagsgade 5, 1353 Copenhagen, Denmark

[*]: corresponding authors: Claudia Sabine Bruhn (claudia.bruhn@awi.de); Uwe John (uwe.john@awi.de)

Originally published in *Harmful Algae*, https://doi.org/10.1016/j.hal.2021.101978

**Abstract**

Harmful algal blooms (HABs) are occurring more frequently in the world's oceans, probably as a consequence of climate change. HABs have not been considered a serious concern in the Arctic, even though the Arctic warms faster than any other region. While phycotoxins and toxin-producing phytoplankton have been found in Arctic waters on several occasions, there is a lack of information on seasonal succession of species and whether the occurrence of harmful species correlates with the presence of their respective phycotoxins. Hence, there is no baseline to assess future changes of HABs in this area. Here, we investigated two periods, from winter to spring and from the spring bloom until summer, in Disko Bay, West Greenland and followed the succession of toxins and their producers using metabarcoding, as well as analyses of particulate and dissolved toxins. We observed a typical seasonal succession with a spring bloom dominated by diatoms, followed by dinoflagellates in summer, with the two most important potentially toxic taxa found being *Pseudo-nitzschia* spp. and *Alexandrium ostenfeldii*. The *Pseudo-nitzschia* spp. peak correlated with a clear increase in particulate domoic acid, reaching 0.05 pg/L. Presence of *Alexandrium ostenfeldii* could be linked to an increase in spirolides, up to 56.4 pg/L in the particulate phase. Generally, the majority of detected dissolved toxins followed the succession pattern of the particulate toxins with a delay in time. Our results further show that

Arctic waters are a suitable habitat for various toxin producers and that the strong seasonality of this environment is reflected by changing abundances of different toxins that pose a potential threat to the ecosystem and its beneficiaries.

**Keywords:** Arctic, phytoplankton, protist, time series, harmful algal bloom

## 1. Introduction

Phytoplankton responses to ongoing and future environmental change will significantly affect earth system processes at many scales. These primary producers are the photosynthetic base of marine food webs and responsible for approximately half of the global oxygen production (Falkowski, 1994; Field *et al.*, 1998). In the Arctic, climate change is progressing at a much faster rate than the global average (Overpeck *et al.*, 1997; McBean *et al.*, 2005; IPCC 2007), hence the Arctic is one of the quickest changing ecosystems in the world, warming at a significantly higher rate than other regions (Moritz *et al.*, 2002; Mauritsen, 2016). An increased risk of future HAB events in the Arctic is therefore anticipated, as potential HAB species from temperate regions may migrate further north and establish themselves in the Arctic ecosystems.

Greenland is dependent on a healthy marine ecosystem. The fishing industry provides Greenland's most important marketable goods for export (Brett, 2003; Vahl & Kleemann, 2019) and many private households are dependent on marine resources, like hunting marine mammals, for regular sustenance (Vahl & Kleemann, 2019). The marine ecosystem, which is the fundament of these resources, heavily relies on a direct link from diatoms via copepods to marine mammals in spring, when considering latitudes as high as most of Greenland. In the Arctic, a more pronounced microbial loop, as it is typical for temperate regions, is usually observed in summer. At this time, microbial biomass is generally relatively low, making the direct short food web link, which is dominant in spring, much more relevant to food production for the native population (Hobson & Welch, 1992; Seuthe *et al.*, 2011). This increases the possible impact of a change in the microbial spring diversity on the Greenlandic population. Besides the beneficial impact of microbial eukaryotes, some of them can form harmful algal blooms (HABs), which can have adverse effects on the marine ecosystem function and services. Only a few studies have described succession dynamics of primary producers and HAB species in particular in the Arctic (Marquardt *et al.*, 2016), although it is crucial to know the status quo for identifying future risks and recognizing changes of the plankton community structure and therefore changes in the entire ecosystem.

General consensus exists about a global increase in HABs (Van Dolah, 2000; Hallegraeff, 2003; Anderson *et al.*, 2012), and many of the factors promoting HABs are linked to the effect of climate change (Hallegraef, 2010; Wells *et al.*, 2015). Increased water temperature and water column stratification are a direct result of increased atmospheric $CO_2$ levels and therefore global warming (IPCC, 2014; McCarthy *et al.*, 2015), and both factors are broadly recognized as a risk factor for HABs (Peperzak, 2003; Ralston *et al.*, 2014; Wells *et al.*, 2015). Possible effects of melting glaciers, a known result of climate change, are changing water salinity and nutrient upwelling events from lower ocean layers by promoting subsurface meltwater plumes (Meire *et al.*, 2017). Additionally, melting land-terminating glaciers may wash out nutrients from freshly thawed permafrost, carrying terrestrial nutrients into the ocean (McCarthy *et al.*, 2015; Wadham *et al.*, 2016; Meire *et al.* 2017), and therefore potentially increasing the risk for future HABs even further.

Some HAB species and toxins have already been detected in the Arctic. Presence of domoic acid (DA)-producing *Pseudo-nitzschia* species has been shown off West Greenland, Iceland, and in Barrow Strait, Beaufort Sea, Baffin Bay as well as subarctic parts of Norway (Hasle, 2002; Hansen *et al.*, 2011; Harðardóttir *et al.*, 2015; Lundholm *et al.*, 2018). The toxin itself was detected in phytoplankton in West Greenland, reaching as far as 71 °N (Elferink *et al.*, 2017). In 2017, *Pseudo-nitzschia* spp. occurrences caused elevated DA contents in *Mytilus edulis*, resulting in a local harvesting ban close to Dønna, Norway at 66°5’ N (HAEDAT, 2017).

The vast majority of toxigenic species are dinoflagellates (Smayda, 1997), and their toxins have also been detected in Arctic waters. Paralytic shellfish poisoning (PSP) toxins exceeded the limit of 800 µg/kg shellfish in 2003 in the Attu region (67°50’ N-68°10’ N, 53°00’ W-54°00’ W) at the west coast of Greenland (Baggesen *et al.*, 2012). In August 2005, saxitoxin-producing *Alexandrium catenella* (formerly reported as *A. tamarense*, now renamed as *A. catenella*; John *et al.*, 2014), was found in the same area and considered as the causative agent of the PSP event (Baggesen *et al.*, 2012). Pectenotoxin-1 was found at levels of 467 µg/kg shellfish in the Chuckchi Sea at approximately 74 °N, well exceeding the safety regulation for consumption (Gao *et al.*, 2019). Spirolides are potentially toxic hazards, which have not yet been confirmed to be a threat to humans in situ (Richard *et al.*, 2000; Munday *et al.*, 2012). Spirolides have by now not been shown to be produced by other species than *A. ostenfeldii* (Cembella *et al.*, 2000; 2001). Some *A. ostenfeldii* strains are capable of producing other, probably more harmful toxins, such as paralytic shellfish poisoning (PSP) toxins and gymnodimines (GYM) (Munday *et al.*, 2012; Martens *et al.*, 2017). In Uummannaq Fjord in West Greenland (around 71 °N), *A. ostenfeldii* was found in 2012 (Tillmann *et al.*, 2014). *Alexandrium ostenfeldii* was also observed in the Russian Arctic, albeit without evidence of toxin-producing activity (Okolodkov *et al.*, 1996). Azaspiracid-producing *Amphidoma languida* was found in the Subarctic Irminger Sea

(Tillmann *et al.*, 2015), and *Azadinium* spp. and *Amphidoma* spp. have been observed along the coast of Norway (Tillmann *et al.*, 2018).

HABs can severely affect higher trophic levels, including humans and animals (Bates *et al.*, 2018) and consequently result in negative health and economic consequences. Higher trophic levels such as marine mammals have been reported to bioaccumulate toxins in the Arctic, and HABs thus represent a rarely studied and hidden risk (Lefebvre *et al.*, 2016). As many known HAB species have been detected in the Arctic and Subarctic, a potential for HAB development exists, although the record of actual Arctic HAB events seems to be relatively low. Part of this may be due to a study bias, because the Arctic is less accessible for routine field studies. This is reflected by reports of snapshot or transect studies, mainly from research cruises, which do not account for the yearly development in the highly seasonal environment as done by monitoring programs. However, only long-term datasets can reveal overall changes in the community, dynamics and resulting threats that may be caused by HABs (Hinder *et al.*, 2012). Our study therefore provides a characterization of the natural succession and presence of HAB species during two field periods of approximately three months length each. We will particularly focus on the dynamics of different potential HAB species and their succession patterns around the spring bloom season to evaluate the risk for HAB events in the future.

## 2. Material and methods

### 2.1 Site description and Sampling procedure

The sampling stations were located close to the Arctic Station in Qeqertarsuaq, Disko Island, West Greenland. Water samples were taken with a 25 L Niskin Water sampler (KC Denmark) in an area of approximately 6 km x 2 km (69°11'000'' N to 69°15'014'' N and 53°25'036'' W to 53°31'015'' W), depending on the conditions of sea ice or the presence of icebergs (Fig. 1). The area was sampled in the time periods May 1, 2017 to July 27, 2017, and February 10, 2018 to April 23, 2018 as close to noon as possible. Sampling was performed every second week at three distinct stations, except for winter when only one station was sampled but at a higher frequency of approximately every four days. Sampling of dissolved toxins was performed with SPATT (Solid Phase Adsorption Toxin Tracking) samplers at another, more enclosed location (69°15'060'' N, 53°46'024'' W) (Fig. 1). The sampling location for the SPATT samplers was selected as a compromise for being safe from icebergs, good accessibility throughout the year, and qualitative proximity to the original sampling stations.

Sampling containers were pre-treated with 3 % hydrochloric acid and rinsed with fresh water thoroughly between samplings. The containers were flushed twice with the respective

sample before collecting 10 L of seawater from 5, 10, 20, 30 and 40 m depth. Salinity and temperature were measured manually from the sampled waters until May 14. From May 2017 on, a SonTek CastAway-CTD or a Seabird SBE 911plus CTD were used for additional oceanographic data. Comparability of the values was ensured by measuring in parallel with the different devices. To restrict degradation of the samples, they were stored cool and dark before being processed within 24 hours after sampling.

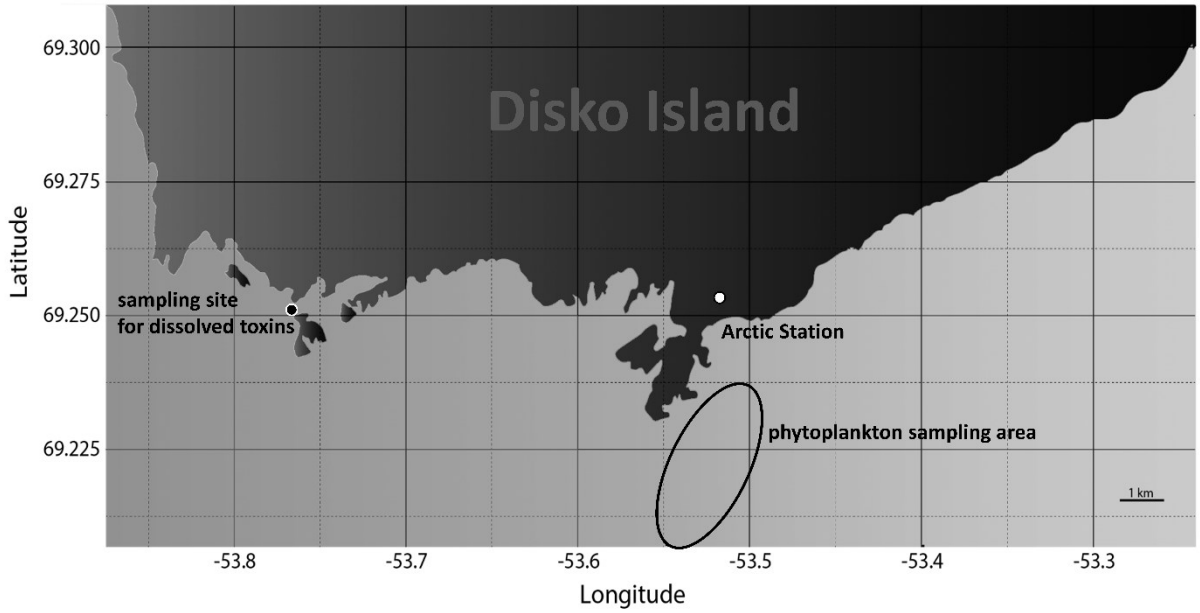


***Figure 1: Sampling stations.*** *The phytoplankton sampling area off the south coast of Disko Island, the sampling site for dissolved toxins, and the location of the research base Arctic Station.*

## 2.2 Sample preparation and analysis

Water samples from different depths at the same sampling station were pooled before the following treatments were performed:

Samples for inorganic nutrient measurements (ammonium, nitrate, nitrite, phosphate and silicate) were transferred from the pooled sample to polypropylene bottles (50 mL) and frozen immediately at -20 °C. Nutrient samples were analyzed with a continuous-flow autoanalyzer (Evolution III, Alliance Instruments, France) based upon standard seawater analytical methods for determination of nitrate and nitrite (Armstrong *et al.*, 1967), ammonium (Koroleff, 1969), silicate (Grasshoff *et al.*, 1983), and phosphate (Eberlein & Kattner, 2000).

For chlorophyll *a* analyses, 1 L of pooled sample was filtered through glass microfiber filters (Whatman GF/F, Whatman, UK; nominal pore size: 0.7 µm), packed in aluminum foil and frozen at -20 °C until analysis, maximum four weeks after sampling. Chlorophyll *a* was extracted

from the filters by incubation in 10 mL of methanol (modified after EPA method 445.0-1, Arar & Collins, 1997) at -20 °C overnight. The extract was measured at 665 nm (TD-700 fluorometer, Turner Designs, USA, calibrated with *Anacystis nidulans* chlorophyll, Sigma-Aldrich).

For POC and PON analysis, 1 L of pooled sample was filtered through pre-combusted glass microfiber filters (Whatman GF/F, Whatman, UK; nominal pore size: 0.7 µm) and frozen in pre-combusted glass vials before analysis. For analysis, the wet filters were dried at 50 °C overnight. Half of the dried filter was acidified with 300 µL 0.2 N HCl and again dried overnight at 50 °C, the other half was frozen as a backup. The acidified and dried filters were packed in tin foil and analyzed on a Euro Elemental Analyzer 3000 CHNS-O (HEKAtech GmbH, Germany). POC:PON ratios from February 10 through 21 were excluded because of very low cell biomass.

### 2.3 Metabarcoding

The remaining pooled water sample was filtrated through a series of filters for size fractionation. A 200 µm nylon mesh was used to decrease the amount of debris and larger zooplankton. As the size fraction above 200 µm was discarded, some larger phytoplankton cells and colonies were removed as a consequence. The filtrate was subsequently size fractionated in three filtration steps with a 20 µm nylon mesh (filtering 47.5 L), and polycarbonate filters with pore sizes of 3 µm (filtering 3 L) and 0.2 µm (filtering 1 L) using a vacuum pump at minimum -500 mbar. The size fractions will hereafter be referred to as picoplankton (0.2 µm to 3 µm), nanoplankton (3 µm to 20 µm) and microplankton (20 µm to 200 µm). DNA was extracted with a NucleoSpin Soil kit (Macherey-Nagel, Germany). Metabarcoding libraries were prepared according to 16S Metagenomic Sequencing Library Preparation protocol by Illumina, with the primers being adapted for the eukaryotic V4-region (Piredda *et al.*, 2016). After sequencing with the Illumina MiSeq system, the clustering and annotation of OTUs (Operational Taxonomic Units) was performed utilizing a pipeline developed in house (as described by Sprong *et al.*, 2020) with the reference database PR$^2$ (version 4.11.1, Guillou *et al.*, 2012). To gain further insight and a better-curated system, the taxonomic groups of dinoflagellates, diatoms and haptophytes were additionally annotated on taxonomic trees (Elferink *et al.*, 2017) and subsequently manually curated. Further, the data was normalized, fungi and metazoan sequences were removed, as well as singletons and doubletons as potential artifacts. This and further data preparation was done in R, version 3.6 with RStudio, version 1.3.959 and the packages effects, ggplot2, plyr, phyloseq, and vegan.

### 2.4 Toxin analysis

Two distinct approaches were used to monitor the toxins presented in Table 2. For particulate toxin content, plankton net (pore size 20 µm, 40 cm diameter; Hydro-Bios, Kiel, Germany) samples were hauled from 40 m depth at the same locations and time points as the water samples. We estimate that a maximum of approximately 5000 L water was filtered with each net tow, depending on the density of particles in the water (Brander *et al.* 1993). The dense plankton net sample was diluted with surface water and stored cold a few hours until processing to minimize cell death and lysis. Most zooplankton (and some larger phytoplankton cells and colonies) was removed by a 200 µm mesh filtration, the samples were collected on a 20 µm mesh, split in four even aliquots with a pipette and pelleted by centrifugation. Pellets were frozen at -20 °C until toxin extraction. Two aliquots were spiked with 0.9 g of lysing matrix D (Thermo Savant, Illkirch, France) and with methanol and 0.03 M acetic acid, respectively. The cells were lysed and extracted in a FastPrep homogenizer (Thermo Savant) by reciprocal shaking at 6.5 m/s, and subsequently centrifuged at 16,100 x g for 15 min. After filtering the supernatant through Ultrafree MC Filter units (Millipore), one aliquot was analyzed for hydrophilic paralytic shellfish poisoning (PSP) toxins by ion-pair chromatography coupled to post-column derivatization and fluorescence detection as detail in Van de Waal *et al.* (2015). The other aliquot was analyzed for lipophilic phycotoxins by reversed phase liquid chromatography coupled to tandem mass spectrometry (LC-MS/MS) as detailed in Krock *et al.* (2008) with additional mass transitions for goniodomin A and desmethyl-goniodomin A (m/z 786.5 → 733.5 and m/z 772.5 → 719.5, respectively).

Dissolved toxins were sampled by solid phase absorption toxin tracking (SPATT, MacKenzie *et al.*, 2004). SPATT samplers with Diaion HP20 (Sigma, Deisenhofen, Germany) were prepared as described in Krock *et al.* (2020) before deployment. The samplers were not placed in the sampling area for particulate plankton, because this location was too open and iceberg occurrences would have interfered with the samplers. Instead, SPATT samplers were deployed in a small bay in the vicinity (69°15'060'' N, 53°46'024'' W), at a depth of 8.5 m below surface. SPATT sampler monitoring was performed between May 1, 2017 and April 30, 2018, where they were exchanged approximately once per month with a time span ranging from 18 d in the times with higher primary production up to 43 d during less productive phases. From September 19, 2017 to October 18, 2017 it was not possible to deploy new samplers. After retrieval, the samplers were air dried at room temperature and subsequently frozen at -20 °C until analysis. SPATT sampler were desalted by rinsing three times with deionized water and subsequently dried over night at 50 °C. The dry resin was transferred to 50 mL centrifugation tubes and stored at -20 °C until extraction. For extraction, 30 mL methanol were added to the resin and gently shaken overnight. Subsequently, the methanolic resin suspension was poured into a glass

chromatography column and methanol was eluted dropwise until reaching the surface of the resin layer. Subsequently, the centrifugation tube was rinsed with 25 mL methanol and the methanol was added to the resin column. Finally, the resin was extracted with additional 100 mL methanol. The combined eluates were collected in a glass flask and concentrated to approximately 1 mL in a rotary evaporator. The extract was spin filtered (0.45 µm pore size) and the filtrate transferred into an HPLC vial, taken to dryness under a gentle nitrogen stream and finally reconstituted in 200 µL methanol. SPATT samples were analyzed for lipophilic phycotoxins as described above.

## 3. Results

### 3.1 Seasonal biomass, Nutrients and temperature

The biomass markers POC, PON and chlorophyll *a* all peaked at the sampling in the end of March 2017. All three values behaved largely the same in their tendencies of increasing and decreasing with slight variations in the strength of in- and decrease (Figure 4C). Chlorophyll *a* levels peaked at 3.41 µg/L, POC at 0.65 µg/L and PON at 0.07 µg/L. In summer (May-July) 2017, silicate, nitrate and phosphate were decreasing with time (Fig 2A). Ammonium levels varied, but did not show a clear trend. Nitrite levels stayed low, with a slightly higher level in the beginning of this season (Fig. 2A). With progression from spring to summer, water temperature increased continuously and the POC:PON-ratio decreased (Fig. 2B). Levels of nitrate, silicate and phosphate were overall higher in winter than in summer. Nitrite stayed low at levels comparable to the summer season. Silicate had a slight increasing trend, whereas nitrate and phosphate levels were approximately the same throughout the season. Ammonium levels varied again, overall being a bit lower than in summer (Fig. 2A). The water temperature in winter was uniformly low at approximately 1.5 °C, while the POC:PON followed an upwards trend (Fig. 2B).

### 3.2 Potentially toxic species

Using the IOC-UNESCO taxonomic reference list for defining potentially toxic taxa (Moestrup *et al.*, 2009), eleven potentially toxic taxa of eight genera were detected as OTUs (Table 1). It was possible to identify five toxigenic taxa to species level, namely *Alexandrium catenella*, *Alexandrium ostenfeldii*, *Dinophysis acuminata*, *Gonyaulax spinifera*, and *Protoceratium reticulatum*. Because the genera *Alexandrium*, *Dinophysis*, *Phalacroma* (toxicity under debate with hints for toxicity, Reguera *et al.*, 2014), *Prorocentrum*, *Nitzschia* and *Pseudo-nitzschia* contain several toxin-producing species, the reads for these genera were included. The total number of OTU reads from potentially toxic species equalled 1.7 % of all detected OTU reads.

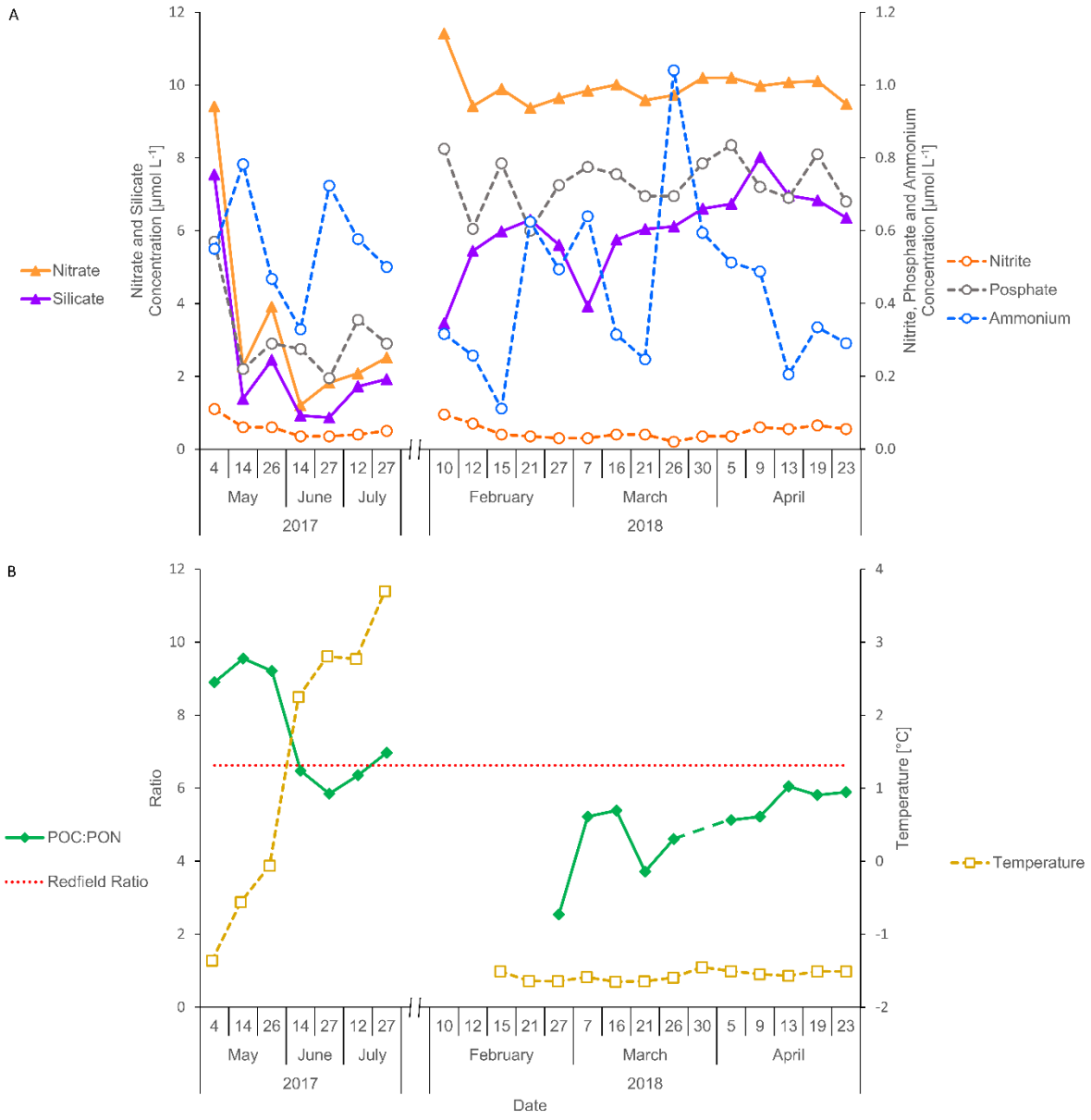


***Figure 2: Nutrients and contextual data.*** *Macronutrients in solution (A), particulate nutrients in comparison to the Redfield ratio and in context with temperature (B). POC:PON ratios from February 10 through 21 were excluded because of very low biomass and resulting biased ratios. The POC:PON for March 30 was not measured, as indicated with a dashed line. Temperature readings were mathematically averaged analogously to the physical water samples. The temperature readings of February 10 and 12 were not included due to CTD malfunction.*

***Table 1: Statistics of potential HAB species.*** *Singletons, doubletons and tripletons were removed from the pool before assessing the numbers. The per mill value of total detected OTUs values was rounded to three decimal places.*

| *HAB Taxon* | *Number of assigned different OTUs* | *Per mill of total amount of reads* |
|---|---|---|
| *Alexandrium catenella* | 2 | 0.373 |
| *Alexandrium ostenfeldii* | 7 | 7.048 |
| *Alexandrium* spp. | 33 | 0.076 |
| *Dinophysis acuminata* | 5 | 0.511 |
| *Dinophysis* spp. | 17 | 0.02 |
| *Gonyaulax spinifera* | 2 | 0.034 |
| *Phalacroma* spp. | 5 | 0.654 |
| *Prorocentrum* spp. | 22 | 4.028 |
| *Protoceratium reticulatum* | 1 | 0.040 |
| *Nitzschia* spp. | 9 | 0.396 |
| *Pseudo-nitzschia* spp. | 4 | 3.989 |
| Total | 107 | 17.169 |

### 3.3 Seasonal succession pattern of potential HAB species

We were able to assign 26,993 different OTUs via PR$^2$ in the combined datasets from 2017 and 2018, of which 1,179 could not be assigned to anything more specific than Eukaryota and 37 OTUs were assigned to unclassified Opisthokonta, meaning that it was not possible to completely exclude the possibility of the OTUs to represent a protist species. After excluding fungi, land plants, and animals, 24,698 potential protist-representing OTU reads were left and analyzed for the succession pattern on different phylogenetic levels after normalizing (Fig. 3). HAB relevant dinoflagellates, diatoms and haptophytes were evaluated from the normalized OTU metabarcoding and put into context with the overall protist succession. Potential toxin producers were mainly found in the microplankton size fraction, while they were not present in picoplankton and present to a much lesser extent in the nanoplankton size fraction (Fig. 3B and C). The peak percentage of potentially toxic dinoflagellates was in July 2017 (Fig. 3B), whereas the peak for potentially toxic diatoms was observed in May 2017 (Fig. 3C).

### 3.4 Temporal toxin content

In spring, the phytoplankton biomass peaked on May 26 2017, probably due to a diatom bloom. Most particulate toxins (from cell pellets) reached their highest values more than 47 days later on July 12 and 27 (Fig. 4A, B). The dissolved toxin fraction, which was in contrast measured for almost the entire year, appeared latest three months thereafter in the time period October 18 to November 18. Both in the particulate and dissolved phase, spirolides (SPX) and pectenotoxins (PTX) clustered together, while only dissolved okadaic acid (OA) was associated with these toxins.

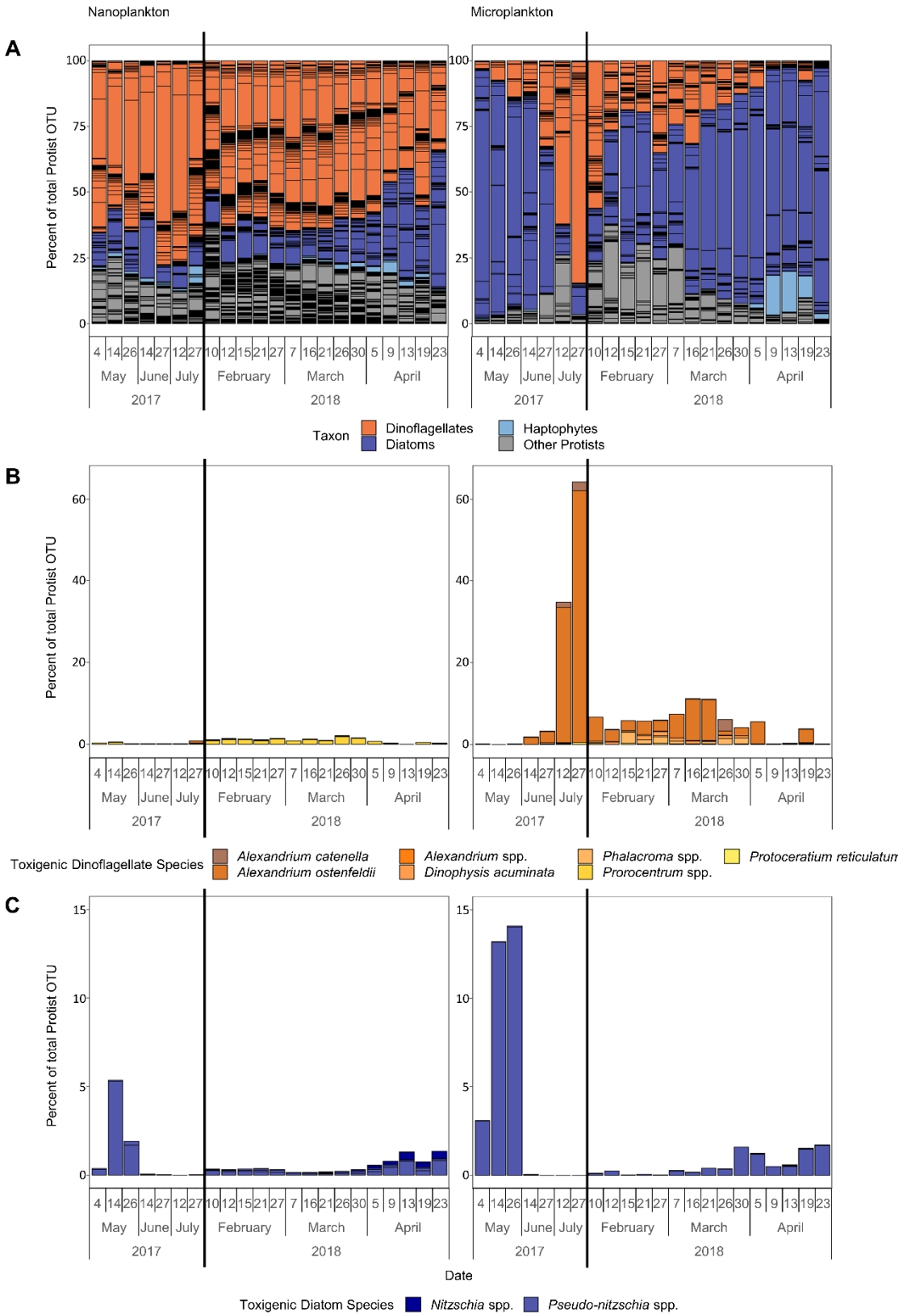


***Figure 3: Succession of toxic species in the OTU analysis.*** *Normalized total protist OTU data (A), progression of potentially toxic dinoflagellates (B), and progression of potentially toxic diatoms (C) are shown. Solid black vertical lines indicate discontinuous measurement.*

Dissolved gymnodimine A (GYM A) and azaspiracid-1 (AZA 1) also clustered together. GYM A, OA, dinophysistoxins (DTX), yessotoxins (YTX), and AZA 1 were only detected in the dissolved phase, whereas DA was the only toxin solely detected in the particulate phase. All other analyzed toxins were either not detected at all or detected in both phases, but at different time points (Table 2). The most abundant toxin group was SPX, which was present and measureable in all sample types. Additionally, DA and PTX were present, although DA could only be detected in the particulate phase. In contrast, GYM only had comparably low amounts detected in the liquid phase (Table 2 and Figure 4).

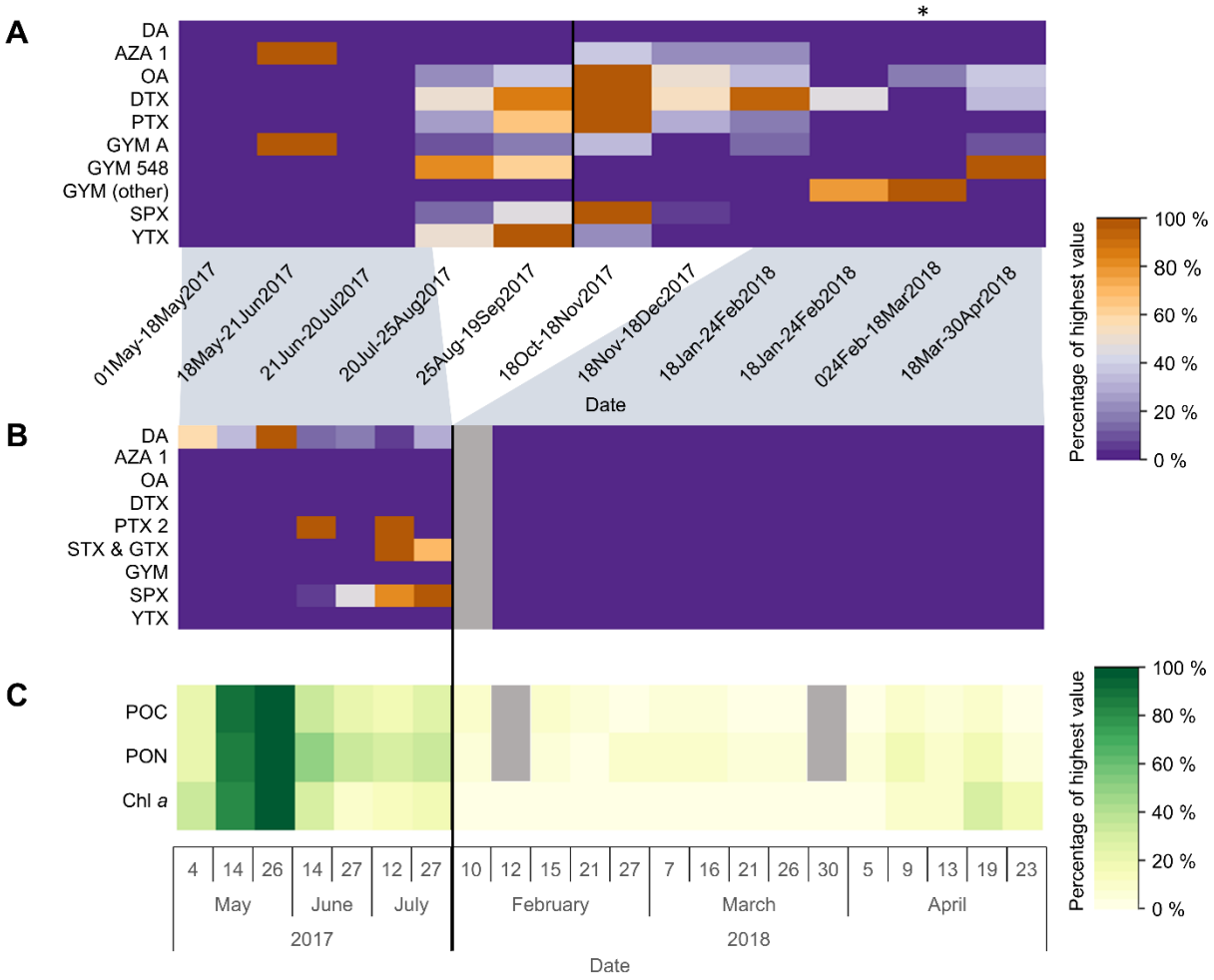


***Figure 4: Toxin content over time.*** *Toxin content patterns in liquid phase (A) and solid phase (B) as well as biomass as context (C), normalized along the time scale. Grey areas are indicating no measured value for the particular time point. Solid black lines indicate a discontinuous measurement. The sampling with the asterisk (*) was done approximately 10 km apart from the usual sampling spot due to weather-related inaccessibility of the original location. For data analysis, values measured below detection limit were set as 0. Numbers next to GYM toxins indicate m/z of the respective measured species.*

***Table 2: Measured absolute maxima in toxin content and corresponding sampling dates.*** *Amounts of dissolved toxins are expressed in picogram per plankton haul (PH). nd = below detection limit. nm = not measured.*

| | *pg/PH particulate* | *pg/sample Detection limit* | *Sampling time point* | *pg/sample dissolved* | *Detection limit* | *Sampling time frame* |
|---|---|---|---|---|---|---|
| *AZA1* | nd | 75.00 | - | 57.00 | 8.82 | 18.05.-21.06.2017 |
| *DA* | 81010.10 | 447.76 | 26.05.2017 | nd | 110.08 | - |
| *DTX1* | nd | 1136.36 | - | 37232.29 | 750.00 | 18.01.-24.02.2018 |
| *DTX1 Isomer* | nm | - | - | 24876.44 | 750.00 | 18.12.-18.01.2018 |
| *DTX2* | nd | 12500.00 | - | nd | 375.00 | - |
| *GDA* | nd | 6944.44 | - | nd | 545.45 | - |
| *GTX 1* | nd | 0.058 | - | nm | - | - |
| *GTX 2* | nd | 0.002 | - | nm | - | - |
| *GTX 3* | 5686153.85 | 0.003 | 27.07.2017 | nm | - | - |
| *GTX 4* | nd | 0.048 | - | nm | - | - |
| *GTX 5* | nd | 0.012 | - | nm | - | - |
| *GYM A* | nd | 6.25 | - | 289.00 | 0.34 | 18.05.-21.06.2017 |
| *GYM_494* | nm | - | - | 37.20 | 0.34 | 18.12.-18.01.2018 |
| *GYM_522* | nm | - | - | 48.12 | 0.34 | 18.01.-24.02.2018 |
| *GYM_548* | nm | - | - | 41.98 | 0.34 | 24.02.-18.03.2018 |
| *GYM_582* | nm | - | - | 34.10 | 0.34 | 18.01.-24.02.2018 |
| *OA* | nd | 2205.88 | - | 22669.10 | 1041.67 | 18.10.-18.11.2017 |
| *PTX2* | 25154.32 | 375.00 | 14.06.2017 | 56293.71 | 155.84 | 18.10.-18.11.2017 |
| *PTX2sa* | nm | - | - | 6993.01 | 155.84 | 18.10.-18.11.2017 |
| *SPX 1* | 30882.35 | 83.33 | 12.07.2017 | 3158.14 | 0.86 | 18.10.-18.11.2017 |
| *SPX A* | 121915.82 | 83.33 | 27.07.2017 | 2386.05 | 0.86 | 18.10.-18.11.2017 |
| *SPX C* | 113041.07 | 83.33 | 12.07.2017 | 39860.47 | 0.86 | 18.10.-18.11.2017 |
| *SPX G* | 113041.07 | 83.33 | 12.07.2017 | 1646.51 | 0.86 | 18.10.-18.11.2017 |
| *20-Me-SPX G* | 283454.28 | 83.33 | 27.07.2017 | 11441.86 | 0.86 | 18.10.-18.11.2017 |
| *STX* | 1571184.98 | 0.002 | 12.07.2017 | nm | - | - |
| *dc-STX* | nd | 0.003 | - | nm | - | - |
| *Neo STX* | nd | 0.022 | - | nm | - | - |
| *YTX* | nd | 37500.00 | - | nd | 750.00 | - |
| *YTX Isomer* | nd | 37500.00 | - | 6866.36 | 750.00 | 25.08.-18.09.2017 |

## 4. Discussion

### 4.1 Seasonality in context of nutrient availability

The aim of this study was to reveal the natural succession pattern of HAB species and their phycotoxins in order to assess a potential future risk on the Arctic marine ecosystem. We observed a clear seasonal reciprocal trend of dinoflagellates and diatoms in terms of community dominance (Fig. 3A), with diatoms dominating in spring and dinoflagellates afterwards. This supports previous observations of diatoms dominating the spring bloom biomass, which then quickly consume the nutrients in the mixed layer (Tammilehto *et al.*, 2017), giving way to

mixotrophic organisms such as dinoflagellates in the summer period (Raymont, 1980; Smayda & Trainer, 2010; Flynn *et al.*, 2019). This is in accordance with our data, where the nutrients in the spring season were quickly depleted in correlation with high diatom abundance in the microplankton size fraction (Fig. 2, 3). After the nutrient depletion, the relative dinoflagellate OTU dominance and ammonium levels were increasing (Fig. 2A), as also shown by Glibert (2016).

### 4.2 Overall contribution of HAB species OTUs

In total, eleven potentially toxic dinoflagellate and diatom taxa were found, of which five dinoflagellates were identified to species level. While the overall OTU richness was diverse, the eleven potentially toxic taxa seen in our study contributed to only 1.7 % of total OTU reads (including all size fractions). Hence, we did not observe a HAB, but the respective species were present and an imbalance and further changes in the ecosystem has the potential for HABs to develop in the near future. As expected, the most important size fraction for detected OTUs of HAB species was the microplankton (>20 µm) (Fig. 3). Among these, *Alexandrium ostenfeldii* was the most important dinoflagellate, contributing at times to more than 60 % of all microplankton OTU reads, and peaking together with the overall contribution of dinoflagellates in this size fraction. This larger dinoflagellate contribution of OTUs was taking place after the spring bloom peak at relatively low Chl *a*, POC and PON content. Additionally, the high copy number of ribosomal operons in dinoflagellate genomes often leads to an overestimation of their absolute contribution to the community in metabarcoding approaches because a single cell can contain several copies of the genes relevant for metabarcoding (Guo *et al.*, 2016). This may indicate a rather low absolute abundance of *A. ostenfeldii* at the cellular level and a method-based overestimation of dinoflagellates in general. Still, the contribution to the overall OTUs of *A. ostenfeldii* was notable, and most prominent in July. The most abundant toxic diatom taxon based on the OTU data was the genus *Pseudo-nitzschia*, which contributed about 14 % of all microplankton OTU reads at the time of the spring bloom peak. The danger of HAB events partly lies in their spatiotemporal unpredictability, as they are often influenced by wind-induced upwelling or other non-seasonal events (Zingone & Oksfeldt; Enevoldsen, 2000; Pitcher & Weeks, 2006). A strongly seasonal environment such as the Arctic may be different, as the potentially toxic organisms strongly correlate with the overall seasonal bloom pattern in the present study. On the other hand, it is known that the exact composition of the Arctic spring bloom varies considerably from year to year (Hegseth & Tverberg, 2013; Fragoso *et al.*, 2017), which may imply similar risks in this region.

### 4.3 Dissolved and particulate toxin prevalence of diatom-related domoic acid

Various phycotoxins have been observed in Subarctic and Arctic regions, but their seasonal occurrence has not yet been assessed. So far, field surveys took place during the spring bloom event and the summer months afterwards, looking at snapshots or transects (e.g. Baggesen *et al.*, 2012; Tillmann *et al.*, 2014; Elferink *et al.*, 2017, 2020 a, b). This is the first study to include the temporal component in context with nutrients, community structure, and biomass to allow for a developmental analysis of presence of toxins in an Arctic coastal region. The overall pattern shows a toxin succession which starts with particulate toxins occurring first and dissolved toxins later. The shift from particular into the dissolved toxin fraction (Fig. 4) may result from continuous leaking and excretion of the source organisms, but also from lysed and grazed organisms due to increased grazing pressure over time (Cembella, 2003; Ianora *et al.*, 2011).

After spirolides (SPX), domoic acid (DA) had the highest measured content in the particulate phase, with the highest level reaching 0.05 pg/L in late May. Compared to other non-Arctic regions, we observed orders of magnitude lower levels of DA (Bates *et al.*, 2018; Torres Palenzuela *et al.*, 2019). The increase in amount of DA in spring co-aligned with both the peak in Chl *a* and the OTU peak of *Pseudo-nitzschia* spp. Previous findings of particulate DA found between July 28 and August 8 in 2012 in the Uumannaq Fjord, Vaigat Strait and Disko Bay, were also linked to *Pseudo-nitzschia* spp. presence in metabarcoding samples (Elferink *et al.*, 2017). In April 2012, June 2013 and June 2014, DA-producing *P. delicatissima* was isolated from the Disko Bay area as well (Lundholm *et al.*, 2018). In 2007, toxic *P. seriata* was found around Nuuk (Hansen *et al.*, 2011) and in 2011 in Disko Bay (Tammilehto *et al.*, 2012). The non-toxic *P. arctica* has also been detected before in Disko Bay (Percopo *et al.*, 2016), suggesting that, in our case, there was probably a mixture of toxic and non-toxic species present. Several different *Pseudo-nitzschia* species co-occur in Arctic waters in spring, but the OTU sequences have not provided enough phylogenetic resolution allowing us to assign *Pseudo-nitzschia* spp. to species level.

Ecophysiological experiments have shown that DA cell quota increases during silicate and phosphate limitation, whereas nitrogen is required for the production, as DA is an amino acid derivative (Bates *et al.*, 2018). Our field data (Fig. 2) support these findings, as silicate and phosphate were depleted at the time around the DA peak. Ammonium was still available at a relatively high concentration, not following a downwards trend like the other nutrients and possibly providing nitrogen for DA-production (Wohlrab *et al.*, 2019). Nitrite was only present in very little densities throughout the study and nitrate was also depleted along silicate and phosphate. Previous laboratory experiments with *Pseudo-nitzschia* strains from the Disko Bay area showed that the presence of herbivorous copepods induced DA production (Harðardóttir *et al.*, 2015; Lundholm *et al.*, 2018). Copepods, which are typical diatom grazers in the Arctic,

increase in biomass and grazing activity around the spring bloom in Disko Bay (Dünweber *et al.*, 2010). The ammonium concentration in our data may additionally indicate copepod presence and their ammonium excretion and grazing activity (Corner & Newell, 1967). This implies that a combination of nutrient limitation and grazer cues may have increased particulate DA-levels. DA was the only toxin exclusively detectable in the particulate phase and not as dissolved toxin. Spatial differences could have led to the detection of DA in one location and not in the other. However, neither PSP toxins nor DA are adsorbing well to the SPATT material, resulting in a possible method bias. DA may either still be present, because it has previously been commonly found in the dissolved phase applying different detection methods (Lane *et al.*, 2010; Pagou & Hallegraeff, 2012; Geuer *et al.*, 2019). Alternatively, DA could have not been present in the water, because it presumably only leaks out of cells at high intracellular DA concentrations in the stationary growth phase of DA producers (Lundholm *et al.*, 2004; Gai *et al.*, 2018).

### 4.4 Dissolved and particulate toxin prevalence of dinoflagellate-related toxins

The measured variety of toxins produced by dinoflagellates was much greater and the temporal distribution therefore more complex. The most obvious peak of toxins related to dinoflagellates was observed in July for particulate toxins and in October and November for dissolved toxins. Spirolide (SPX) contents in the particulate phase clustered together with pectenotoxin (PTX) contents. This pattern of toxin clustering repeated itself time-delayed in the dissolved toxins, although these toxins also clustered together with okadaic acid (OA), one gymnodimine (GYM) and a yessotoxin isomer (YTX, Fig. 4). This suggests that the causative organisms kept the majority of toxins intracellularly and afterwards released the toxins into the water, probably due to cell death. The time gap between particulate and dissolved toxins may have been smaller than presented due to unmeasured toxin contents in the discontinuous measurements from particulate toxins and metabarcoding samples. Nevertheless, this does not affect the overall tendency of dissolved toxin patterns to repeat after the particulate toxin patterns.

The highest peaks in recorded particulate SPX in our data coincided with the metabarcoding peak of *Alexandrium ostenfeldii* in late July 2017. Currently, *A. ostenfeldii* is the only known producer of SPX (Cembella *et al.*, 2000; 2001), but the organism is also associated to the production of paralytic shellfish toxins (PST, including saxitoxin;STX and gonyautoxins;GTX), and gymnodimines (GYM) (Salgado *et al.*, 2015; Van de Waal *et al.*, 2015). In August 2012, SPX-producing *A. ostenfeldii* strains were also documented in the Disko Bay area (Tillmann *et al.*, 2014). The same seasonal occurrence appeared in the northern Baltic Sea with the highest *A. ostenfeldii* abundance in the warm periods of July and August (Hakanen *et al.*, 2012), and in July 2013 in the Netherlands (Van de Waal *et al.*, 2015). Hence, *A. ostenfeldii* typically appears in the

warmer months after the initial spring bloom peak, both in temperate and Arctic areas. Three GYM toxins peaked in January to March in the dissolved phase. We did not observe the community structure in the time period before this measurement, so it remains speculative which organism produced the toxins. GYM was first reported to be produced by *Karenia selliformis* (reported as *Gymnodinium* sp.; Seki *et al.*, 1996), which was not found in our metabarcoding analyses. Another source of GYM is *A. ostenfeldii* (reported as *A. peruvianum*; Van Wagoner *et al.*, 2011; Martens *et al.*, 2017). However, GYM was present at different time periods than SPX, so *A. ostenfeldii* most likely can be excluded as the GYM-producing species. This indicates that in all probability there are other, yet unidentified GYM-producing organisms in the West Greenland region. The occurrence of PTX, OA, and YTX could also not be linked to causative organisms. Possible causative organisms for these toxins that were detected in the metabarcoding data comprise *Dinophysis acuminata* (OA, DTX, PTX), *Dinophysis* spp. (OA, DTX, PTX), *Gonyaulax spinifera* (YTX), *Prorocentrum* spp. (OA) and *Protoceratium reticulatum* (YTX). In the relative OTU abundance of these species, no obvious temporal distribution patterns were found that coincide with the toxin patterns. For instance, in Japanese waters, *Dinophysis acuminata*, a potential producer of OA, DTX and PTX, appeared in the warmer months May, June and July and additionally in October, November and December (Nishitani *et al.*, 2002). This bi-annual succession pattern cannot be observed in the metabarcoding data, but more or less in the dissolved toxin pattern, where we have a peak of OA and PTX in late summer and a peak of a DTX Isomer in winter. For some dinoflagellates like *Dinophysis* spp., a patchy occurrence in thin layers in the water column has been reported, which can result in sampling bias (Escalera *et al.*, 2012). Single cells of *Dinophysis* were seen in inspections by microscopy of plankton net samples, which sampled the whole water column (this study). The samples used for metabarcoding were a pooled approach of different depths and not a fully integrated sample of all depths. This may have resulted in missing the distinct water column layer of occurrence for the organisms. This highlights the importance of passive sampling of dissolved toxins, which was able to detect DTX, OA and GYM in contrast to the sampling approach for particulate toxins, where none of these toxins were detected.

Azaspiracid-1 was detected in the dissolved phase but not in the particulate phase. *Azadinium* cells, producing azaspiracid-1, are below 20 µm in size, and may hence have been missed in the particulate toxin phase based on 20 µm plankton net hauls. Only one OTU belonging to the genus *Azadinium* was detected in the sequenced data, but was excluded with subsequent curation and analyses of data due to its low read numbers. A new *Azadinium* species named *Azadinium perforatum* has recently been described for West Greenlandic waters (Tillmann *et al.*, 2020), suggesting the possibility that the DNA signature of other, AZA-producing species may have not yet been implemented in the databases that were been used for

identification of our OTU data. This shows the need for the development of more and larger references databases so that less species remain invisible in a background of non-assigned reads/sequences.

## 5. Conclusions

In conclusion, the investigated area in Disko Bay, West Greenland did not exhibit an HAB event in the examined period, but presence of several HAB species and their toxins in the expected succession pattern of diatoms during the spring bloom event, followed by dinoflagellates in summer. The toxins usually appear first in the phytoplankton and are later on found dissolved in water. The observed seasonal dynamics of HAB species and toxins can be used as a baseline for HAB potential for this area and for comparison for future HAB events.

## Funding

Funding provided by the Danish Research Council for Nature and Universe was given to Nina Lundholm. Financial support for Claudia Sabine Bruhn, Uwe John, and Bernd Krock was provided by the PACES research program of the Alfred-Wegener-Institute, Helmholtz-centre for polar and marine research. Sylke Wohlrab was funded by the Ministry for Science and Culture of Lower Saxony and the Volkswagen Foundation through the “Niedersächsisches Vorab” grant program (grant number ZN3285).

## Acknowledgements

We are grateful to Nancy Kühne for her technical assistance in the laboratory. The toxin analyses were supported by Thomas Max and Annegret Müller, whom we thank for their technical aid in the laboratory. We thank Kai-Uwe Ludwichowski for the nutrient analysis.

The expeditions were conducted within the framework of the Disko Marine Basis Program, Arctic Station, Greenland and was financially and logistically supported under the PACES II Programme of the Alfred Wegener Institute, Helmholtz Centre for Polar and Marine Research, Germany. The Helmholtz Institute for Functional Marine Biodiversity is a collaboration between the Alfred Wegener Institute, Helmholtz-Centre for Polar and Marine Research, and the Carl-von-Ossietzky University Oldenburg, initially funded by the Ministry for Science and Culture of Lower Saxony and the Volkswagen Foundation through the “Niedersächsisches Vorab” grant program (grant number ZN3285).

## References

'HAEDAT Event NO-17-038', 2017 <http://haedat.iode.org/viewEvent.php?eventID=5915> [accessed 29 April 2020]

Anderson, D. M., Cembella, A. D., Hallegraeff, G. M. (2012). Progress in Understanding Harmful Algal Blooms: Paradigm Shifts and New Technologies for Research, Monitoring, and Management. *Annu. Rev. Mar. Sci.*, **4**, 143-176.

Arar, E. J., Collins, G. B. (1997). Method 445.0 In Vitro Determination of Chlorophyll *a* and Pheophytin a in Marine and Freshwater Algae by Fluorescence. *U.S. Environmental Protection Agency, Washington, DC*, 1-22.

Armstrong, F. A. J., Stearns, C. R., Strickland, J. D. H. (1967). The measurement of upwelling and subsequent biological process by means of the Technicon Autoanalyzer® and associated equipment. *Deep-Sea Res. Oceanogr. Abstr.*, **14**, 381-389.

Baggesen, C., Moestrup, Ø., Daugbjerg, N., Krock, B., Cembella, A. D., Madsen, S. (2012). Molecular phylogeny and toxin profiles of *Alexandrium tamarense* (Lebour) Balech (Dinophyceae) from the west coast of Greenland. *Harmful Algae*, **19**, 108-116.

Bates, S. S., Hubbard, K. A., Lundholm, N., Montresor, M., Leaw, C. P. (2018). *Pseudo-nitzschia*, *Nitzschia*, and domoic acid: New research since 2011. *Harmful Algae*, **79**, 3-43.

Brander, K. M., Milligan, S. P., Nichols, J. H. (1993). Flume tank experiments to estimate the volume filtered by high-speed plankton samplers and to assess the effect of net clogging. *J. Plankton Res.*, **15**(4), 385-401.

Brett, D. (Ed.). (2003). Europe Review 2003/4: The Economic and Business Report (World of Information Reviews Series) (15th ed.). *Walden Publishing Ltd.*

Cembella, A. D., Lewis, N. I., Quilliam, M. A. (2000). The marine dinoflagellate *Alexandrium ostenfeldii* (Dinophyceae) as the causative organism of spirolide shellfish toxins. *Phycologia*, **39**(1), 67-74.

Cembella, A. D. (2003). Chemical ecology of eukaryotic microalgae in marine ecosystems. *Phycologia*, **42**(4), 420–447.

Cembella, A. D., Bauder, A. G., Lewis, N. I., Quilliam, M. A. (2001). Association of the gonyaulacoid dinoflagellate *Alexandrium ostenfeldii* with spirolide toxins in size-fractionated plankton. *J. Plankton Res.*, **23**(12), 1413-1419.

Corner, E. D. S., Newell, B. S. (1967). On the nutrition and metabolism of zooplankton; IV. The forms of nitrogen excreted by *Calanus*. *J. Mar. Biolog. Assoc. UK.*, **47**(1), 113-120.

Dolah, F. M. Van. (2000). Marine Algal Toxins: Origins, Health Effects, and Their Increased Occurrence. *Environ. Health Perspect.*, **108**, 133-141.

Dünweber, M., Swalethorp, R., Kjellerup, S., Nielsen, T. G., Arendt, K. E., Hjorth, M., Tönnesson, K., Møller, E. F. (2010). Succession and fate of the spring diatom bloom in Disko Bay, western Greenland. *Mar. Ecol. Prog. Ser.*, **419**, 11-29.

Eberlein, K., Kattner, G. (1987). Automatic method for the determination of ortho-phosphate and total dissolved phosphorus in the marine environment. *Fresenius' Zeitschrift Für Analytische Chemie*, *326*, 354-357.

Elferink, S., John, U., Neuhaus, S., & Wohlrab, S. (2020a). Functional Genomics Differentiate Inherent and Environmentally Influenced Traits in Dinoflagellate and Diatom Communities. *Microorganisms*, **8**(567), 1-22.

Elferink, S., Neuhaus, S., Wohlrab, S., Toebe, K., Voß, D., Gottschling, M., Lundholm, N., Krock, B., Koch, B. P., Zielinski, O., Cembella, A., John, U. (2017). Molecular diversity patterns among various phytoplankton size-fractions in West Greenland in late summer. *Deep-Sea Res. Pt. I*, **121**, 54-69.

Elferink, S., Wohlrab, S., Neuhaus, S., Cembella, A., Harms, L., & John, U. (2020). Comparative Metabarcoding and Metatranscriptomic Analysis of Microeukaryotes Within Coastal Surface Waters of West Greenland and Northwest Iceland. *Front. Mar. Sci.*, **7**(439), 1-20.

Escalera, L., Pazos, Y., Dolores, M., Reguera, B. (2012). A comparison of integrated and discrete depth sampling for monitoring toxic species of Dinophysis. *Mar. Pollut. Bull.*, **64**, 106-113.

Falkowski, P. G. (1994). The role of phytoplankton photosynthesis in global biogeochemical cycles. *Photosynth. Res.*, **39**, 235-258.

Field, C. B., Behrenfeld, M. J., Randerson, J. T. (1998). Primary Production of the Biosphere: Integrating Terrestrial and Oceanic Components. *Science*, **281**, 237-241.

Flynn, K. J., Mitra, A., Anestis, K., Anschütz, A. A., Calbet, A., Duarte Ferreira, G., Gypens, N., Hansen, P. J., John, U., Lapeyra Martin, J., Mansour, J. S., Maselli, M., Medić, N., Norlin, A., Not, F., Pitta, P., Romano, F., Saiz, E., Schneider, L. K., Stolte, W., Traboni, C. (2019). Mixotrophic protists and a new paradigm for marine ecology: where does plankton research go now?, **41**, 375-391.

Fragoso, G. M., Poulton, A. J., Yashayaev, I. M., Head, E. J. H., Purdie, D. A. (2017). Spring phytoplankton communities of the Labrador Sea (2005 - 2014): pigment signatures, photophysiology and elemental ratios. *Biogeosciences*, *14*, 1235-1259.

Gai, F. F., Hedemand, C. K., Louw, D. C., Grobler, K., Krock, B., Moestrup, Ø., Lundholm, N. (2018). Morphological, molecular and toxigenic characteristics of Namibian *Pseudo-nitzschia* species – including *Pseudo-nitzschia bucculenta* sp. nov. *Harmful Algae*, **76**, 80-95.

Gao, C., Lin, S., Chen, M., Hong, J., Liu, C. (2019). Toxicon Prevalence of phycotoxin contamination in shellfish from the Northern Bering Sea and the Chukchi Sea. *Toxicon*, **167**, 76-81.

Geuer, J. K., Krock, B., Leefmann, T., Koch, B. P. (2019). Quantification, extractability and stability of dissolved domoic acid within marine dissolved organic matter. *Mar. Chem*., **215**, 103669.

Glibert, P. M. (2016). Margalef revisited: A new phytoplankton mandala incorporating twelve dimensions, including nutritional physiology. *Harmful Algae*, **55**, 25-30.

Grasshoff, K., Ehrhardt, M., Kremling, K. (1983). Methods of Seawater Analysis (2nd ed.). *John Wiley & Sons: Weinheim, Germany.*

Guillou, L., Bachar, D., Audic, S., Bass, D., Berney, C., Bittner, L., Boutte, C., Burgaud, G., de Vargas, C., Decelle, J., del Campo, J., Dolan, J. R., Dunthorn, M., Edvardsen, B., Holzmann, M., Kooistra, W. H. C. F., Enrique, L., Le Bescot, N. , Logares, R., Mahé, F., Massana, R., Montresor, M., Morard, R., Not, F., Pawlowski, J., Probert, I., Sauvadet, A.-L., Siano, R., Stoeck, T., Vaulot, D., Zimmermann, P., Christen, R. (2013). The Protist Ribosomal Reference database ($PR^2$): a catalog of unicellular eukaryote Small Sub-Unit rRNA sequences with curated taxonomy. *Nucleic Acids Res. Spec. Publ*., **41**, 597-604.

Guo, L., Sui, Z., Liu, Y. (2016). Quantitative analysis of dinoflagellates and diatoms community via Miseq sequencing of actin gene and v9 region of 18S rDNA. *Sci. Rep*., (October), 1-9.

Hakanen, P., Suikkanen, S., Franzén, J., Franzén, H., Kankaanpää, H., Kremp, A. (2012). Bloom and toxin dynamics of *Alexandrium ostenfeldii* in a shallow embayment at the SW coast of Finland, northern Baltic Sea. *Harmful Algae*, **15**, 91-99.

Hallegraeff, G. M. (2010). Ocean climate change, phytoplankton community responses, and harmful algal blooms: a formidable predictive challenge. *J. Phycol*., **46**, 220-235.

Hallegraeff, G. M., Anderson, D. M., Cembella, A. D. (2003). Manual on Harmful Marine Microalgae. *UNESCO Publishing*.

Hansen, L. R., Soylu, S. í, Kotaki, Y., Moestrup, Ø., Lundholm, N. (2011). Toxin production and temperature-induced morphological variation of the diatom *Pseudo-nitzschia seriata* from the Arctic. *Harmful Algae*, **10**(6), 689-696.

Harðardóttir, S., Pančić, M., Tammilehto, A., Krock, B., Møller, E. F., Nielsen, T. G., Lundholm, N. (2015). Dangerous Relations in the Arctic Marine Food Web: Interactions between Toxin Producing *Pseudo-nitzschia* Diatoms and *Calanus* Copepodites. *Mar. Drugs*, **13**(June), 3809-3835.

Hasle, G. R. (2002). Are most of the domoic acid-producing species of the diatom genus *Pseudo-nitzschia* cosmopolites? *Harmful Algae*, **1**, 137-146.

Hegseth, E. N., Tverberg, V. (2013). Effect of Atlantic water in flow on timing of the phytoplankton spring bloom in a high Arctic fjord (Kongsfjorden, Svalbard). *J. Marine Syst.*, **113-114**, 94-105.

Hinder, S. L., Hays, G. C., Edwards, M., Roberts, E. C., Walne, A. W., Gravenor, M. B. (2012). Changes in marine dinoflagellate and diatom abundance under climate change. *Nat. Clim. Change*, **2**, 271-275.

Hobson, K. A., Welch, H. E. (1992). Determination of trophic relationships within a high Arctic marine food web using $\delta^{13}C$ and $\delta^{15}N$ analysis. *Mar. Ecol. Prog. Ser.*, **84**, 9-18.

Ianora, A., Bentley, M. G., Caldwell, G. S., Casotti, R., Cembella, A. D., Engström-Öst, J., Halsband, C., Sonnenschein, E., Legrand, C., Llewellyn, C. A., Paldavičienë, A., Pilkaityte, R., Pohnert, G., Razinkovas, A., Romano, G., Tillmann, U., Vaiciute, D. (2011). The Relevance of Marine Chemical Ecology to Plankton and Ecosystem Function: An Emerging Field. *Mar. Drugs*, **9**, 1625-1648.

John, U., Litaker, R. W., Montresor, M., Murray, S., Brosnahan, M. L., Anderson, D. M. (2014). Formal Revision of the *Alexandrium tamarense* Species Complex (Dinophyceae) Taxonomy: The Introduction of Five Species with Emphasis on Molecular-based (rDNA) Classification. *Protist*, **165**(6), 779-804.

Koroleff, F. (1969). Direct determination of ammonia in natural waters as indophenol blue. International Council for the Exploration of the Sea.

Krock, B., Schloss, I. R., Trefault, N., Tillmann, U., Hernando, M., Deregibus, D., Antoni, J., Almandoz, G. O., Hoppenrath, M. (2020). Detection of the phycotoxin pectenotoxin-2 in waters around King George Island, Antarctica. *Polar Biol.*, **43**, 263-277.

Lane, J. Q., Roddam, C. M., Langlois, G. W., Kudela, R. M. (2010). Application of Solid Phase Adsorption Toxin Tracking (SPATT) for field detection of the hydrophilic phycotoxins domoic acid and saxitoxin in coastal California. *Limnol. Oceanogr.: Methods*, **8**, 645-660.

Lefebvre, K. A., Quakenbush, L., Frame, E., Burek Huntington, K., Sheffield, G., Stimmelmayr, R., Bryan, A., Kendrick, P., Ziel, H., Goldstein, T., Snyder, J. A., Gelatt, T., Gulland, F., Dickerson, B., Gill, V. (2016). Prevalence of algal toxins in Alaskan marine mammals foraging in a changing arctic and subarctic environment. *Harmful Algae*, **55**, 13-24.

Lundholm, N., Hansen, P. J., Kotaki, Y. (2004). Effect of pH on growth and domoic acid production by potentially toxic diatoms of the genera *Pseudo-nitzschia* and *Nitzschia*. *Mar. Ecol. Prog. Ser*., **273**, 1-15.

Lundholm, N., Krock, B., John, U., Skov, J., Cheng, J., Pančić, M., Wohlrab, S., Rigby, K., Gissel Nielsen, T., Selander, E., Harðardóttir, S. (2018). The distribution and impacts of harmful algal bloom species in eastern boundary upwelling systems. *Harmful Algae*, **85**, 33-52.

MacKenzie, L., Beuzenberg, V., Holland, P., McNabb, P., Selwood, A. (2004). Solid phase adsorption toxin tracking (SPATT): a new monitoring tool that simulates the biotoxin contamination of filter feeding bivalves. *Toxicon*, **44**, 901-918.

Marquardt, M., Vader, A., Stübner, E. I., Reigstad, M., Gabrielsen, T. M. (2016). Strong Seasonality of Marine Microbial Eukaryotes in a High-Arctic Fjord (Isfjorden, in West Spitsbergen, Norway). Appl. Environ. *Microbiol.*, **82**(6), 1868-1880.

Martens, H., Tillmann, U., Harju, K., Dell'Aversano, C., Tartaglione, L., Krock, B. (2017). Toxin Variability Estimations of 68 *Alexandrium ostenfeldii* (Dinophyceae) Strains from The Netherlands Reveal a Novel Abundant Gymnodimine. *Microorganisms*, **5**(29), 1-24.

Mauritsen, T. (2016). Greenhouse warming unleashed. *Nat. Geosci*., **9**(4), 268-269.

McBean, G., Alekseev, G., Chen, D., Førland, E., Fyfe, J., Groisman, P. Y., King, R., Melling, H., Vose, R., Whitfield, P. H. (2005). Arctic Climate: Past and Present. *Arctic Climate Impacts Assessment (ACIA)*, 21-60.

McCarthy, G. D., Haigh, I. D. (2015). Ocean impact on decadal Atlantic climate variability revealed by sea-level observations. *Nature*, **521**, 508-510.

Meire, L., Mortensen, J., Meire, P., Sejr, M. K., Rysgaard, S., Nygaard, R., Huybrechts, P., Meysman, F. J. R. (2017). Marine-terminating glaciers sustain high productivity in Greenland fjords. *Glob. Change Biol.*, **23**(12), 1-14.

Moestrup, Ø., Akselmann-Cardella, R., Churro, C., Fraga, S., Hoppenrath, M., Iwataki, M., Larsen, J., Lundholm, N., Zingone, A. (2009). IOC-UNESCO Taxonomic Reference List of Harmful Micro Algae.

Moritz, R. E., Bitz, C. M., Steig, E. J. (2002). Dynamics of Recent Climate Change in the Arctic. *Science*, **297**, 1497-1503.

Munday, R., Quilliam, M. A., LeBlanc, P., Lewis, N., Gallant, P., Sperker, S. A., Ewart, H. S., MacKinnon, S. L. (2012). Investigations into the Toxicology of Spirolides, a Group of Marine Phycotoxins. *Toxins*, **4**(1), 1-14.

Nishitani, G., Sugioka, H., Imai, I. (2002). Seasonal distribution of species of the toxic dinoflagellate genus *Dinophysis* in Maizuru Bay (Japan), with comments on their autofluorescence and attachment of picophytoplankton. *Harmful Algae*, **1**, 253-264.

Okolodkov, Y. B., Dodge, J. D. (1996). Biodiversity and biogeography of planktonic dinoflagellates in the Arctic Ocean. *J. Exp. Mar. Biol. Ecol*., **202**(1), 19-27.

Overpeck, J., Hughen, K., Hardy, D., Bradley, R., Case, R., Douglas, M., Finney, B., Gajewski, K., Jacoby, G., Jennings, A., Lamoureux, S., Lasca, A., Macdonald, G., Moore, J., Retelle, M., Smith, S., Wolfe, A., Zielinski, G. (1997). Arctic Environmental Change of the Last Four Centuries. *Science*, **278**, 1251-1257.

Pachauri, R. K., Reisinger A. (Eds., Core Writing Team). IPCC, 2007: Climate Change 2007: Synthesis Report. Contribution of Working Groups I, II and III to the Fourth Assessment Report of the Intergovernmental Panel on Climate Change. *IPCC, Geneva, Switzerland*, 104 pp.

Pachauri, R. K., Meyer, L. A. (Eds., Core Writing Team). IPCC, 2014: Climate Change 2014: Synthesis Report. Contribution of Working Groups I, II to the Fifth Assessment Report of the Intergovernmental Panel on Climate Change. *IPCC, Geneva, Switzerland*, 151 pp.

Pagou, K. A., Hallegraeff, G. M. (Eds.). (2012). Proceedings of the 14th international conference on harmful algae. International Society for the Study of Harmful Algae and Intergovernmental Oceanographic Commission of UNESCO 2012.

Peperzak, L. (2003). Climate change and harmful algal blooms in the North Sea. *ACTA Oecol*., **24**, S139-S144.

Percopo, I., Ruggiero, M. V., Balzano, S., Gourvil, P., Lundholm, N., Tammilehto, A., Vaulot, D. (2016). *Pseudo-nitzschia arctica* sp. nov., a new cold-water cryptic *Pseudo-nitzschia* species within the *P. pseudodelicatissima* complex. *J. Phycol*., **52**, 184-199.

Piredda, R., Tomasino, M. P., Erchia, A. M. D. (2016). Diversity and temporal patterns of planktonic protist assemblages at a Mediterranean LTER site.

Ralston, D. K., Keafer, B. A., Brosnahan, M. L., Anderson, D. M. (2014). Temperature dependence of an estuarine harmful algal bloom: Resolving interannual variability in bloom dynamics using a degree-day approach. Limnol. *Oceanogr*., **59**(4), 1112-1126.

Raymont, J. E. G. (1980). Plankton and Productivity in the Oceans (2nd ed., Vol. 2). *Pergamon Press Ltd.: Oxford, England.*

Reguera, B., Riobó, P., Rodríguez, F., Díaz, P. A., Pizarro, G., Paz, B., Franco, J. M., Blanco, J. (2014). Dinophysis Toxins: Causative Organisms, Distribution and Fate in Shellfish*. Mar. Drugs*, 394-461.

Richard, D., Arsenault, E., Cembella, A. D., Quilliam, M. A. (2000). Investigations into the toxicology and pharmacology of spirolides, a novel group of shellfish toxins. (G. M. Hallegraeff, S. I. Blackburn, C. J. Bolch, & R. J. Lewis, Eds.), Harmful Algal Blooms 2000. *International Oceanographic Commission (UNESCO), Paris*.

Salgado, P., Riobó, P., Rodríguez, F., Franco, J. M., Bravo, I. (2015). Differences in the toxin profiles of *Alexandrium ostenfeldii* (Dinophyceae) strains isolated from different geographic origins: Evidence of paralytic toxin, spirolide, and gymnodimine. *Toxicon*, **103**, 85-98.

Seki, T., Satake, M., MacKenzie, A. L., Kaspar, H. F., Yasumoto, T. (1996). Gymnodimine, a novel toxic imine isolated from the Foveaux Strait oysters and *Gymnodinium* sp. Harmful and Toxic Algal Blooms. (T. Yasumoto, Y. Oshima and Y. Fukuyo, Eds.), *Intergovernmental Oceanographic Commission of UNESCO* 495-498.

Seuthe, L., Töpper, B., Reigstad, M., Thyrhaug, R., Vaquer-Sunyer R. (2011). Microbial communities and processes in ice-covered Arctic waters of the northwestern Fram Strait (75 to 80° N) during the vernal pre-bloom phase. *Aquat. Microb. Ecol*., **64**, 253-266.

Smayda, T. J. (1997). Harmful algal blooms: Their ecophysiology and general relevance to phytoplankton blooms in the sea. *Limnol. Oceanogr*., **42**(5), 1137-1153.

Smayda, T. J., Trainer, V. L. (2010). Dinoflagellate blooms in upwelling systems: Seeding, variability, and contrasts with diatom bloom behaviour. *Prog. Oceanogr*., **85**, 92-107.

Tammilehto, A., Gissel, T., Krock, B., Friis, E., Lundholm, N. (2012). *Calanus* spp. - Vectors for the biotoxin, domoic acid, in the Arctic marine ecosystem? *Harmful Algae*, **20**, 165-174.

Sprong, P. A. A., Fofonova, V., Wiltshire, K. H., Neuhaus, S., Ludwichowski, K. U., Käse, L., Androsov, A., Metfies, K. (2020). Spatial dynamics of eukaryotic microbial communities in the German Bight. *J. Sea Res*., **163**, 101914.

Tammilehto, A., Watts, P. C., Lundholm, N. (2017). Isolation by Time during an Arctic Phytoplankton Spring Bloom*. J. Eukaryot. Microbiol*., **64**, 248-256.

Tillmann, U., Edvardsen, B., Krock, B., Smith, K. F., Paterson, R. F., Voß, D. (2018). Diversity, distribution, and azaspiracids of Amphidomataceae (Dinophyceae) along the Norwegian coast. *Harmful Algae*, **80**, 15-34.

Tillmann, U., Gottschling, M., Nézan, E., Krock, B. (2015). First records of *Amphidoma languida* and *Azadinium dexteroporum* (Amphidomataceae, Dinophyceae) from the Irminger Sea off Iceland. *Mar. Biodivers. Rec*., **8**, 1-11.

Tillmann, U., Kremp, A., Tahvanainen, P., Krock, B. (2014). Characterization of spirolide producing *Alexandrium ostenfeldii* (Dinophyceae) from the western Arctic. *Harmful Algae*, **39**, 259-270.

Tillmann, U., Wietkamp, S., Krock, B., Tillmann, A., Voss, D., Gu, H. (2020). Amphidomataceae (Dinophyceae) in the western Greenland area, including description of *Azadinium perforatum* sp. nov. *Phycologia*, **59**(1), 63-88.

Torres Palenzuela, J. M., Gonzáles Vilas, L., Bellas, F. M., Garet, E., González-Fernández, Á., Spyrakos, E. (2019). *Pseudo-nitzschia* Blooms in a Coastal Upwelling System: Remote Sensing Detection, Toxicity and Environmental Variables. *Water*, **11**, 1-24.

Vahl, B., Kleemann, N. (Eds.). (2019). Greenland in figures. *Statistics Greenland.*

Van de Waal, D. B., Tillmann, U., Martens, H., Krock, B., van Scheppingen, Y., John, U. (2015). Characterization of multiple isolates from an *Alexandrium ostenfeldii* bloom in The Netherlands. *Harmful Algae*, **49**, 94-104.

Wadham, J. L., Hawkings, J., Telling, J., Chandler, D., Alcock, J., Lawson, E. (2016). Sources, cycling and export of nitrogen on the Greenland Ice Sheet. *Biogeosciences Discuss*., **13**, 1-30.

Van Wagoner, R. M., Misner, I., Tomas, C., Wright, J. L. C. (2011). Occurrence of 12-methylgymnodimine in a spirolide-producing dinoflagellate *Alexandrium peruvianum* and the biogenetic implications. Tetrahedron Lett., 52(33), 4243-4246.Wells, M. L., Trainer, V. L., Smayda, T. J., Karlson, B. S. O., Trick, C. G., Kudela, R. M., Ishikawa, A., Bernard, S., Wulff, A., Anderson, D. M., Cochlan, W. P. (2015). Harmful algal blooms and climate change: Learning from the past and present to forecast the future. *Harmful Algae*, **49**, 68-93.

Wohlrab, S., John, U., Klemm, K., Eberlein, T., Forsberg Grivohiannis, A. M., Krock, B., Frickenhaus, S., Bach, L., Rost, B., Riebesell, U., Van de Waal, D. B. (2019). Ocean acidification increases domoic acid contents during a spring to summer succession of coastal phytoplankton. *Harmful Algae*, **92**, 101697.

# Chapter 3

**Supplementary**

**Material**

| Particulate toxins | | | | | | | | | | | | | | |
|---|---|---|---|---|---|---|---|---|---|---|---|---|---|---|
| date | 04.05.2017 | 14.05.2017 | 26.05.2017 | 14.06.2017 | 27.06.2017 | 12.07.2017 | 27.07.2017 | | | | | | | |
| DA [pg/planktonhaul] | 46666.67 | 26717.17 | 81010.10 | 11767.68 | 13704.55 | 3312.83 | 23706.29 | | | | | | | |
| GYM [pg/planktonhaul] | 0.00 | 0.00 | 0.00 | 0.00 | 0.00 | 0.00 | 0.00 | | | | | | | |
| SPX1 [pg/planktonhaul] | 0.00 | 0.00 | 0.00 | 0.00 | 16216.98 | 30882.35 | 23381.71 | | | | | | | |
| SPX-A [pg/planktonhaul] | 0.00 | 0.00 | 0.00 | 6918.24 | 50943.40 | 73534.96 | 121915.82 | | | | | | | |
| SPX-G [pg/planktonhaul] | 0.00 | 0.00 | 0.00 | 0.00 | 54905.66 | 113041.07 | 108418.00 | | | | | | | |
| 20-me-SPX-G [pg/planktonhaul] | 0.00 | 0.00 | 0.00 | 24109.01 | 112924.53 | 207436.18 | 283454.28 | | | | | | | |
| SPX-C [pg/planktonhaul] | 0.00 | 0.00 | 0.00 | 12704.40 | 52075.47 | 77497.23 | 63570.39 | | | | | | | |
| GONA [pg/planktonhaul] | 0.00 | 0.00 | 0.00 | 0.00 | 0.00 | 0.00 | 0.00 | | | | | | | |
| OA [pg/planktonhaul] | 0.00 | 0.00 | 0.00 | 0.00 | 0.00 | 0.00 | 0.00 | | | | | | | |
| DTX2 [pg/planktonhaul] | 0.00 | 0.00 | 0.00 | 0.00 | 0.00 | 0.00 | 0.00 | | | | | | | |
| DTX1 [pg/planktonhaul] | 0.00 | 0.00 | 0.00 | 0.00 | 0.00 | 0.00 | 0.00 | | | | | | | |
| AZA1 [pg/planktonhaul] | 0.00 | 0.00 | 0.00 | 0.00 | 0.00 | 0.00 | 0.00 | | | | | | | |
| PTX2 [pg/planktonhaul] | 0.00 | 0.00 | 0.00 | 25154.32 | 0.00 | 24963.24 | 0.00 | | | | | | | |
| YTX [pg/planktonhaul] | 0.00 | 0.00 | 0.00 | 0.00 | 0.00 | 0.00 | 0.00 | | | | | | | |
| GTX 2/3 [pg/planktonhaul] | 0 | 0 | 0 | 0 | 0 | 2390622.62 | 5686153.85 | | | | | | | |
| STX [pg/planktonhaul] | 0 | 0 | 0 | 0 | 0 | 1571184.98 | 0 | | | | | | | |
| | | | | | | | | | | | | | | |
| | | | | | | | | | | | | | | |
| date | 12.02.2018 | 15.02.2018 | 21.02.2018 | 27.02.2018 | 07.03.2018 | 16.03.2018 | 21.03.2018 | 26.03.2018 | 30.03.2018 | 05.04.2018 | 09.04.2018 | 13.04.2018 | 19.04.2018 | 23.04.2018 |
| DA [pg/planktonhaul] | 0.00 | 0.00 | 0.00 | 0.00 | 0.00 | 0.00 | 0.00 | 0.00 | 0.00 | 0.00 | 0.00 | 0.00 | 851.20 | 631.06 |
| GYM [pg/planktonhaul] | 0.00 | 0.00 | 0.00 | 0.00 | 0.00 | 0.00 | 0.00 | 0.00 | 0.00 | 0.00 | 0.00 | 0.00 | 0.00 | 0.00 |
| SPX1 [pg/planktonhaul] | 0.00 | 0.00 | 0.00 | 0.00 | 0.00 | 0.00 | 0.00 | 0.00 | 0.00 | 0.00 | 0.00 | 706.24 | 0.00 | 0.00 |
| SPX-A [pg/planktonhaul] | 0.00 | 0.00 | 0.00 | 0.00 | 0.00 | 0.00 | 0.00 | 747.17 | 2615.09 | 0.00 | 0.00 | 0.00 | 2751.57 | 0.00 |
| SPX-G [pg/planktonhaul] | 0.00 | 0.00 | 0.00 | 0.00 | 0.00 | 0.00 | 0.00 | 0.00 | 0.00 | 0.00 | 0.00 | 0.00 | 0.00 | 0.00 |
| 20-me-SPX-G [pg/planktonhaul] | 1012.58 | 1427.67 | 6283.02 | 4901.89 | 1969.81 | 8830.19 | 9962.26 | 1613.21 | 4183.02 | 3809.43 | 3705.66 | 5283.94 | 14785.23 | 1196.02 |
| SPX-C [pg/planktonhaul] | 0.00 | 0.00 | 0.00 | 0.00 | 0.00 | 2609.43 | 2994.34 | 0.00 | 0.00 | 0.00 | 0.00 | 0.00 | 0.00 | 1107.97 |
| GONA [pg/planktonhaul] | 0.00 | 0.00 | 0.00 | 0.00 | 0.00 | 0.00 | 0.00 | 0.00 | 0.00 | 0.00 | 0.00 | 0.00 | 0.00 | 0.00 |
| OA [pg/planktonhaul] | 0.00 | 0.00 | 0.00 | 0.00 | 0.00 | 0.00 | 0.00 | 0.00 | 0.00 | 0.00 | 0.00 | 0.00 | 0.00 | 0.00 |
| DTX2 [pg/planktonhaul] | 0.00 | 0.00 | 0.00 | 0.00 | 0.00 | 0.00 | 0.00 | 0.00 | 0.00 | 0.00 | 0.00 | 0.00 | 0.00 | 0.00 |
| DTX1 [pg/planktonhaul] | 0.00 | 0.00 | 0.00 | 0.00 | 0.00 | 0.00 | 0.00 | 0.00 | 0.00 | 0.00 | 0.00 | 0.00 | 0.00 | 0.00 |
| AZA1 [pg/planktonhaul] | 0.00 | 0.00 | 0.00 | 0.00 | 0.00 | 0.00 | 0.00 | 0.00 | 0.00 | 0.00 | 0.00 | 0.00 | 0.00 | 0.00 |
| PTX2 [pg/planktonhaul] | 0.00 | 0.00 | 0.00 | 0.00 | 0.00 | 0.00 | 0.00 | 0.00 | 0.00 | 0.00 | 0.00 | 0.00 | 0.00 | 0.00 |
| YTX [pg/planktonhaul] | 0.00 | 0.00 | 0.00 | 0.00 | 0.00 | 0.00 | 0.00 | 0.00 | 0.00 | 0.00 | 0.00 | 0.00 | 0.00 | 0.00 |
| GTX 2/3 [pg/planktonhaul] | 0 | 0 | 0 | 0 | 0 | 0 | 0 | 0 | 0 | 0 | 0 | 0 | 0 | 0 |
| STX [pg/planktonhaul] | 0 | 0 | 0 | 0 | 0 | 0 | 0 | 0 | 0 | 0 | 0 | 0 | 0 | 0 |

## Dissolved Toxins

| SPATT | | | | | | | | | | | | | | | |
|---|---|---|---|---|---|---|---|---|---|---|---|---|---|---|---|
| start | 01.05.2017 | 18.05.2017 | 21.06.2017 | 20.07.2017 | 25.08.2017 | 18.09.2017 | 18.10.2017 | 18.11.2017 | 18.12.2017 | 18.01.2018 | 24.02.2018 | 18.03.2018 | | | |
| end | 18.05.2017 | 21.06.2017 | 20.07.2017 | 25.08.2017 | 18.09.2017 | 18.10.2017 | 18.11.2017 | 18.12.2017 | 18.01.2018 | 24.02.2018 | 18.03.2018* | 30.04.2018 | | | |
| days | 18 | 34 | 29 | 36 | 24 | 30 | 31 | 30 | 31 | 37 | 22 | 43 | | | |
| DA [pg/sample] | 0.00 | 0.00 | 0.00 | 0.00 | 0.00 | N/A | 0.00 | 0.00 | 0.00 | 0.00 | 0.00 | 0.00 | | | |
| AZA1 [pg/sample] | 0.00 | 57 | 0.00 | 0.00 | 0.00 | N/A | 20.81 | 13.00 | 11.92 | 0.00 | 0.00 | 0.00 | | | |
| DTX1 [pg/sample] | 0.00 | 0.00 | 0.00 | 19110.38 | 32619.44 | N/A | 37232.29 | 11861.61 | 9901.15 | 0.00 | 0.00 | 7677.10 | | | |
| DTX1 Isomer [pg/sample] | 0.00 | 0.00 | 0.00 | 0.00 | 0.00 | N/A | 0.00 | 8187.81 | 24876.44 | 16392.09 | 0.00 | 5024.71 | | | |
| DTX2 [pg/sample] | 0.00 | 0.00 | 0.00 | 0.00 | 0.00 | N/A | 0.00 | 0.00 | 0.00 | 0.00 | 0.00 | 0.00 | | | |
| GONA [pg/sample] | 0.00 | 0.00 | 0.00 | 0.00 | 0.00 | N/A | 0.00 | 0.00 | 0.00 | 0.00 | 0.00 | 0.00 | | | |
| GYM_494 [pg/sample] | 0.00 | 0.00 | 0.00 | 0.00 | 0.00 | N/A | 0.00 | 0.00 | 37.20 | 8.67 | 0.00 | 37.20 | | | |
| GYM_522 [pg/sample] | 0.00 | 0.00 | 0.00 | 0.00 | 0.00 | N/A | 0.00 | 0.00 | 21.13 | 48.12 | 0.00 | 48.12 | | | |
| GYM_548 [pg/sample] | 0.00 | 0.00 | 0.00 | 33.82 | 26.66 | N/A | 0.00 | 0.00 | 0.00 | 0.00 | 41.98 | 41.98 | | | |
| GYM_582 [pg/sample] | 0.00 | 0.00 | 0.00 | 0.00 | 0.00 | N/A | 0.00 | 0.00 | 13.86 | 34.10 | 0.00 | 34.10 | | | |
| GYM A [pg/sample] | 0.00 | 289 | 0.00 | 33.99 | 52.56 | N/A | 103.41 | 0.00 | 39.25 | 0.00 | 0.00 | 33.79 | | | |
| OA [pg/sample] | 0.00 | 0.00 | 0.00 | 5265.08 | 8372.94 | N/A | 22669.10 | 11261.43 | 7477.15 | 0.00 | 3893.97 | 8793.42 | | | |
| PTX2 [pg/sample] | 318.00 | 112.00 | 0.00 | 15734.27 | 41083.92 | N/A | 56293.71 | 15244.76 | 9283.22 | 1045.45 | 791.96 | 1423.08 | | | |
| PTX2sa [pg/sample] | 0.00 | 0.00 | 0.00 | 776.22 | 1431.82 | N/A | 6993.01 | 3653.85 | 2744.76 | 0.00 | 0.00 | 491.26 | | | |
| SPX1 [pg/sample] | 0.00 | 0.00 | 0.00 | 790.70 | 2288.37 | N/A | 3158.14 | 15.35 | 0.00 | 0.00 | 0.00 | 0.00 | | | |
| SPXA [pg/sample] | 0.00 | 0.00 | 0.00 | 497.67 | 1227.91 | N/A | 2386.05 | 87.91 | 83.72 | 0.00 | 0.00 | 0.00 | | | |
| SPXG [pg/sample] | 0.00 | 0.00 | 0.00 | 383.72 | 762.79 | N/A | 1646.51 | 97.67 | 0.00 | 0.00 | 0.00 | 0.00 | | | |
| SPXC [pg/sample] | 0.00 | 0.00 | 0.00 | 5674.42 | 18511.63 | N/A | 39860.47 | 2074.42 | 1176.74 | 0.00 | 0.00 | 0.00 | | | |
| 20-Me-SPX G [pg/sample] | 0.00 | 0.00 | 0.00 | 1469.77 | 4976.74 | N/A | 11441.86 | 716.28 | 365.58 | 0.00 | 0.00 | 0.00 | | | |
| YTX [pg/sample] | 0.00 | 0.00 | 0.00 | 0.00 | 0.00 | N/A | 0.00 | 0.00 | 0.00 | 0.00 | 0.00 | 0.00 | | | |
| YTX Isomer [pg/sample] | 0.00 | 0.00 | 0.00 | 3317.97 | 6866.36 | N/A | 1534.56 | 0.00 | 0.00 | 0.00 | 0.00 | 0.00 | | | |

| BIOMASS | | 04.05.2017 | 14.05.2017 | 26.05.2017 | 14.06.2017 | 27.06.2017 | 12.07.2017 | 27.07.2017 | |
|---|---|---|---|---|---|---|---|---|---|
| µg/mL | POC | 0.13695762 | 0.58701825 | 0.64842287 | 0.23397345 | 0.1328826 | 0.13054062 | 0.17559228 | |
| µg/mL | PON | 0.01538938 | 0.06147151 | 0.0704178 | 0.03612385 | 0.02272415 | 0.02055386 | 0.02519114 | |
| µg/L | Chl *a* | 1.5 | 3.41 | 4.21 | 1.25 | 0.37 | 0.52 | 0.76 | |
| | | | | | | | | | |
| | | | | | | | | | |
| | | 10.02.2018 | 12.02.2018 | 15.02.2018 | 21.02.2018 | 27.02.2018 | 07.03.2018 | 16.03.2018 | |
| µg/mL | POC | 0.06840125 | N/A | 0.06371959 | 0.04328883 | 0.01636097 | 0.03346165 | 0.03141414 | |
| µg/mL | PON | 0.00373564 | N/A | 0.00493894 | 0.00079789 | 0.00644227 | 0.00640959 | 0.00583208 | |
| µg/L | Chl *a* | 0.01 | 0.02 | 0.02 | 0.01 | 0.01 | 0.04 | 0.03 | |
| | | | | | | | | | |
| | | | | | | | | | |
| | | | | | | | | | |
| | | 21.03.2018 | 26.03.2018 | 30.03.2018 | 05.04.2018 | 09.04.2018 | 13.04.2018 | 19.04.2018 | 23.04.2018 |
| µg/mL | POC | 0.0140108 | 0.01617518 | N/A | 0.02378826 | N/A | 0.06612664 | 0.0498228 | 0.07078776 |
| µg/mL | PON | 0.00377187 | 0.00351215 | N/A | 0.00464008 | N/A | 0.01267147 | 0.00824059 | 0.01218555 |
| µg/L | Chl *a* | 0.06 | 0.06 | 0.08 | 0.12 | 0.43 | 0.38 | 1.26 | 0.71 |

| sample | date | Samp_Loc | size_fraction | Samp_Method | chlorophyll [ug/l] | NO3[umol/l] | NO2[umol/l] | Si[umol/l] | PO4[umol/l] | NH4[umol/l] | Temperature [°C] | Salinity [PSU] | ctd_type | POC[ug/ml] | PON[ug/m] |
|---|---|---|---|---|---|---|---|---|---|---|---|---|---|---|---|
| II_1_NB_3_DNA | 04.05.2017 | II | B 3um | niskin_sampler | 1.083423619 | 9.41 | 0.11 | 7.55 | 0.57 | 0.55 | -1.36 | 36.20 | manual | 0.13695762 | 0.01538938 |
| II_1_NB_20_DNA | 04.05.2017 | II | C 20um | niskin_sampler | 1.083423619 | 9.41 | 0.11 | 7.55 | 0.57 | 0.55 | -1.36 | 36.20 | manual | 0.13695762 | 0.01538938 |
| II_3_NB_3_DNA | 14.05.2017 | II | B 3um | niskin_sampler | 2.462983026 | 2.28 | 0.06 | 1.38 | 0.22 | 0.78 | -0.56 | 36 | manual | 0.58701825 | 0.06147151 |
| II_3_NB_20_DNA | 14.05.2017 | II | C 20um | niskin_sampler | 2.462983026 | 2.28 | 0.06 | 1.38 | 0.22 | 0.78 | -0.56 | 36 | manual | 0.58701825 | 0.06147151 |
| II_4_NB_3_DNA | 26.05.2017 | II | B 3um | niskin_sampler | 3.040808956 | 3.91 | 0.06 | 2.45 | 0.29 | 0.47 | -0.06111876 | 32.9627371 | CastAway | 0.64842287 | 0.0704178 |
| II_4_NB_20_DNA | 26.05.2017 | II | C 20um | niskin_sampler | 3.040808956 | 3.91 | 0.06 | 2.45 | 0.29 | 0.47 | -0.06111876 | 32.9627371 | CastAway | 0.64842287 | 0.0704178 |
| II_5_NB_3_DNA | 14.06.2017 | II | B 3um | niskin_sampler | 0.902853016 | 1.21 | 0.04 | 0.93 | 0.28 | 0.33 | 2.249180462 | 33.1784005 | CastAway | 0.23397345 | 0.03612385 |
| II_5_NB_20_DNA | 14.06.2017 | II | C 20um | niskin_sampler | 0.902853016 | 1.21 | 0.04 | 0.93 | 0.28 | 0.33 | 2.249180462 | 33.1784005 | CastAway | 0.23397345 | 0.03612385 |
| II_7_NB_3_DNA | 27.06.2017 | II | B 3um | niskin_sampler | 0.267244493 | 1.83 | 0.04 | 0.87 | 0.20 | 0.72 | 2.806801538 | 32.8505188 | SeaBird | 0.1328826 | 0.02272415 |
| II_7_NB_20_DNA | 27.06.2017 | II | C 20um | niskin_sampler | 0.267244493 | 1.83 | 0.04 | 0.87 | 0.20 | 0.72 | 2.806801538 | 32.8505188 | SeaBird | 0.1328826 | 0.02272415 |
| II_8_NB_3_DNA | 12.07.2017 | II | B 3um | niskin_sampler | 0.375586854 | 2.09 | 0.04 | 1.73 | 0.36 | 0.58 | 2.770328483 | 33.070862 | SeaBird | 0.13054062 | 0.02055386 |
| II_8_NB_20_DNA | 12.07.2017 | II | C 20um | niskin_sampler | 0.375586854 | 2.09 | 0.04 | 1.73 | 0.36 | 0.58 | 2.770328483 | 33.070862 | SeaBird | 0.13054062 | 0.02055386 |
| II_9_NB_3_DNA | 27.07.2017 | II | B 3um | niskin_sampler | 0.548934633 | 2.52 | 0.05 | 1.93 | 0.29 | 0.50 | 3.698250776 | 32.8997695 | SeaBird | 0.17559228 | 0.02519114 |
| II_9_NB_20_DNA | 27.07.2017 | II | C 20um | niskin_sampler | 0.548934633 | 2.52 | 0.05 | 1.93 | 0.29 | 0.50 | 3.698250776 | 32.8997695 | SeaBird | 0.17559228 | 0.02519114 |
| II_10_NB_3_DNA | 10.02.2018 | II | B 3µm | niskin_sample | 0.01 | 11.41 | 0.10 | 3.46 | 0.83 | 0.32 | | | | | |
| II_10_NB_20_DNA | 10.02.2018 | II | C 20µm | niskin_sample | 0.01 | 11.41 | 0.10 | 3.46 | 0.83 | 0.32 | | | | | |
| II_11_NB_3_DNA | 12.02.2018 | II | B 3µm | niskin_sample | 0.02 | 9.42 | 0.07 | 5.45 | 0.61 | 0.26 | | | | 0.06840125 | 0.00373564 |
| II_11_NB_20_DNA | 12.02.2018 | II | C 20µm | niskin_sample | 0.02 | 9.42 | 0.07 | 5.45 | 0.61 | 0.26 | | | | 0.06840125 | 0.00373564 |
| II_12_NB_3_DNA | 15.02.2018 | II | B 3µm | niskin_sample | 0.02 | 9.89 | 0.04 | 5.98 | 0.79 | 0.11 | -1.506990913 | 33.4022489 | SeaBird | 0.06371959 | 0.00493894 |
| II_12_NB_20_DNA | 15.02.2018 | II | C 20µm | niskin_sample | 0.02 | 9.89 | 0.04 | 5.98 | 0.79 | 0.11 | -1.506990913 | 33.4022489 | SeaBird | 0.06371959 | 0.00493894 |
| II_13_NB_3_DNA | 21.02.2018 | II | B 3µm | niskin_sample | 0.01 | 9.37 | 0.04 | 6.30 | 0.60 | 0.62 | -1.639556852 | 33.3859811 | SeaBird | 0.04328883 | 0.00079789 |
| II_13_NB_20_DNA | 21.02.2018 | II | C 20µm | niskin_sample | 0.01 | 9.37 | 0.04 | 6.30 | 0.60 | 0.62 | -1.639556852 | 33.3859811 | SeaBird | 0.04328883 | 0.00079789 |
| II_14_NB_3_DNA | 27.02.2018 | II | B 3µm | niskin_sample | 0.01 | 9.64 | 0.03 | 5.61 | 0.73 | 0.49 | -1.643568092 | 33.4202122 | SeaBird | 0.01636097 | 0.00644227 |
| II_14_NB_20_DNA | 27.02.2018 | II | C 20µm | niskin_sample | 0.01 | 9.64 | 0.03 | 5.61 | 0.73 | 0.49 | -1.643568092 | 33.4202122 | SeaBird | 0.01636097 | 0.00644227 |
| II_15_NB_3_DNA | 07.03.2018 | II | B 3µm | niskin_sample | 0.04 | 9.85 | 0.03 | 3.93 | 0.78 | 0.64 | -1.587212917 | 33.4258803 | SeaBird | 0.03346165 | 0.00640959 |
| II_15_NB_20_DNA | 07.03.2018 | II | C 20µm | niskin_sample | 0.04 | 9.85 | 0.03 | 3.93 | 0.78 | 0.64 | -1.587212917 | 33.4258803 | SeaBird | 0.03346165 | 0.00640959 |
| V_16_NB_3_DNA | 16.03.2018 | V | B 3µm | niskin_sample | 0.03 | 10.01 | 0.04 | 5.76 | 0.76 | 0.31 | -1.648598026 | 33.4268208 | SeaBird | 0.03141414 | 0.00583208 |
| V_16_NB_20_DNA | 16.03.2018 | V | C 20µm | niskin_sample | 0.03 | 10.01 | 0.04 | 5.76 | 0.76 | 0.31 | -1.648598026 | 33.4268208 | SeaBird | 0.03141414 | 0.00583208 |
| V_17_NB_3_DNA | 21.03.2018 | V | B 3µm | niskin_sample | 0.06 | 9.59 | 0.04 | 6.05 | 0.70 | 0.25 | -1.644742917 | 33.4268748 | SeaBird | 0.0140108 | 0.00377187 |
| V_17_NB_20_DNA | 21.03.2018 | V | C 20µm | niskin_sample | 0.06 | 9.59 | 0.04 | 6.05 | 0.70 | 0.25 | -1.644742917 | 33.4268748 | SeaBird | 0.0140108 | 0.00377187 |
| V_18_NB_3_DNA | 26.03.2018 | V | B 3µm | niskin_sample | 0.06 | 9.72 | 0.02 | 6.12 | 0.70 | 1.04 | -1.594067012 | 33.434016 | SeaBird | 0.01617518 | 0.00351215 |
| V_18_NB_20_DNA | 26.03.2018 | V | C 20µm | niskin_sample | 0.06 | 9.72 | 0.02 | 6.12 | 0.70 | 1.04 | -1.594067012 | 33.434016 | SeaBird | 0.01617518 | 0.00351215 |
| V_19_NB_3_DNA | 30.03.2018 | V | B 3µm | niskin_sample | 0.08 | 10.20 | 0.04 | 6.61 | 0.79 | 0.59 | -1.450889625 | 33.4465975 | SeaBird | | |
| V_19_NB_20_DNA | 30.03.2018 | V | C 20µm | niskin_sample | 0.08 | 10.20 | 0.04 | 6.61 | 0.79 | 0.59 | -1.450889625 | 33.4465975 | SeaBird | | |
| V_20_NB_3_DNA | 05.04.2018 | V | B 3µm | niskin_sample | 0.12 | 10.20 | 0.04 | 6.74 | 0.84 | 0.51 | -1.505095515 | 33.4481495 | SeaBird | 0.02378826 | 0.00464008 |
| V_20_NB_20_DNA | 05.04.2018 | V | C 20µm | niskin_sample | 0.12 | 10.20 | 0.04 | 6.74 | 0.84 | 0.51 | -1.505095515 | 33.4481495 | SeaBird | 0.02378826 | 0.00464008 |
| V_21_NB_3_DNA | 09.04.2018 | V | B 3µm | niskin_sample | 0.43 | 9.98 | 0.06 | 8.02 | 0.72 | 0.49 | -1.546393087 | 33.4473482 | SeaBird | | |
| V_21_NB_20_DNA | 09.04.2018 | V | C 20µm | niskin_sample | 0.43 | 9.98 | 0.06 | 8.02 | 0.72 | 0.49 | -1.546393087 | 33.4473482 | SeaBird | | |
| V_22_NB_3_DNA | 13.04.2018 | V | B 3µm | niskin_sample | 0.38 | 10.08 | 0.06 | 6.97 | 0.69 | 0.21 | -1.569569142 | 33.4155435 | SeaBird | 0.06612664 | 0.01267147 |
| V_22_NB_20_DNA | 13.04.2018 | V | C 20µm | niskin_sample | 0.38 | 10.08 | 0.06 | 6.97 | 0.69 | 0.21 | -1.569569142 | 33.4155435 | SeaBird | 0.06612664 | 0.01267147 |
| V_24_NB_3_DNA | 23.04.2018 | V | B 3µm | niskin_sample | 0.71 | 9.48 | 0.06 | 6.35 | 0.68 | 0.29 | -1.509411532 | 33.3914045 | SeaBird | 0.07078776 | 0.01218555 |
| V_24_NB_20_DNA | 23.04.2018 | V | C 20µm | niskin_sample | 0.71 | 9.48 | 0.06 | 6.35 | 0.68 | 0.29 | -1.509411532 | 33.3914045 | SeaBird | 0.07078776 | 0.01218555 |

# Synthesis

## Functional transition patterns of the protist community

The presented dissertation provides new insights into species and functional group transition patterns in context with environmental parameters and harmful algal bloom toxins in Disko Bay, West Greenland. It focused on different seasonal phases, which can be divided into the time leading up to the spring bloom, the spring bloom itself, and the transition from spring bloom to a summer community. A clear seasonality of the prostist community was observed, being visible both in different functional and different species compositions. The main findings are

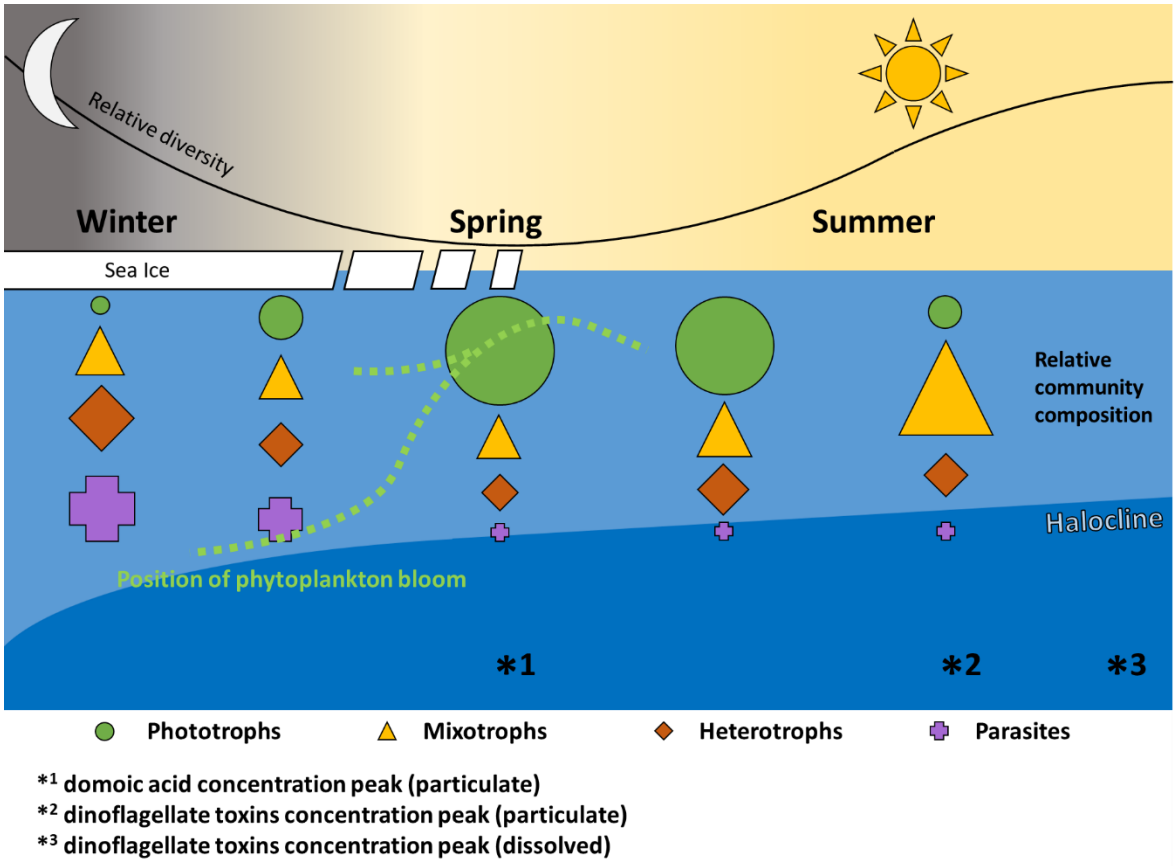


summarized in Figure 5, and will be elaborated in this section.

***Figure 5: Transitional seasonal changes of the pelagic protist community in Disko Bay, West Greenland.*** *All scales are relative and not absolute. The combination of the different sized shapes for the functional groups indicate the functional composition and not the location in the water column. Likewise, the asterisks (*) solely mark the time point and not the position in the water column.*

## Transition from a winter protist community towards the spring bloom

The winter season is usually understudied because of challenging logistics in the Arctic environment (e.g. Kubiszyn *et al.*, 2017), making spring and summer studies much more

common (e.g. Tammilehto *et al.*, 2017; Lafond *et al.*, 2019). The presented seasonal study is therefore elucidating transitional patterns that so far have rarely been investigated. In February 2018, while the days were short and dark and sea ice was building up, a net heterotrophic protist community was detected via metabarcoding in Disko Bay (chapter 1). Similar observations of a net heterotrophic winter protist community have been conducted close to Svalbard, albeit in a system that lacks seasonal sea ice (Kubiszyn *et al.*, 2017). In winter, the biomass of the protist community was generally extremely low with a rather high diversity and high nutrient contents (see chapter 1 and 3, and Fig. 6, shown as Fisher Diversity). The low biomass of the winter community is similar to what was observed north of Svalbard (Błachowiak-Samołyk *et al.*, 2015). This fits into the general understanding of the Arctic pelagic ecosystem with the winter being a season of very low biomass because of very low energy inflow via light into the ecosystem.

Harmful algal blooms are phenomena that are usually detected in seasons with higher biomass (e.g. Nishitani *et al.*, 2002; Hakanen *et al.*, 2012), meaning that HAB toxins would not be expected to be present in the Arctic winter with its low biomass. The highest content of most dinoflagellate-related toxins was indeed detected in autumn between October 18 and November 18 (see chapter 3). Nevertheless, dissolved dinoflagellate-related toxins were present throughout the whole winter. Similar to this, the presence of the HAB species *Prorocentrum minimum* in the form of blooms have already been detected in a warm temperate estuary in winter (Springer *et al.*, 2005), showing that HABs are not always timely limited to the biomass-rich seasons. However, the Arctic environment is only remotely comparable to the aforementioned area, because an estuary is most likely more influenced by its river, and not seasonal changes. Therefore, it can be assumed that the detected dissolved toxins in winter can be accounted to long retention times of the toxins released by organisms that have been more active in the seasons prior (see chapter 3).

During late winter (February and early March), many parasitic and heterotrophic organisms were present in the waters. Parasites in winter have already been found in temperate regions (Morán *et al.*, 2018), and in Antarctica (Cleary *et al.*, 2016), possibly even being associated with openings in the sea ice (Clarke *et al.*, 2019). This suggests the possibility of parasite prevalence as the typical winter community in areas with seasonal sea ice. Other heterotrophs, combined with a very low biomass have been found in Disko Bay in winter before (Levinsen *et al.*, 2002), which confirms the presented findings of heterotrophy being part of a typical winter community in the studied area. Due to the challenging cultivation of the highly abundant parasites and heterotrophs in comparison to phototrophs (del Campo *et al.*, 2013), there are knowledge gaps existing regarding the autecology of the unique members of the winter protist community. Marine protistal parasites – to our knowledge so far – only persevere without their hosts for a

very limited amount of time (Alacid *et al.*, 2015; Reñé *et al.*, 2017; John *et al.*, 2019). However, the parasites found in the presented study were mostly present in the picoplankton size fraction, indicating that a substantial part of them was most likely existing outside of their host cells, which are usually much larger than picoplankton (Gómez *et al.*, 2009; Alacid *et al.*, 2015). This suggests that the parasites in winter are possibly following a yet-to-be-understood survival strategy in the harsh winter conditions in absence, or at least low abundance, of most of their host cells.

Most of the diatoms are typical spring bloom species, also in the Arctic (Tammilehto *et al.*, 2017; Krause *et al.*, 2018; Lafond *et al.*, 2019, Fig. 7). In the investigated winter period, diatoms have been present in very low relative abundance. In a study north of Svalbard, other phototrophic organisms have been detected in winter as well (Błachowiak-Samołyk *et al.*, 2014; Vader *et al.*, 2014). In the presented case, surviving pelagic phototrophs have been found to be the species that were seeding the subsequent spring bloom, overgrowing the former winter community in the presented work (chapter 1). This resulted in a decline in diversity (Fig. 6), further showing that few species were successfully superseding the winter community.

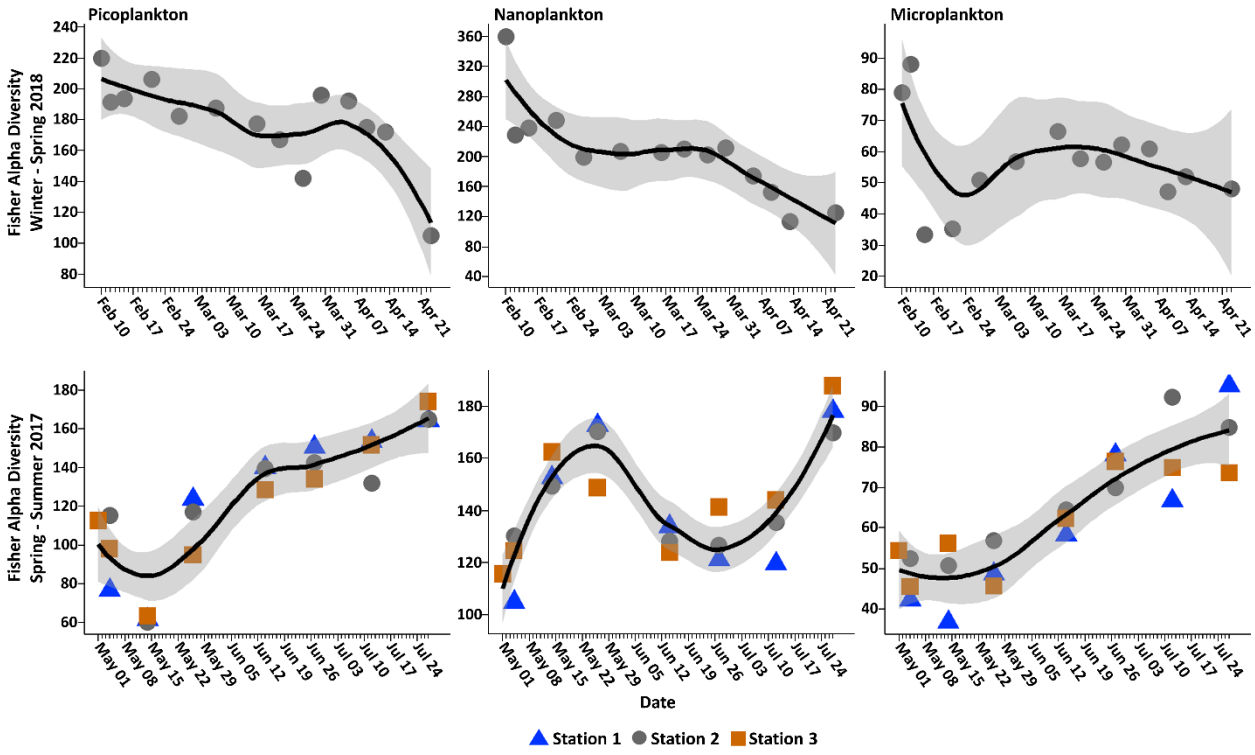


***Figure 6: Fisher Alpha Diversity Measure of all time points, comparing the different seasons.*** *The black line represents a loess regression with the grey area representing the 95 % confidence interval.*

At the end of winter, high amounts of dissolved nutrients are available, indicating that scarce chemical resources are not the limiting factor in protist growth at this time of the year (chapter

3). In Arctic areas with sea ice, such as Disko Bay, the limiting factor is often discussed to be light (Terrado *et al.*, 2008; Leu *et al.*, 2015). Contrasting to this, studies have shown that many diatoms only need very little light to grow (Arrigo *et al.*, 2012; Spall *et al.*, 2014; Massicotte *et al.*, 2020). In laboratory experiments, the photosynthetic activity of diatom resting spores was also quickly reactivated when light was available again (Kvernvik *et al.*, 2018). In the observed case, the phytoplankton bloom initiated at lower depths at a PAR of approximately 0.24 µmol $m^{-2}s^{-1}$, coinciding with the mixed layer depth at 55 m, also showing that light intensity was not the most important factor. Still, the light spectral composition and daily insolation time changed with the progressing year. Interestingly, the phytoplankton later on was visible as two layers of fluorescence within the mixed layer at different depths, combining into one layer later on. The location of the spring bloom initiation suggests an interplay between shallowing of the mixed layer depth and changing of the light spectral composition as factors in the spring bloom initiation.

*Key messages regarding the transition from winter to spring*

- The mixed layer depth continuously shallowed towards spring, while the sea ice melted and declined, and the light spectral composition and insolation time changed.
- The spring bloom initiated at a depth of approximately 55 m, coinciding with the now shallowed mixed layer depth.
- The winter community had a high relative abundance of parasites and heterotrophs, and some mixotrophs.
- The diversity in winter in all size fractions was higher than in spring or summer (Fisher Diversity Measure).
- Dissolved HAB toxins derived from dinoflagellates were present in winter – although they are most likely the remnants of earlier seasons.

## The spring bloom and its termination

In the two field trips, both the onset of the spring bloom of 2017 (chapter 1) and the transition from the spring bloom to the summer community 2018 (chapter 2) were examined with metabarcoding, Chl *a* analyses, POC and PON analyses, and nutrient analyses. With microscopic methods, the species richness in summer has been detected to be generally higher than in the other seasons in a study close to Svalbard (Kubiszyn *et al.*, 2017). However, the presented study shows the opposite of this: the diversity of the protist community was lowest during its most productive season in spring (chapters 1 and 2, Fig. 6). Microscopic methods are generally biased

towards larger protist species, excluding a lot of the diversity of smaller or similar-looking species, as shown e.g. for dinoflagellates by Smith *et al.* (2017). Metabarcoding on the other hand has its own limitations: dinoflagellates are known to have high copy numbers of ribosomal operons, often leading to their overestimation in metabarcoding (Guo *et al.*, 2016). Additionally, metabarcoding is selective for the organisms that have the PCR target site conserved in a specific way to be targetable by the used primers. In the past, metabarcoding was known to e.g. select against haptophytes. However, the usage of haptophyte-optimized primers are an attempt to include as many eukaryotes as possible (Piredda *et al.*, 2016), giving the opportunity to investigate different size fractions in depth. After all, it is believed that metabarcoding is a more objective way of assessing the protist community and is probably more in line with the real community than studies based on microscopy, because it is taking smaller organisms into account as well and does not discriminate against similar looking species. In chapters 1

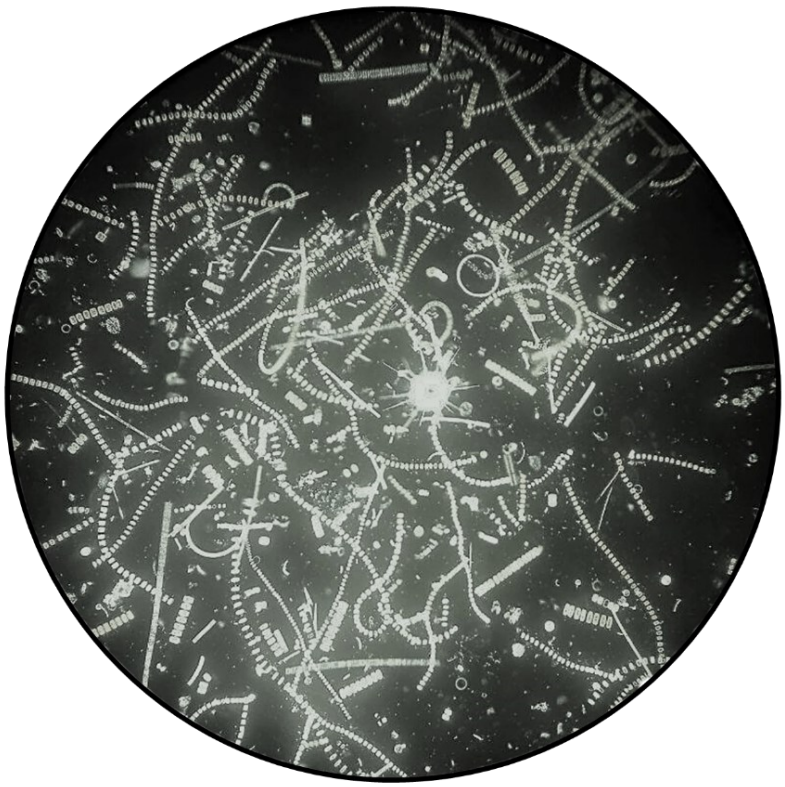

***Figure 7: Phase contrast microscopic example picture of the spring bloom community of 2017.*** *The spring bloom community of 2017 was rather typical with many centric diatoms and only a few pennate diatoms or heterotrophs, such as the radiolarian in the center of this picture.*

and 2, the overall Chl *a* peak correlated with a high share of phototrophs in the microplankton size fraction ASVs, while the other size fractions had a much lower share of phototrophs. This shows that the bloom itself was mostly driven by the microplankton size fraction. The RUE of the spring bloom was the highest that was measured throughout all the observed community

transitions, which underlines the importance of the spring bloom event for biomass creation. In fact, in sub-Arctic waters, the magnitude of the phytoplankton blooms were found to directly influence the amount of energy that was made available for higher trophic levels (Sigler *et al.*, 2014). In conclusion, a spring community with high productivity and a relatively low diversity was confirmed for Disko Bay. The bloom event efficiently provides biomass for higher trophic levels and is therefore indeed one of the most important periods for the marine ecosystem.

The termination of the spring bloom in the presented study was most likely driven by a combination of lack of silicate (see chapter 3, Fig. 2) and an increase in copepod grazing activity. Silicate is essential to sustain growth and biomass production of diatoms, which have their outer shell based on this element. Transitions from phototrophic diatoms towards more mixotrophic dinoflagellates driven by silicate limitation have already been observed on several occasions in temperate regions (Liang *et al.*, 2019; Xiang *et al.*, 2019), and seem to be a general succession pattern in protist ecology (Smayda & Trainer, 2010; Flynn *et al.*, 2019). Copepods are known to be the most important mesozooplankton in Arctic waters (Arashkevich *et al.*, 2002; Ashjian *et al.*, 2003), making them the next trophic level after protists. Calanoid copepods are the most prevalent grazers in Disko Bay (Møller & Nielsen, 2020), and are known to quickly increase their grazing activity when protist biomass increases, but preferring phototrophs over heteroptrophs as a food source (Forest *et al.*, 2011). This could mean that the phototrophic spring bloom event was terminated both by lack of silicate as a nutrient and by additional grazing from higher trophic levels, which specifically targeted the phototrophic diatoms. At the time of bloom termination, levels of the HAB toxin DA also increased in the particulate phase (chapter 3). In other studies, it was found that DA production of diatoms increased when subjected to grazing by herbivorous copepods (Harðardóttir *et al.*, 2015; Lundholm *et al.*, 2018), possibly as a defense mechanism of the diatoms against grazing. This fits into the hypothesis of the spring bloom termination induced by grazing, because the termination of the bloom coincides with the increase in particulate DA and the increase of the potential DA-producers *Nitzschia* and *Pseudo-nitzschia* spp. (see chapter 3).

*Key messages regarding the spring bloom and its termination*

- The spring bloom was characterized by microplanktonic diatoms.
- The spring bloom was a time of highest RUE and lowest diversity.
- It was most likely terminated by lack of silicate and grazing pressure.
- Particulate DA increased, possibly as a consequence of grazing.

## The transition towards summer

While studies from winter and the onset of the spring bloom are relatively scarce (Marquardt *et al.*, 2016; Massicotte *et al.*, 2020), studies in the logistically easier spring and summer periods are much more common (e.g. Hop *et al.*, 2019; Lafond *et al.*, 2019; Elferink *et al.*, 2020). However, most studies from the Arctic are transect or snapshot-studies, only investigating a short amount of time (Baggesen *et al.*, 2012; Tillmann *et al.*, 2014; Elferink *et al.*, 2017). In the presented study, it was possible to observe the transition processes from spring to summer, showing a steady replacement of the phototrophs in the microplankton size fraction by mixotrophs (chapter 2). In contrast to this, heterotrophs were more abundant than mixotrophs in the nanoplankton size fraction, which is in accordance to a study from Antarctica (Gast *et al.*, 2018). This suggests that smaller size fractions generally behave differently than bigger size fractions. Fisher diversity showed that in summer, the diversity was higher than in spring, although not as high as in winter (Fig. 6), while the RUE was much lower in summer than in spring. This shows that with protists, RUE is not proportional to diversity as proposed before with plants (Hector *et al.*, 1999; Loureau *et al.*, 2012), where a high diversity was generally considered beneficial for an ecosystem's RUE. This might be because planktonic protists, and in particular mixotrophs, have a lower correlation of traits and nutrient uptake than plants, resulting in a different RUE. Mixotrophs are more flexible in their ecological niches, being able to adapt to different trophic modes depending on available resources. The nutrient scarce summer period is probably selecting for a more generalist ecological approach of the protists, as also reviewed in Stoecker & Levrentyev (2018), which is in accordance to the relative increase of constitutive mixotrophic dinoflagellates, replacing the phototrophic diatoms in the presented study (chapter 2).

Most toxin producing species are known to be dinoflagellates (Smayda, 1997). Constitutive mixotrophic dinoflagellates were increasing in relative abundance towards the summer period, posing the question if this is a season of increased dinoflagellate toxin production as well. Potentially toxic dinoflagellate species have indeed been increasing in abundance towards summer as well (chapter 3). Particulate dinoflagellate-related toxins also increased towards summer, confirming the hypothesis of a natural succession towards toxic dinoflagellates in summer. The general prevalence of mixotrophs in summer in Disko Bay has been described before (Levinsen *et al.*, 2000), including the potentially toxigenic *Alexandrium ostenfeldii* (Tillmann *et al.*, 2014). In the presented study, the potentially toxigenic dinoflagellate taxa *Alexandrium catenella* (saxitoxins), *A. ostenfeldii* (spirolides, gymnodimines), other *Alexandrium* spp. (possibly toxigenic), *Dinophysis acuminata* (ocadaic acids, dinophysistoxins, pectenotoxins), *Gonyaulax spinifera*, *Phalacroma* spp. (toxicity under debate, Reguera *et al.*, 2014), *Prorocentrum* spp. (ocadaic acids), and *Protoceratium reticulatum* (yessotoxins) were

found and linked to the detected toxins in the water or in the particulate phase. This confirms that many toxigenic dinoflagellates are present in Disko Bay and that they, too, follow the seasonal transition patterns.

*Key messages regarding the seasonal community transition towards summer*

- The spring bloom community was able to utilize the given resources better than the summer community (shown in a lower RUE).
- The diversity in summer was higher than the diversity in spring, but lower than the diversity in winter.
- Microplanktonic phototrophs were gradually replaced by mixotrophs towards summer.
- The mixotrophs were mostly comprising constitutive mixotrophic dinoflagellates.
- Mixotrophs had an ecological advantage over phototrophs when nutrient levels and grazing pressure were higher.
- The smaller size fractions also had a high relative abundance of heterotrophic protists, both in spring and summer.
- Dinoflagellate toxins were produced by the upcoming mixotrophic dinoflagellates in summer.

## Functional transitions in comparison to species transitions

Protist transition patterns are usually assessed by species (Marquardt *et al.*, 2016; Massicotte *et al.*, 2020). Here, the relatively new approach of illuminating the functional/trophic modes of the respective protist taxa was utilized. This approach has already been proven to be especially useful for the marine protist communities, giving a different insight into the community patterns than only assessing the species (Mitra *et al.*, 2016; Gran-Stadniczeñko *et al.*, 2019; Flynn *et al.*, 2019). The presented study confirms that the heterotroph-phototroph-dichotomy does not reflect the marine protist community, as already elaborated e.g. in Flynn *et al.* (2013). Furthermore, it shows that there are many transitions in between the most prevalent trophic modes in the protist community, most drastic in the microplankton size fraction. However, transition patterns between different organisms were observable that were operating in the same trophic mode but were replacing each other in transitional progressions as well (chapter 2, *Porosira glacialis* and *Thalassiosira antarctica* var. *borealis*). This shows that there are still differences in the niches within one trophic mode and that the most comprehensive investigation should include both approaches: functional traits and species. In the Arctic, setting found organisms to their respective trophic mode has already been done in a Svalbard fjord

(Kubiszyn *et al.*, 2017). However, the utilized microscopic approach had the limitation of not assessing the protist community in all size fractions, because microscopy is usually biased towards larger species, as elaborated before.

During the progression from winter to summer, several different trophic modes increased and decreased in their relative abundance and importance within the protist community: as mixotrophs, parasites and heterotrophs are the most prevalent trophic modes in winter, phototrophic diatoms overgrew everything during the spring bloom and, after silicate depletion, opened up the phototrophic niche to constitutive mixotrophs (Figure 5). Parasitism as a very widespread trophic mode in winter was a relatively new finding. Parasites have been found in Antarctic winter communities under the sea ice before (Cleary *et al.*, 2016; Clarke *et al.*, 2019), suggesting that they are a normal part of the winter community in the Polar Regions. Their prevalence in the picoplankton size fraction suggests that a majority of them was present in their free-living stage. It is not clear how they survive in the winter and who their host organisms are. In laboratory experiments, they only survive a few hours to days without their hosts (Alacid *et al.*, 2015; Reñé *et al.*, 2017; John *et al.*, 2019). This shows that there is still a lot to be understood about the protist winter community, and in particular about the parasites that are widespread in winter. The overall prevalence of mixotrophs, especially in smaller size fractions and in summer, demonstrated their overall importance in the Arctic environment. Before, mixotrophs have already been hypothesized to be the most prevalent trophic mode for most of the year in the Arctic, making use of the scarce resources and being relative generalists (Stoecker *et al.*, 2018). With the results of the presented studies, this hypothesis could be refined to the statement that mixotrophs dominate the microplankton size fraction throughout most of the year except for the spring bloom, while smaller size fractions show differences to this (such as in Gast *et al.*, 2018).

The approach of this work proves that the ecological niches change during the seasons, which is not surprising, taking the strong seasonality of the Arctic into account. Additionally, it shows that mixotrophy is indeed one of the most important trophic modes in the Arctic, albeit with differences in the size fractions. The functional transitions as opposed to the species transitions give a different insight into the mode the ecosystem is operating in at the studied moment.

## Arctic pelagic protist communities in context with climate change

The presented study can be used as a baseline reference for future changes in the Arctic. With the multitude of different accompanying factors and analyses, it will probably be possible to

strengthen potential links of environmental causes and their effects on the protist community with further studies. Potential future changes in light of climate change can already be speculated. In general, climate change is having a huge impact on the Arctic, warming it up twice as quickly as any other region in the world (Moritz *et al.*, 2002; Mauritsen *et al.*, 2016). With retreating sea ice and increased melt water from the declining glaciers and ice sheets (Arrigo *et al.*, 2008; Meire *et al.*, 2017), this naturally also influences the marine protist community, which is the basis of the marine food web, being responsible for a significant amount of the Earth's primary production (Falkowski *et al.*, 1994; Field *et al.*, 1998). Warming temperature with decreasing sea ice will most likely result in higher phytoplankton biomass in the Arctic, as growing seasons elongate and higher temperatures result in increased growth rates (Bopp *et al.*, 2005; Dutkiewicz *et al.*, 2013; Cabré *et al.*, 2015). According to a modeling approach, species richness will probably decrease with the increase in biomass, with many species migrating polewards (Henson *et al.*, 2021). The low species richness and high biomass is comparable to the time of the spring communities investigated in this study, which had low diversity but high biomass. However, this might have implications for quicker nutrient depletion, probably accelerating the transition towards a more generalist constitutive mixotroph summer community and therefore also increasing the possibility of blooms of toxigenic dinoflagellates. It was already shown that different nutrient limitations of either carbon or nitrogen or phosphorus could lead to a higher cell quota of specific toxins (Van de Waal *et al.*, 2014), making this scenario more likely. Overall, this study provided a significant step towards understanding the pelagic protist communities and their transitional patterns to and from the spring bloom event. It will help to assess the aforementioned future changes in the Arctic context.

## Future perspectives

The presented study is a comprehensive picture of protist community transitions from winter to summer. Nevertheless, it has not been part of the study to collect data on the transitions from summer to winter. To get a complete picture, it should be studied how the community developed over the fall season into the low biomass and high diversity community that was seen in winter. The best way to approach this would be to study the ecosystem for one to several consecutive years (similar to the Green Edge project or MOSAiC). This way, it could be determined if the findings truly were reflecting the regular succession patterns and timing or if the investigated years were peculiarities.

One of the drawbacks of metabarcoding, which was the most important method of this study, is the potential overrepresentation of dinoflagellates due to large copy numbers of the target genes. With flow cytometry, a quantitative level could be brought to the semi-quantitative

metabarcoding ASV reads. In addition, fluorescence of chlorophyll could also to some extend provide information about the trophic modes of the analyzed organisms when using this method. However, organisms that organize in colonies such as chain-building diatoms would be difficult to assess with flow cytometry. If it is possible to optimize the method for such protists, it would be possible to significantly decrease one of the bigger drawbacks of metabarcoding for evaluating environmental microbial communities.

Protists are key players of the marine ecosystem and are undoubtedly very important for primary production and therefore for providing the base for the marine food web. However, the analyses of the ecosystem would be more complete if prokaryotes were included in the study as well. Marine prokaryotes can regenerate nutrients and therefore influence the ecosystem via the microbial loop (Pomeroy *et al.*, 2007). Additionally to prokaryotes, marine fungi may be important for remineralizing nutrients or as parasites in the marine ecosystem as well. They may play important roles in the protist community that would be easily overlooked because of artificial exclusion after metabarcoding analyses. Moreover, it was speculated how copepods as the next trophic level could influence the protist community, especially as a factor in terminating the spring bloom and DA production as a response to grazing. This could be proven with additional analyses of the copepod community as the next trophic level in this ecosystem. It could be studied how many and which copepods are present at what times, estimating the grazing pressure on the protist community. This way, it would be possible to not only look into the protist community itself, but also into direct interactions with other organisms in the ecosystem, ultimatively leading to a better understanding of the whole ecosystem and the interconnections between the different levels.

# References

Eighty years of Redfield (2014) *Nat Geosci* **7**: 849.

Alacid, E., Reñé, A., and Garcés, E. (2015) New Insights into the Parasitoid *Parvilucifera sinerae* Life Cycle: The Development and Kinetics of Infection of a Bloom-forming Dinoflagellate Host. *Protist* **166**: 677–699.

Anderson, D.M., Cembella, A.D., and Hallegraeff, G.M. (2012) Progress in Understanding Harmful Algal Blooms: Paradigm Shifts and New Technologies for Research, Monitoring, and Management. *Ann Rev Mar Sci* **4**: 143–176.

Anderson, D.M., Fachon, E., Pickart, R.S., Lin, P., Fischer, A.D., Richlen, M.L., *et al.* (2021) Evidence for massive and recurrent toxic blooms of *Alexandrium catenella* in the Alaskan Arctic. *PNAS* **118**: 1–11.

Arashkevich, E., Wassmann, P., Pasternak, A., and Wexels Riser, C. (2002) Seasonal and spatial changes in biomass, structure, and development progress of the zooplankton community in the Barents Sea. *J Mar Syst* **38**: 125–145.

Arrigo, K.R., Perovich, D.K., Pickart, R.S., Brown, Z.W., Dijken, G.L. Van, Lowry, K.E., *et al.* (2012) Under Arctic Sea Ice. *Science* **336**: 1408.

Arrigo, K.R., van Dijken, G., and Pabi, S. (2008) Impact of a shrinking Arctic ice cover on marine primary production. *Geophys Res Lett* **35**: 1–6.

Ashjian, C.J., Campbell, R.G., Welch, H.E., Butler, M., and van Keuren, D. (2003) Annual cycle in abundance, distribution, and size in relation to hydrography of important copepod species in the western Arctic Ocean. *Deep Res Part I* **50**: 1235–1261.

Baggesen, C., Moestrup, Ø., Daugbjerg, N., Krock, B., Cembella, A.D., and Madsen, S. (2012) Molecular phylogeny and toxin profiles of *Alexandrium tamarense* (Lebour) Balech (Dinophyceae) from the west coast of Greenland. *Harmful Algae* **19**: 108–116.

Błachowiak-Samołyk, K., Wiktor, J.M., Hegseth, E.N., Wold, A., Falk-Petersen, S., and Kubiszyn, A.M. (2015) Winter Tales : the dark side of planktonic life. *Polar Biol* **38**: 23–36.

Bopp, L., Aumont, O., Cadule, P., Alvain, S., and Gehlen, M. (2005) Response of diatoms distribution to global warming and potential implications : A global model study. **32**: 2–5.

Brett, D. ed. (2003) Europe Review 2003/4: The Economic and Business Report (World of Information Reviews Series), 15th ed. Walden Publishing Ltd.

Buch, E. (1990) A monograph on the physical environment of Greenland Waters, Danish Meteorologiocal Institute.

Cabré, A., Marinov, I., and Leung, S. (2015) Consistent global responses of marine ecosystems to future climate change across the IPCC AR5 earth system models. *Clim Dyn* 1253–1280.

Calil, P.H.R., Doney, S.C., Yumimoto, K., and Eguchi, K. (2011) Episodic upwelling and dust deposition as bloom triggers in low - nutrient, low - chlorophyll regions. **116**: 1–16.

Christy, M. (1923) The common teasel as a carnivorous plant. *Jour Botany* **61**:33–45.

Clarke, L.J., Bestley, S., Bissett, A., and Deagle, B.E. (2019) A globally distributed Syndiniales parasite dominates the Southern Ocean micro-eukaryote community near the sea-ice edge. *ISME J* **13**: 734–737.

Cleary, A.C. and Durbin, E.G. (2016) Unexpected prevalence of parasite 18S rDNA sequences in winter among Antarctic marine protists. **38**: 401–417.

del Campo, J., Balagué, V., Forn, I., Lekunberri, I., and Massana, R. (2013) Culturing Bias in Marine Heterotrophic Flagellates Analyzed Through Seawater Enrichment Incubations. *Microb Ecol* **66**: 489–499.

Deppeler, A. L., and Davidson, A. T. (2017) Southern Ocean Phytoplankton in a Changing Climate. *Front. Mar. Sci.* **4**:40.

Dutkiewicz, S., Scott, J.R., and Follows, M.J. (2013) Winners and losers: Ecological and biogeochemical changes in a warming ocean. **27**: 463–477.

Elferink, S., Neuhaus, S., Wohlrab, S., Toebe, K., Voß, D., Gottschling, M., *et al.* (2017) Molecular diversity patterns among various phytoplankton size-fractions in West Greenland in late summer. *Deep Res Part I* **121**: 54–69.

Elferink, S., Wohlrab, S., Neuhaus, S., Cembella, A., Harms, L., and John, U. (2020) Comparative Metabarcoding and Metatranscriptomic Analysis of Microeukaryotes Within Coastal Surface Waters of West Greenland and Northwest Iceland. *Front Mar Sci* **7**: 1–20.

Falkowski, P.G. (1994) The role of phytoplankton photosynthesis in global biogeochemical cycles. *Photosynth Res* **39**: 235–258.

Faure, E. and Not, F. (2019) Mixotrophic protists display contrasted biogeographies in the global ocean. *ISME J* 1072–1083.

Fawcett, S.E. and Ward, B.B. (2011) Phytoplankton succession and nitrogen utilization during the development of an upwelling bloom. **428**: 13–31.

Field, C.B., Behrenfeld, M.J., and Randerson, J.T. (1998) Primary Production of the Biosphere: Integrating Terrestrial and Oceanic Components. *Science* **281**: 237–241.

Fischer, A.D., Brosnahan, M.L., and Anderson, D.M. (2018) Quantitative Response of *Alexandrium catenella* Cyst Dormancy to Cold Exposure. *Protist* **169**: 645–661.

Flynn, K.J., Mitra, A., Anestis, K., Anschütz, A.A., Calbet, A., Duarte Ferreira, G., *et al.* (2019) Mixotrophic protists and a new paradigm for marine ecology: where does plankton research go now? *J Plankton Res* **41**: 375–391.

Flynn, K.J., Stoecker, D.K., Mitra, A., Raven, J.A., Glibert, P.M., Hansen, P.J., *et al.* (2013) Misuse of the phytoplankton – zooplankton dichotomy: the need to assign organisms as mixotrophs within plankton functional types. *J Plankt Res* **35**: 3–11.

Forest, A., Galindo, V., Darnis, G., Pineault, S., Lalande, C., Tremblay, J.-É., and Fortier, L. (2011) Carbon biomass , elemental ratios (C:N) and stable isotopic composition ($\delta^{13}C$, $\delta^{15}N$) of dominant calanoid copepods during the winter-to-summer transition in the Amundsen Gulf (Arctic Ocean). *J Plankton Res* **33**: 161–178.

Fuchs, V.E. and Whittard, W.F. (1930) The East Greenland Pack-Ice and the Significance of Its Derived Shells. *Geogr J* **76**: 419–425.

Gast, R.J. (2018) Mixotrophic Activity and Diversity of Antarctic Marine Protists in Austral Summer. *Front Mar Sci* **5**: 1–12.

Gobler, C.J. (2020) Climate Change and Harmful Algal Blooms: Insights and perspective. *Harmful Algae* **91**: 101731.

Gomez, F. (2011) Heterotroph. In: Gargaud M. et al. (eds) *Encyclopedia of Astrobiology*. Springer, Berlin, Heidelberg.

Gómez, F., Moreira, D., and López-García, P. (2009) Life cycle and molecular phylogeny of the dinoflagellates *Chytriodinium* and *Dissodinium*, ectoparasites of copepod eggs. *Eur J Protistol* **45**: 260–270.

Gran-Stadniczeñko, S., Egge, E., Hostyeva, V., Logares, R., Eikrem, W., and Edvardsen, B. (2019) Protist Diversity and Seasonal Dynamics in Skagerrak Plankton Communities as Revealed by Metabarcoding and Microscopy. *J Eukaryot Microbiol* **66**: 494–513.

Grandiger, R. and Ikävalko, J. (1998) Organism incorporation into newly forming Arctic sea ice in the Greenland Sea. *J Plankton Res* **20**: 871–886.

Guo, L., Sui, Z., and Liu, Y. (2016) Quantitative analysis of dinoflagellates and diatoms community via Miseq sequencing of actin gene and v9 region of 18S rDNA. *Sci Rep* 1–9.

Hakanen, P., Suikkanen, S., Franzén, J., Franzén, H., Kankaanpää, H., and Kremp, A. (2012) Bloom and toxin dynamics of *Alexandrium ostenfeldii* in a shallow embayment at the SW coast of Finland, northern Baltic Sea. *Harmful Algae* **15**: 91–99.

Hallegraeff, G.M., Anderson, D.M., and Cembella, A.D. (2003) Manual on Harmful Marine Microalgae, UNESCO Publishing.

Hansen, M.O., Nielsen, T.G., Stedmon, C.A., and Munk, P. (2012) Oceanographic regime shift during 1997 in Disko Bay, Western Greenland. *Limnol Oceanogr* **57**: 634–644.

Harðardóttir, S., Pančić, M., Tammilehto, A., Krock, B., Møller, E.F., Nielsen, T.G., and Lundholm, N. (2015) Dangerous Relations in the Arctic Marine Food Web: Interactions between Toxin Producing *Pseudo-nitzschia* Diatoms and *Calanus* Copepodites. *Mar Drugs* **13**: 3809–3835.

Hector, A., Schmid, B., Beierkuhnlein, C., Caldeira, M.C., Diemer, M., Dimitrakopoulos, P.G., *et al.* (1999) Plant Diversity and Productivity Experiments in European Grasslands. *Science* **286**: 1123–1127.

Henson, S.A., Cael, B.B., Allen, S.R., and Dutkiewicz, S. (2021) Future phytoplankton diversity in a changing climate. *Nat Commun* **12**: 1–8.

Hobson, K.A. and Welch, H.E. (1992) Determination of trophic relationships within a high Arctic marine food web using $\delta^{13}C$ and $\delta^{15}N$ analysis. *Mar Ecol Prog Ser* **84**: 9–18.

Hodapp, D., Hillebrand, H., and Striebel, M. (2019) "Unifying" the Concept of Resource Use Efficiency in Ecology. *Front Ecol Evol* **6**: 1–14.

Hop, H., Assmy, P., Wold, A., Sundfjord, A., Daase, M., Duarte, P., *et al.* (2019) Pelagic Ecosystem Characteristics Across the Atlantic Water Boundary Current From Rijpfjorden, Svalbard, to the Arctic Ocean During Summer (2010-2014). *Front Mar Sci* **6**: 1–21.

Hudson, S. (2007) DayLength. Based on the Fortran code published on ftp://climate1.gsfc.nasa.gov/wiscombe/Solar_Rad/SunAngles/sunae.f which in turn is based on Michalsky, J. (1988): The Astronomical Almanac's algorithm for approximate solar position (1950-2050), Solar Energy **40**: 227–235.

Jékely, G. (2007) Origin of phagotrophic eukaryotes as social cheaters in microbial biofilms. *Biol. Direct* **2**: 3.

John, U., Lu, Y., Wohlrab, S., Groth, M., Janouškovec, J., Kohli, G.S., *et al.* (2019) An aerobic eukaryotic parasite with functional mitochondria that likely lacks a mitochondrial genome. *Sci Adv* **5**: 1–11.

Karlson, B., Andersen, P., Arneborg, L., Cembella, A., Eikrem, W., John, U., *et al.* (2021) Harmful algal blooms and their effects in coastal seas of Northern Europe. *Harmful Algae* **102**: 101989.

Krause, J.W., Duarte, C.M., Marquez, I.A., Assmy, P., Fernández-Méndez, M., Wiedmann, I., *et al.* (2018) Biogenic silica production and diatom dynamics in the Svalbard region during spring. *Biogeosciences* **15**: 6503–6517.

Kubiszyn, A.M., Wiktor, J.M., Wiktor Jr., J.M., Griffiths, C., Kristiansen, S., and Gabrielsen, T.M. (2017) The annual planktonic protist community structure in an ice-free high Arctic fjord (Adventfjorden, West Spitsbergen). *J Mar Syst* **169**: 61–72.

Kvernvik, A.C., Hoppe, C.J.M., Lawrenz, E., Prášil, O., Greenacre, M., Wiktor, J.M., and Leu, E. (2018) Fast Reactivation of Photosynthesis in Arctic Phytoplankton during the Polar Night. *Phycol Soc Am* **54**: 461–470.

Lafond, A., Leblanc, K., Quéguiner, B., Moriceau, B., Leynaert, A., Cornet, V., *et al.* (2019) Late spring bloom development of pelagic diatoms in Baffin Bay. *Elem Sci Anthr* **7**: 1–24.

Larsen, A., Flaten, G.A.F., Sandaa, R.-A., Castberg, T., Thyrhaug, R., Erga, S.R., Jacquet, S., and Bratbak, G. (2004) Spring phytoplankton bloom dynamics in Norwegian coastal waters: Microbial community succession and diversity. *Limnol. Oceanogr.* **49**(1): 180–190.

Laskar, J. (1986) Secular terms of classical planetary theories using the results of general theory. *Astron Astrophys* **157**: 59–70.

Lefebvre, K.A., Quakenbush, L., Frame, E., Burek Huntington, K., Sheffield, G., Stimmelmayr, R., *et al.* (2016) Prevalence of algal toxins in Alaskan marine mammals foraging in a changing arctic and subarctic environment. *Harmful Algae* **55**: 13–24.

Leles, S.G., Mitra, A., Flynn, K.J., Tillmann, U., Stoecker, D., Jin, H., *et al.* (2019) Sampling bias misrepresents the biogeographical significance of constitutive mixotrophs across global oceans. 418–428.

Leu, E., Mundy, C.J., Assmy, P., Campbell, K., Gabrielsen, T.M., Gosselin, M., *et al.* (2015) Arctic spring awakening – Steering principles behind the phenology of vernal ice algal blooms. *Prog Oceanogr* **139**: 151–170.

Levinsen, H., Nielsen, T.G., and Hansen, B.W. (2000) Annual succession of marine pelagic protozoans in Disko Bay, West Greenland, with emphasis on winter dynamics. *Mar Ecol Prog Ser* **206**: 119–134.

Levinsen, H. and Nielsen, T.G. (2002) The trophic role of marine pelagic ciliates and heterotrophic dinoflagellates in Arctic and temperate coastal ecosystems: A cross-latitude comparison. *Limnol Oceanogr* **47**: 427–439.

Liang, Y., Zhang, G., Wan, A., Zhao, Z., Wang, S., and Liu, Q. (2019) Nutrient-limitation induced diatom-dinoflagellate shift of spring phytoplankton community in an off shore shell fish farming area. *Mar Pollut Bull* **141**: 1–8.

Liebig, J. von (1840) Die organische Chemie in ihrer Anwendung auf Agricultur und Physiologie.

Lundholm, N., Krock, B., John, U., Skov, J., Cheng, J., Pančić, M., *et al.* (2018) Introduction of domoic acid production in diatoms - types of grazers and diatoms are important. *Harmful Algae* **85**: 33–52.

Marañón, E. (2009) Phytoplankton size structure. *Elements of physical oceanography: A derivate of the encyclopedia of ocean sciences* **85**.

Marquardt, M., Vader, A., Stübner, E.I., Reigstad, M., and Gabrielsen, T.M. (2016) Strong Seasonality of Marine Microbial Eukaryotes in a High-Arctic Fjord (Isfjorden, in West Spitsbergen, Norway). *Appl Environ Microbiol* **82**: 1868–1880.

Massicotte, P., Amiraux, R., Amyot, M.-P., Archambault, P., Ardyna, M., Arnaud, L., *et al.* (2020) Green Edge ice camp campaigns: understanding the processes controlling the under-ice Arctic phytoplankton spring bloom. *Earth Sysem Sci Data* **12**: 151–176.

Mauritsen, T. (2016) Greenhouse warming unleashed. *Nat Geosci* **9**: 268–269.

McBean, G., Alekseev, G., Chen, D., Førland, E., Fyfe, J., Groisman, P.Y., *et al.* (2005) Arctic Climate: Past and Present. *Arct Clim Impact Assess* 21–60.

McCann, K.S. (2000) The diversity–stability debate. *Nature* **405**: 228–233.

Meire, L., Mortensen, J., Meire, P., Sejr, M.K., Rysgaard, S., Nygaard, R., *et al.* (2017) Marine-terminating glaciers sustain high productivity in Greenland fjords. *Glob Chang Biol* **23**: 1–14.

Meltofte, H. (2017) What is the Arctic and who are Arctic waders?

Mitra, A., Flynn, K.J., Tillmann, U., Raven, J.A., Caron, D., Stoecker, D.K., et al. (2016) Defining Planktonic Protist Functional Groups on Mechanisms for Energy and Nutrient Acquisition: Incorporation of Diverse Mixotrophic Strategies. *Protist* **167**: 106–120.

Møller, E.F. and Nielsen, T.G. (2000) Plankton community structure and carbon cycling off the western coast of Greenland, with emphasis on sources of DOM for the bacterial community. *Aquat Microb Ecol* **22**: 13–25.

Morán, X.A.G., Calvo-Díaz, A., Arandia-Gorostidi, N., and Huete-Stauffer, T.M. (2018) Temperature sensitivities of microbial plankton net growth rates are seasonally coherent and linked to nutrient availability. *Environ Microbiol* **20**: 3798–3810.

Moritz, R.E., Bitz, C.M., and Steig, E.J. (2002) Dynamics of Recent Climate Change in the Arctic. *Science (80)* **297**: 1497–1503.

Morlighem, M., Williams, C.N., Rignot, E., An, L., Arndt, J.E., Bamber, J.L., *et al.* (2017) BedMachine v3: Complete Bed Topography and Ocean Bathymetry Mapping of Greenland From Multibeam Echo Sounding Combined With Mass Conservation. *Geophys Res Lett* 11051–11061.

Motyka, R.J., Truffer, M., Fahnestock, M., Mortensen, J., Rysgaard, S., and Howat, I. (2011) Submarine melting of the 1985 Jakobshavn Isbræ floating tongue and the triggering of the current retreat. *J Geophys Res* **116**: 1–17.

Nejstgaard, J.C., Tang, K.W., Steinke, M., Dutz, J., Koski, M., Antajan, E., and Long, J.D. (2007) Zooplankton grazing on *Phaeocystis*: a quantitative review and future challenges. *Biogeochemistry* **83**: 147–172.

Niemi, A., Michel, C., Hille, K., and Poulin, M. (2011) Protist assemblages in winter sea ice: setting the stage for the spring ice algal bloom. *Polar Biol* **34**: 1803–1817.

Nishitani, G., Sugioka, H., and Imai, I. (2002) Seasonal distribution of species of the toxic dinoflagellate genus Dinophysis in Maizuru Bay (Japan), with comments on their autofluorescence and attachment of picophytoplankton. *Harmful Algae* **1**: 253–264.

Odum, H.T. (1957) Trophic Structure and Productivity of Silver Springs, Florida. *Ecol Monogr* **27**: 55–112.

Overpeck, J., Hughen, K., Hardy, D., Bradley, R., Case, R., Douglas, M., *et al.* (1997) Arctic Environmental Change of the Last Four Centuries. *Science (80- )* **278**: 1251–1257.

Panel, T.I., Change, C., Nations, U., Programme, E., Ipcc, T., Report, F.A., *et al.* IPCC 2007, Climate Change 2007: Impacts, Adaptation and Vulnerability.

Parkinson, C.L. and Cavalieri, D.J. (2002) A 21 year record of Arctic sea-ice extents and their regional, seasonal and monthly variability and trends. *Ann Glaciol* **34**: 441–446.

Pavlov, A.K., Taskjelle, T., Kauko, H.M., Hamre, B., Hudson, S.R., Assmy, P., *et al.* (2017) Altered inherent optical properties and estimates of the underwater light field during an Arctic under-ice bloom of *Phaeocystis pouchetii*. *J Geophys Res Ocean* **122**: 4939–4961.

Paytan, A. and Mclaughlin, K. (2007) The Oceanic Phosphorus Cycle.

Peretó, J. (2011) Phototroph. In: Gargaud M. *et al.* (eds) *Encyclopedia of Astrobiology*. Springer, Berlin, Heidelberg.

Piredda, R., Tomasino, M.P., Erchia, A.M.D., Manzari, C., Pesole, G., Montresor, M., *et al.* (2017) Diversity and temporal patterns of planktonic protist assemblages at a Mediterranean LTER site. *FEMS Microbiol Ecol* **93**: 1–14.

Pomeroy, L.R., Williams, P.J., Azam, F., and Hobbie, J.E. (1998) The Microbial Loop. *Oceanography* **20**: 28–33.

Porsild, M.P. (1906) The Danish Arctic Station.

Ptacnik, R., Solimini, A.G., Andersen, T., Tamminen, T., Brettum, P., Lepisto, L., *et al.* (2008) Diversity predicts stability and resource use efficiency in natural phytoplankton communities. *PNAS* **105**: 5134–5138.

Raymont, J.E.G. (1980) Plankton and Productivity in the Oceans, 2nd ed. Pergamon Press, Ltd.

Redfield, A.C. (1934) On the proportions of organic derivatives in sea water and their relation to the composition of plankton. *James Johnstone Meml Vol* 176–192.

Redfield, A.C., Ketchum, B.H., and Richards, F.A. (1963) The influence of organisms on the composition of seawater. In *The Sea, Volume 2: the Composition of Sea-Water Comparative and Descriptive Oceanography*. Hill, M.N. (ed). Harvard University Press, pp. 26–77.

Reguera, B., Riobó, P., Rodríguez, F., Díaz, P.A., Pizarro, G., Paz, B., *et al.* (2014) Dinophysis Toxins: Causative Organisms, Distribution and Fate in Shellfish. Mar Drugs 394–461.

Reñé, A., Alacid, E., Figueroa, R.I., Rodríguez, F., and Garcés, E. (2017) Life-cycle, ultrastructure, and phylogeny of *Parvilucifera corolla* sp. nov. (Alveolata, Perkinsozoa), a parasitoid of dinoflagellates. *Eur J Protistol* **58**: 9–25.

Riedel, A., Michel, C., Gosselin, M., and LeBlanc, B. (2008) Winter – spring dynamics in sea-ice carbon cycling in the coastal Arctic Ocean. *J Mar Syst* **74**: 918–932.

Rózanska, M., Gosselin, M., Poulin, M., Wiktor, J.M., and Michel, C. (2009) Influence of environmental factors on the development of bottom ice protist communities during the winter – spring transition. *Mar Ecol Prog Ser* **386**: 43–59.

Ryther, J.H. and Dunstan, W.M. (1971) Nitrogen, Phosphorus, and Eutrophication in the Coastal Marine Environment. *Science* **171**: 1008–1013.

Sakshaug, E., and Skjoldal, H. R. (1989) Life at the Ice Edge. *Ambio* **18**(1): 60–67.

Sigler, M.F., Stabeno, P.J., Eisner, L.B., Napp, J.M., and Mueter, F.J. (2014) Deep-Sea Research II Spring and fall phytoplankton blooms in a productive subarctic ecosystem, the eastern Bering Sea , during 1995 – 2011. *Deep Res Part II* **109**: 71–83.

Smayda, T.J. (1997) Harmful algal blooms: Their ecophysiology and general relevance to phytoplankton blooms in the sea. *Limnol Oceanogr* **42**: 1137–1153.

Smayda, T.J. and Trainer, V.L. (2010) Progress in Oceanography Dinoflagellate blooms in upwelling systems: Seeding, variability, and contrasts with diatom bloom behaviour. *Prog Oceanogr* **85**: 92–107.

Smith, K.F., Kohli, G.S., Murray, S.A., Rhodes, L.L., Smith, K.F., Kohli, G.S., *et al.* (2017) Assessment of the metabarcoding approach for community analysis of benthic-epiphytic dinoflagellates using mock communities. **8330**.

Smith, S. V. (1984) Phosphorus versus nitrogen limitation. *Limnol Oceanogr* **29**: 1149–1160.

Sommer, U. and Lengfellner, K. (2008) Climate change and the timing, magnitude, and composition of the phytoplankton spring bloom. *Glob Chang Biol* **14**: 1199–1208.

Spall, M.A., Pickart, R.S., Brugler, E.T., Moore, G.W.K., Thomas, L., and Arrigo, K.R. (2014) Deep-Sea Research II Role of shelfbreak upwelling in the formation of a massive under-ice bloom in the Chukchi Sea. *Deep Res Part II* **105**: 17–29.

Springer, J.J., Burkholder, J.M., Glibert, P.M., and Reed, R.E. (2005) Use of a real-time remote monitoring network (RTRM) and shipborne sampling to characterize a dinoflagellate bloom in the Neuse Estuary, North Carolina , USA. *Harmful Algae* **4**: 533–551.

Stefels, J. and van Boeckel, W.H.M. (1993) Production of DMS from dissolved DMSP axenic cultures of the marine phytoplankton species *Phaeocystis* sp. *Mar Ecol Prog Ser* **97**: 11–18.

Stoecker, D.K. and Lavrentyev, P.J. (2018) Mixotrophic Plankton in the Polar Seas: A Pan-Arctic Review. *Front Mar Sci* **5**: 1–12.

Tammilehto, A., Watts, P.C., and Lundholm, N. (2017) Isolation by Time During an Arctic Phytoplankton Spring Bloom. *J Eukaryot Microbiol* **64**: 248–256.

Tanner, J. (2021) Obliquity of the ecliptic, nutation and latitudes of the Arctic and Antarctic Circles.

Terrado, R., Lovejoy, C., Massana, R., and Vincent, W.F. (2008) Microbial food web responses to light and nutrients beneath the coastal Arctic Ocean sea ice during the winter – spring transition. *J Mar Syst* **74**: 964–977.

Tillmann, U., Gottschling, M., Nézan, E., and Krock, B. (2015) First records of *Amphidoma languida* and *Azadinium dexteroporum* (Amphidomataceae, Dinophyceae) from the Irminger Sea off Iceland. *Mar Biodivers Rec* **8**: 1–11.

Tillmann, U., Kremp, A., Tahvanainen, P., and Krock, B. (2014) Characterization of spirolide producing *Alexandrium ostenfeldii* (Dinophyceae) from the western Arctic. *Harmful Algae* **39**: 259–270.

Vader, A., Marquardt, M., Meshram, A.R., and Gabrielsen, T.M. (2015) Key Arctic phototrophs are widespread in the polar night. *Polar Biol* **38**: 13–21.

Vahl, B. and Kleemann, N. eds. (2019) Greenland in figures, Statistics Greenland.

Van de Waal, D.B., Smith, V.H., Declerck, S.A.J., Stam, E.C.M., and Elser, J.J. (2014) Stoichiometric regulation of phytoplankton toxins. *Ecol Lett* **17**: 736–742.

Van Dolah, F.M. (2000) Marine Algal Toxins: Origins, Health Effects, and Their Increased Occurrence. *Environ Health Perspect* **108**: 133–141.

Verity, P.G., Brussaard, C.P., Nejstgaard, J.C., van Leeuwe, M.A., Lancelot, C., and Medlin, L.K. (2007) Current understanding of *Phaeocystis* ecology and biogeochemistry, and perspectives for future research. *Biogeochemistry* **83**: 311–330.

Ward, B. A. (2019) Mixotroph ecology: More than the sum of its parts. *PNAS* **116**(13): 5846–5848.

Weisse, T., Tande, K., Verity, P., Hansen, F., and Gieskes, W. (1994) The trophic significance of *Phaeocystis* blooms. *J Mar Syst* **5**: 67–79.

Whittaker, R. H., and Margulis, L. (1978) Protist classification and the kingdoms of organisms. *BioSystems* **10**: 3–18.

Winder, M. and Cloern, J.E. (2010) The annual cycles of phytoplankton biomass. 3215–3226.

de Wit, C. T. (1992) Resource use efficiency in agriculture. *Agric. Syst*. **40**: 125–151.

Xiang, C., Tan, Y., Zhang, H., Liu, J., Ke, Z., and Li, G. (2019) The key to dinoflagellate (*Noctiluca scintillans*) blooming and outcompeting diatoms in winter off Pakistan, northern Arabian Sea. *Sci Total Environ* **694**: 133396.

## Acknowledgements

The success of this dissertation would not have been possible without the help of various people along my path. First and foremost, I want to thank my main supervisor Dr. Uwe John for giving me the chance to write proposals with him and to eventually conduct this research with his support. I want to thank Dr. Sylke Wohlrab for always having an open ear for my questions, ideas and thoughts. Also, I want to thank Prof. Dr. Nina Lundholm for her continuous support. It was amazing and an unforgettable experience to set my foot on Greenland for the first time with you three. I also want to thank the additional members of my thesis advisory committee: Prof. Dr. Boris Koch, Prof. Dr. Tilmann Harder, and Dr. Christoph Völker, who were always available when I had questions. Prof. Dr. Per Juel Hansen was a great co-author, always willing to give his take on a particular topic and investing a lot of time into my project. Dr. Bernd Krock was a knowledgeable addition to my co-authors for my very first publication. Thanks also go to Prof. Dr. Bente Edvardsen, who agreed on being one of my reviewers.

During my field trips, I had the privilege to meet more wonderful people: Dr. Regin Rønn, Kjeld Akaraaq Mølgaard, Abel Brandt, and Johannes Mølgaard. The time on Disko working with you changed me, and showed me a completely different world.

But also the work back home at AWI gave me unforgettable impressions. Thank you for Annegret Müller, Claudia Burau, Kai-Uwe Ludichowski, Dr. Florian Koch, Dr. Jan Tebben, and Prof. Dr. Allan Cembella for helping me to do my analyses. It was great to get to know different methods and to see how different parts of the ecological chemistry section are working.

Thank you, Nancy Kühne, for technical help and help in coordinating everything. Also, talking to you and sharing thoughts became an important part of my time at AWI. Thank you, Konstantinos Anestis for being the best office mate I could imagine and all the stories that we shared. I'd invite you to an instant coffee and some almonds any time. Thank you to Dr. Jessica Kegel for your valuable advice. Thank you to Sabrina Wilms, Dr. Stephanie Elferink, Cora Hörstmann, Antonia Uthoff, and all other people who were part of the Eco-Evo-gang over the years. It was a pleasure to get to know you and to tackle the daily madness of work in science with you.

I want to thank my wonderful family for always supporting me. My parents Sylvia and Arno, my sister Stefanie and my brother-in-law Simon. I am grateful for having you. Thank you Stella for the wonderful cover of my dissertation. This meant a lot to me. Last but not least, I was blessed with friends who were there when I needed them the most. It feels good to know that you always have my back.